Pyrano-Furo-Pyridones:

Design, Synthesis and Morphological Profiling of a Novel Pseudo Natural Product Class

Dissertation

Zur Erlangung des akademischen Grades eines
Doktors der Naturwissenschaften (Dr. rer. nat.)
von der Fakultät für Chemie und Chemische Biologie
an der Technischen Universität Dortmund

vorgelegt von
M. Sc. Andreas Christoforow
Geboren am 13.08.1989
In Nishnajaja Alarca, Kirgistan

Dortmund 2019

Die vorliegende Arbeit entstand im Zeitraum von Februar 2016 bis September 2019 unter der Anleitung von Prof. Dr. Dr. h.c. Herbert Waldmann an der Fakultät für Chemie und Chemische Biologie der Technischen Universität Dortmund und dem Max-Planck-Institut für molekulare Physiologie in Dortmund.

1. Gutachter: Prof. Dr. Dr. h.c. Herbert Waldmann

2. Gutachter: Prof. Dr. Markus Kaiser

Results presented in this thesis contributed to the following publications:

A. Christoforow, J. Wilke, A. Binici, A. Pahl, S. Sievers, H. Waldmann, "Design, Synthesis and Phenotypic Profiling of Pyrano-Furo-Pyridone Pseudo Natural Products", *Accepted Manuscript in Angewandte Chemie International Edition*, **2019**, 10.1002/anie.201907853

A. Binici, "Synthesis and Biological Investigation of Pyrano-Furo-Pyridone Pseudo Natural Products", *Master Thesis,* **2019**

Table of Contents

Abstract

The design and synthesis of novel biologically relevant chemical matter finds valuable inspiration in nature´s evolutionary pre-validated molecular repository. Biology-oriented synthesis (BIOS) exploits the power of evolution to generate privileged natural product-like scaffolds. However, the guiding natural products (NPs) restrain the exploration of total NP-like chemical space and the associated target space which renders BIOS limited in the discovery of novel chemotypes and their biological activities. Combining NP-inspired strategies with fragment-based compound design bears the potential to overcome these limitations by *de novo* combination of NP-derived fragments to unprecedented and biosynthetically inaccessible compound classes termed pseudo natural products (pseudo NPs).

In the course of this project pyrano-furo-pyridones (PFPs) were designed as a novel class of pseudo NPs and synthesized by combination of biosynthetically rarely related 2-pyridone and dihydropyrane NP-fragments in three isomeric arrangements. Cheminformatic analysis indicated that PFPs resemble drugs and related compounds that occupy NP-like chemical space not covered by existing NPs. Morphological profiling by means of the target-agnostic "cell painting" assay enabled unbiased biological investigation of the novel pseudo NP class and guided the discovery of PFPs as structurally novel inhibitors of mitochondrial complex I and inducers of reactive oxygen species. These results further establish the concept of pseudo NPs as a novel guiding principle for library design in small molecule drug and probe discovery.

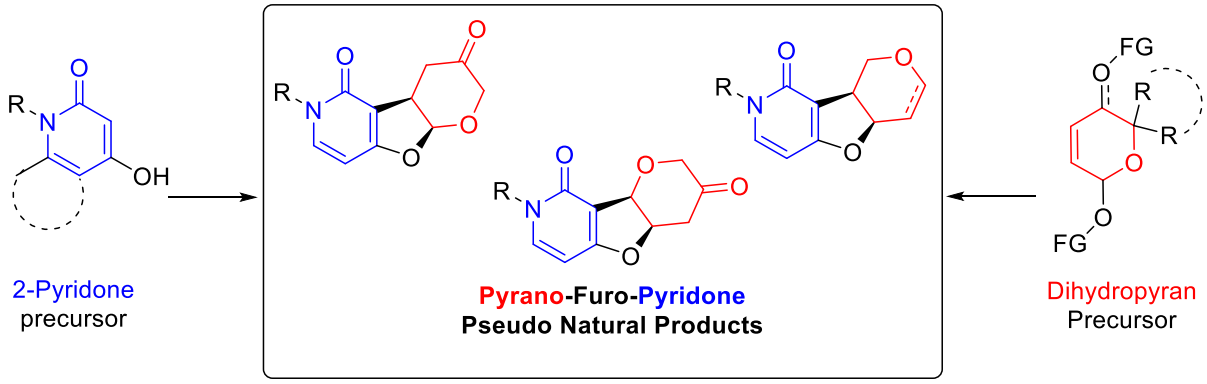

Graphical Abstract. Synthetic combination of NP derived 2-pyridone and dihydropyran fragments leads to unprecedented pyrano-furo-pyridone pseudo NPs.

Kurzzusammenfassung

Von der Natur evolutionär vorselektierte Moleküle inspirieren die Gestaltung und Synthese von neuen biologisch relevanten Substanzen. Im Zuge der Biologie-orientierten Synthese (BIOS) werden aus Naturstoffen mit interessanter biologischer Aktivität privilegierte und naturstoffähnliche Molekülgerüste abgeleitet. Die Wahl eines Naturstoffes begrenzt hierbei jedoch die Erforschung des gesamten naturstoffähnlichen chemischen Raumes und der zugehörigen biologischen Aktivität. Somit ist das BIOS Konzept eingeschränkt in der Entdeckung neuer Chemotypen und deren biologischer Relevanz. Die Kombination von naturstoff-inspirierten Synthesestrategien mit Konzepten des fragmentbasierten Strukturdesigns ermöglicht es diese Einschränkungen zu überwinden, indem naturstoff-abgeleitete Fragmente zu neuartigen und biosynthetisch unzugänglichen Verbindungsklassen, sogenannten Pseudo-Naturstoffen, kombiniert werden.

Im Rahmen dieses Projekts wurden Pyrano-Furo-Pyridone (PFP) als neuartige Klasse von Pseudo-Naturstoffen entworfen und synthetisiert, indem 2-Pyridon und Dihydropyran Naturstofffragmente in drei isomeren Anordnungen kombiniert wurden. Chemoinformatische Analysen zeigten, dass PFP den chemischen Raum von naturstoffähnlichen Wirkstoffen einnehmen, welcher jedoch nicht von existierenden Naturstoffen abgedeckt wird. Die morphologische Profilierung in einem sogenannten „Cell Painting“-Test ermöglichte die unvoreingenommene biologische Untersuchung der neuen Pseudo-Naturstoffklasse sowie die Entdeckung von PFP als strukturell neue Inhibitoren des mitochondrialen Komplexes I und die damit verbundene Zunahme reaktiver Sauerstoffspezies. Dies bestätigt das Pseudo-Naturstoff Konzept als neuartiges Leitprinzip für das Design von Substanzbibliotheken zur Erforschung von biologisch relevanten niedermolekularen Wirkstoffen und chemischen Sonden.

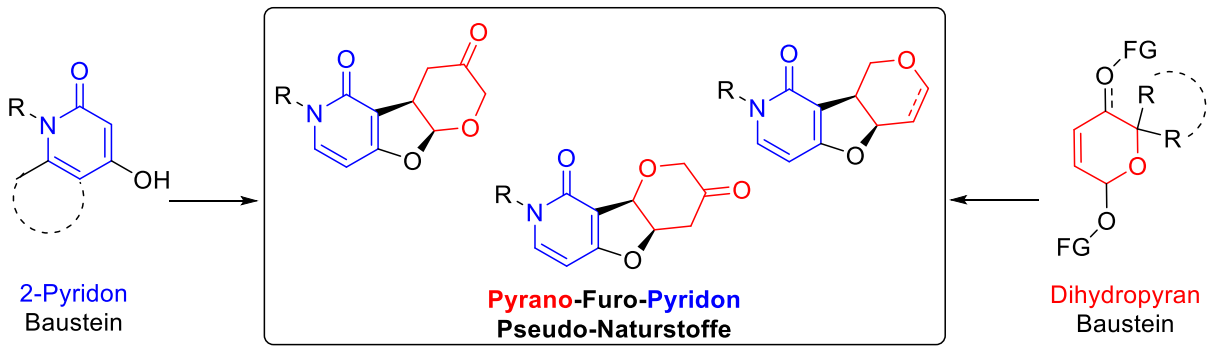

Kurzzusammenfassung. Pyrano-furo-pyridon pseudo Naturstoffe lassen sich durch die synthetische Kombination von naturstoffabgeleiteten 2-Pyridon und Dihydropyran Bausteinen darstellen.

1. Introduction

Identifying tools that shed light on known and novel biological phenomena lies at the heart of Chemical Biology. A deeper understanding of disease- and non-disease states requires tools with distinct features regarding selectivity, efficacy and potency to identify, characterize and elucidate molecular mechanisms of interactions between proteins and their modulators. Eventually, the discovery of powerful tools in Chemical Biology has a direct impact on the development of effective, potent and safe drugs.[1]

In contrast to genetic alterations, small molecules can be applied in adjustable doses and often in a reversible manner, allowing precise control over a biological process in terms of time and magnitude.[2] In addition, employing small molecules to modulate a specific function of one or multiple proteins enables the investigation of a biological process of interest without the necessity to remove or change the protein itself.[1, 3] In forward chemical genetics[4], the successful identification of a small molecule eliciting a desired biological effect strongly depends on the composition of the substance library which is supposed to be screened. With the number of hypothetically synthesizable and drug-like molecules being estimated between 10^{20} and 10^{30},[5] it is of major importance to choose a promising point of departure for the exploration of vast chemical space.

1.1. Natural Product Inspired Compound Collections

Natural products (NPs) have proven to be a reliable and rich source of biologically relevant chemical matter as it was recently shown that 28% of all US Food and Drug Administration (FDA) approved first-in-class drugs between 1999 and 2013 are either NPs (15%) or NP-derived (13%).[6] This significant impact on drug discovery ultimately results from increased hit rates of NPs and their analogues compared to purely chemically synthesized compounds which is attributed to a different and broader coverage of chemical space.[7] NPs were selected and optimized by nature over thousands of years by evolutionary pressure. Thus, their structures and scaffolds can be viewed as privileged for molecular interactions with their respective targets.[8] Despite their obvious predestination for drug discovery, the application of NPs and derivatives thereof still faces significant reluctance in the pharmaceutical industry.[9] This discrepancy can be rationalized by difficulties in isolation of suitable quantities of a desired NP from complex mixtures and challenging multi-step synthesis which may restrict structure-activity relationship (SAR) studies.[8] However, approaches to overcome these limitations

include diversity-oriented synthesis (DOS), biology-oriented synthesis (BIOS), complexity-to-diversity (CtD) and NP-fragment based ligand discovery.[10-13]

1.1.1. Diversity-Oriented Synthesis

The goal of DOS is to build up stereochemical and scaffold diversity in a small number of synthetic transformations. To this end, a common three-step strategic approach is followed consisting of the build-, the couple- and the pair-phase (Figure 1). Initially, chiral building blocks with orthogonal sets of functional groups are synthesized employing robust asymmetric syntheses. In the couple-phase these building blocks are joined ideally under full stereocontrol. The building and coupling provide the fundament of stereochemical diversity. In the final pair-phase, intramolecular coupling reactions are performed to link complementary functional groups resulting in compounds with high scaffold diversity. Compared to commercial libraries, DOS-derived compound classes have a higher stereochemical content and a higher fraction of sp^3-hybridised centers. This higher degree of complexity is also a common feature of numerous NPs. Hence, DOS-derived compound libraries can be considered NP-like which is also reflected in their enhanced biological performance.[10]

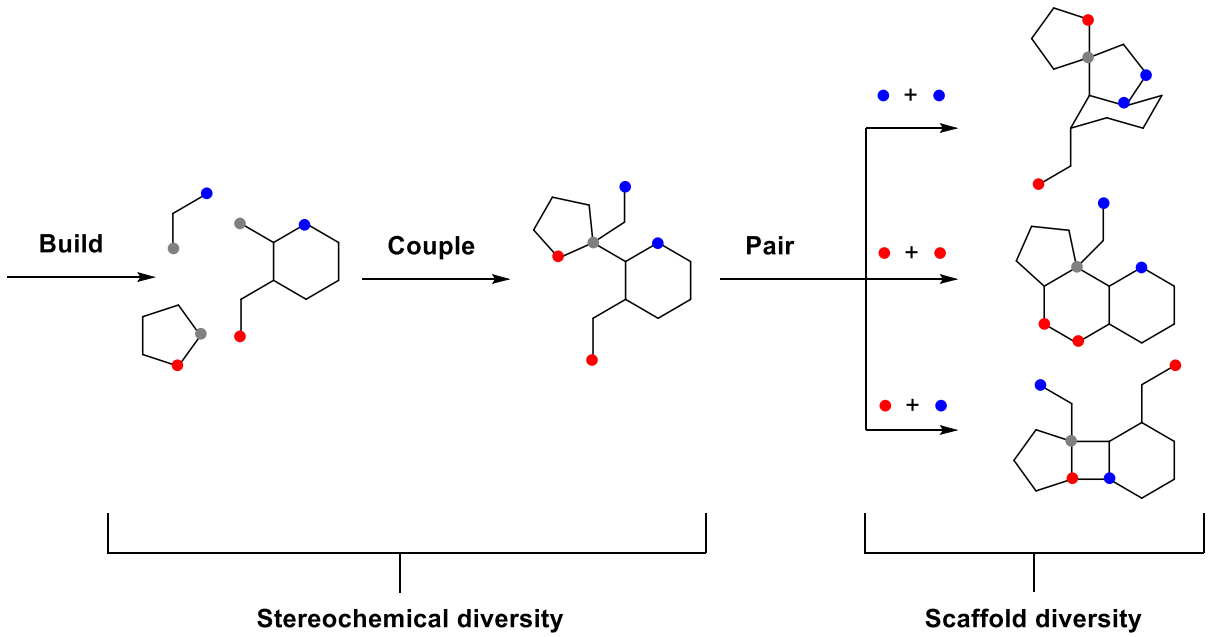

Figure 1. General concept of diversity-oriented synthesis (DOS). Grey dots indicate the functional groups for coupling. Blue and red dots indicate functional groups for pairing.

1.1.2. Biology-Oriented Synthesis

The strategy of BIOS employs nature´s pre-validated structures of bioactive NPs as leading scaffolds which are reduced to less complex frameworks with retained kind of bioactivity. These serve then as privileged starting points for the synthesis of NP-inspired compound collections ensuring reliable and efficient synthetic tractability (Figure 2).[11] The BIOS approach initially required cheminformatic analysis of NPs and their embedded scaffolds. This was visualized in a tree-like structural classification of NPs (SCONP) allowing the mapping of known NP chemical space and navigation from complex structures to simpler frameworks and single-ring building blocks.[14] Annotation of biological relevance and implementation as hierarchical guiding criterion during structure simplification additionally assures that the kind of bioactivity encoded in the scaffolds is retained while potency might drop.[11] Numerous examples based on the BIOS strategy were reported and extensively reviewed having an average library size of 200 – 500 compounds with a hit rate of 0.5 – 1.5%. Collectively, BIOS enabled thorough SAR studies which ultimately resulted in the successful discovery of various NP-inspired bioactive compounds.[11, 15-16]

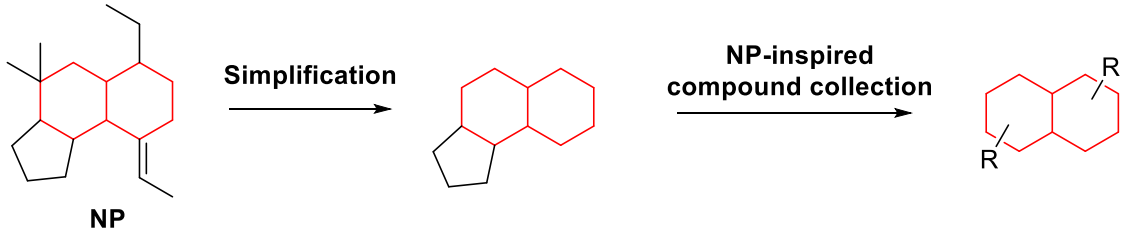

Figure 2. General concept of biology-oriented synthesis (BIOS). The simplified core scaffold is indicated in red.

However, selection of a guiding NP and its linked molecular target renders the BIOS approach biased in the exploration of chemical and biological space. The covered chemical space by BIOS is dictated by the guiding NPs listed in the dictionary of natural products (DNP) which represent only the characterized NPs and hence only a relatively small fraction of the total NP-like chemical space.[17]

1.1.3. Ring Distortion Strategy

In a total synthesis or drug discovery effort, the complex structures of NPs are usually regarded as the final product. Yet, through appropriate chemical modifications of orthogonal functional characteristics embedded in the NP scaffolds, they can be applied as privileged starting points

for the exploration of NP-like chemical space. In that sense, the ring distortion/modification approach aims for significant disruption of overall topology of the parent NP by manipulation of core ring systems to achieve a high degree of scaffold diversity. Hence, it was termed as the complexity-to-diversity (CtD) strategy which stands in contrast to traditional optimization efforts intending to improve potency or drug-like properties of NPs.[12]

In nature, the biosynthesis of complex NPs is composed of diverse arrays of various enzymes which transform common intermediates into distinct secondary metabolites. Inspired by this, enzymes are replaced in CtD by chemoselective reactions which enable the strategic manipulation of a suitable NP through ring-cleavage, ring-rearrangement, ring-fusion and modification of ring-size (expansion or contraction) and/or its oxidation state (e.g. aromatization) as illustrated in Figure 3.

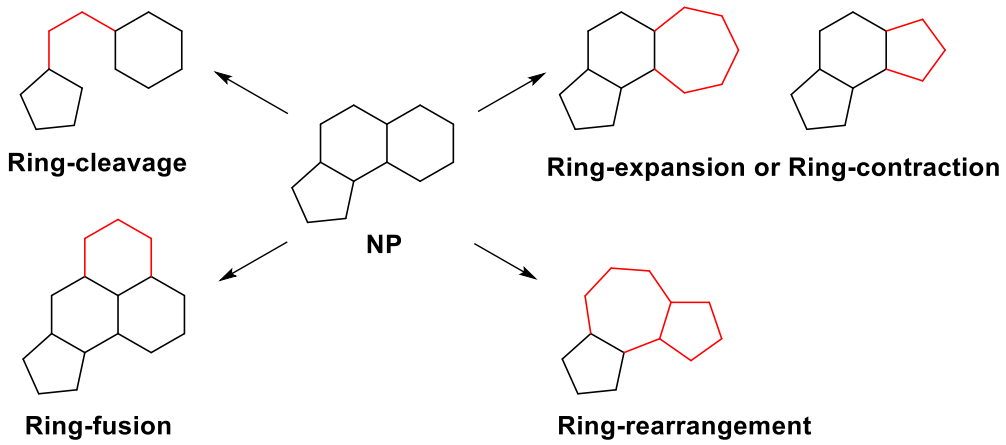

Figure 3. General concept of complexity-to-diversity strategy (CtD). Changes to the NP scaffold are indicated in red.

The diversification of several NPs including gibberellic acid[12], adrenosterone[12], quinine[12], abietic acid[18], yohimbine[19], sinomenine[20] and lycorine[21] outlined the proof of concept. The biological relevance of CtD generated NP-derived products was demonstrated in a recent example employing pleuromutilin as the parent NP for diversification resulting in structurally diverse and highly complex derivatives (Figure 4). Subsequent biological evaluation in a phenotypic assay for anticancer activity revealed the ring-contraction product of pleuromutilin **P1**, which was further elaborated to ferroptocide **P5**, as a rapid inducer of ferroptotic cell death by inhibiting thioredoxin.[22]

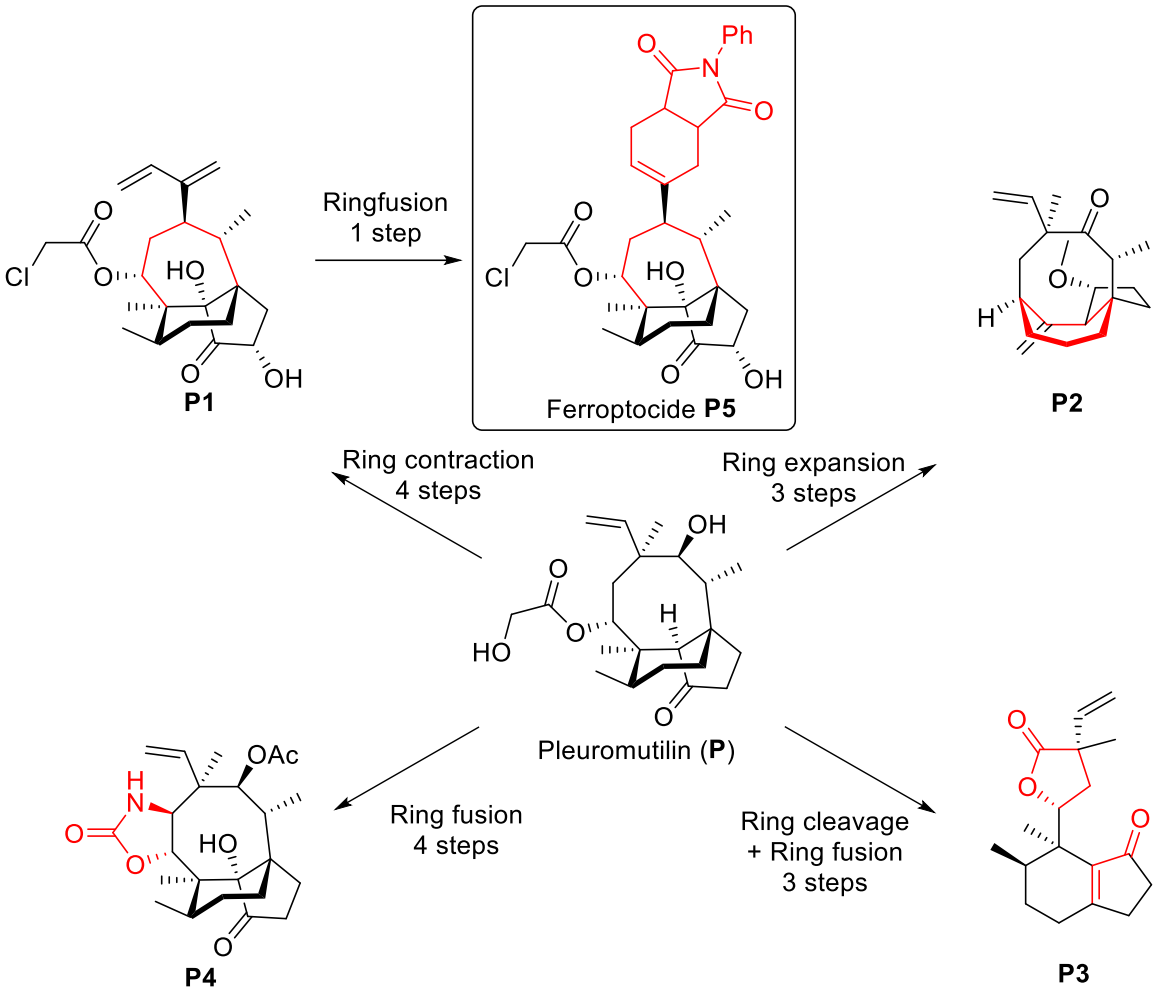

Figure 4. Diversification (indicated in red) of pleuromutilin (**P**) leads to a thioredoxin inhibitor and inducer (**P5**) of ferroptosis.

CtD is limited by the guiding NPs as they need to be available in sufficient amounts. Furthermore, the employed NPs require orthogonal functional groups for selective diversification of the core scaffold. From a practical point of view, the fast exploration of NP-like chemical space from a selected NP might be impaired by laborious screening of suitable reaction conditions to achieve a desired transformation, and/or isolation and characterization of complex isomers derived from an unanticipated reactivity of the NP.

1.1.4. Natural Product Fragments

Fragment-based drug design (FBDD) has gained increasing attention especially by the pharmaceutical industry as it seems to overcome high attrition rates during classic lead discovery approaches such as high throughput screening of combinatorial chemistry derived libraries. FBDD is based on the investigation of low-affinity pharmacophores and the

identification of their exact binding modes to the target protein of interest by X-ray crystallography or NMR spectroscopy. From a determined anchor point, the fragments can then be grown to form new interactions with the binding pocket applying structure-based drug design. This leads to high quality lead compounds which can readily be optimized. Although it was demonstrated that FBDD rapidly explores large areas of chemical space while requiring smaller libraries than usually applied during high-throughput screening (HTS), there is an inherited impairment of the obtained chemical leads regarding their complexity and diversity. As most libraries screened during FBDD consist of fragments derived from known drugs or drug candidates, the explored chemical space should be regarded as previously examined containing predominantly sp^2- and nitrogen-rich structures while lacking sp^3 carbons and stereogenic centers.[23-24]

To overcome the limitations of FBDD and the lack of straightforward synthetic accessibility to most NPs, Over *et al.* applied a modified SCONP algorithm to perform fragmentation, filtering and clustering of more than 180 000 NP structures from the DNP to arrive at 2000 clusters of NP-fragments. A principal component analysis and subsequent graphical representation revealed that NP-derived fragments cover distinctly different chemical space to synthetic and drug-like fragments. Furthermore, it was shown that the distribution of NP-derived fragment properties resembles the distribution of properties extracted from the DNP, especially in terms of three dimensionality induced by a high number of sp^3-configured centers. In a sense, NP-fragments sufficiently represent the complexity and diversity of NP structures suggesting that usage of NP-fragments in FBDD has the potential to identify structurally novel modulators of established drug targets. This approach was validated by the discovery of several phosphatase inhibitors and stabilizers of an inactive p38α MAP kinase conformation with truly novel chemotypes.[13]

1.1.5. Pseudo Natural Products

Klein *et al.* applied a gene transfer and expression technology in which yeast cells were engineered to produce 74 novel scaffold-sized (200-350 Da) compounds from diverse genetic material and immediately screened for biological activity by a functional Brome Mosaic Virus replication assay.[25] Following the concept of coevolution which refers to a continuous development of secondary metabolites and their cellular target proteins, the 74 active compounds identified by this synthetic biology effort can be regarded as prevalidated hits.[16] Beside their physicochemical properties satisfying the requirements for drug- and fragment

likeness, more than 75% of the found compounds have not been described previously and 20% exhibit entirely novel chemotypes.[25]

Conceptually, Klein´s approach can be regarded as a recombination of NP-fragments through different arrays of classes of NP associated genes. The concept of pseudo NPs mimics the engineered biosynthetic assembly of unrelated NP-fragments by synthetically recombining privileged NP derived building blocks. This generates substance libraries extending NP-like chemical space beyond the structures of NPs and thereby potentially unveiling yet unknown biological phenomena (Figure 5). This approach merges the concepts of BIOS with NP-fragments in capturing the biological relevance of NPs together with an expedient exploration of chemical space through fragments.

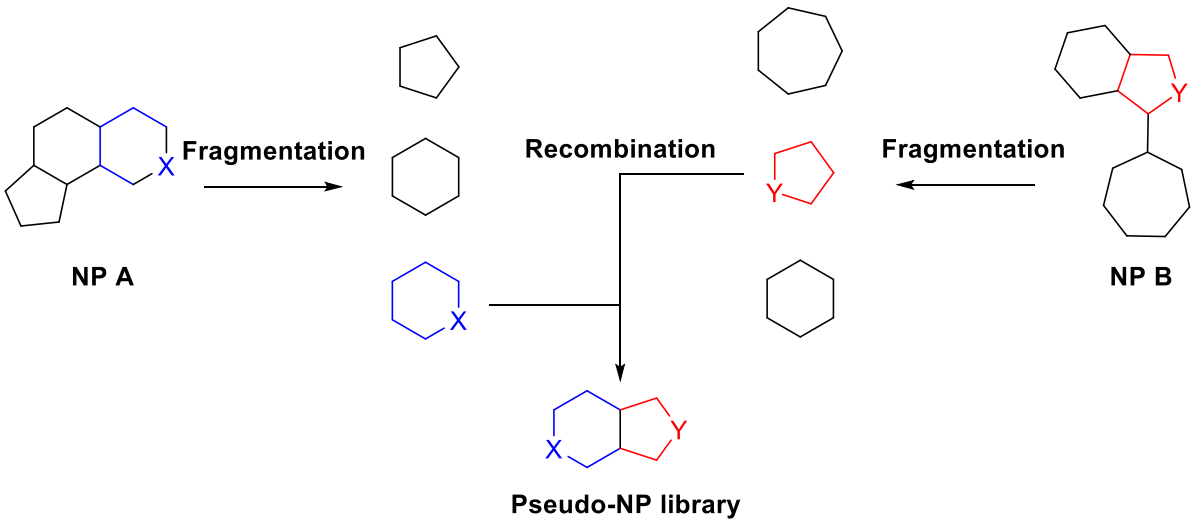

Figure 5. General concept of pseudo Natural Products (pseudo NPs). Fragments of interest (indicated in blue and red) are identified and subsequently synthetically recombined.

Following the basic design guidelines introduced for pseudo NPs has the potential to increase likelihood for biological activity.[26] In this regard, NPs employed to derive the fragments should have diverse bioactivities. Fragments selected for recombination should be biosynthetically unrelated to incorporate distinct structural features for binding to molecular targets, and ideally contain complementary heteroatoms to ensure structural diversity. Since a three-dimensional scaffold is crucial for spatial binding in protein pockets[27], the recombination of fragments should also incorporate sufficient stereogenic centers.

Table 1 illustrates six possible connection types for the design of pseudo NPs which are also observed in NPs.[28] The first entry represents a simple link between two fragments through a bond which can be regarded as a monopodal connection (Table 1, entry 1). An increase in

complexity can be achieved when two fragments share one atom and are therefore connected as a spiro compound (Table 1, entry 2). When sharing two atoms, the fragments are connected edge by edge (Table 1, entry 3). With three shared atoms, additional three-dimensional complexity is gained as a bridgehead is installed between the two fragments (Table 1, entry 4). A bipodal connection links the two fragments throughout four atoms of the molecule. Here, both attachment points can be connected through either one or multiple bonds (Table 1, entry 5). With multiple bonds in place, the newly formed molecule must be analyzed carefully as a third fragment might have inevitably been incorporated, now connecting the other two fragments. Finally, a mixture of a bridged fusion and a bipodal connection represents the most complex way of attaching two fragments to each other (Table 1, entry 6). As is the case for bipodal connected fragments, multiple bonds installed between the two fragments inevitably lead to the incorporation of a third fragment. However, the actual connection type suitable for a new class of pseudo NPs will ultimately depend on the imbedded functionalities of chosen fragments and the synthetic feasibility to exploit these for fragment recombination.

Entry	NP-Fragments	Connection Type	Pseudo NP Products	Natural Product Example
1		Monopodal Connection	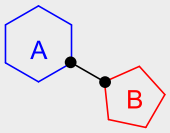	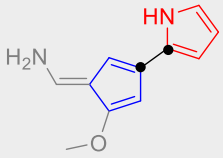 Tambjamine A
2	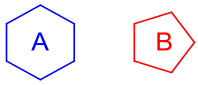	Spiro Fusion	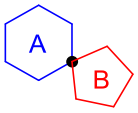	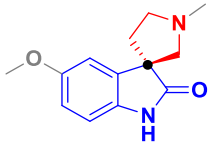 (–)-Horsfiline
3		Edge Fusion	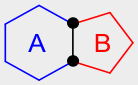	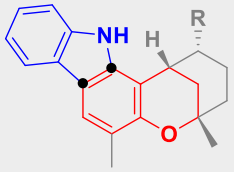 Murraya Alkaloids
4	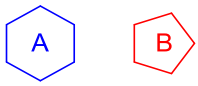	Bridged Fusion	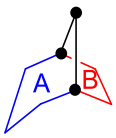	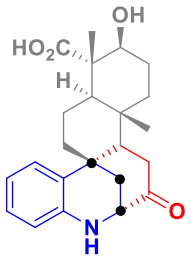 Sespenine
5		Bipodal Connection	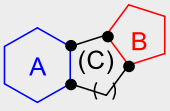 n=0-2	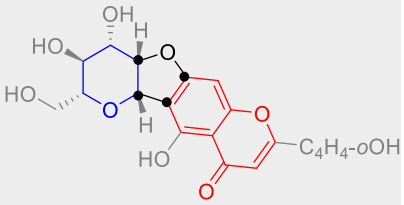 Chafuroside A
6	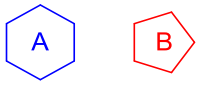	Bridged Bipodal Connection	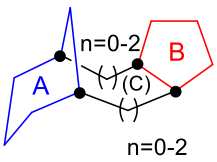 n=0-2	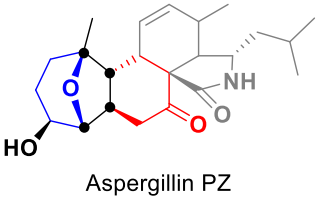 Aspergillin PZ

Table 1. Frequent connection types for two fragments observed in NPs.

The first example of pseudo NPs as a new guiding principle for small molecule drug discovery was demonstrated by the discovery of chromopynones as structurally novel glucose uptake inhibitors targeting glucose transporters GLUT-1 and -3 (Figure 6).[26] Using a multi-component one-pot synthesis, oxygen-rich chromanes, a substructure widely occurring in a

variety of bioactive NPs, were combined with nitrogen-containing tetrahydropyrimidines, representing a core fragment of an antibiotic class. As this bridged fusion of the two fragments is not encountered in nature, cheminformatic analysis of atom connectivity patterns confirmed that chemical space occupied by chromopynones does not overlap with the space defined by NPs and BIOS compounds. Noticeably, the generated novel molecular framework restricted the glucose uptake ability of cancer cells by inhibition of GLUT-1 and -3, which denotes a novel biological effect not observed for chromane or tetrahydropyrimidine containing NPs. Furthermore, copper-catalyzed 3+2 cycloaddition reactions were employed to fuse the biosynthetically unrelated indole and tropane NP-fragments providing a stereogenically complex library of indotropanes.[29] From these, myokinasib was identified as a selective and isoform-specific inhibitor of MLCK1.

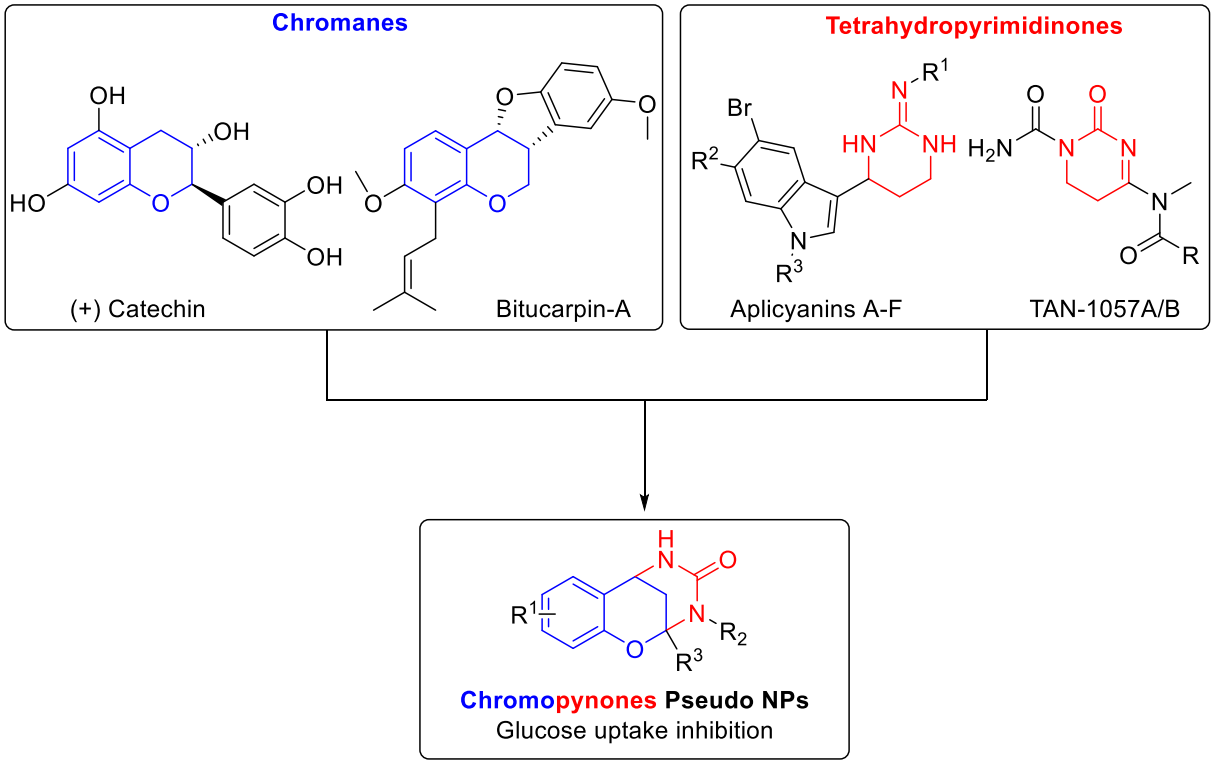

Figure 6. Design of chromopynone Pseudo NPs from chromane and tetrahydropyrimidone fragments.

Fragmentation of NPs and subsequent reconnection in alternative arrangements represents a pioneering strategy based on reconfiguration of privileged chemical matter to enable exploration of larger areas of biologically relevant chemical space not covered by nature. This introduces new nature-inspired molecular frameworks to small molecule drug and probe discovery bearing the potential to elicit interesting biological phenomena. Furthermore, the unexplored yet biological relevant chemical space as intentionally covered by pseudo NPs might spark the discovery of entirely novel biology and mechanisms of action. However, the

concept of pseudo NPs, their underlying design principles as well as their biological characterization still require further validation by different structural classes of *de novo* combined NP-fragments. The aim of this research was to provide additional affirmation of the pseudo NP concept by exploring the chemistry and biological relevance of a novel structure class of pseudo NPs.

1.2. Phenotypic Assays in Drug and Probe Discovery

The screening of small molecule libraries with the aim to investigate the functions of proteins and biological processes is referred to as chemical genetics.[30] This designation indicates the relatedness to classical genetics in which the identity of genes and their function in a specific pathway is evaluated by screening mutant libraries of an organism and investigating their phenotype. In contrast to reverse chemical genetics (RCG), which aims for the identification of a small molecule modulator of a protein of interest in target-based assays, forward chemical genetics (FCG) uses small molecules to identify proteins that regulate distinct cellular processes.[31-33] For FCG the lack of knowledge about the identity of a specific target or a hypothesis about its physiological role entails the necessity to observe the phenotypic effects of a compound minimally on cell-based level, if not tissue- or organism-based, ultimately leading to an increased translatability of disease relevant assays.[32, 34] Furthermore, recent technological advances in computation and high-throughput multiplex microscopy have provided an unbiased approach for the morphological profiling of chemically perturbed cells to support small molecule drug and probe discovery.[35-36]

1.2.1. Phenotypic Screening

The dominance of target-based screening in the pharmaceutical industry over the last three decades is in clear contrast to the success rate it delivered compared to phenotypic drug discovery as a paradigm changing analysis revealed. Out of 50 first-in-class new small-molecular entities discovered between 1999 and 2008, 28 (56%) clinically approved drugs emerged from a phenotypic approach, while 17 (34%) were found in a target-based manner.[37] This result is taken into account as a revival of interest in phenotypic screening is witnessed throughout the drug discovery and chemical biology community.[33]

In fact, FCG offers three major advantages over target-based approaches. First, phenotypic approaches have the power to address poorly understood diseases for which a molecular target is not known because an appropriate assay is capable to abstract complex mechanistic interconnections to a simpler disease-relevant and traceable phenotype.[34] Secondly, the ability to capture a cohesive picture of investigated regulatory pathways merged with proceeding development of advanced cellular models including organoids, 3D cell culture and induced pluripotent stem cells, recapitulates human disease biology more realistically. This eventually increases the clinical potential of a phenotypic hit.[31] Finally, by sampling a larger volume of molecular target space, FCG has the ability to identify compounds that act through unprecedented mechanisms of action, potentially leading to the discovery of first-in-class drugs.[37]

The complexity of FCG is reflected in the challenges and risks associated with it. Besides technical hurdles during assay development and a high false-positive hit rate, the establishment of a clear structure activity relationship (SAR) is not trivial and not always feasible due to the multi-factorial character of phenotypic data. Target identification carries another risk for failure, and it represents a major point of consideration during strategic discussions especially in the pharmaceutical industry. Although the knowledge of a target is not required for approval, the absence of a molecular target is likely to complicate safety assessment and medicinal chemistry efforts to overcome toxicological issues with a phenotypically derived compound.[31] However, constant progress in target identification technologies might lower the barrier of concern for FCG and actually ignite new RCG projects for previously unknown mechanisms of action originating from phenotypic approaches.[34] Hence, FCG and RCG should be regarded as complementary approaches, rather than competing research alternatives for the discovery and development of drugs and chemical probes with novel molecular mechanisms of action.

While phenotypic screening is capable in capturing human disease relevance, it still restricts the covered biological target space by focusing on a distinct phenotype of interest. For the chemically driven discovery approach of pseudo NPs, in which novel chemical matter is generated without any hint towards a specific biological activity, phenotypic screening is inapplicable to cover a broad range of molecular mechanisms in a reasonable manner.

1.2.2. Morphological Profiling

Technological advancements in microscopy and computation have enabled experimental methods that measure hundreds to thousands of distinct properties of a biological sample in an image-based single assay. Data generated from these multiplexed assays can be translated into specific morphological profiles allowing comparison and clustering among each other. Although technically related to phenotypic screening, morphological profiling aims at a different goal. Phenotypic screens focus on changes of a single process or cell function, whereas profiling measures a broad spectrum of features from each sample in an unbiased manner to reveal differences and similarities to other samples.[35]

While other multiplexed assays such as measurement of gene expression, protein levels and metabolites tend to be low- to medium throughput,[38] microscopy image-based profiling which tracks the morphological changes of a biological sample (therefore also referred to as morphological profiling) is particularly suitable for high-throughput measurement. This is due to a highly automatable assay set-up (multi-well plates and pipetting robot) as well as the compatibility with various biological samples, for examples cells, tissues or organisms, and sophisticated computational methods. These algorithms extract meaningful information from a broad range of measured properties to enable the comparison among individual patterns. The crucial readout is typically not the identity of each measured feature but the discovered difference itself.[35]

In a pioneering report[36], Gustafsdottir *et al.* introduced a multiplex morphological profiling assay to measure diverse cellular states upon chemical perturbation employing fluorescent markers for distinct cellular components (Figure 7).[39-40] In the so-called "cell painting assay", altogether six stains with varying detection wavelengths were used for imaging in five channels to visualize six cellular components/organelles, namely nuclei, endoplasmic reticulum, nucleoli, actin, Golgi apparatus and mitochondria. Thereby subtle changes in hundreds of features including intensity, texture, form and localization, elicited upon compound treatment were captured by microscopy imaging with single-cell resolution. Applying the open-source software CellProfiler[41], 824 morphological features per cell were extracted, reduced in dimension and the resulting morphological fingerprints were clustered to give several mechanistic or structurally related groups of compounds. Based on these morphological comparisons the authors proposed potential applications in drug discovery by identifying new mechanisms of action, scaffold hopping and library enrichment.[35-36]

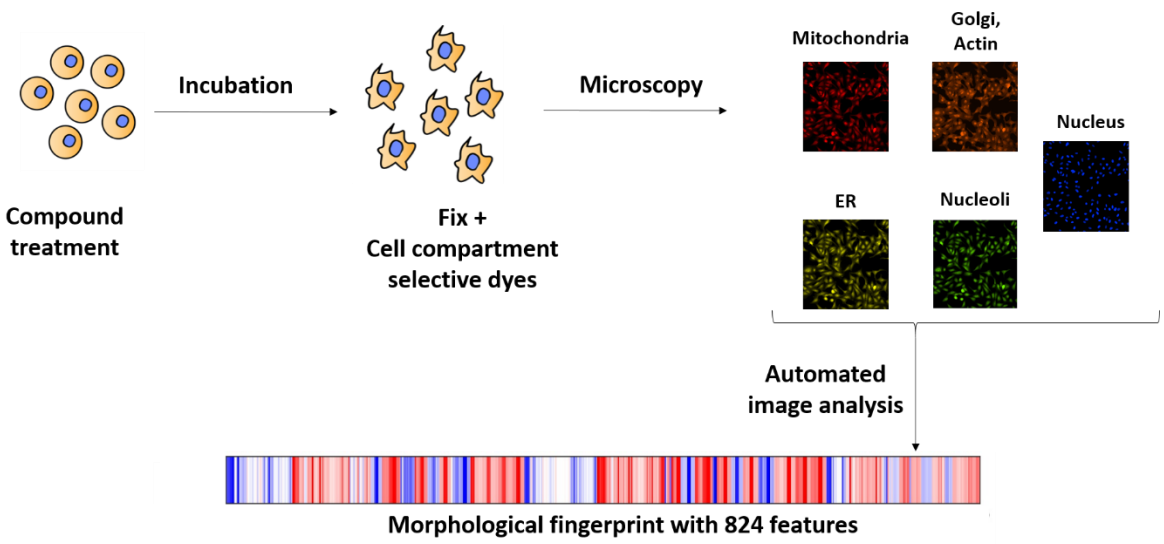

Figure 7. General concept of morphological profiling using the high-content image-based cell painting assay.

Indeed, in a follow up study multiplexed high-dimensional profiling was employed to determine and to enrich biological performance diversity of small-molecule libraries. Clemens *et al.* demonstrated that a compound collection selected due to their activity in the cell painting assay had an increased hit frequency in a panel of 96 cell-based high-throughput screening (HTS) projects. Furthermore, compound clustering and selection according to diversity in morphological fingerprints was shown to lead to overall higher HTS performance diversity compared to randomly selected compounds or structurally diverse compound collections. It was concluded that chemical structure diversity is not necessarily correlated to diverse biological performance and that libraries with diverse assay performance patterns should rather be designed according to a maximum in heterogeneity of morphological data. Finally, the authors pointed out that some bioactivities cannot be detected by the cell painting assay and that each identified profile type should have a few structurally similar compounds in the cluster to ensure the validity of the data.[42]

In another report, stereoisomers of disubstituted azetidines were analyzed in the cell painting assay. It was shown that comparison of the multidimensional profiles of stereoisomers enables differentiation in biological activity and modes of action arising exclusively from alternative configurations of stereoisomeric azetidines.[43] Although this analysis highlights the power of morphological profiling as realized in the cell painting assay to detect structural nuances and their distinct effect on morphological changes, the full potential of this multiplexed assay was not yet entirely exploited as for example target identification efforts by means of cell painting data analysis and guidance remains an unaddressed challenge.

In the context of pseudo NPs, unbiased morphological profiling has the great potential to identify bioactivity in general and in "real-time".[44] As novel compounds are synthesized with yet unknown biological activity an unbiased cell-based assay monitoring changes in cell morphology increases the chances to detect perturbing compounds which can then be prioritized for subsequent targeted assays. In addition, morphological profiles of pseudo NPs can be compared to reference compounds for mechanism-of-action hypothesis generation and compared among each other to assess biological performance diversity and general trends in structure-phenotype-relationship (SPR).

2. Aim of the Thesis

NP-inspired compound collections derived from BIOS, CtD or NP-fragments are in general enriched with biological relevant chemical matter as they exploit nature´s privileged structures which were selected over millions of years through evolutionary pressure.[11-13] Although such NP-inspired compound collections deliver enhanced hit rates in forward chemical genetics screens, they are burdened with some limitations. To overcome these limitations, it was envisioned merging the concepts of BIOS with those of NP-fragments to define and validate a novel design principal for *de novo* small molecule probe and drug discovery termed pseudo NPs.

With preliminary reports on the design and concept of pseudo NPs already published[26, 29], the aim of this thesis is to expand the strategy on different NP-fragment classes and to verify its applicability for the discovery of potential new tools in chemical biology and drug discovery.

In a first step, suitable NP-fragments for recombination will be identified and the chemotypes composing the library will be designed according to accessible reactions. Next, the feasibility of synthetic routes will be evaluated and optimized to allow a highly modular synthesis of the pseudo NPs by fast and diverse combination of various NP-fragments. Subsequently, the synthesized pseudo NP library will be evaluated with cheminformatic tools to visualize the covered chemical space.

As pseudo NPs aim for a privileged exploration of yet undefined NP-like chemical space, there is an inevitable need for an appropriate biological assay to capture a wide range of biological space. Hence, the synthesized pseudo NP library will be subjected for morphological profiling in a cell painting assay and subsequent investigation of the relation between molecular structure and phenotype should disclose potential biological activity as well as a hypothesis for mode of action.

Insights from the morphological profiling will be translated to targeted cell-based assays for validation of the derived target hypothesis to ultimately verify pseudo NPs as a reliable and versatile design principle for the discovery of entirely novel tool compounds for chemical biology and drug discovery.

3. Results and Discussion

3.1. Design of the Pyrano-Furo-Pyridone Library

Following the guidelines for the design of pseudo NPs as described in 1.1.5., it was envisioned to combine 2-pyridones with dihydropyrans (DHPs). The 2-pyridone scaffold is part of numerous NP-structures with diverse biological activities including the pyridone alkaloid camptothecin which is a topoisomerase I targeting anti-cancer drug[45], and apiosporamide which is an antifungal NP[46]. DHPs represent a commonly found substructure of various classes of biologically relevant NPs such as the dihydropyranone-based flavonoid pinocembrin and the iridoid catalpol which are endowed with antioxidant[47] and neuritogenic activity[48], respectively (Scheme 1). Out of the six connection types described in Table 1 (see 1.1.5.), 2-pyridone and DHP fragments can be combined theoretically in three different ways without changing oxidation states or introducing odd bond angles. These are simple connection through one bond, fragment fusion edge by edge or combination by a bipodal connection (Scheme 1).

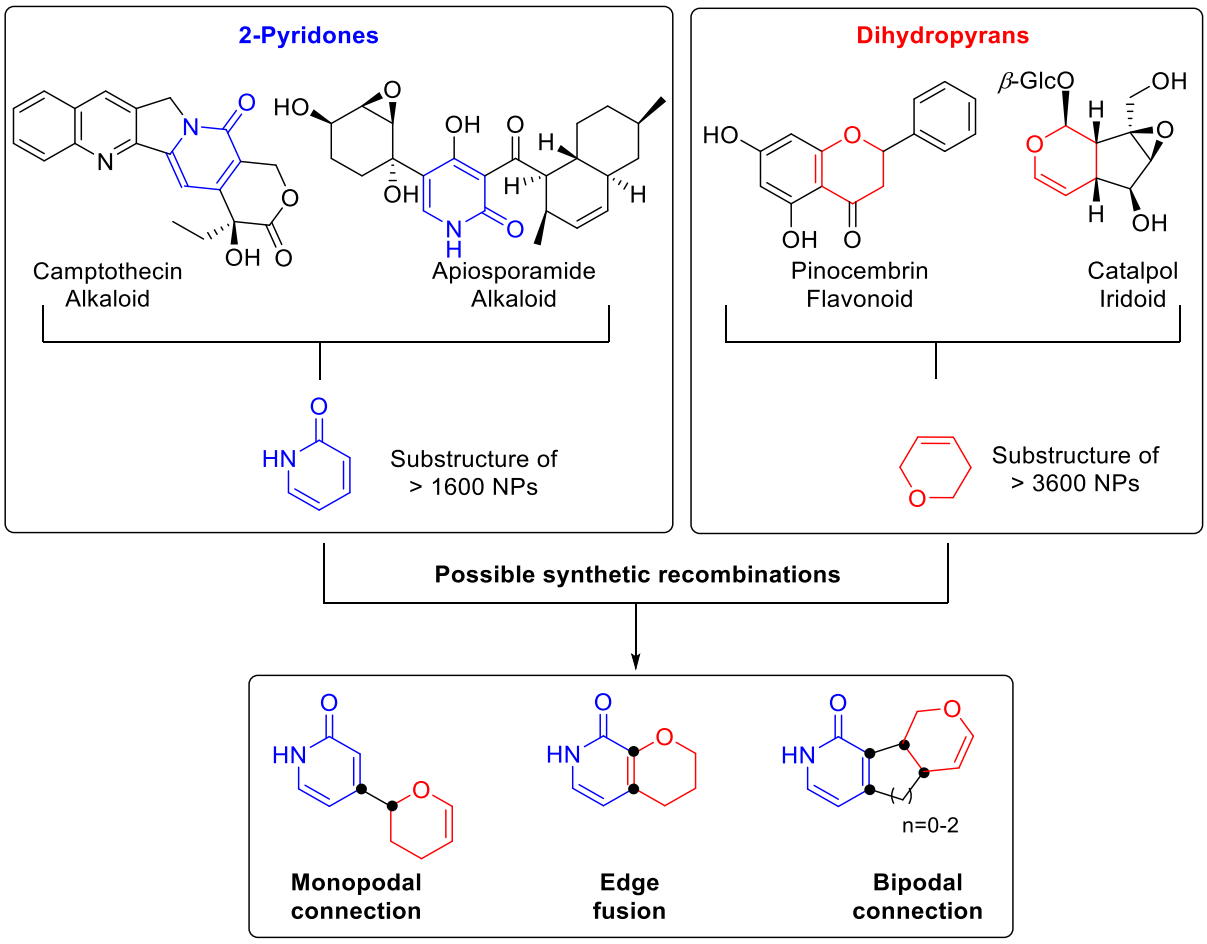

Scheme 1. NPs containing 2-pyridone or dihydropyran fragments and their potential synthetic recombination.

To assess if and which combinations of 2-pyridones and DHPs already exist in nature, all permutations of the combinations of *N*-methyl-2-pyridone with dihydropyrane (DHP) or tetrahydropyrane (THP) in a monopodal, bipodal or edge-on connection type were analyzed. Therefore, a substructure search for the respective combinations was carried out in the DNP[49] (Version 27.2, Scheme 2). Altogether 121 natural products containing examples for combinations between *N*-methyl-2-pyridone with DHPs and *N*-methyl-2-pyridone with THPs were found. The DNP Version 27.2 has approximately a total of 40 000 entries, giving a coverage of 0.3% of the reported NP chemical space by the shown combinations. This substructure search confirmed that combinations of 2-pyridones with DHPs or THPs in monopodal connection or edge fusion are rarely found in NPs while a bipodal connection of the two fragments is not observed in nature.

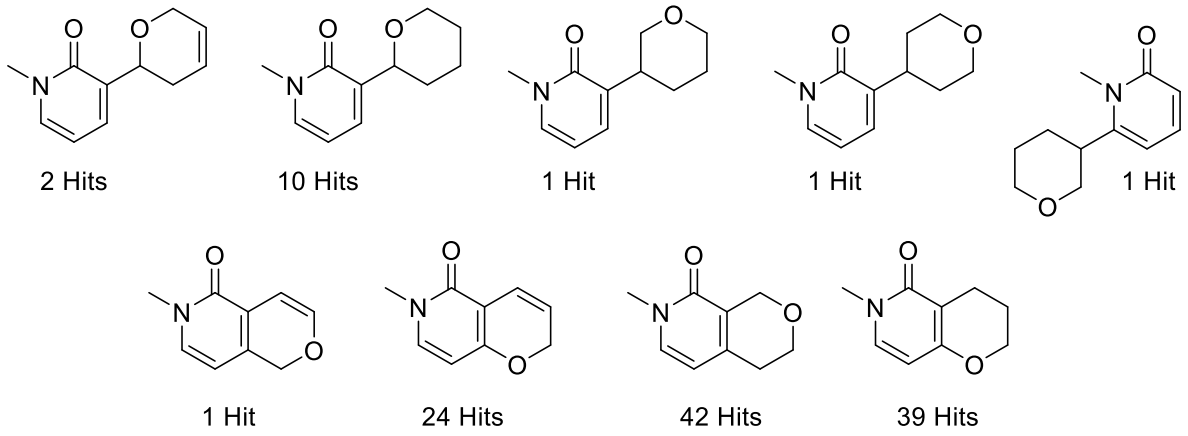

Scheme 2. Combinations of N-methyl-2-pyridone with THP or DHP for which NP examples were found in DNP.

A bipodal connection offers the opportunity to incorporate multiple stereocenters upon fragment fusion as well as a third NP-fragment. Systematic browsing of the Scifinder database for a suitable bipodal connection between a 2-pyridone and DHP fragment (see the Experimental Part 5.2.) revealed that Bartlett *et al.* reported molecules with general scaffold **A** from a combination of 2-pyrones (**1**) and a few 2-pyridones (**2**) with difunctionalized DHPs (**3**) (Scheme 3). With two stereocenters being generated through incorporation of a common dihydrofuran NP-subunit[50], scaffold **A** comprises all desired features for a bipodal connection. It was envisioned to employ this strategy for a variety of 2-pyridones terming this novel pseudo NP class eventually pyrano-furo-pyridones (PFPs).

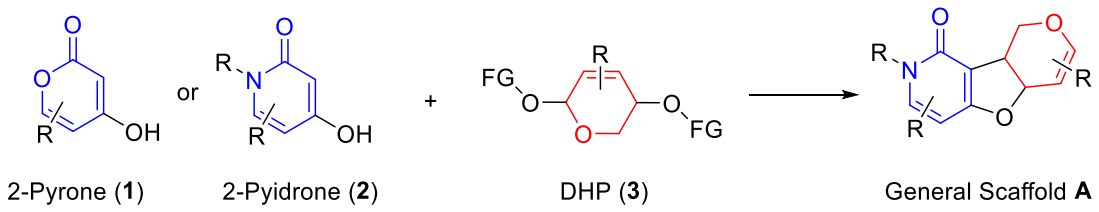

Scheme 3. General scaffold **A** is accessible through a bipodal recombination strategy of 2-pyridones and DHPs.

General scaffold **A** was selected as an initial model for the design of the PFP pseudo NP compound library. Further literature searches revealed that depending on the functionalization of the DHP building block and the applied catalyst two additional attachment point isomers (**B** and **C**) can be accessed in which the oxygen of the DHP subunit is shifted around the six-membered pyran ring.[51] It was envisioned to synthesize a pseudo NP library of various derivatives of scaffolds **A-C** (Scheme 4).

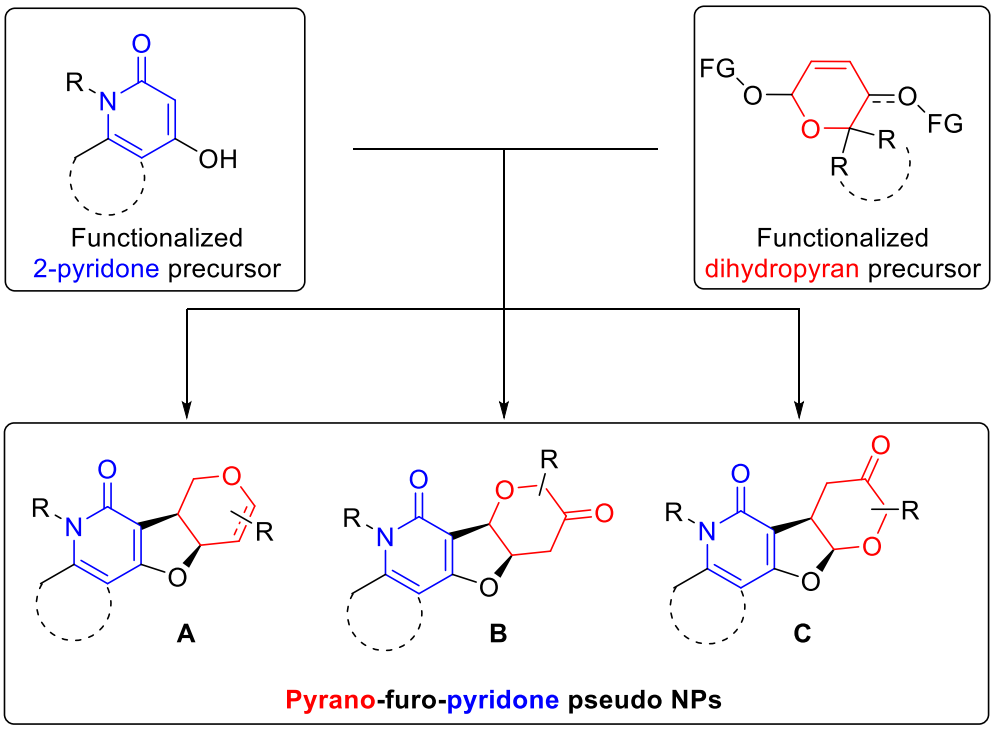

Scheme 4. Design of the pyrano-furo-pyridone (PFP) pseudo NP library from 2-pyridones and DHPs.

3.2. Synthesis Strategy

Besides the advantageous features of a bipodal connection, scaffolds **A-C** were also selected due to their shared or closely related building blocks, allowing a highly modular synthetic approach. Scaffold **A** is generated by a palladium-catalyzed allylic alkylation cascade (Pd-AAC) from bis-nucleophilic 4-hydroxy-2-pyridones (**2**) and bis-electrophilic 3,6-dihydro-2*H*-

pyrans (**3**, DHPs) carrying an allylic carbonate and an anomeric siloxy leaving group. This allows the regioselective and stereoconvergent preparation of *cis*-fused furo[3,2-*c*]pyridones (Scheme 5, general scaffold **A**).[50] The synthesis of **B** employs 4-hydroxy-2-pyridones as bis-nucleophiles (**2**), as well. In contrast, the bis-electrophile here is a dihydropyranone (**4**, also abbreviated as DHP) equipped with an anomeric acetate leaving group and a Michael acceptor functionality. Under palladium-catalyzed conditions, a two-step reaction sequence occurs consisting of initial allylic alkylation and subsequent intramolecular oxa-Michael-cyclization to construct *cis*-fused furo[3,2-*b*]pyridones (Scheme 5, general scaffold **B**).[51] Using stoichiometric amounts of quinine instead of a palladium catalyst causes an inversion of reactivity and therefore a change in the reaction sequence. In this case initial diastereoselective Michael addition followed by an intramolecular transacetalization results in *cis*-fused furo[2,3-*b*]pyridones (Scheme 5, general scaffold **C**).[51]

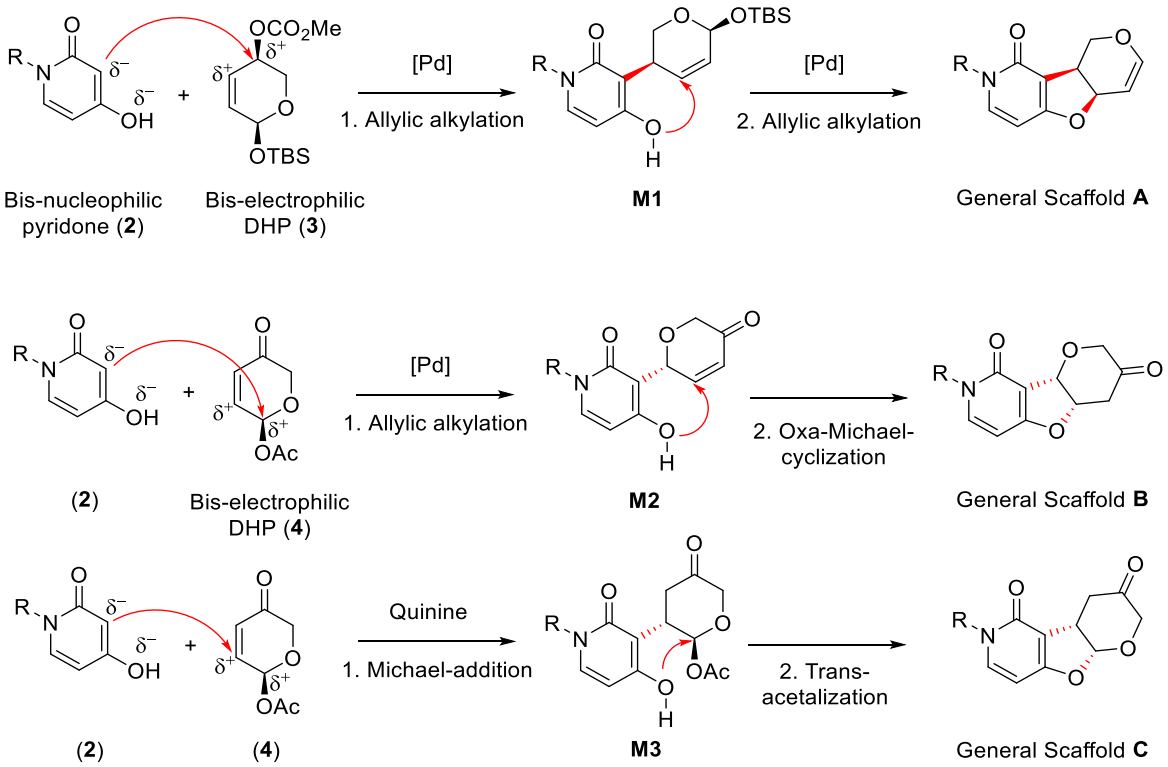

Scheme 5. General synthetic strategy for the preparation of pyrano-furo-pyridone scaffolds **A**, **B** and **C**.

All three reaction routes are based on the utilization of a 4-hydroxy-2-pyridone as a bis-nucloephile and DHPs with varying functional groups as bis-electrophiles. Hence, by adjusting the appropriate catalytic system and/or conditions a small number of pyridones and DHPs can lead to various combinations of the two fragments allowing the expedient exploration of chemical space around scaffolds **A**, **B** and **C**.

3.3. Synthesis of Functionalized Precursors

3.3.1. Synthesis of 2-Pyridones

2-Pyrones are known to react with primary amines to give *N*-substituted 2-pyridones.[52] This well-established method was employed to rapidly introduce a high diversity of substituents on the pyridone fragment (**2**) by treatment of 4-hydroxy-6-methyl-pyrone **(1a)** with the respective primary amines (Scheme 6). *N*-substitution ranged from simple hydrogen (**2a**), methyl (**2b**) and isopentyl (**2d**) or (hetero)-alkyl rings (**2c**, **2e**, **2f**) to benzyl (**2g**), substituted benzyl groups (**2h-k**) and heteroaryl groups (**2l-p**). In addition, variation of the linker length between pyridone and aryl- or heteroaryl groups was investigated by introduction of a second methylene group (**2s**, **2t**) or exclusion of a linker (**2q**, **2r**). Furthermore, some NP-derived pyrones and pyridones were commercially available (**1b** and **2u-za**). 4-Hydroxy-2-pyridones can be regarded as the enol form of cyclic 1,3-dicarbonyl bis-nucleophiles with a nucleophilic position at C3 and at the phenolic oxygen.

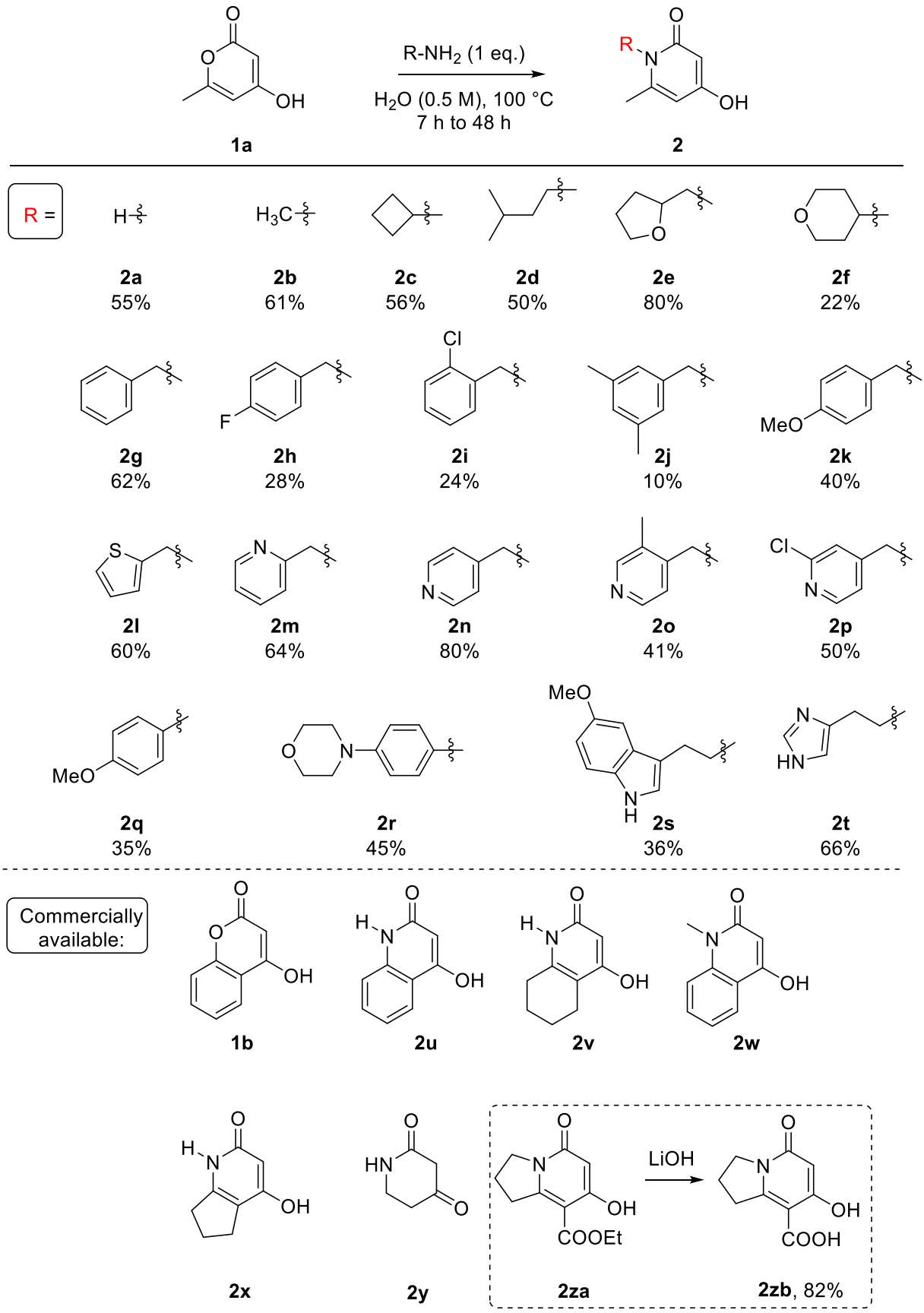

Scheme 6. Synthesis of various 4-hydroxy-2-pyridones (**2**).

3.3.2. Synthesis of Dihydropyrans

The key reaction to build up the DHP core scaffold was discovered by Achmatowizc *et al.* and consists of treating furfuryl alcohol substrates with an appropriate oxidant.[53] For the synthesis of difunctionalized DHPs, an established protocol was used applying *meta*-chloroperoxybenzoic acid (*m*CPBA) as an oxidant for the initial Achmatowizc rearrangement. Subsequent protection of the anomeric alcohol with *tert*-butyldimethylsilyl chloride (TBSCl), diastereoselective substrate-controlled Luche-reduction of the keto group and transformation to corresponding carbonates yielded bis-functionalized DHPs.[50] Following this route, C6-unsubstituted difunctionalized bis-electrophilic DHP **3a** and C6-methylated DHP **3b** were synthesized on a multi gram scale with overall yields of 23% and 10%, respectively (Scheme 7). The rather low yields can be attributed to the use of excessive amounts of *m*CPBA in the first step which generates *meta*-chlorobenzoic acid as a by-product. This and unreacted *m*CPBA was laborious to remove from the reaction mixture requiring multiple washing and chromatography steps even in subsequent reactions ultimately resulting in a high loss of desired products.

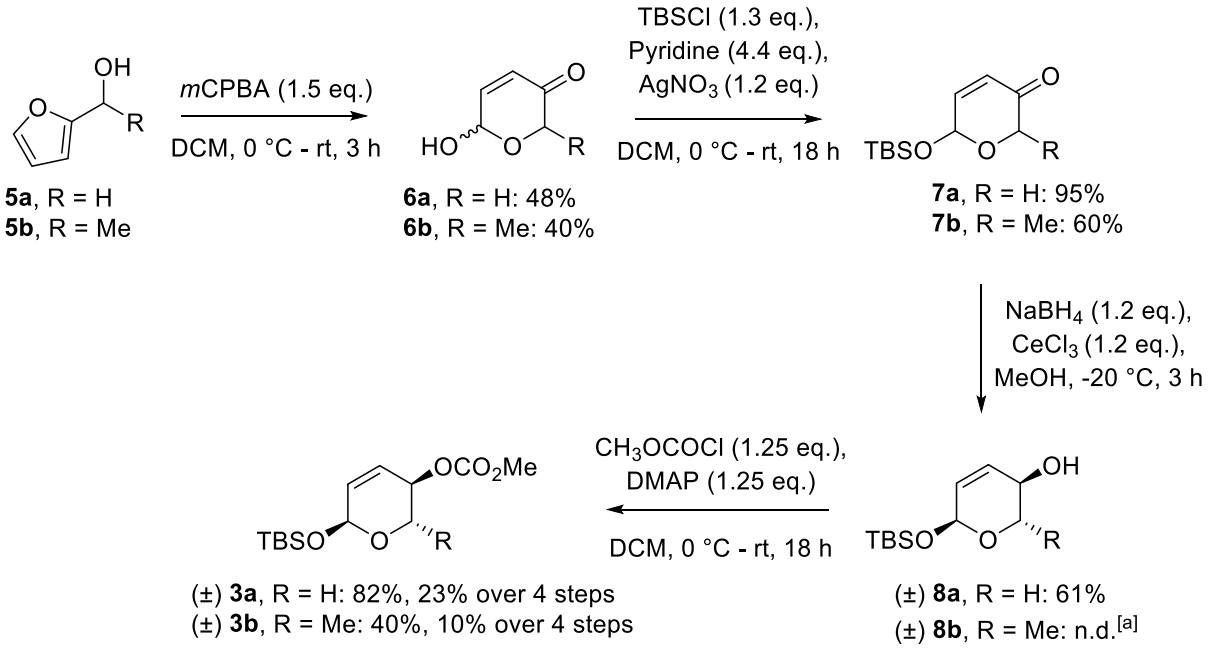

Scheme 7. Synthesis of bis-funcitionalized DHPs **3a** and **3b** from furyl alcohols.
[a] n.d.: product was used directly in next step without isolation.

Alternative reaction conditions for the Achmatowicz rearrangement were recently published by Plutschack *et al.*[54]. The authors demonstrated that various furfuryl derivatives can be transformed to their corresponding dihydropyranones in a photo-redox catalyzed transformation employing only 0.1 mol% of $Ru(bpy)_3Cl_2 \bullet 6H_2O$ as the photocatalyst and

almost equimolar amounts of $Na_2S_2O_8$ as an oxidant for the excited state of the photocatalyst. The robustness of the reaction and good water solubility of formed by-products was encouraging to develop a batch photo reactor and to investigate the reported conditions.

The transformation of (±)-1-(2-furyl)ethanol (**5b**) to 6-hydroxy-2-methyl-2H-pyran-3(6H)-one (**6b**) was chosen as a model reaction for the establishment of a batch photo reactor (Table 2). Results from the first-generation reactor (see the Experimental Part 5.1.1.) were promising (Table 2, entry 1) as the product could be isolated in 72% yield and with very high purity after aqueous work-up. Notably, temperature control between 20 and 25 °C was crucial to avoid formation of orange and black precipitants at the vessel walls and an associated decrease in yield (entry 2 and 3). With increasing scale, the photo reactor was slightly modified to the second generation (see the Experimental Part 5.1.1.) allowing a larger reaction volume and appropriate temperature maintenance around 24 °C by compressed air flow over an isopropanol bath (entry 4). Eventually, the reaction could be performed on a multigram scale giving the desired product in 67% yield after four hours and in high purity after aqueous work-up (entry 5).

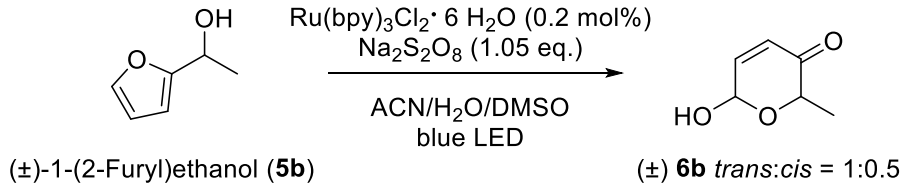

(±)-1-(2-Furyl)ethanol (**5b**) (±) **6b** *trans*:*cis* = 1:0.5

Entry	Scale, Conc.	Temp., Time, Set-up	Yield[a], Notes
1	1.00 mmol, 0.25 M	rt, 2 h, 1st reactor	72%, high purity after aqueous work-up
2	5.00 mmol, 0.25 M	30 °C, 6 h, 1st reactor	39%, orange precipitate formed at vessel wall
3	15.0 mmol, 0.5 M	> 30 °C, 3 h, 1st reactor	37%, orange and black precipitate formed at vessel wall
4	15.0 mmol, 0.25 M	24 °C, 4 h, 2nd reactor	49%, high purity after aqueous work-up
5	44.6 mmol, 0.25 M	24 °C, 4 h, 2nd reactor	67%, high purity after aqueous work-up

Table 2. Evaluation of a batch photo reactor for photo-catalyzed Achmatowicz rearrangement.
[a] isolated yield

(±) 1-(2-Furyl)ethanol (**5b**) and 2-(furan-2-yl)propan-2-ol (**5c**) were transformed by photo-catalyzed Achmatowicz reaction to the respective dihydropyranone derivatives **6b-c** and subsequently functionalized according to the previously described reaction sequence (Scheme 8). The high purity of Achmatowicz rearrangement products allowed following reactions without necessity for chromatographic purification, except after the last step in which diastereomers had to be separated chromatographically. Hence, the yield for C6-methylated DHP **3b** could be increased from 10 to 44% over four steps and C6-dimethylated DHP **3c** could be synthesized in 33% yield over five steps.

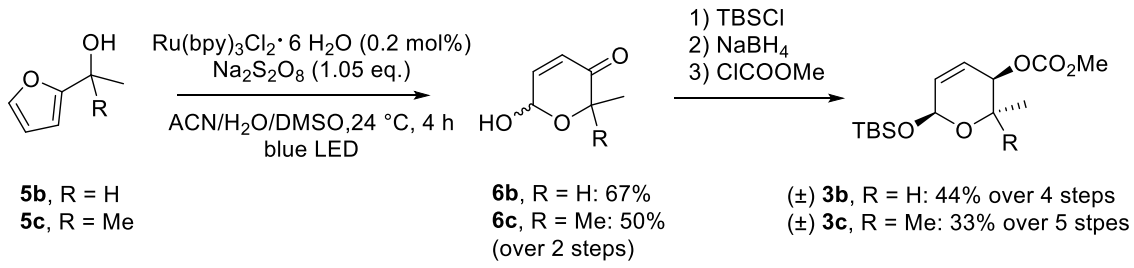

Scheme 8. Synthesis of bis-functionalized DHPs **3b** and **3c** employing a photo-catalyzed Achmatowicz rearrangement.

In analogy, bis-electrophilic DHPs **4** with an anomeric acetate group were synthesized (Scheme 9). DHP **4a** and **4b** could be synthesized from readily available furyl alcohol derivatives in two steps with 36% and 60% overall yield, respectively. In a three-step synthesis, DHPs **4c** and **4d** were synthesized through photo-catalyzed Achmatowicz rearrangement of corresponding furyl alcohols and subsequent acetate protection of the anomeric alcohol in 28% and 74% overall yield, respectively.

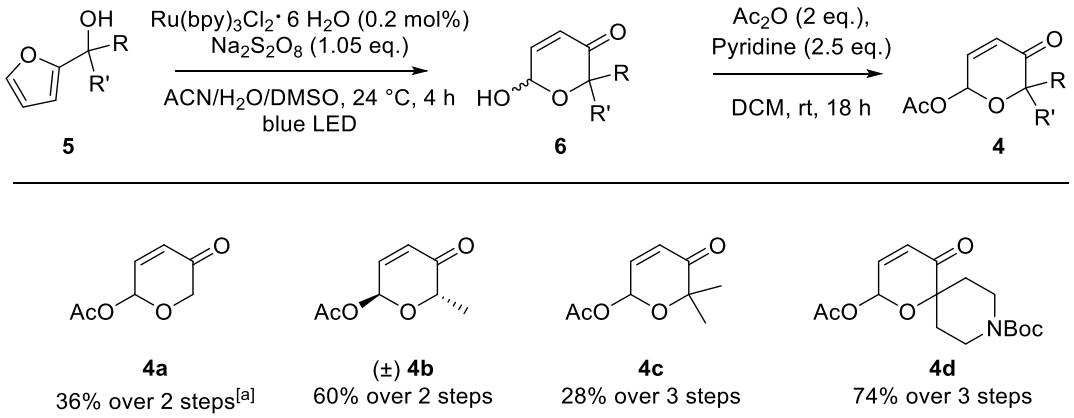

Scheme 9. Synthesis of acetylated DHPs **4**.
[a] Achmatowicz reaction was carried out with *m*CPBA.

3.4. Synthesis of Pyrano-Furo-Pyridones

Within the concept of pseudo NPs, the *de novo* generated molecular architectures have no predecessors. Thus, a link between the absolute configuration of a pseudo NP and its potential biological activity is unknown. To cover more accessible configurational space, the pyrano-furo-pyridone library was synthesized in racemic fashion.

3.4.1. Synthesis of General Scaffold A Isomers

Initially, literature known fusion of DHP **3a** with 4-hydroxy-6-methyl-2-pyrone (**1a**) by Pd-AAC was carried out as a model reaction to furnish pyrano-furo-pyrone **9a** as a representative structure of isomers **A** (Table 3, entry 1).[50] A significant point to evaluate was the scalability of Pd-AAC and its applicability with pyridones as bis-nucleophiles. Hence, the model reaction was scaled up by a factor of two leading to a decrease in yield from 55% to 18% (entry 2). Increased concentration, prolongation of reaction time, increase of catalyst loading to 10 mol% or addition of triethyl amine (NEt_3) left the yield at rather low levels between 21% and 28% (entries 3-5). On a 0.70 mmol scale a satisfying yield of 81% could only be achieved with high catalyst loadings of 20 mol% in toluene at a compound concentration of 0.05 M (entry 6). Noteworthy, for entry 6 the procedure was slightly modified by adding the first 10 mol% of palladium catalyst in the beginning of the reaction and another 10 mol% after six hours reaction time. This indicated that $Pd(PPh_3)_4$ might degrade over the course of reaction and thereby leading to lower yields for entries 1-5 in Table 3.

With the stability of the catalyst being crucial for high yields, in a following optimization cycle the focus was set on the screening of various catalysts and ligands (entries 7-13). Allylpaladium(II) chloride dimer in combination with 2-dicyclohexylphosphino-2′,4′,6′-triisopropylbiphenyl (XPhos) gave 60% yield on 0.35 mmol scale but the yield dropped to 10% on a 0.70 mmol scale (entries 7 and 8). Second generation Xphos palladium precatalyst (Pd-Xphos G2) and [1,1′-bis(diphenylphosphino)ferrocene]dichloropalladium(II) ($Pd(dppf)Cl_2$) were also not suitable for the reaction (entries 9 and 10). Interestingly, with tris(tris(3,5-bis(trifluoromethyl)phenyl)phosphine)palladium(0) (abbreviated as superstable Pd(0) catalyst[55]) the product could be obtained after 14 days at room temperature in THF with 95% yield (entry 11). The reaction time could be drastically reduced to one hour by irradiating the reaction mixture in the microwave (MW) at 100 °C without noticeable influence on the yield (entry 12). Furthermore, the superior catalytic activity of superstable Pd(0) was demonstrated

by giving similar results with a lower catalyst loading of 5 mol% and on increased scale (entry 13). Noteworthy, the application of superstable Pd(0) in palladium catalyzed allylic alkylation reactions was not reported before in the literature.

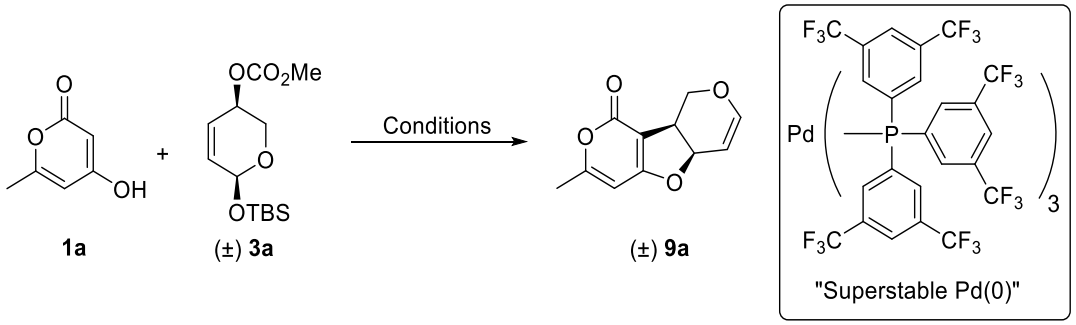

Entry	Scale	Conc.	Solvent	Additive	Time, Temp.	Cat.	Yield[a]
1	0.35 mmol	0.1 M	Toluene,	/	24 h, rt	$Pd(PPh_3)_4$ (5 mol%)	55%
2	0.70 mmol	0.1 M	Toluene	/	24 h, rt	$Pd(PPh_3)_4$ (5 mol%)	18%
3	0.70 mmol	0.1 M	Toluene,	NEt_3 (1 eq.)	48 h, rt	10 mol% $Pd(PPh_3)_4$	25%
4	0.70 mmol	0.5 M	Toluene	/	24 h, rt	$Pd(PPh_3)_4$ (5 mol%)	28%
5	0.70 mmol	0.5 M	Toluene	NEt_3 (1 eq.)	24 h, rt	$Pd(PPh_3)_4$ (5 mol%))$_4$	21%
6	0.70 mmol	0.05 M	Toluene	/	24 h, rt	$Pd(PPh_3)_4$ (20 mol%)[b]	81%
7	0.35 mmol	0.05 M	Toluene	Cs_2CO_3 (1.1 eq.)	24 h, rt	$[PdCl(allyl)]_2$ (5 mol%), Xphos (15 mol%)	60%
8	0.70 mmol	0.05 M	Toluene	Cs_2CO_3 (1.1 eq.)	24 h, rt	$[PdCl(allyl)]_2$ (5 mol%), Xphos (15 mol%)	10%
9	0.35 mmol	0.05 M	Toluene	$CaCO_3$ (1.1 eq.)	24 h, rt	Pd-Xphos G2 (5 mol%)	traces
10	0.35 mmol	0.05 M	Toluene	$CaCO_3$ (1.1 eq.)	24 h, rt	$Pd(dppf)Cl_2$ (5 mol%)	10%
11	0.35 mmol	0.01 M	THF	/	14 d, rt	Superstable Pd(0) (20 mol%)	95%

12	0.35 mmol	0.01 M	THF	/	1 h, 100 °C MW	Superstable Pd(0) (20 mol%)	94%
13	0.70 mmol	0.01 M	THF	/	1 h, 100 °C MW	Superstable Pd(0) (5 mol%)	86%

Table 3. Optimization studies on Pd-AAC for the synthesis of **9a**.
[a] isolated yield
[b] Pd-catalyst was added in two portions at two distinct time points

The generated tricyclic scaffold **9a** was found to be unstable under aqueous and/or acidic condition due to a Ferrier-rearrangement (Scheme 10).[56] The synthesized furo[3,4-*c*]pyran is a highly reactive glycal in which the 1,3-keto-enolate group of the pyrone substructure serves as a leaving group when treated with e.g. DMSO/H_2O (4:1) or MeOH, thus leading to a ring opening of the dihydrofuran substructure. This hypothesis was further validated by NMR experiments in which **9a** was dissolved in a mixture of deuterated DMSO/H_2O or MeOH, respectively. After incubation for 24 hours at room temperature the obtained spectra for the treatment with deuterated DMSO/H_2O (4:1) showed a distinct shift of peaks suggesting the structure of **NMR-1** (see Supplemental Spectra S1). For the deuterated MeOH mixture a spectrum with two signal sets was obtained for which all peaks could be assigned to their corresponding structure **NMR-2a** and **NMR-2b** (see Supplemental Spectra S2).

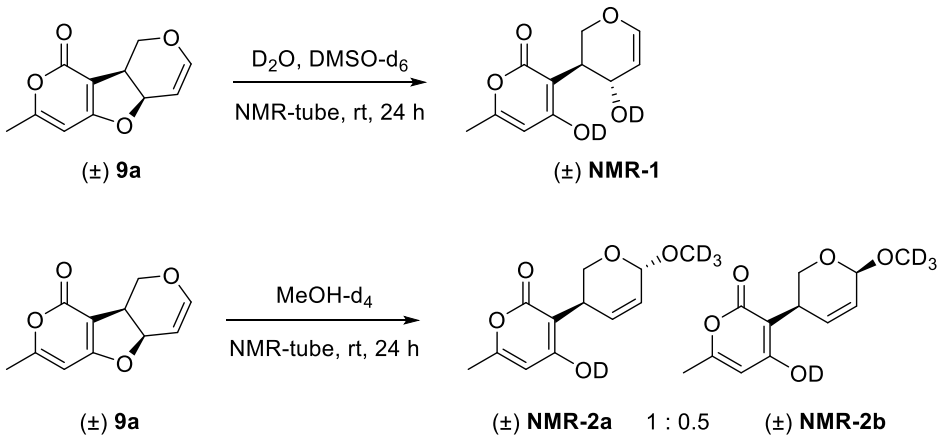

Scheme 10. NMR-experiments with **9a** validate a Ferrier-rearrangement occurring in deuterated DMSO/H_2O (4:1) or MeOH.

It was hypothesized that reduction of the glycal double bond would prevent Ferrier-rearrangement. In fact, optimized conditions for a catalytic reduction of **9a** with H_2 over Pd/C in toluene (Table 4, entry 4) gave a ring-fused product **10a** which was stable in aqueous

medium. As a side product of the reaction, compound **11a** was identified by means of NMR analysis.

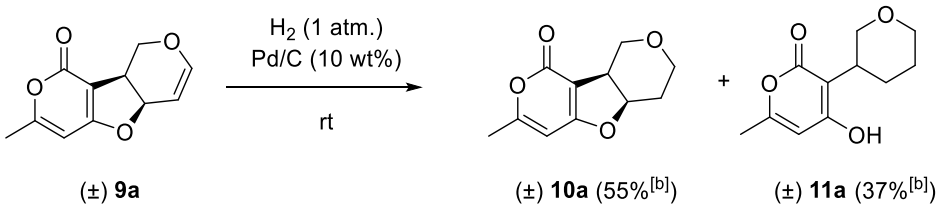

(±) **9a** (±) **10a** (55%[b]) (±) **11a** (37%[b])

Entry	Solvent	Time	Ratio[a] (10a:11a:9a)
1	THF	4.5 h	0:1:0
2	THF	10 min	1.8:1:0
3	DCM	24 h	3.3:1:4
4	Toluene	7 h	3:1:0

Table 4. Optimization of the catalytic heterogenous hydrogenation of **9a**.
[a] determined by analytical HPLC-MS.
[b] Yield for entry four after preparative HPLC

With the optimized catalytic system in hand, it was proceeded to evaluate 4-hydroxy 2-pyridones (**2**) as bis-nucleophiles in Pd-AAC with DHPs. For that purpose, 4-hydroxy-1,6-dimethylpyridin-2(1H)-one (**2b**) was reacted with DHP **3a** in the presence of superstable Pd(0) on a one gram scale to provide the desired product **9c** in 66% yield (Scheme 11). For better solubility of the 2-pyridone, the solvent was changed from THF to a THF/DMF 3:1 mixture. Encouraged by this result, the optimized reaction conditions were then successfully applied for diverse Pd-AAC ring-fusions of various 2-pyridones with DHP **3a** (Scheme 11). Due to the instability of the glycal substructure of pyridone-furo[3,2-*c*]pyrans, the majority of Pd-AAC products **9** were quickly purified by flash chromatography and directly subjected to heterogenous hydrogenation giving in total a subset of 16 PFP pseudo NPs **10** and two 2-pyrone derivatives (**10a** and **10b**) with general scaffold **A**. The scope of *N*-substitution ranged from hydrogen, methyl and (hetero)carbocycles to benzyl, substituted benzyl groups and various heteroaryl-substituents. Furthermore, tetracyclic PFPs **10b** and **10r-t** could be synthesized as well. Notably, the reduction step for **9n** and **9q** was not successful and additional Pd-AAC products **9** were isolated for **9a**, **9c-e** and **9g-i**.

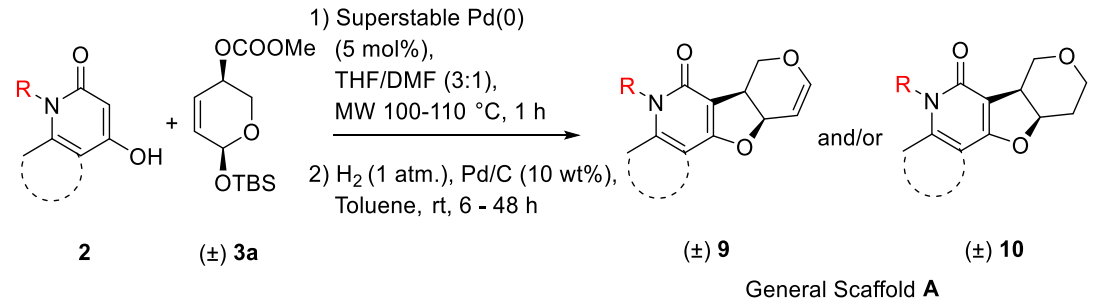

9a, 86%[1]
10a, 47%[2]

10b, 33%[2, [a]]

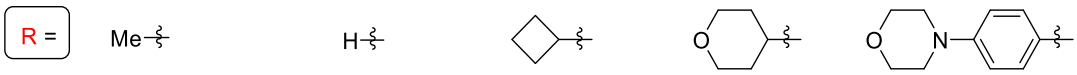

9c, 66%[1] (1g scale)
10c, 21%[2]

9d, 98%[1]
10d, 10%[2]

9e, 74%[1]
10e, 17%[2]

10f, 10%[2]

9g, 33%[1]
10g, 3%[2]

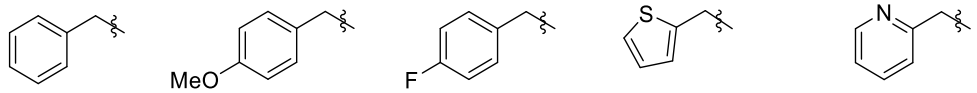

9h, 48%[1, [a]]
10h, 24%[2]

9i, 77%[1]
10i, 13%[2]

10j, 40%[2]

10k, 16%[2]

10l, 38%[2]

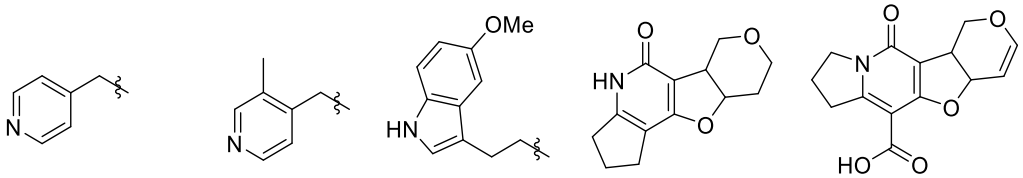

10m, 30%[2]

9n, 74%[1]

10o, 23%[2]

10p, 32%[2]

9q, 7%[1]

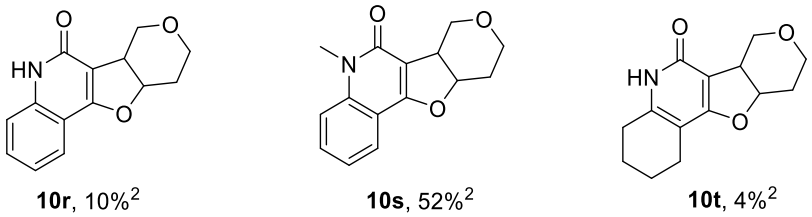

10r, 10%[2]

10s, 52%[2]

10t, 4%[2]

Scheme 11. Synthesis of general scaffold **A** derivatives by Pd-AAC employing various pyridones **2** and DHP **3a**.
1) Yield for the Pd-AAC step.
2) Yield after the heterogenous reduction over two steps.
[a] $Pd(Ph_3)_4$ was used as a catalyst.

Due to steric and electronic incompatibility of C6-substituted DHP **3b**-*trans* and superstable Pd(0) (see 3.4.2.), the catalyst had to be replaced by $Pd(Ph_3)_4$ in the Pd-AAC of DHP **3b**-*trans*

with various pyridones (**2**). The resulting eleven examples of PFP pseudo NPs **12** and **13** were shown to have a *cis*-fused bipodal connection with the newly installed methyl group having relative *trans*-relation to the furo-pyrone ring in example **12a** by means of a 2D-NOESY experiment (Scheme 12, see Supplemental Spectra S3, cross-peaks detected for H12/H10 and H10/H9). Notably, when pyridones **2h** and **2k** were used, cyclic acetal isomers of **12f** and **13g** could be isolated as side products (see also 3.4.2.). In addition, unreduced Pd-AAC products **12** were isolated for examples **12a** and **12d-f**.

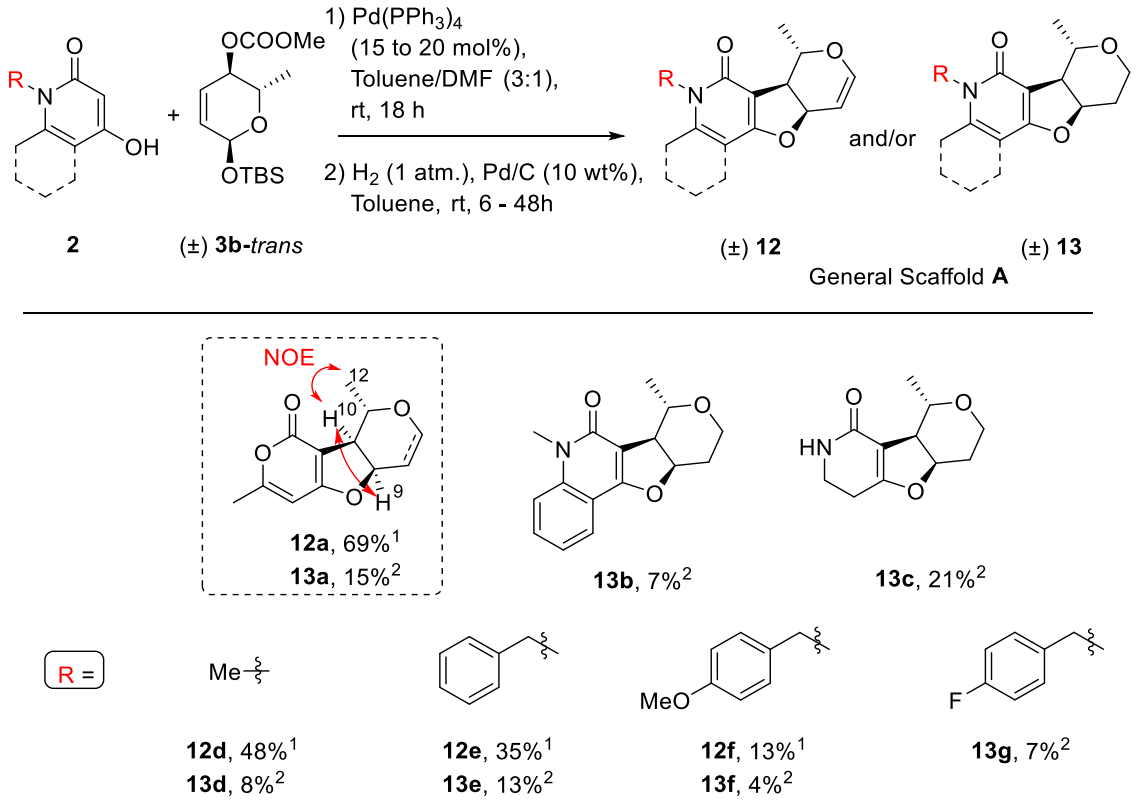

Scheme 12. Synthesis of general scaffold **A** derivatives by Pd-AAC employing various pyridones **2** and DHP **3b**-*trans*.
1) Yield for the Pd-AAC step.
2) Yield after the heterogenous reduction over two steps.

The ring-opened isomers **11** and **14** (Scheme 13) represent a monopodal connection between 2-pyridones and tetrahydropyrans (THPs). Therefore, the side products from heterogenous reductions were also isolated, characterized and used in biological testing. The tendency for the phenolic ether to be cleaved during heterogenous reduction seems to be more pronounced for the C6-methylated DHP derivatives **14**, as in total eight compounds could be isolated compared to three molecules for the C6-unsubstituted DHP derivatives **11** (Scheme 13).

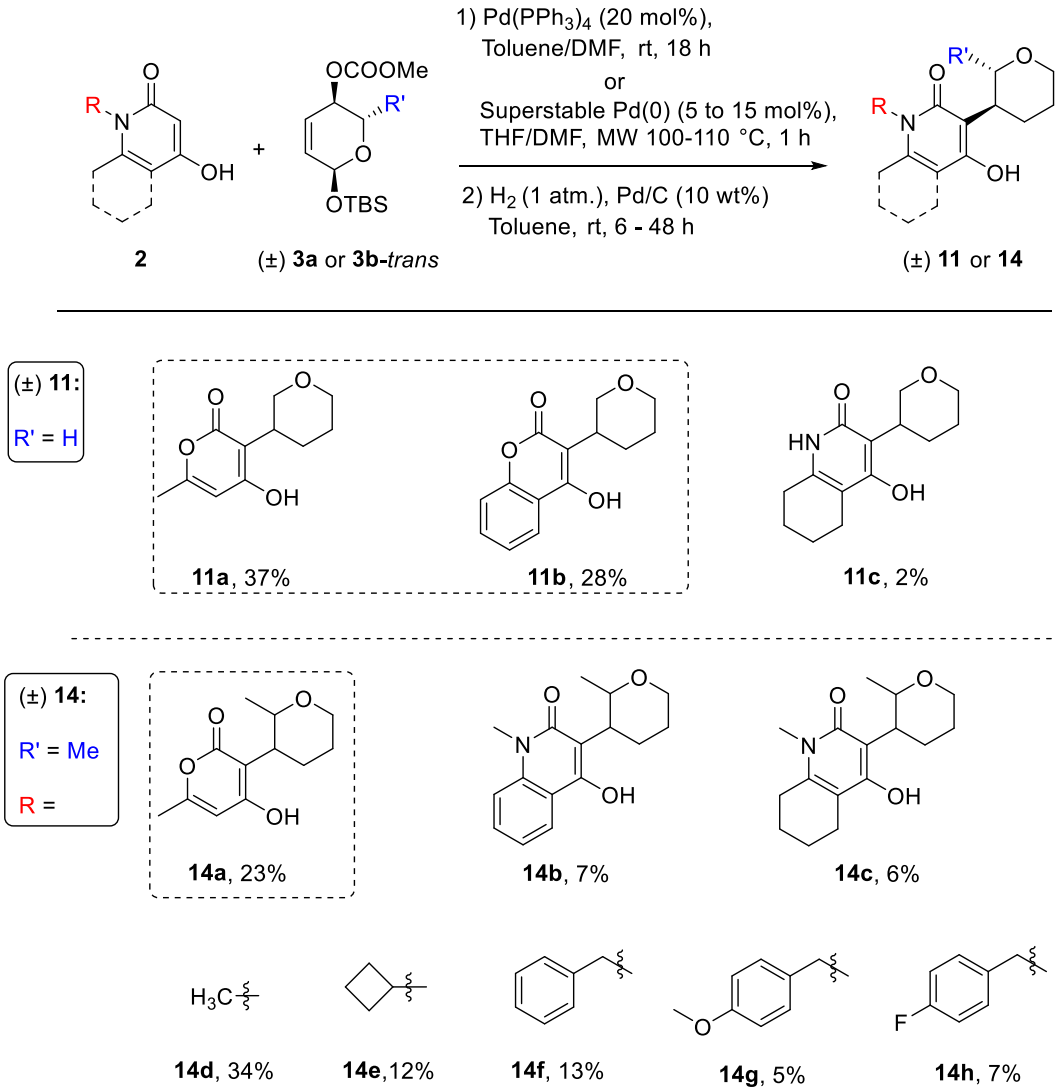

Scheme 13. Isolated monopodal connected side products **11** and **14** after heterogenous reduction of Pd-AAC products. Yields are given over two steps.

3.4.2. Allylic Alkylation Cascade vs. Tsuji-Trost-Transacetalization Cascade

Employing superstable Pd(0) as the catalyst in an attempted Pd-AAC of pyridone **2b** and C6-methylated DHP **3b**-*trans* resulted in a new regioisomeric product **15a** incorporating a cyclic acetal with *cis* relation of the methyl group and the *cis*-fused furo-pyridone residue, as determined by 1D- and 2D-NMR (Scheme 14, see Supplemental Spectra S4, cross-peaks detected for H12/H8).

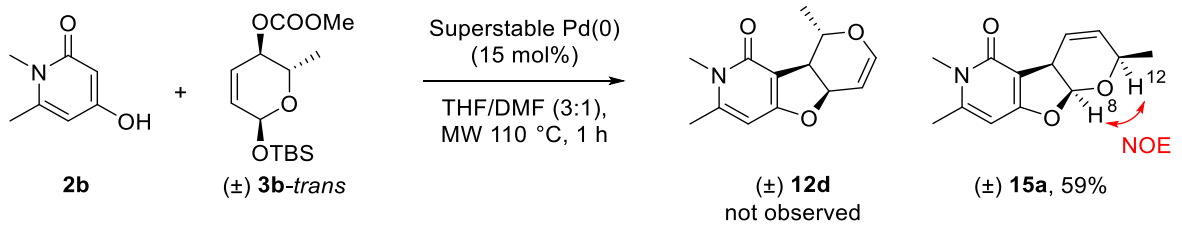

2b (±) **3b**-*trans* (±) **12d** not observed (±) **15a**, 59%

Scheme 14. Synthesis of an unexpected cyclic acetal isomer **15a** from pyridone **2b** and DHP **3b**-*trans* employing superstable Pd(0).

An explanation for the formation of the observed cyclic acetal regio-isomer is proposed in Scheme 15. Initially, a π-allyl palladium complex **M4** is formed from superstable Pd(0) and DHP **3b**-*trans*. Due to steric repulsion between the large tris(3,5-bis(trifluoromethyl)phenyl)phosphine ligands on palladium and the C6 methyl of DHP **3b**-*trans*, combined with the electron withdrawing character of the phosphine ligands, a nucleophilic displacement on the opposite site of the π-allyl palladium complex by another Pd(0) species is facilitated to generate the isomeric π-allyl palladium complex **M5**. Such displacements have been observed and discussed in the literature before.[57] In the formed **M5** isomer, steric repulsion between the phosphine ligands and the OTBS group is very likely and therefore a fast equilibrium between both π-allyl palladium complexes **M4** and **M5** is suggested. However, attack of the soft nucleophilic[58] pyridone **2** at the C3 position of **M5** anti to palladium and OTBS, is less sterically demanding than attack anti to palladium and next to methyl at C5. Therefore, the C3-allylated pyridone intermediate **M6** is formed, and an irreversible 5-*exo*-*trig* oxa-acetalization yields the final Tsuji-Trost transacetalization cascade product **15**.

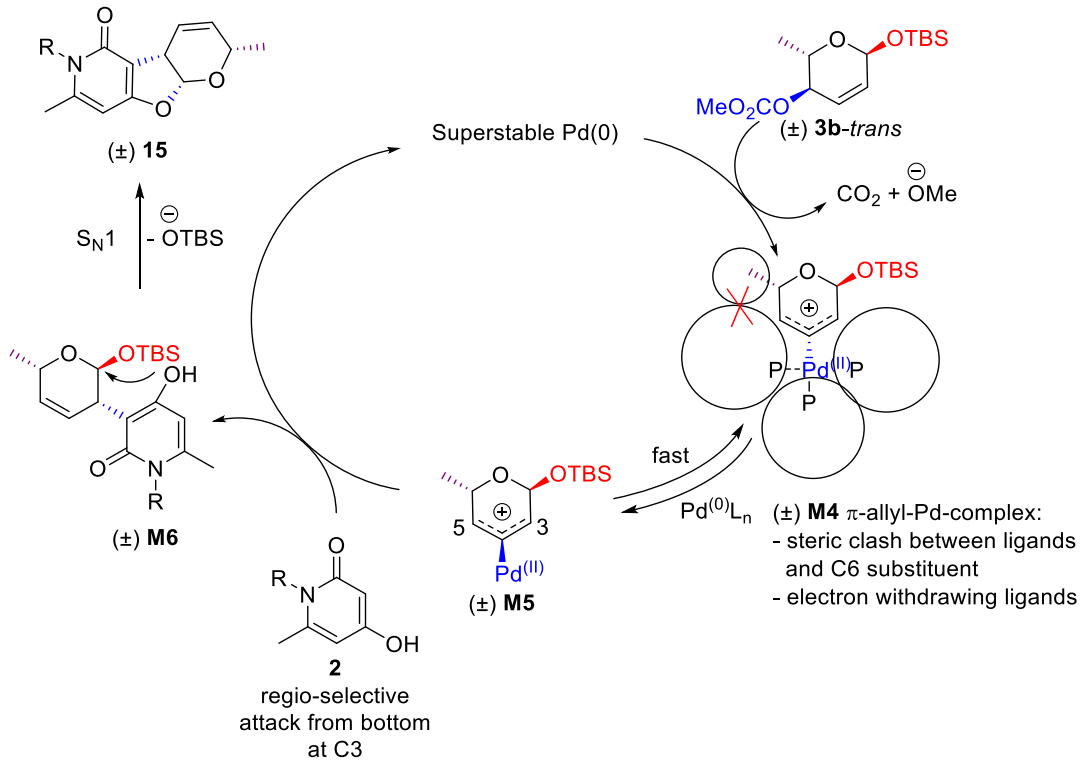

Scheme 15. Proposed mechanism for the formation of cyclic acetal isomer **15** by a Tsuji-Trost transacetalization cascade.

This unexpected reactivity was exploited to generate eight examples of regio-isomeric cyclic acetals **15** and five examples of subsequently reduced derivatives **16** (Scheme 16). The core scaffold of this substance class resembles general scaffold **C** in which the methylene-carbonyl moiety is replaced by a C-C double bond. Pyridone *N*-substituents ranged from hydrogen, methyl, cyclobutyl to various substituted benzyl groups. Additionally, one tetracyclic example **15h** could be isolated in very low yield as well.

Notably, for ortho-chloro-benzyl pyridone **2i** and thiophenyl substituted pyridone **2l** mixtures of Pd-AAC products and Tsuji-Trost transacetalization products were formed (Scheme 16, **12i** + **15i**; **12j** + **15j**) which were separated by preparative HPLC. Furthermore, pyridones containing hetero-atoms in the *N*-substituents with distinct distance to the pyridone ring gave only Pd-AAC products (Scheme 16, **12k-m**) in low yields. Hence, the nature of the pyridone nucleophile has also an impact on the suggested mechanism for the formation of Tsuji-Trost transacetalization products which requires additional investigation.

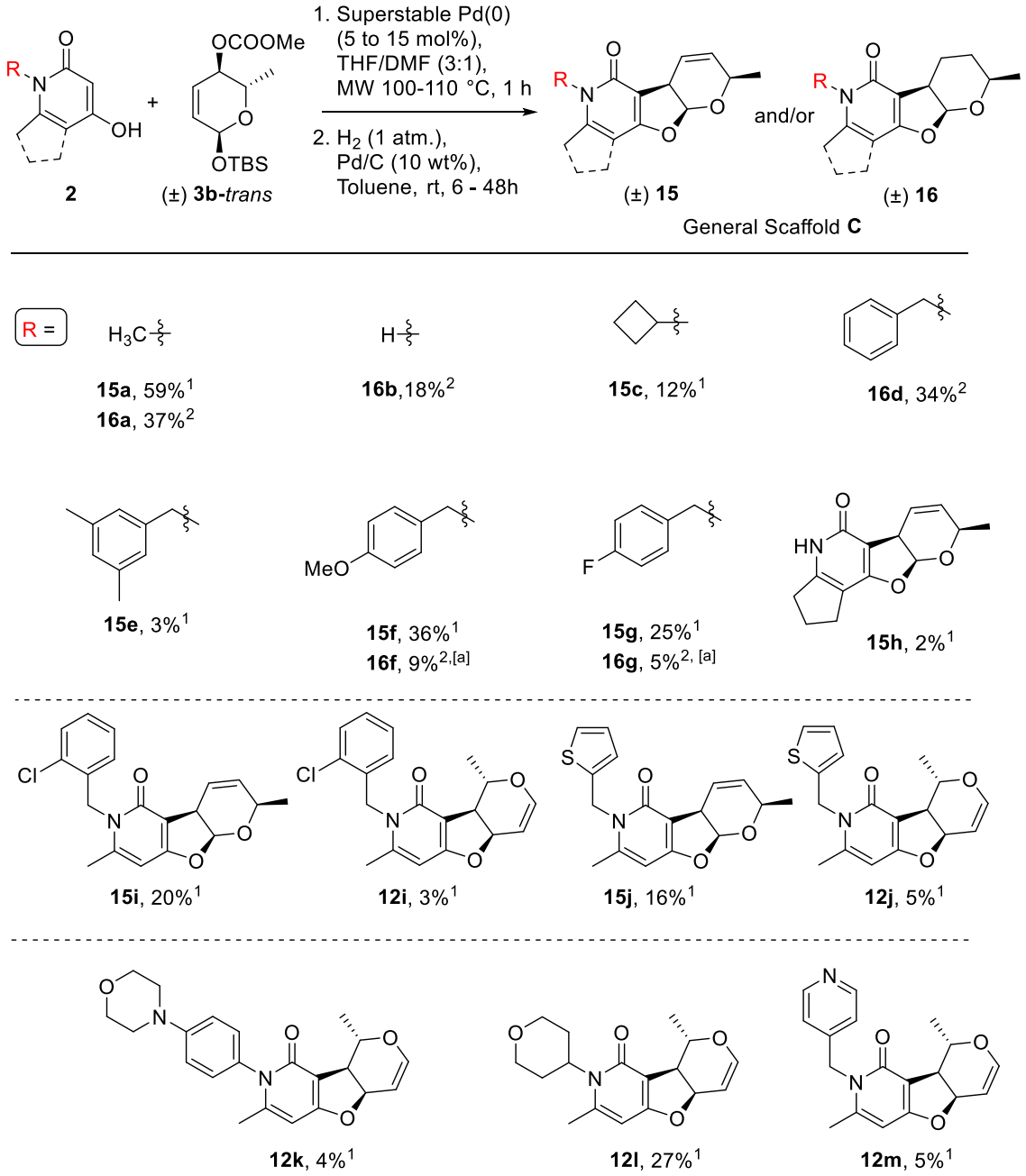

Scheme 16. Synthesis of PFP cyclic acetal isomers **15** and **16** through a superstable Pd(0) catalyzed Tsuji-Trost transacetalization cascade.
1) Yield for the Tsuji-Trost transacetalization cascade step.
2) Yield after the heterogenous reduction over two steps.
[a] $Pd(Ph_3)_4$ was used as a catalyst.

To further evaluate the effects influencing the outcome of palladium catalyzed fusion of DHP **3b**-*trans* with bis-nucleophilic pyridones **2** the reaction between DHP **3b**-*trans* and pyridone **2k** was investigated in more detail. Employing superstable Pd(0) as a catalyst, formation of a Tsuji-Trost transacetalization product was observed (Table 5, entry 2). In contrast, employing $Pd(Ph_3)_4$ resulted in the formation of a mixture of Pd-AAC and Tsuji-Trost transacetalization

product (entry 1). Hence, bidentate catalysts were screened for the selective formation of the Pd-AAC product as it was hypothesized that these could stabilize the initially formed π-allyl palladium complex. With bis[1,2-bis(diphenylphosphino)ethane]palladium(0) ($Pd(dppe)_2$) as the catalyst only starting material was recovered (entry 3). Nevertheless, employing 2.5 mol% allylpalladium(II) chloride dimer ($[PdCl(allyl)]_2$) and 7.5 mol% Xantphos in the presence of triethylamine afforded the desired Pd-AAC product **12d** in 61% yield as the sole product (entry 4).

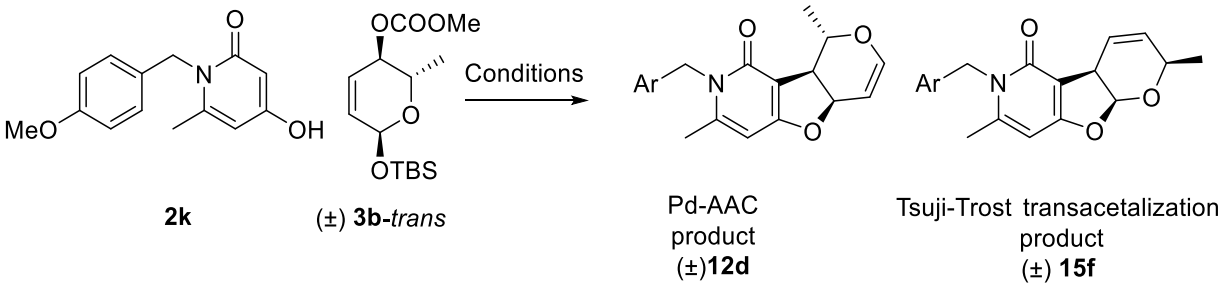

2k (±) **3b**-*trans*

Entry	Solvent	Catalyst	Additive	Time / Temp.	Yield 12d:15f
1	Toluene/DMF (3:1)	$Pd(PPh_3)_4$ (15 mol%)	/	24 h, rt	13% : 14%
2	THF/DMF (3:1)	Superstable Pd(0) (5 mol%)	/	1 h, 100 °C MW	0% : 36%
3	THF/DMF (3:1)	$Pd(dppe)_2$ (5 mol%)	NEt_3 (2 eq.)	24 h, rt	starting material
4	THF/DMF (3:1)	$[PdCl(allyl)]_2$ (2.5 mol%) Xantphos (7.5 mol%)	NEt_3 (2 eq.)	24 h, rt	61% : 0%

Table 5. Screening of catalysts and conditions for the selective synthesis of Pd-AAC product **12d**.

It is hypothesized that Xanthphos-Pd(0) steers the reaction selectively towards a Pd-AAC[50] because of its ability to stabilize the first π-allyl palladium complex **M7** and suppress a nucleophilic displacement by another Pd(0) species (Scheme 17). Regioselective attack of the soft pyridone nucleophile **2** from top[58] at C5 of **M7** (opposite to palladium) is then sterically and electronically[59] favored, leading to the formation of an allyl-pyridone intermediate **M1** which can undergo a second Tsuji-Trost reaction in a 5-*exo*-*trig* cyclization to give **12**. Noteworthy, attempted Pd-AAC with DHP **3b**-*cis* and C6-dimethylated DHP **3c** failed to give any product probably due to steric hindrance at C5 (neighbouring methyl-group) and C3 (neighbouring OTBS-group) in the respective first π-allyl palladium complexes.

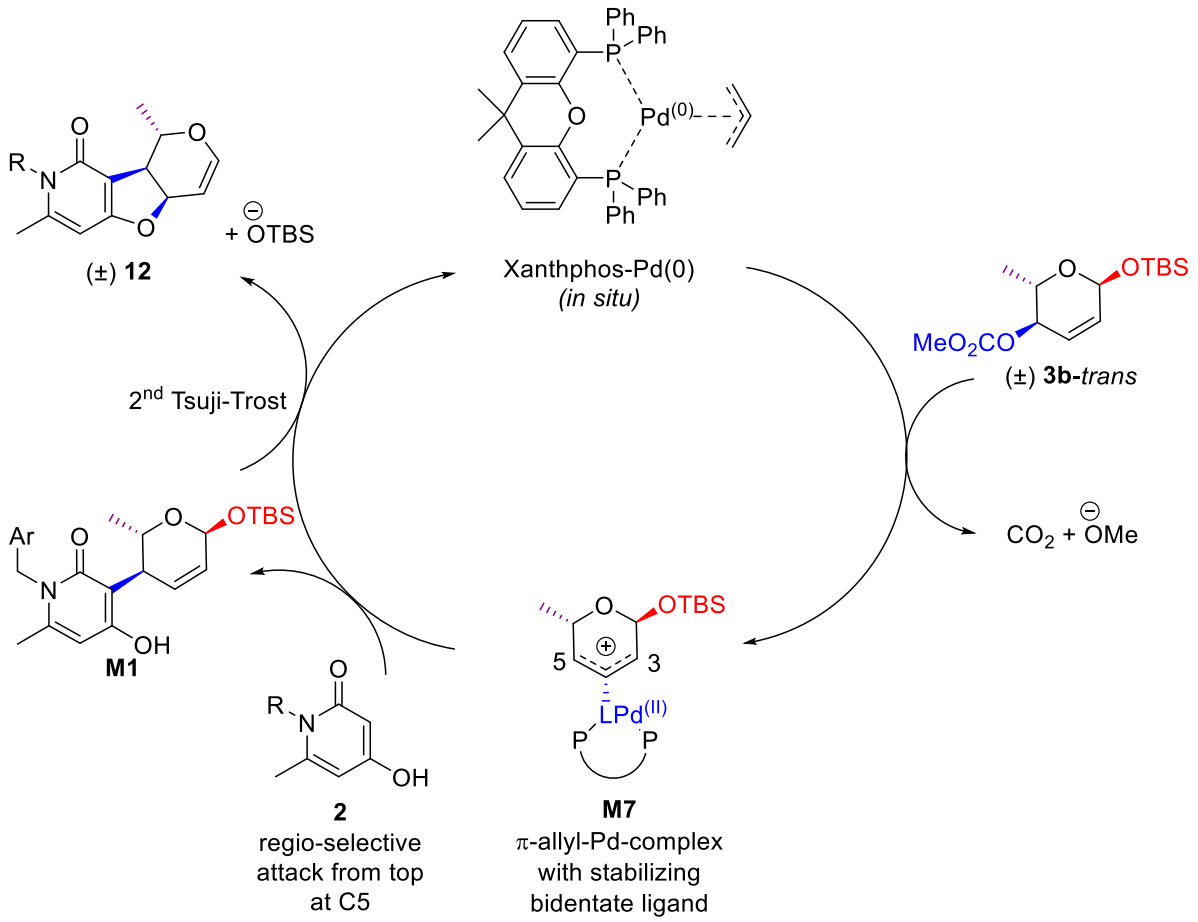

Scheme 17. Proposed mechanism for the Pd-AAC with DHP **3b**-*trans* and 2-pyridones **2** employing Xanthos-Pd(0).

3.4.3. Derivatization of Isomers A

The inherent reactivity of the glycal double bond in isomer **A** was exploited as a chemical handle to further explore the area of chemical space occupied by the new pseudo NP class and the influence of substituents on the stability. For instance, compound **9a** was treated with *N*-bromosuccinimide (NBS) and silver nitrate ($AgNO_3$) to brominate the glycal double bond regioselectively at C3.[60] Subsequent Suzuki-Miyaura coupling with aryl-boronic acids gave the C3 arylated analouges **17b-d** (Scheme 18). Reaction of **9a** with *tert*-butyl acrylate in a mild palladium-catalyzed oxidative cross coupling[61] yielded exclusively the *E*-isomer of **17e** (Scheme 18).

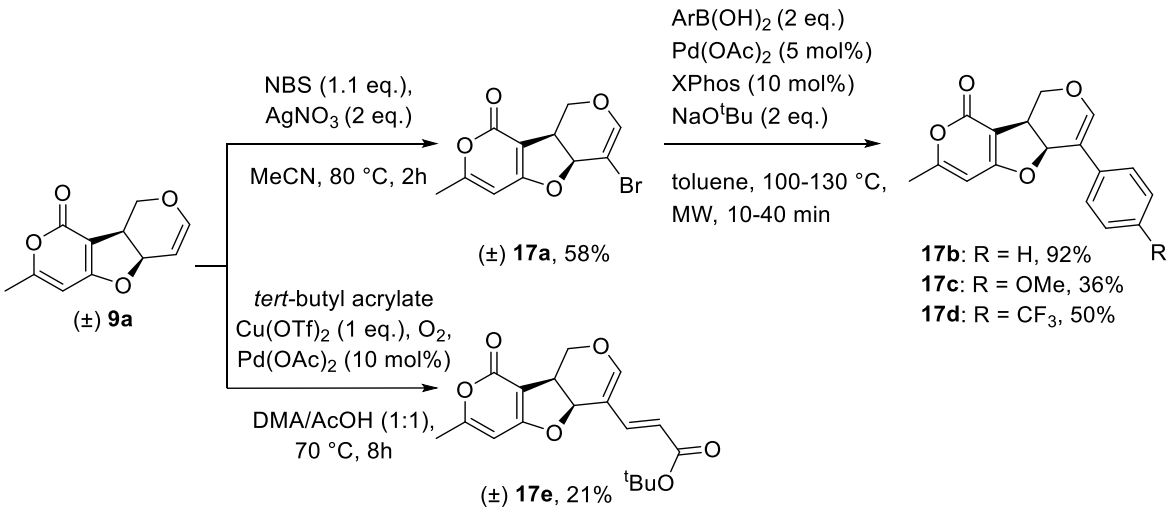

Scheme 18. Functionalization of **9a** at C3 of the glycal moiety.

Alternatively, compound **9c** and **9k** were subjected to a Pd(II) catalyzed Heck-type *C*-glycosidation with various arylboronic acids (Scheme 19).[62-63] Notably, an isomerization of the glycal double bond into the dihydrofuran system was observed. This double bond could selectively be reduced with $Pd(OH)_2$ as exemplified for **18a** to give product **18h**.

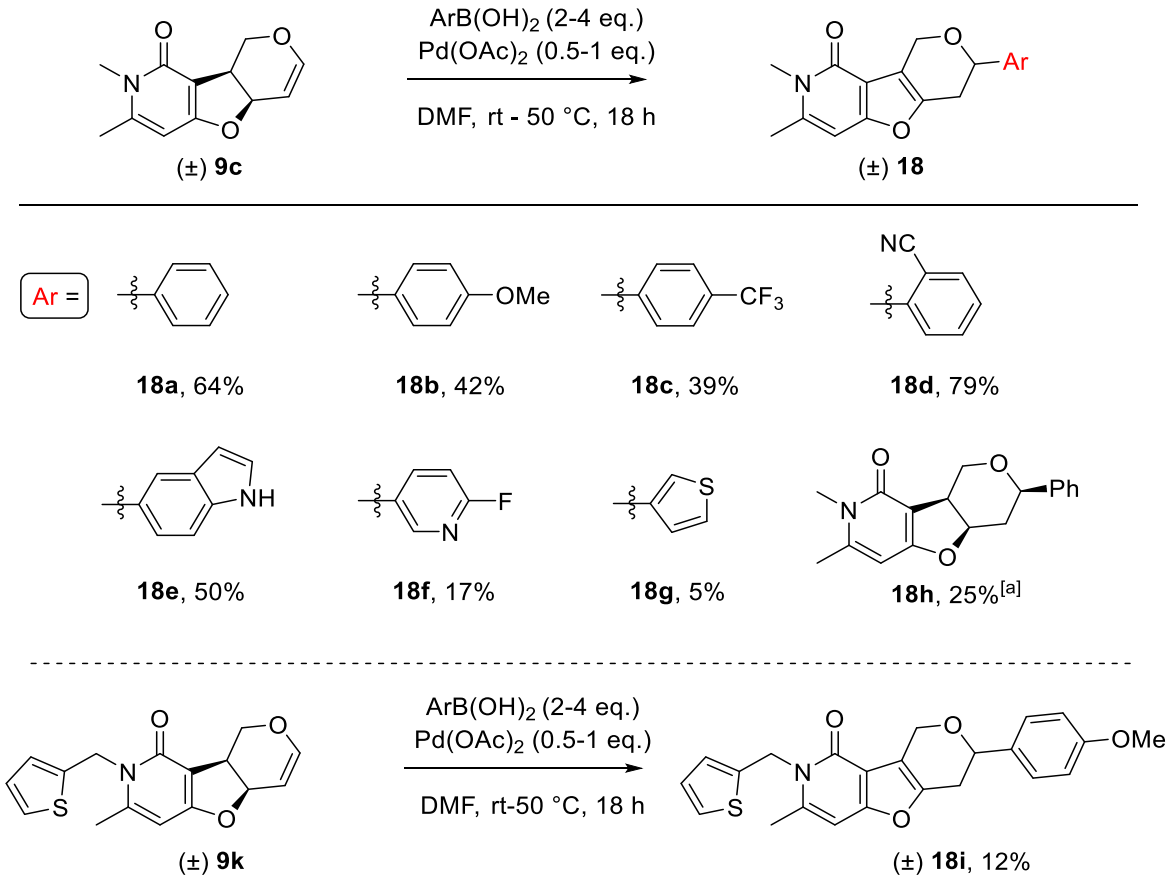

Scheme 19. Pd(II) catalyzed Heck-type *C*-glycosidation of **9c** and **9k** with arylboronic acids.
[a] Product after heterogenous reduction with 10 wt% $Pd(OH)_2$.

For this reaction a proposed mechanism is shown in Scheme 20. In the initial step, a transmetalation between $Pd(OAc)_2$ and the arylboronic acid occurs to generate an aryl-Pd^{II}-OAc species. This undergoes a *syn*-insertion (carbopalladation) into the glycal double bond to give the σ-complex I **M8** from which a subsequent β-hydride elimination occurs to afford vinyl ether **M9**. A β-heteroatom elimination side reaction as described by Ramnauth *et al.*[63] was not observed under these conditions. **M9** is likely to coordinate to a H-Pd^{II}-OAc species and then undergo a 1,2 migratory insertion to form the second σ-complex II **M11**. Finally, a second β-hydride elimination yields the observed *C*-glycosidation product **18** with the double bond isomerized into the furan ring system. It is proposed that the last step is the driving force of the reaction as it leads to aromatization of the dihydrofuran to a furan moiety. The liberated H-Pd^{II}-OAc species is likely to undergo reductive elimination to form acetic acid and uncoordinated Pd(0), thereby aborting a catalytic cycle. Furthermore, the necessity of a high palladium loading of 0.5 to 1 equivalent indicated rather a stochiometric consumption of palladium acetate than a catalytic activity.

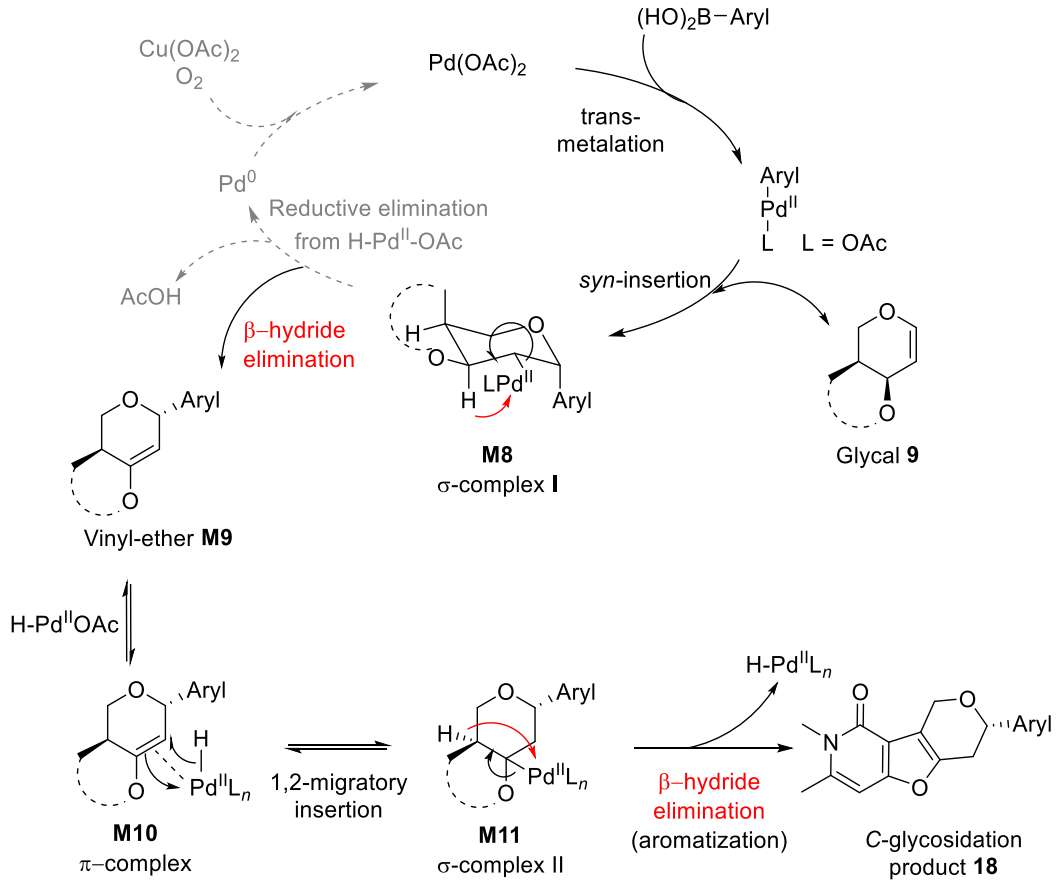

Scheme 20. Proposed mechanism for the Pd(II) catalyzed Heck-type *C*-glycosidation of glycal PFPs and isomerization of the double bond.

To prove this hypothesis and close the catalytic cycle, the *C*-glycosidation of **9c** and phenylboronic acid was performed under oxidative conditions employing an excess of $Cu(OAc)_2$ and oxygen as reported by Xiong *et al.* (Scheme 21).[62] This allowed a reduction of the palladium acetate loading to 10 mol%, since under oxidative conditions and in the presence of $Cu(OAc)_2$ the $Pd^{II}(OAc)_2$ is regenerated from Pd(0) and thereby the catalytic cycle is closed (Scheme 20, indicated in grey).

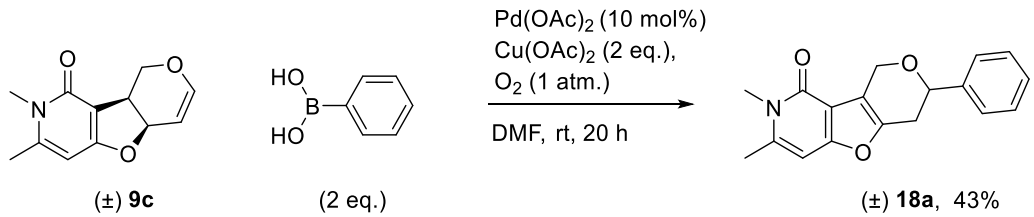

Scheme 21. Pd(II) catalyzed *C*-glycosidation of glycal PFPs under oxidative conditions.

Another functionalization of isomer **A** transforming the tricyclic 6-5-6 to a 6-5-5 ring arrangement was reported by Bartlett *et al.* for the corresponding pyrones.[50] First a hydrobromination of the glycal double bond was carried out followed by a reductive ring contraction initiated by sodium borohydride reduction of the acetal carbon for a total of seven examples (Scheme 22). The scope included literature known pyrone example **20a**, *N*-methylated and variously *N*-arylated pyridones (**20b-f**) and one tetracyclic example **20g**. The resulting primary alcohol methylene moiety was determined to be *trans* to the *cis*-fused furo-pyridone residue by means of 2D-NOESY (Scheme 22, see Supplemental Spectra S5, cross-peaks detected for H12/H8).

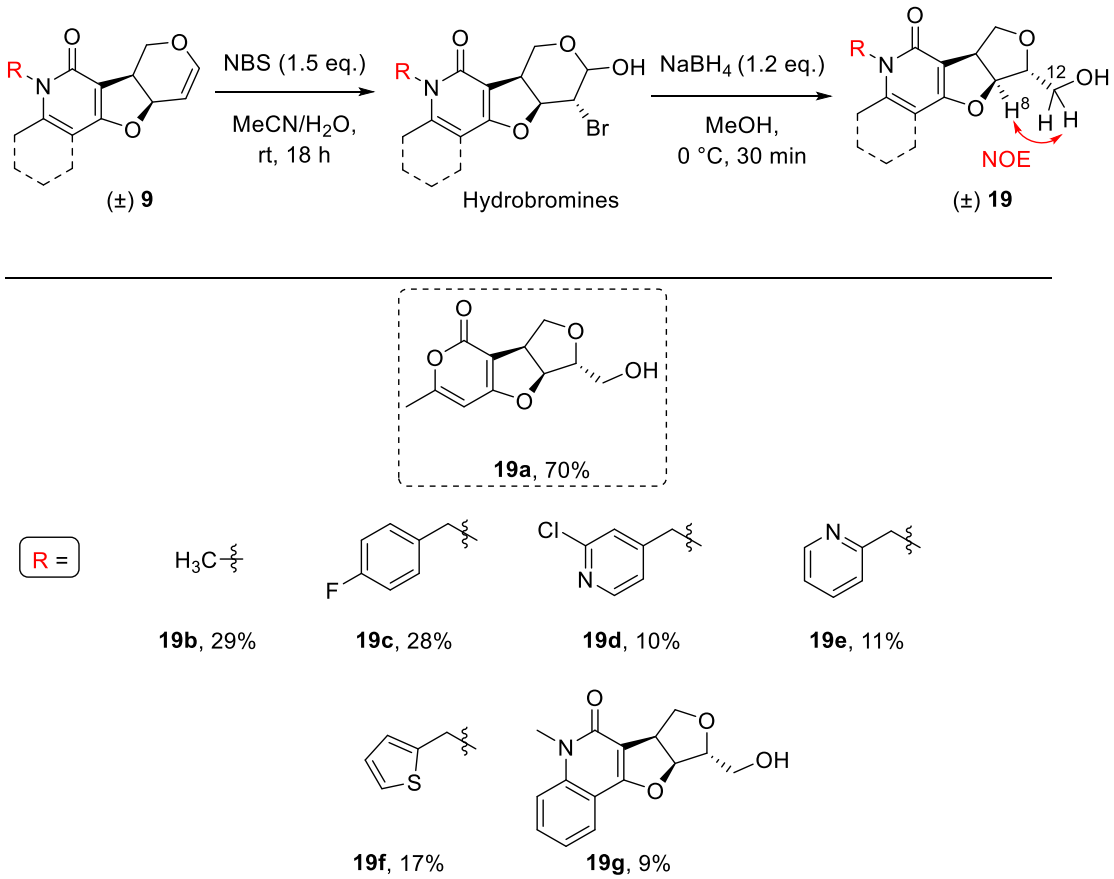

Scheme 22. Synthesis of 6-5-5 ring arrangement isomers of general scaffold **A**. Yields are given over two steps.

3.4.4. Synthesis of General Scaffold B Isomers

The synthesis of isomers of general scaffold **B** was carried out by a Tsuji-Trost oxa-Michael cascade reaction of pyridones **2** and DHPs **4**. Mechanistically, this reaction was proposed to proceed through an initial oxidative addition of palladium to the allylic acetate moiety of **4** to generate the π-allyl-Pd-complex **M12.** Subsequent S_N2-like substitution at C2 of **M12** with a soft 1,3-dicarbonyl nucleophile[58] **2** and a final 5-*exo*-*trig* oxa-Michael cyclization of intermediate **M2** affords the Tsuji-Trost oxa-Michael products **20**-**24** (Scheme 23).[51]

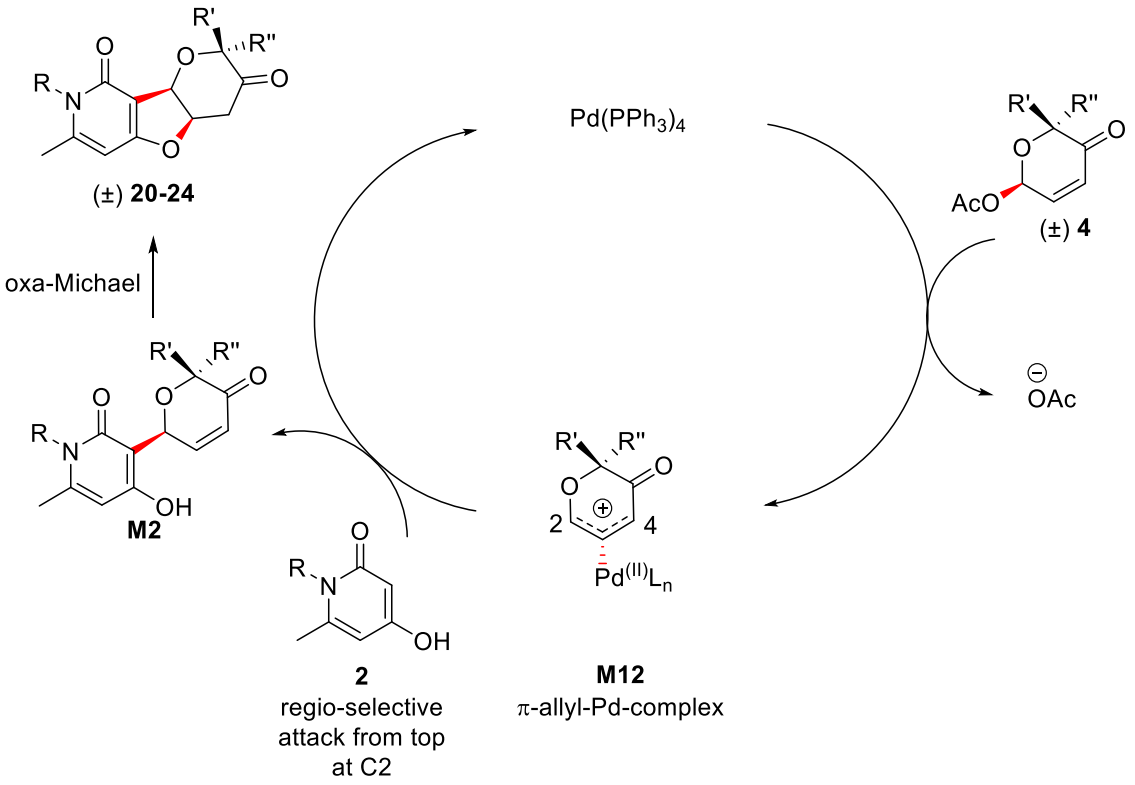

Scheme 23. Proposed mechanism for the formation of Tsuji-Trost oxa-Michael cascade products **20**-**24**.

According to a literature procedure[51] for pyrones as bis-nucleophiles (Scheme 24, example **22k**), the synthesis of PFP isomers **B** was achieved in a Tsuji-Trost oxa-Michael cascade for a total of 27 examples by reaction of various 4-hydroxy-2-pyridones (**2**) with acetylated DHPs **4a-c** at room temperature and under palladium catalysis in a THF/DMF 3:1 mixture and one equivalent of triethyl amine as an additive (Scheme 24). All three DHP substrates **4a-c** could be fused with pyridones carrying various *N*-substituents and functional groups demonstrating the high robustness of this cascade reaction. For instance, methoxy and halogen substituents in various positions on benzyl- or heteroaryl-substituents could be installed. On average, employing DHP **4a** in the Tsuji-Trost oxa-Michael cascade with various pyridones resulted in higher yields compared to its C6-substituted derivates **4b** and **4c**.

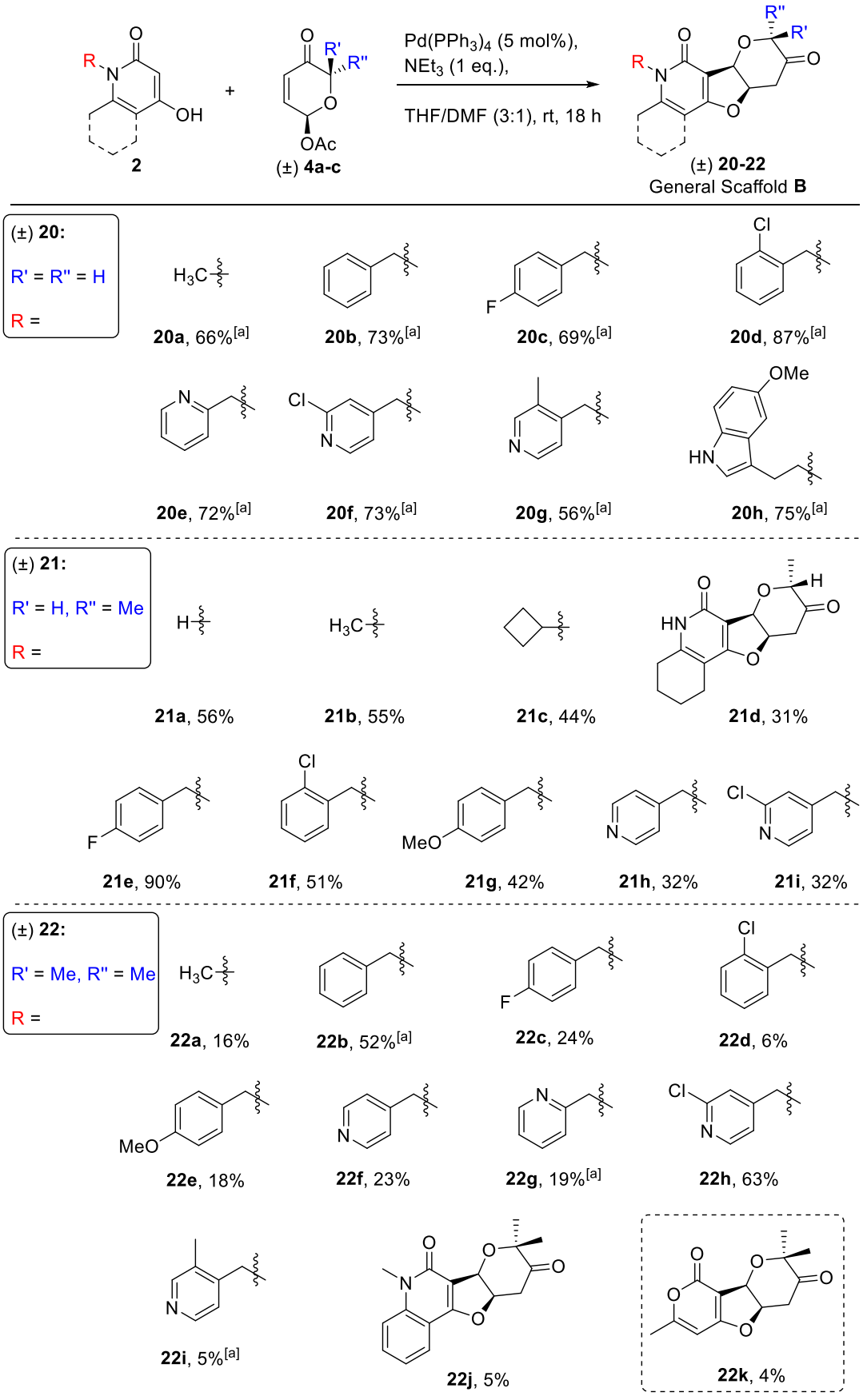

Scheme 24. Synthesis of derivatives of general scaffold **B** by Tsuji-Trost oxa-Michael cascade employing various pyridones **2** and DHPs **4a-c**.
[a] Allyl-Pd(II)-chloride dimer + Xanthphos was used as a catalyst.

Employing DHP **4d** in the Tsuji-Trost oxa-Michael cascade, a total of ten tetra- and penta-cyclic examples for spiro-*N*-Boc-piperidine PFPs could be synthesized (Scheme 25). For the selective removal of the Boc protecting group, the pseudo NPs were treated with a mixture of trimethylsilyl trifluoromethanesulfonate (TMSOTf) and 2,6-lutidine in DCM to avoid a ring-opening side reaction.[64] In general, the deprotected secondary amines were purified by preparative HPLC applying acetonitrile/water mixtures with 0.1% trifluoroacetic acid (TFA) as an additive and therefore the products were isolated as the corresponding TFA salts.

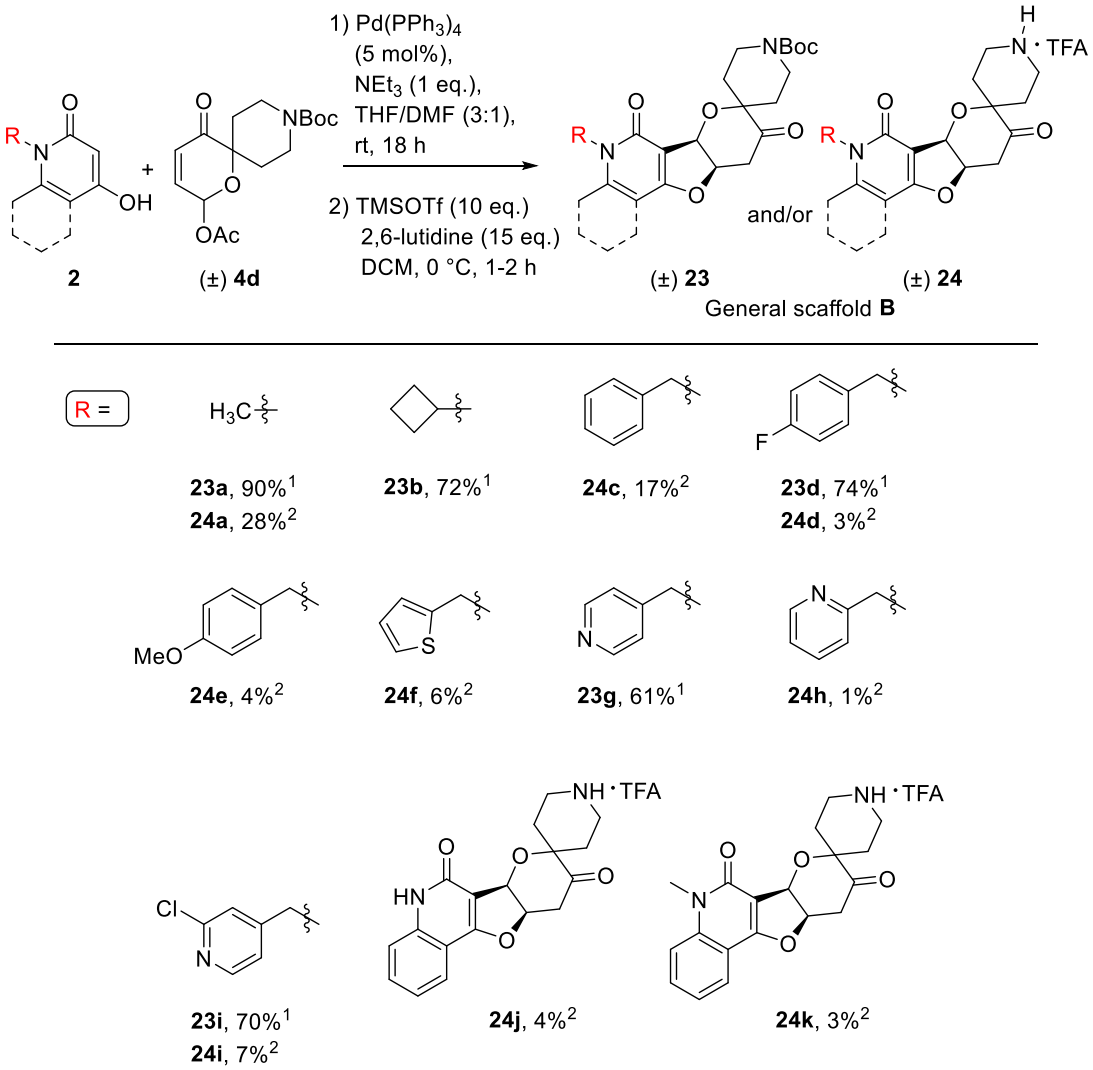

Scheme 25. Synthesis of Tsuji-Trost oxa-Michael cascade products employing various pyridones **2** and DHP **4d**.
1) Yield for the Tsuji-Trost oxa-Michael cascade step.
2) Yield after the Boc-deprotection over two steps.

When using HCl for removal of the Boc-group, a side reaction occured in which the phenolic ether is cleaved and a new glycal moiety is installed in the pyranone substructure. As the resulting connection-type represents a monopodal link between the pyridone and the DHP

fragments, ten ring-opened products were also isolated, characterized and used in biological testing (Scheme 26).

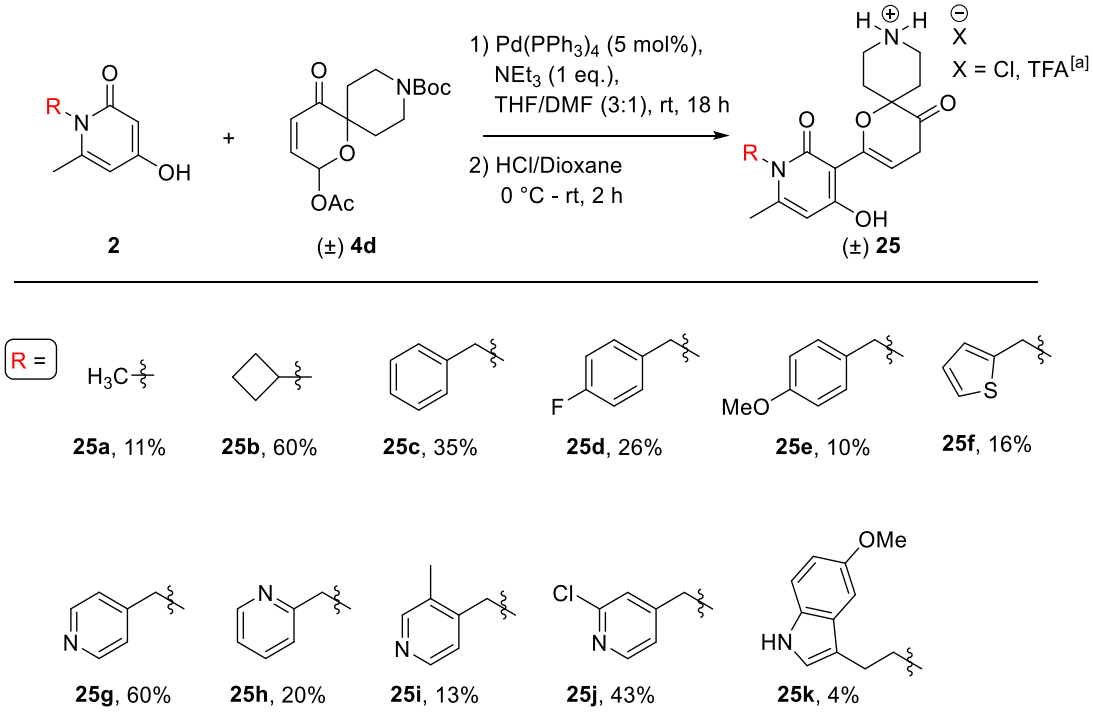

Scheme 26. Isolated monopodal connected side products after treatment with HCl of Tsuji-Trost oxa-Michael products. Yields are given over two steps.
[a] Products were isolated as TFA salts when purified by prep. HPLC.

3.4.5. Synthesis of General Scaffold C Isomers

A Michael-transacetalization cascade reaction between pyridones **2** and DHPs **4** was employed to synthesize isomers of general scaffold **C**. The mechanism is suggested to commence with an initial diastereoselective Michael addition of **2** opposite to the acetoxy group of **4**, followed by a 5-*exo*-*tet* intramolecular S_N2-like transacetalization of **M3** to afford the final cascade products **26-30**. According to the literature, quinine was speculated to mediate both steps in a dual activation mode through double hydrogen bonding interactions with the tertiary amine abstracting a proton from the phenolic nucleophile of **M3** and with the secondary alcohol activating the Michael acceptor in **4** as well as the acetate leaving group of **M3**, respectively (Scheme 27).[51] Noteworthy, although quinine is chiral, asymmetric induction was not reported by the inventors of this cascade reaction.[51]

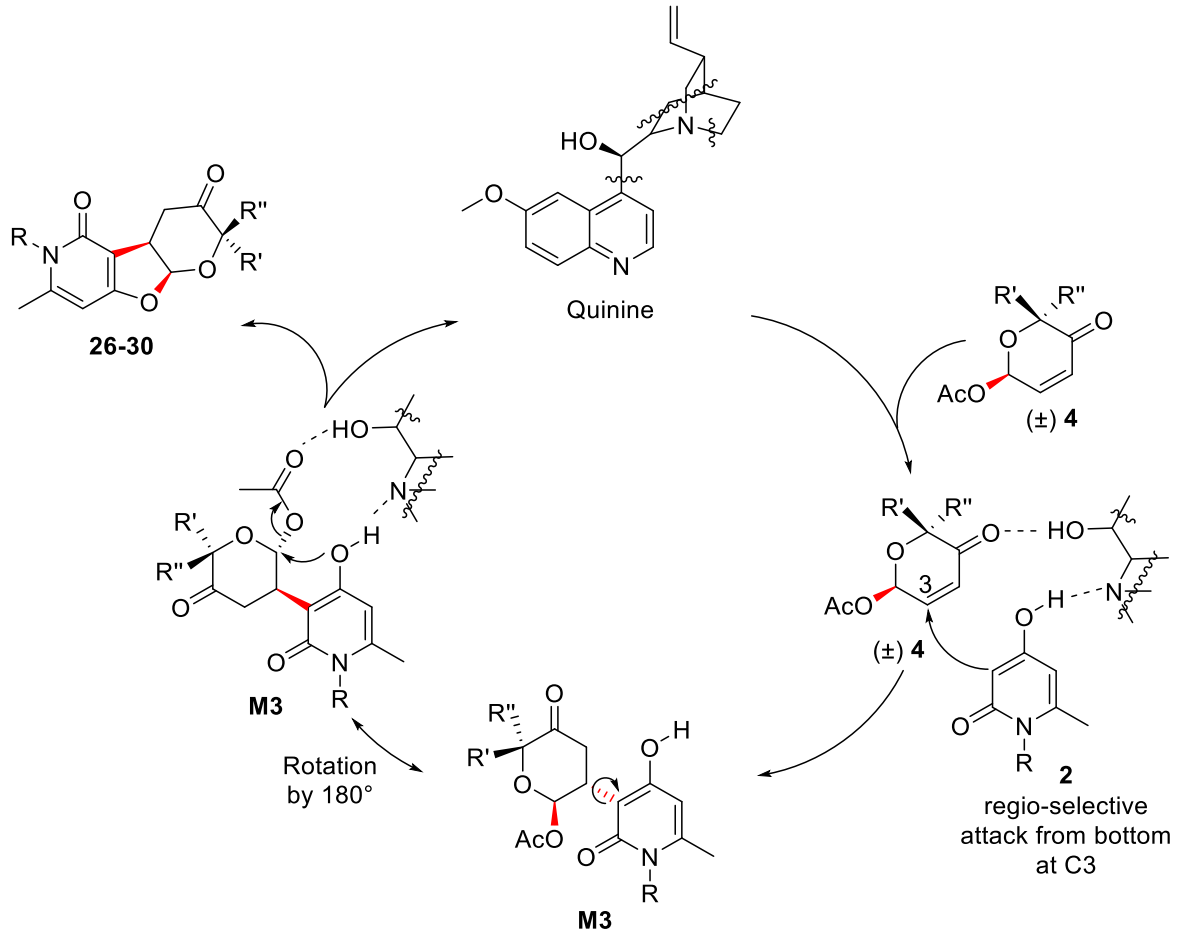

Scheme 27. Proposed mechanism for the formation of Michael transacetalization cascade products **26**-**30**.

According to the literature protocol[51] for pyrones as bis-nucleophiles, the synthesis of PFP isomers **C** was achieved in a Michael transacetalization cascade for a total of twelve examples by reaction of various pyridones **2** with acetylated DHPs **4a**, **4b** and **4c** at 60 °C in the presence of stoichiometric amounts of quinine (Scheme 28). This allowed the installation of methyl, benzyl and substituted benzyl *N*-substituents on the pyridone subunit when employing DHP **4a** and **4c**. C6-monosubstituted DHP **4b** was employed in only one example because the tertiary amine of quinine can act as an organic base. Under reflux conditions this might lead to base-catalyzed epimerization of the α-carbon next to the acetal in the dihydropyranone moiety of the ring fused products which was observed for **27a** and reported by Yu *et al.* for other examples.[51] Hence, the use of C6-monosubstituted DHP **4b** was avoided in further reactions of this kind. Additionally, one pyrone derivative **26e** was synthesized from **1a** and DHP **4a**.

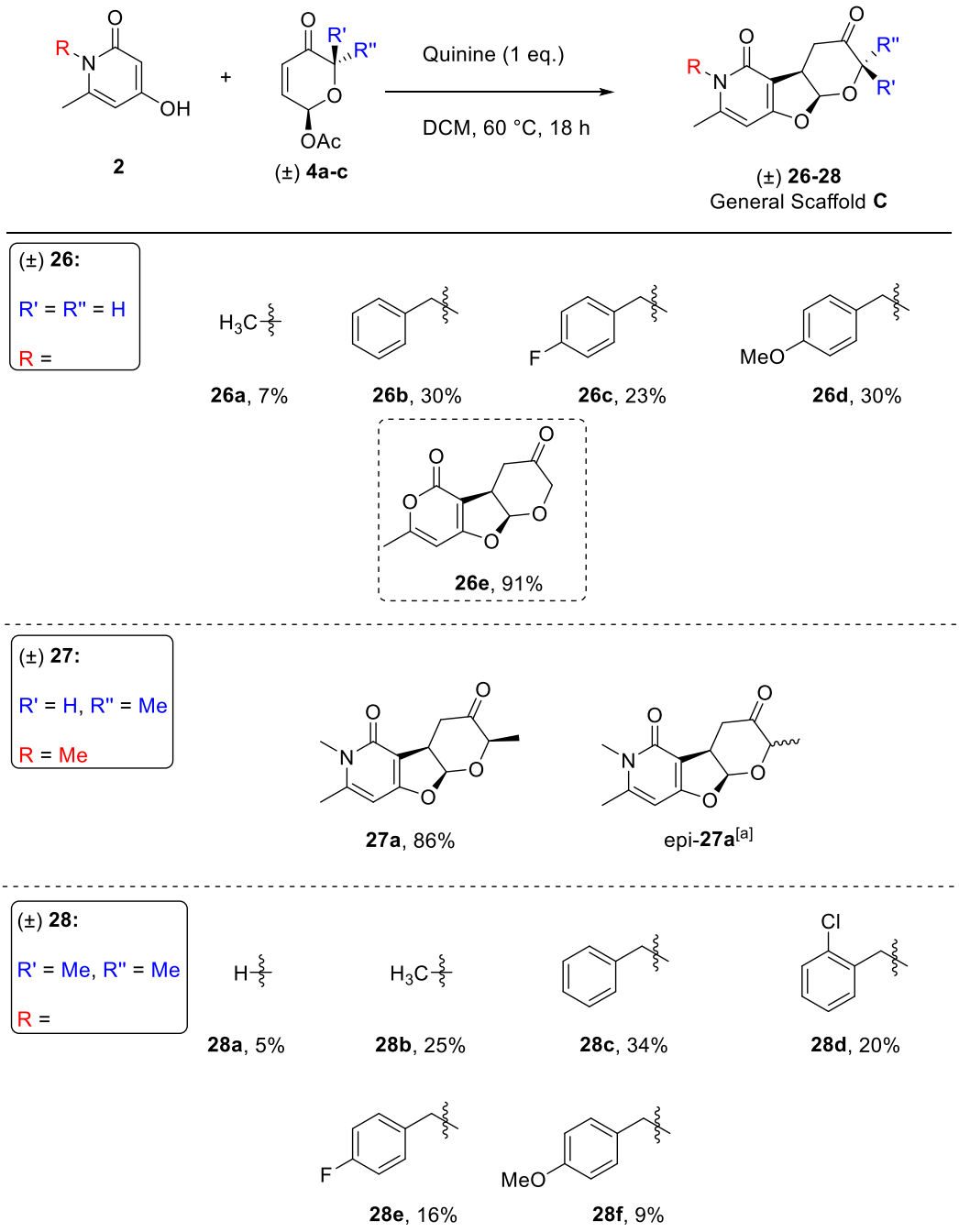

Scheme 28. Synthesis of derivatives of general scaffold **C** by Michael-transacetalization cascade employing various pyridones **2** and DHPs **4a-c**.
[a] Observed by NMR.

Employing the *N*-Boc protected spiro-piperidine DHP **4d**, the fused tetra- and penta-cyclic pseudo NPs of general structure **C** were treated with TFA or HCl to remove the Boc protecting group as demonstrated for 15 examples (Scheme 29). For these regioisomers, no acid-mediated ring-opening was observed. The resulting free amines could be easily isolated through basic aqueous work-up and the majority of products did not require any further chromatographic purification.

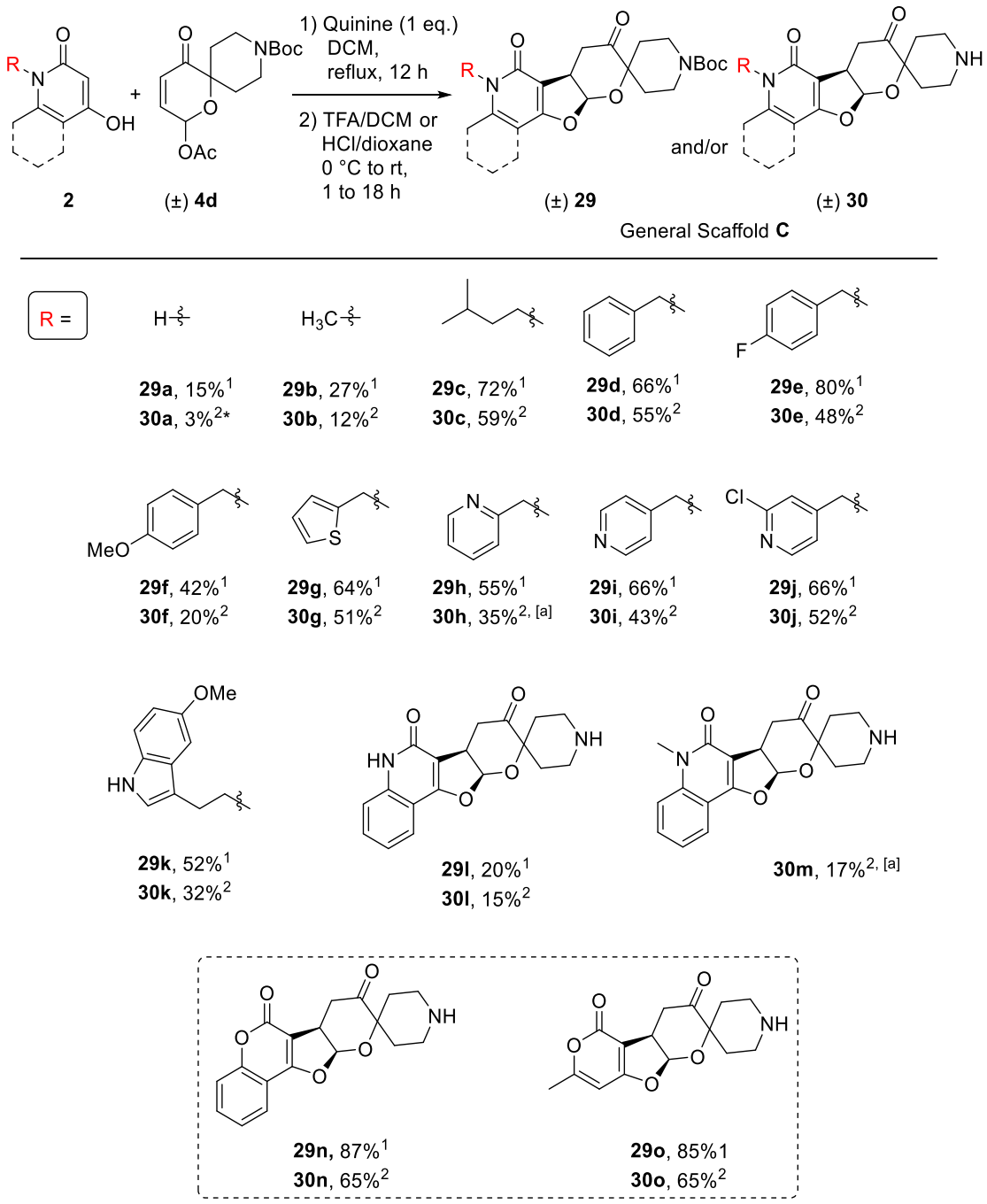

Scheme 29. Synthesis of Michael-transacetalization cascade products employing various pyridones **2** and DHP **4d**.
1) Yield for the Michael-transacetalization cascade step.
2) Yield after the Boc-deprotection over two steps.
[a] Isolated as TFA-salt after purification with prep. HPLC.

3.4.6. Summary of the PFP Synthesis

The synthesis of the PFP pseudo NP library commenced with 4-hydroxy-6-methyl-2-pyridones (**2**), which were obtained from 4-hydroxy-6-methyl-2-pyrone (**1a**) by treatment with various primary amines[65]. Furyl alcohols were subjected to an Achmatowicz rearrangement[53] to establish the six-membered 3,6-dihydro-2*H*-pyran core scaffolds of functionalized DHPs **3** and

4. Bis-functionalized DHP substrates **3** were derived from subsequent protection of anomeric alcohols with TBSCl, diastereoselective substrate-controlled Luche-reduction of the keto group and protection of the resulting secondary alcohols as carbonates. Alternatively, O-acetylation at the anomeric oxygen of Achmatowicz rearrangement products without reduction of the remaining ketone afforded mono-functionalized DHPs **4**.

As summarized in Scheme 30, a palladium-catalyzed allylic alkylation cascade (Pd-AAC) was employed fusing bis-electrophilic difunctionalized DHPs **3a** and **3b** with bis-nucleophilic 4-hydroxy-2-pyridones **2** to obtain PFPs **9** and **12** with general scaffold **A**. Due to a Ferrier-like rearrangement of the glycal moiety instability for some examples of Pd-AAC products was observed. The instability was suppressed by heterogenous reduction of the glycal double bond (Scheme 30, **10** and **13**) for which ring-opened monopodal side products were observed (Scheme 30, **11** and **14**). In addition, direct Heck-type coupling with *tert*-butyl acrylate or regioselective bromination of the glycal double-bond at C3 and subsequent Suzuki-Miyaura coupling with phenylboronic acids was performed (Scheme 30, **17**). Alternatively, direct Pd(II) catalyzed *C*-glycosidation of Pd-AAC products with aryl boronic acids and subsequent isomerization of the pyran double bond into the dihydrofuran ring yielded compounds **18**. In addition, hydrobromination of the glycal moiety and subsequent reductive ring contraction transformed the 6-5-6 ring arrangement into a 6-5-5 system (Scheme 30, **19**). An unprecedented Tsuji-Trost transacetalization cascade was observed employing C6-methylated DHP **3b** as a bis-electrophile when superstable Pd(0) was used as a catalyst. The formed cyclic acetals **15** with general scaffold **C** could be further reduced to increase the sp^3-fraction in the molecules (Scheme 30, **16**).

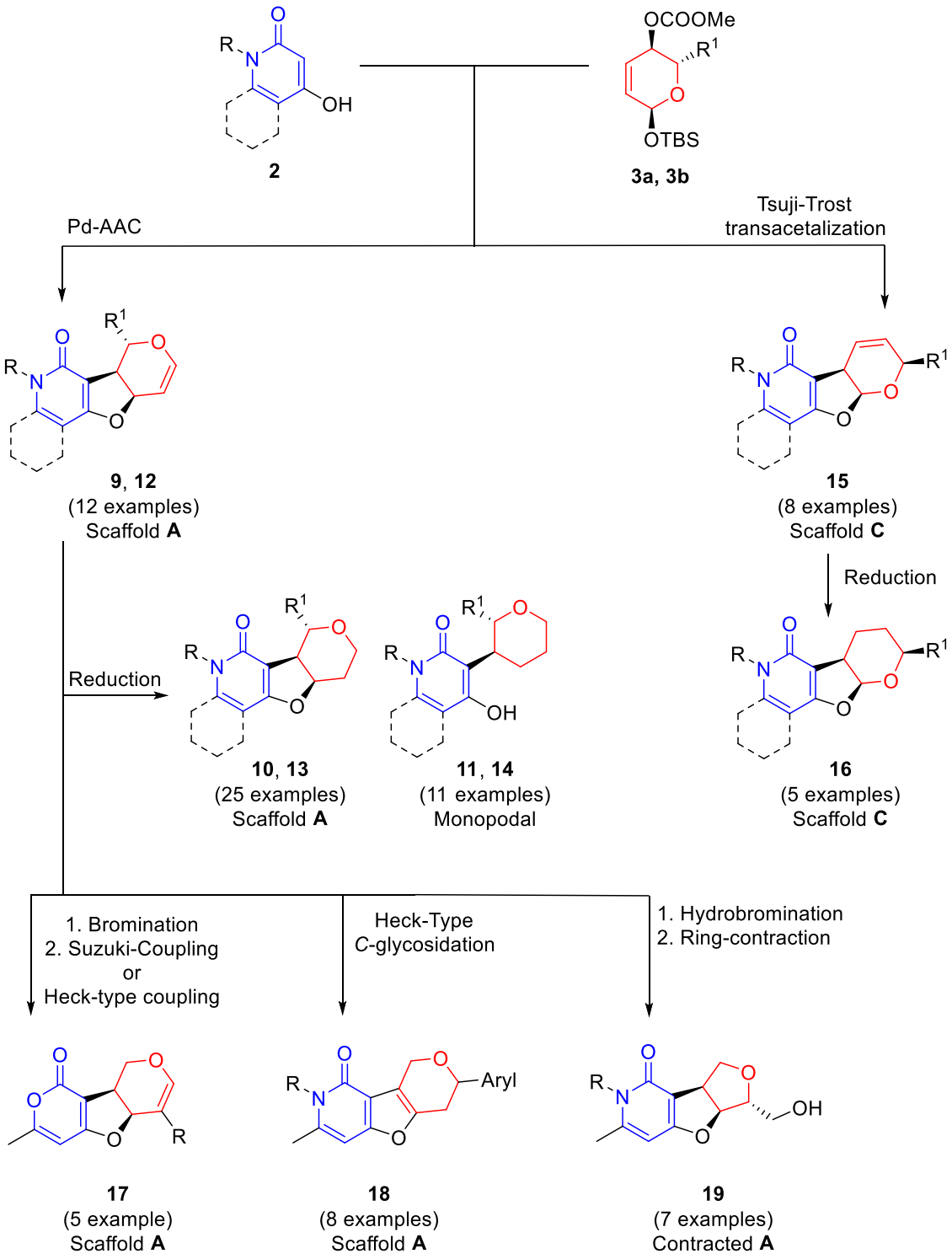

Scheme 30. Synthesis summary for the recombination of 4-Hydroxy-2-pyridones **2** (blue) with DHPs **3a** and **3b** (red) and subsequent reactions.

Additional PFPs with general scaffold **C** (Scheme 31, **26**-**30**) were synthesized by a quinine-mediated Michael addition transacetalization cascade reaction employing bis-nucleophilic 4-hydroxy-2-pyridones **2** and acetylated DHP bis-electrophiles **4a**-**d**. The corresponding regio-isomeric general scaffold **B** (Scheme 31, **20**-**24**) with inversed attachment points between the

pyran fragment and the furopyridone fragment was synthesized by a Tsuji-Trost oxa-Michael cascade. Monopodal connection isomers of **B** were isolated when strong acidic conditions were applied for the Boc deprotection in some examples (Scheme 31, **25**).

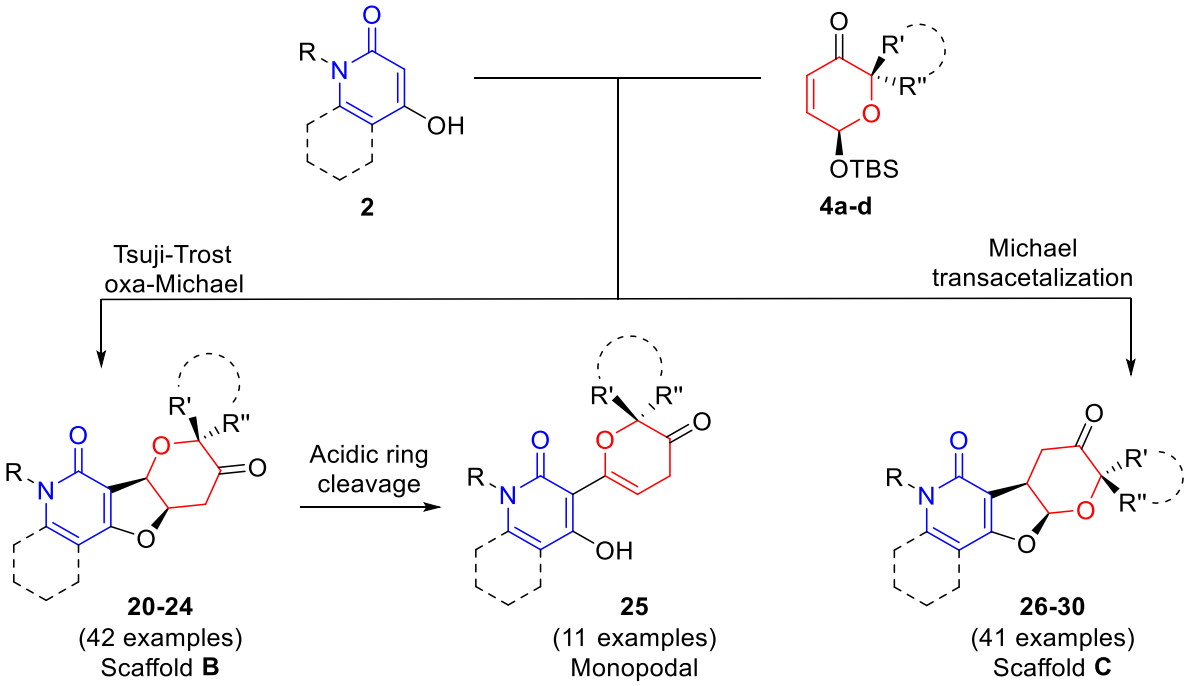

Scheme 31. Synthesis summary for the recombination of 4-Hydroxy-2-pyridones **2** (blue) with DHPs **4a-d** (red).

In total, a library of 162 (+/-)-PFPs with 54 examples for general scaffold **A** (light blue), 42 examples for general scaffold **B** (dark blue), 44 examples for general scaffold **C** (green) and 22 examples for monopodal isomers (grey) was synthesized and subjected for biological testing (Figure 8). In the majority of the cases the yields for the transformations were in the preparatively viable range. All compounds were purified chromatographically if required before they were subjected to biological investigations.

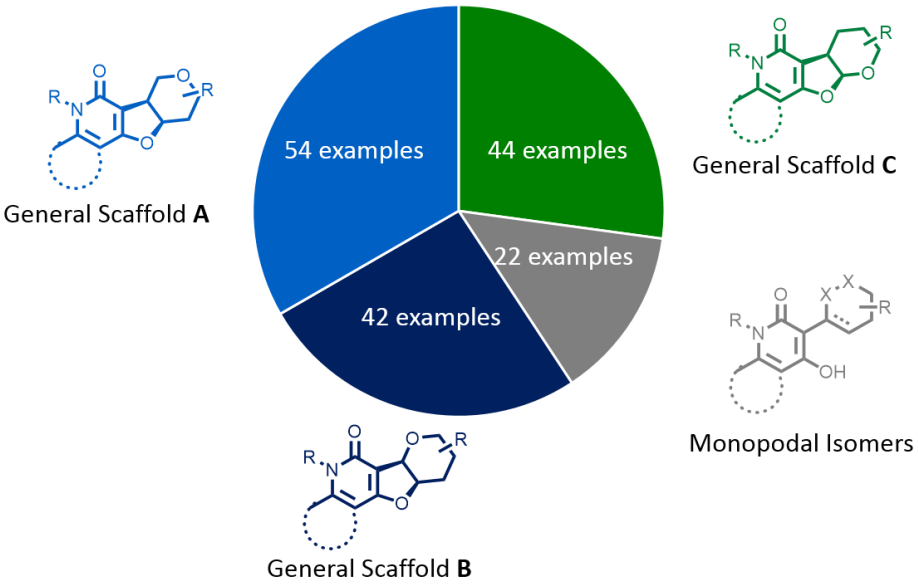

Figure 8. Summary of the library consisting of in total 162 PFP pseudo NPs with general scaffolds **A**, **B**, **C** or monopodal connection type.

3.5. Cheminformatic Analysis

The synthesized PFP pseudo NP compound collection was subjected for cheminformatic analysis to evaluate and visualize the covered chemical space. Therefore, analysis of the distribution of Natural-Product-likeness (NP-likeness) scores, plotting of molecular weight against hydrophobicity and evaluation of molecular shape diversity was carried out.

3.5.1. Natural Product Likeness Scores

The calculation of the Natural Product Likeness Scores was performed by Dr. Axel Pahl

Introduced by Ertl *et al.*, the NP-likeness score is an overall similarity comparison of an analyzed compound collection with the currently known NP structural space.[66] The algorithm deconstructs the molecular structure of a compound of interest into its underlying fragments and summarizes the occurrence of these fragments in NPs compared to their occurrence in commercially available small molecules. The score ranges from -3 to 5, with a higher score indicating higher NP-likeness.

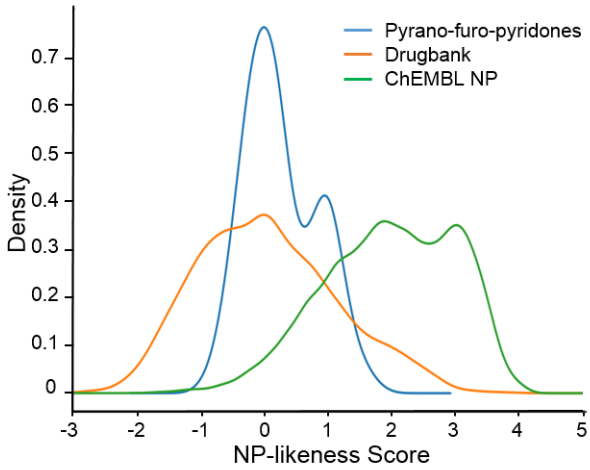

Figure 9. NP-likeness score of PFPs (blue) compared to molecules from Drugbank (orange) and NPs represented in ChEMBL (green curve).

The NP-likeness score of bipodal fused PFPs was evaluated to analyze and compare the occupied chemical space to NP-scores calculated for molecules listed in DrugBank, which represent marketed and experimental drugs[67], and the NP set in the ChEMBL database (Figure 9). The PFP NP-likeness scores range in an area of the graph which is only sparsely covered by NPs. Although this seems counter intuitive on the first glance, this comparison reflects that the novel fragment combinations realized in these scaffolds do not exist in NPs. In contrast, the majority of the PFP NP-likeness scores show substantial overlap with NP-scores calculated for drugs and closely related molecules, indicating that these compounds may be endowed with favorable physicochemical properties endorsing their potential application in drug discovery programs.

3.5.2. Analysis According to Lipinski

Lipinski *et al.* evaluated a compound data set registered for clinical phase II for molecular properties enabling good solubility and cell permeability of an orally active drug.[68] In a statistical analysis four parameters were identified as crucial and it was stated that absorption and permeation are more likely to be poor if the molecule has more than five H-bond donors, the molecular weight (MW) is over 500, the calculated octanol/water partition coefficient (clog P) is over 5 or if there are more than 10 H-bond acceptors present. As the analyzed data set had the least violation of this so-called rule of 5 in the combination of log P and MW (~1%), the assessment of these parameters in a scatter plot has become a rule of thumb to rapidly visualize drug likeness and to evaluate compound collections for drug and probe discovery.

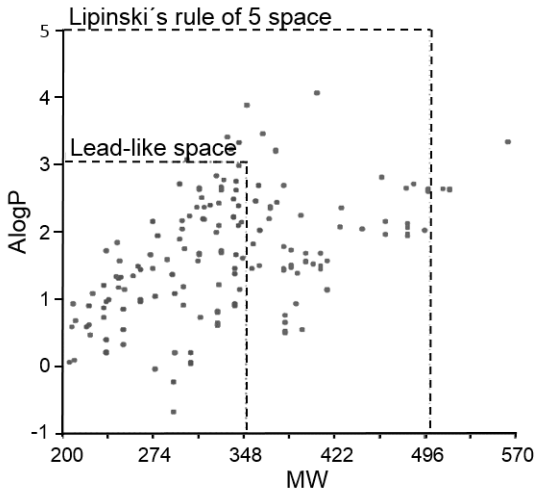

Figure 10. Estimated hydrophobicity (ALogP) vs molecular weight (MW) scatter plot of PFPs.

Using the open-source software "Lead-likeness and Molecular Analysis" (LLAMA), the estimated hydrophobicity (ALogP) was mapped against the respective MW (Figure 10).[69] 158 out of 162 PFP pseudo NPs (98%) fall into the Lipinski's Rule-of-Five space[68] exhibiting an ALogP < 5 and MW < 500 Da. Noteworthy, 61% of the compounds (99 out of 162 PFPs) also fall into lead-like space which is defined as a preferable fraction of chemical space where ALogP < 3 and MW < 350 Da.[70] The low lipophilicity and molecular weight is beneficial in a small molecule drug discovery project as potential hits tend to increase in these values during lead optimization thus running into violations of Lipink´s rule of 5 and potentially poor ADME behavior in later stages of a project.[68, 70]

3.5.3. Assessment of Molecular Shape Diversity

Principal moments of inertia (PMI) plots[27] are based on a computational method for molecular shape assessment using normalized ratios of principal moments of inertia plotted into two-dimensional triangular graphs. The LLAMA algorithm[69] used for the generation of the PMI coordinates randomly determines several 3D conformers of a given compound and minimizes their energy. For the lowest-energy conformer the moments of inertia are calculated in the x, y and z axes and subsequently the PMI plot coordinates I1 are determined by dividing inertia(x) by inertia(z). The I2 coordinates are calculated by dividing inertia(y) by inertia(z). The data is projected in the form of a triangular plot in which the vertices are defined by rod, disk and spherical shapes. Highly three-dimensional molecules will be represented in the upper right corner ([I1, I2] = [1, 1]) while disc-like shapes are found at [0.5, 0.5] and rod-like shapes will

be projected near [0, 1]. Hence, PMI plots allow a rapid assessment and visualization of molecular shape diversity associated with a given compound set

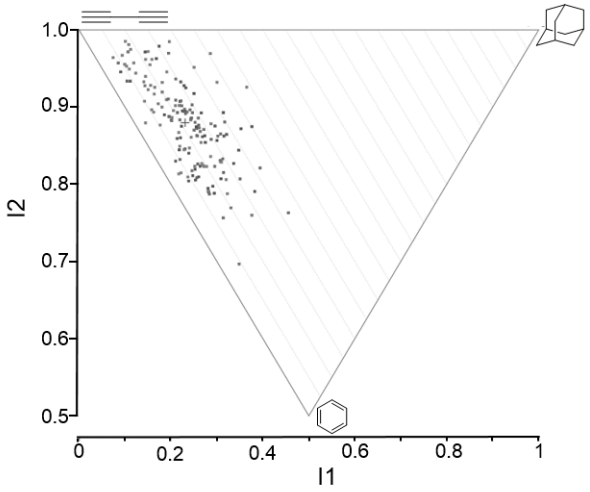

Figure 11. Principal moments of inertia (PMI) plot for PFPs.

Analysis of the three-dimensional character of the PFP compound collection and visualization of the shape distribution in a PMI plot revealed a shift from the linear – disc-like axis towards spherical shape (Figure 11). This indicates an increase in three-dimensional character compared to commercially available compound collections[27, 69] ultimately reflecting that the molecular diversity and high sp^3-content of NPs is conserved in the fragment recombination process of pseudo NPs.

3.5.4. Summary of the Cheminformatic Analysis

Collectively, these data suggest that the analyzed novel PFP pseudo NPs are endowed with advantageous physicochemical properties, increased molecular shape diversity and NP-score distributions not represented by NPs. This observation is consistent with the design principle behind pseudo NPs. PFPs are not accessible by biosynthesis representing a distinct area of chemical space and chemotype which is more than merely the sum of its NP-fragments. For other classes of pseudo NPs a similar trend has previously been observed and reported.[26, 29]

3.6. Morphological Profiling and Biological Evaluation

Morphological Profiling by means of the cell painting assay was performed by the Compound Management and Screening Center Dortmund (COMAS)

Pseudo NPs might be endowed with novel or unexpected bioactivities due to the unprecedented structural assembly of complementary NP-fragments, and they may differ significantly from activities observed for the guiding NPs. Hence, the biological relevance of pseudo NPs should be investigated in a similar manner to newly discovered NPs. To cover a broad spectrum of biological target space, pseudo NPs could either be subjected to multiple individual bioassays or more readily be characterized by target-agnostic phenotypic profiling approaches. Such high-content technologies capture a large number of phenotypic descriptors in a single experiment, thereby allowing an unbiased evaluation of characteristic morphological changes induced by chemical perturbation and eventually simultaneous sampling of various biological phenomena.[35, 71]

In accordance with this concept, the biological relevance of the synthesized PFP pseudo NP library was assessed in a cell painting assay established by the Compound Management and Screening Center Dortmund (COMAS) in a similar manner as introduced and developed by the Carpenter group[35-36, 39-40, 42] (see the Experimental Part 5.3.1.). In this multiplexed assay different cellular compartments are selectively stained by small molecule dyes in the presence of compounds under investigation or reference compounds with annotated biological activity, mode of action or specific targets. Upon compound treatment cells are imaged in high-content fashion and subsequent automated image analysis extracts and quantifies 579 morphological features. These are displayed in a unique fingerprint pattern for each compound and characterize its bioactivity. Similarities between morphological fingerprints are calculated as one minus the correlation distances between two distinct profiles (see the Experimental Part 5.3.1.) and defined as biological similarity ("BioSim"). Comparing the morphological fingerprints of PFPs measured at 10, 30 and 50 µM with those derived from approximately 3500 reference compounds (mostly measured at 10 µM) enabled then mode of action hypothesis generation and inspired further experimental target identification and validation efforts. Subsequently, the cell painting data guided establishment of a qualitative structure-phenotype relationship.[35, 71]

3.6.1. Identification of Bioactivity

In a first step, biological activity *per se* had to be defined. Therefore, the term induction given in [%] was introduced which equals the number of parameters that underwent a significant change in median absolute deviation value upon compound treatment of +/- three-fold of the median determined for the DMSO controls, divided by the total number of 579 measured parameters (see the Experimental Part 5.3.1.).

Applying the induction value as a filter criterion, all PFPs screened at 10 µM with an induction of at least 10% and not more than 80% were considered to potentially elicit most interesting bioactivity. The choice of cut-offs reflects the presumption that compounds with an induction less than 10% will most likely be only low in bioactivity while compounds exceeding 80% induction might have multiple targets or pleiotropic activity. Filtering according to these cut-offs for induction values resulted in five initial hits all of which had a fingerprint profile similarity of higher than 70% to at least one reference compound, hence allowing potential delineation of biological mode of action. To identify compounds with highest potency, the obtained hits were clustered according to induction and biological similarity within the list itself (Table 6; see the Experimental Part 5.3.2.). Two-membered cluster 1 contained the highest inducing PFP pseudo NPs **29k** and **30k** for which a high biological similarity of 84% was determined and which are structurally similar to each other (Tanimoto coefficient, "ChemSim": 0.72) as **30k** is the Boc deprotected version of **29k** (Table 6, entries 1 and 2). These compounds were characterized further since the relatively high biological and chemical similarity suggested similar modes of action. Noteworthy, this and the following analysis allowed only the identification of inducing compounds. Some compounds might have mechanisms of action that are not linked to detectable morphological changes as demonstrated by only 841 out of 3492 references with annotated biological activity exerting an induction of > 10%.

Entry	Compound Nr.	Structure	Induction [%] at 10 µM	Cluster	BioSim [%]	ChemSim
1	**29k**	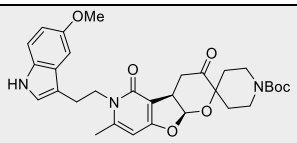	29	1	-	-
2	**30k**	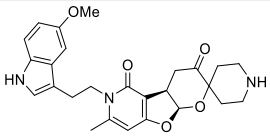	23	1	84	0.72
3	**4d**	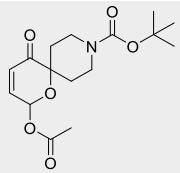	27	2	-	-
4	**28f**	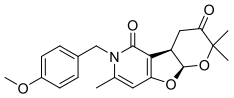	17	3	-	-
5	**4b**	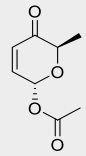	14	4	-	-

Table 6. Filtering the PFP data set measured at 10 µM in the cell painting assay by induction (> 10%; < 80%) and clustering according to highest induction resulted in five hits. Biological similarity (BioSim) calculated to entry 1. ChemSim = chemical similarity.

3.6.2. Concentration-Induction-Phenotype Dependency

The relation between phenotype, induction and applied concentration was determined to validate the choice of induction as a bioactivity indicator. Therefore, the fingerprints of **29k** and **30k** as representative members of the PFP pseudo NPs were compared for each of the two compounds at 10, 30 and 50 µM (Figure 12, see the Experimental Part 5.3.2.).

For compound **29k**, an increase from 29% to 36% induction was observed when the concentration was increased from 10 to 30 µM and the induction remained at 35% when the concentration was further increased to 50 µM. Notably, the biological similarity remained high (> 80%) at all concentrations. For **30k**, the induction increased almost linearly with the concentration as a rise from 23 to 69 to 80% induction was observed when increasing the concentration from 10 to 30 to 50 µM, while the biological similarity remained at an average of 66%.

In addition, weakly active compounds like **29f** with an induction of 4% at 10 µM were active at higher concentrations as an increase to 27% induction at 30 µM and to 40% induction at 50 µM was observed (Figure 12). Although the profile similarities are still above 50%, these values must be regarded with care. This is because the profile of **29f** at 4% induction has substantially less altered parameters than the profiles at 27 or 40% induction and hence a comparison between rich and sparse profiles would inevitable give lower profile similarities and should therefore be avoided in general. However, for the concentration-induction-phenotype analysis of **29f**, an experimental calculation was carried out in which only the parameters of the profile of 10 µM were considered for the similarity calculations to the higher concentration profiles. This resulted in a profile similarity of 89% (between 10 and 30 µM) and 94% (between 10 and 50 µM). Thus, the fingerprint of **29f** at 10 µM is a subset of the fingerprints at 30 and 50 µM, and the initial bioactivity is conserved at higher concentrations.

Finally, compounds being truly inactive in the cell painting assay were identified as well, represented by compound **29i** (Figure 12). For compound **29i** the induction remained under the 5% threshold for activity throughout all measured concentrations (10-50 µM). Noteworthy, low or no activity in the cell painting assay does not represent in general biological irrelevance of a compound as it might exert its activity through a mechanism that is not correlated to a phenotypic change in the given cell line and therefore not detectable by the cell painting assay.

Nevertheless, as in general induction increased with concentration while the shapes of the related fingerprints remained comparable, the choice of induction as a measure for compound bioactivity was justified. Conclusively, this defined compound **29k** and **30k** as the most potent PFPs as they exerted their biological activity (i.e. high induction) already at a low concentration.

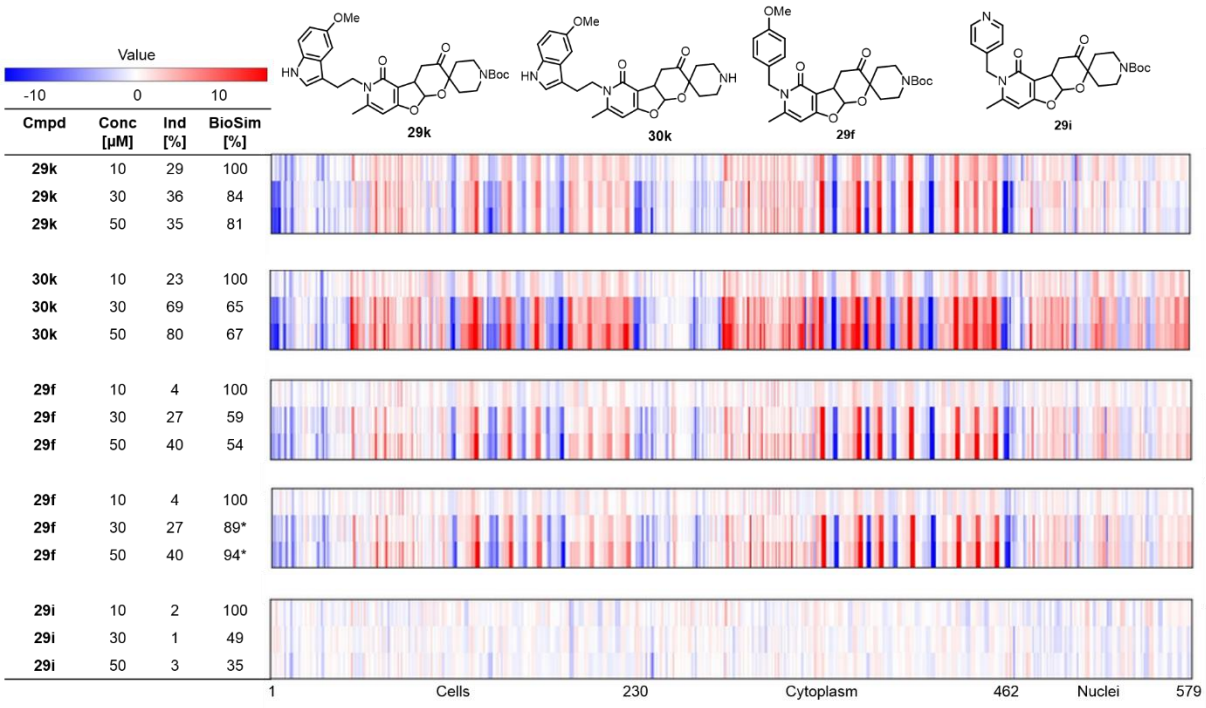

Figure 12. Concentration-induction-phenotype dependency determined for **29k**, **30k**, **29f** and **29i**. The top line in each panel is set as reference fingerprint (100% BioSim) to which subjacent fingerprints are compared, respectively; blue indicates a decreased value of a specific parameter compared to the DMSO control; red indicates an increased value of a specific parameter compared to the DMSO control. Cmpd = compound, Conc = concentration, Ind = induction, BioSim = biological similarity. *) Only the changed parameters of the lower inducing profile were considered for BioSim calculation.

3.6.3. Target Hypothesis Generation

To derive a target or mode of action hypothesis, for **29k** common references found at 10, 30 and 50 µM were determined in a first step. Therefore, only references that were found in the data sets of at least two of the measured concentrations were considered for further analysis (see the Experimental Part 5.3.2.). Next, a cross correlation analysis for the set of profiles of common references with profiles of **29k** and **30k** at all measured concentrations was performed and a cross-correlation matrix was generated (Table 7, see the Experimental Part 5.3.2.).

For **29k** and **30k** at 30 and 50 µM, high biosimilarities (> 83%) were found to reference compounds which inhibit mitochondrial respiration, autophagy, glucose uptake, Wnt- and Hedgehog pathway signaling.[26, 72-75] According to the initially stated hypothesis that similar morphological fingerprints correspond to a similar biological activity, **29k** and **30k** were subsequently investigated by COMAS in cell-based assays monitoring activity in autophagy, glucose uptake and Hedgehog signaling. These pathways could be excluded as potential modes of action because **29k** and **30k** were not or only weakly active in the respective assays.

BioSim	**Aumitin**[75] (10 µM) 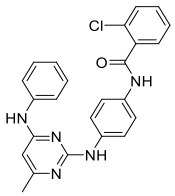	**Chromo-pynone 1**[26] (50 µM) 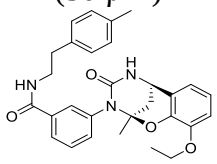	**Lipoxy-genin**[72] (50 µM) 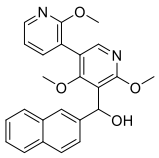	**Pipinib**[74] (30 µM) 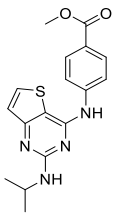	**GW-2974**[73] (10 µM) 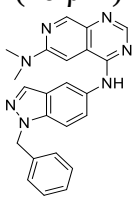
29k (10 µM)	78%	81%	85%	81%	87%
29k (30 µM)	88%	89%	94%	91%	87%
29k (50 µM)	87%	88%	94%	89%	84%
30k (10 µM)	63%	61%	63%	65%	75%
30k (30 µM)	90%	85%	84%	94%	85%
30k (50 µM)	92%	89%	86%	93%	88%
Annotated bioactivity	Autophagy inhibition	Glucose uptake (GLUT) inhibition	Wnt inhibition	Hedgehog (Hh) inhibition	ErbB inhibitor
Target	Mitochondrial complex I	GLUT-1/3	5-LO	(PI4KIIIβ)	ErbB 1/2
In-house observed pathway bioactivity	ROS, GLUT, Wnt, Hh	Autophagy, Wnt, Hh	Autophagy, Hh	Autophagy, Wnt	ROS

Table 7. Cross-correlation analysis. Fingerprints of entries in the y-axis were individually compared to fingerprints of annotated reference compounds on the x-axis. Reference compounds targeting GPCRs were excluded from the analysis as they were found to occur ubiquitous in the whole data set for yet unresolved reasons. BioSim = biological similarity.

However, it was recognized that the regulation of reactive oxygen species (ROS) formation is connected to these developmental and metabolic networks.[76-80] Furthermore, the fingerprints determined for PFP **29k** and **30k** at 30 µM showed 88 and 90% similarity respectively to the fingerprint determined for aumitin at 10 µM, which inhibits mitochondrial respiration by targeting mitochondrial complex I.[75] Inhibition of mitochondrial complexes I and III was reported to induce formation of mitochondrial superoxide which is a specific reactive oxygen

species.[81-82] Thus, PFPs **29k** and **30k** were hypothesized to modulate mitochondrial function by targeting mitochondrial complex I and/or III.

3.6.4. Influence on Mitochondrial Respiration

The Mito Stress Test was performed by Aylin Binici and Julian Wilke

The mode of action hypothesis derived from the cell painting data analysis suggested pseudo NP **29k** to be a modulator of mitochondrial function (see 3.6.3.). Thus, the effect of **29k** on mitochondrial respiration was investigated in a Mito Stress Test employing the Seahorse XF analyzer.[83] With this device the metabolic performance of live cells can be monitored by two distinct fluorophores indicating changes in oxygen concentration and fluctuations in extracellular pH, respectively. This in turn allows the individual observation of oxygen consumption rate (OCR) and extracellular acidification rate (ECAR) in a time- and dose-dependent manner. Whereas OCR reflects the rate of mitochondrial respiration consuming oxygen, ECAR is an indicator of glycolysis since glycolysis-derived lactate is exported together with a proton thereby decreasing the pH. Addition of a mitochondrial respiration inhibitor should cause a decrease of the OCR and, depending on the employed cells, an increase in ECAR, as cells try to compensate the decreased respiration by upregulating glycolysis.

The Mito Stress Test consists of five distinct phases. Initially, the basal respiration of the cells is determined representing glycolysis and respiration under normal conditions (Figure 13[84] and 14). In case of a mitochondrial respiration inhibitor, subsequent compound addition should cause a decrease in OCR, which is counterbalanced by a switch to glycolysis indicated by an increase in ECAR. In a third phase, injection of oligomycin as a mitochondrial ATP synthase inhibitor (complex V) allows the determination of basal respiration required for cellular ATP production. Next, disruption of the proton gradient by addition of trifluoromethoxy carbonylcyanide phenylhydrazone (FCCP) results in an increase of mitochondrial respiration to maximal capacity representing cell respiration under stress. The spare capacity of the cells to respond to an increased energetic demand is the difference of the OCR determined between the basal and maximal respiration. In the final phase, addition of a mixture of the complex I inhibitor rotenone and the complex III inhibitor antimycin A defines the lowest possible OCR related to mitochondrial respiration. The remaining oxygen consumption is caused by mitochondria unrelated processes.

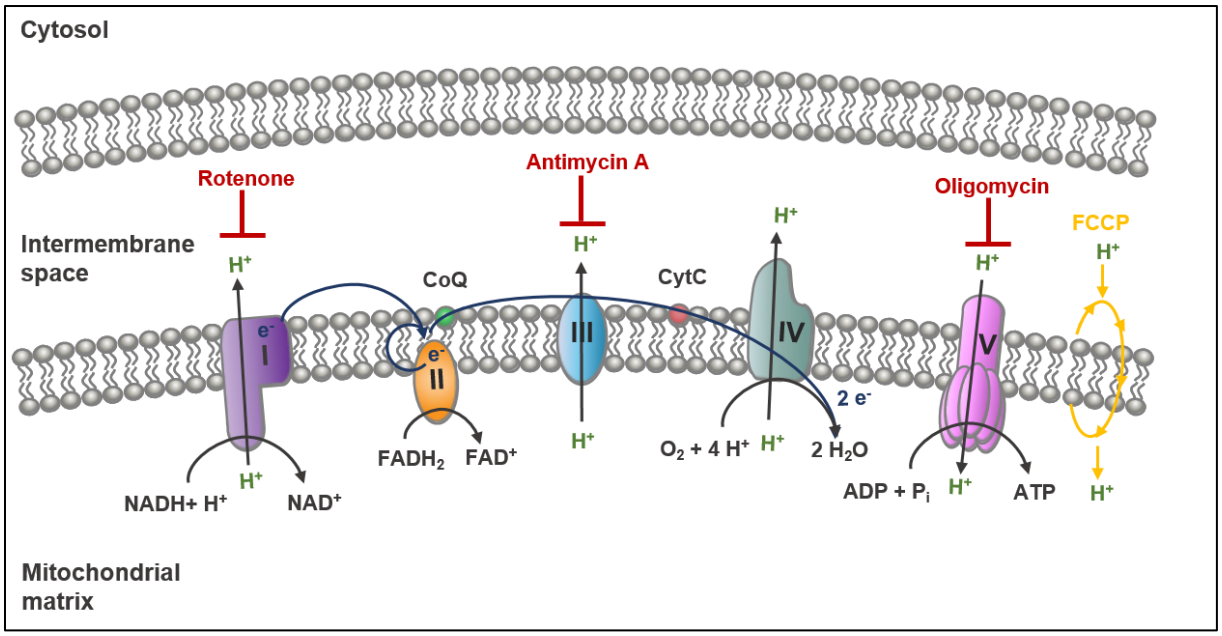

Figure 13. Representative scheme of mitochondrial respiration and inhibitors (red) of respective complexes. Complex I (NADH-CoQ reductase) oxidizes NADH to NAD+ and complex II $FADH_2$ to FAD+. Both, complex I and complex II, transfer electrons to coenzyme Q (CoQ). From CoQ the electrons are passed on to complex IV via complex III and cytochrome C (CytC). Complex IV reduces molecular oxygen to water under consumption of protons. Protons are translocated into the mitochondrial matrix by complex V (ATP synthase). Complex V utilizes the proton gradient between mitochondrial matrix and intermembrane space to generate ATP from ADP and phosphate. Trifluoromethoxy carbonylcyanide phenylhydrazone (FCCP, yellow) acts as a disrupter of the proton gradient.

Following the protocol for the Mito Stress Test (see the Experimental Part 5.3.4.), HeLa cells were treated with 3, 10 and 30 µM of compound **29k** inducing a rapid decrease in OCR and simultaneously an increase in ECAR at 10 and 30 µM compared to the DMSO control (Figure 14). Compared to a full inhibition of mitochondrial respiration by rotenone and antimycin A, PFP **29k** rapidly and dose-dependently induced partial inhibition upon compound treatment as the OCR was not reduced to the OCR level observed for rotenone and antimycin A. Nevertheless, these results indicated the first validation of the mode of action hypothesized for **29k** acting as a modulator of mitochondrial respiration.

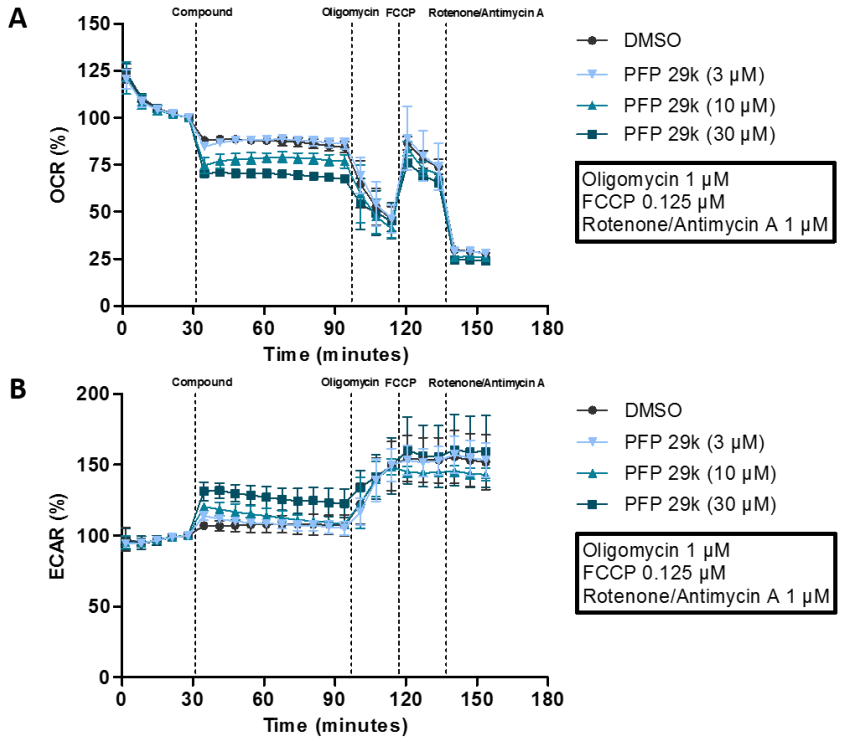

Figure 14. Influence of PFP **29k** on mitochondrial respiration. HeLa cells were treated with compound (3, 10 and 30 µM) or DMSO and the oxygen consumption rate (OCR, **Figure 14A**) and extracellular acidification rate (ECAR, **Figure 14B**) were measured with a Seahorse XF analyzer. Control inhibitors were added successively to the samples. Data are mean values ± SD, n=3.

3.6.5. Influence on Mitochondrial Complexes I-IV

The Semi-Intact Assay for Mitochondrial Respiration was performed by Aylin Binici and Julian Wilke

To further validate the hypothesis of complex I or III inhibition by pseudo NP **29k**, a semi-intact assay for mitochondrial respiration was carried out.[85] With this assay, complex I-, II-, III-, or IV-mediated respiratory activity can be studied in detail by plasma membrane permeabilization and addition of distinct substrates required for the activity of the respective complexes (Figure 15). Hence, adjusting the buffer system with the specific substrates required for the corresponding mitochondrial complexes, the effect of **29k** on each separate complex compared to known specific inhibitors was investigated in the Seahorse XF analyzer (see the Experimental Part 5.3.5.).

When malate/pyruvate were added to permeabilized cells to explore complex I, the OCR decreased upon compound treatment with **29k** at 30 µM, indicating an inhibition of complex I activity as compared to a full inhibition by the known complex I inhibitor rotenone[86] at 1 µM, **29k** partially suppressed complex I (Figure 15A). When succinate or duroquinol were

added to study complex II or IV, respectively, no activity of **29k** was observed (Figure 15B and D). For the investigation of complex III, tetramethylphenylenediamine (TMPD)/ascorbate were provided and a slight decrease in OCR compared to the DMSO control was observed upon addition of **29k** at 30 µM (Figure 15C). This validated the hypothesis of modulation of mitochondrial respiration by PFP pseudo NP **29k** and mitochondrial complex I can be considered as a molecular target. Collectively these results demonstrate that the cell painting assay may be used as a tool for target agnostic multiparametric phenotypic profiling to determine the mode of action of pseudo NPs and other bioactive small molecules.[87-89]

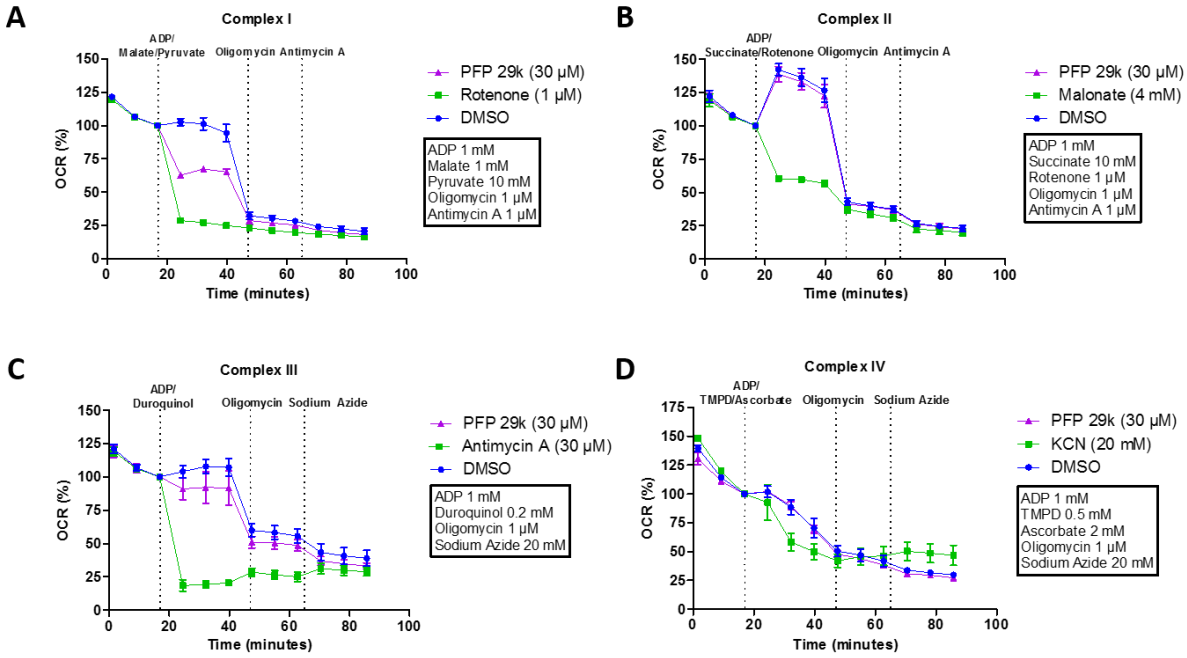

Figure 15. Influence of **29k** on mitochondrial complex I-IV. HeLa cells were permeabilized by Seahorse XF plasma membrane permeabilizer and treated with compound and the respective substrates of the individual complexes. **A**: Effect of PFP **29k** on complex I with malate/pyruvate as substrates and rotenone (1 µM) as control inhibitor. **B**: Effect of PFP **29k** on complex II with succinate as substrate and malonate (2 mM) as control inhibitor. **C**: Effect of PFP **29k** on complex III with duroquinol as substrate and antimycin A (30 µM) as control inhibitor. **D**: Effect of PFP **29k** on complex IV with tetramethylphenylenediamine (TMPD)/ascorbate as substrates and potassium cyanide (20 mM) as control inhibitor. Data are mean values ± SD, n=3.

3.6.6. Comparison to Reported Mitochondrial Complex I and III Inhibitors

Small molecules exhibiting dual inhibitory activity on mitochondrial complex I and III were already described in the literature[90]. However, structural characteristics of PFP **29k** (Table 8, entry 1) do not resemble any of the three major classes of complex I inhibitors[91-93] (entries 2-5) or reported complex III inhibitors[94-95] (entries 6-8). Hence, **29k** represents a truly novel chemotype for mitochondrial complex I inhibition. Essentially, inhibition of complex I leads to electron accumulation within the mitochondrial matrix because electron transfer from the iron-

sulfur centers in complex I to ubiquinone is blocked.[86] This causes an incomplete reduction of cellular oxygen (O_2) to superoxide ($^{\bullet}O_2^-$), a reactive oxygen species (ROS) which damages components of mitochondria including mitochondrial DNA and eventually lead to apoptosis.[82, 96] This oxidative stress can be neutralized by antioxidant defense mechanisms but an imbalance between ROS production and antioxidant defense towards increased levels of ROS is linked to aging and pathogenesis of several diseases.[97] However, recent studies suggest that the altered redox status in cancer cells can be exploited for therapeutic benefits employing ROS inducing agents and thereby selectively triggering cancer-cell toxicity.[98]

Entry	Structure	Name	Annotated Activity
1	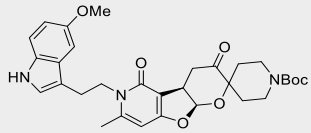	PFP **29k**	Complex I inhibitor
2	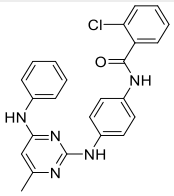	Aumitin	Type A (Pyrimidines) Complex I inhibitor
3	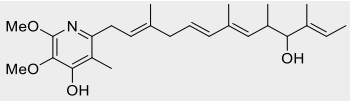	Piericidin A	Type A (4-pyridones) Complex I inhibitor
4	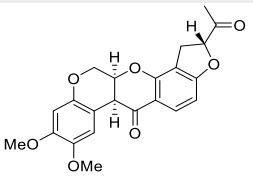	Rotenone	Type B Complex I inhibitor
5	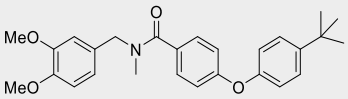	Capsaicinoid CC44	Type C Complex I inhibitor
6	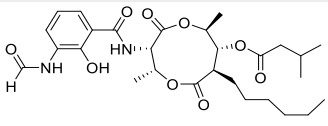	Antimycin A	Complex III inhibitor
7	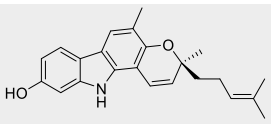	Mahanine	Complex III inhibitor
8	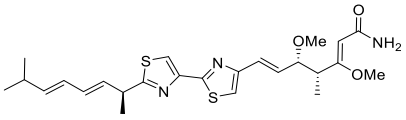	Myxothiazol	Complex III inhibitor

Table 8. Representative mitochondrial complex I and III inhibitors.

Interestingly, a comparison of the morphological fingerprint of **29k** to the profiles of some in-house available complex I and III inhibitors listed in Table 8 revealed that a high biosimilarity of 87% is found between **29k** and aumitin (Figure 16). Even more important, comparing the profile of **29k** to the profiles of complex III inhibitors antimycin A and myxothiazol did not afford any biosimilarity at all. This analysis indicates that **29k** exerts a phenotype that is more similar to phenotypes of known complex I inhibitors than of complex III inhibitors, which is consistent with the results from the semi-intact assay for mitochondrial respiration (see 3.6.5.). Moreover, this analysis demonstrates that the cell painting assay is able to differentiate between closely related mechanisms of action as inhibitors of complex I qualitatively define a distinct phenotype cluster compared to complex III inhibitors.

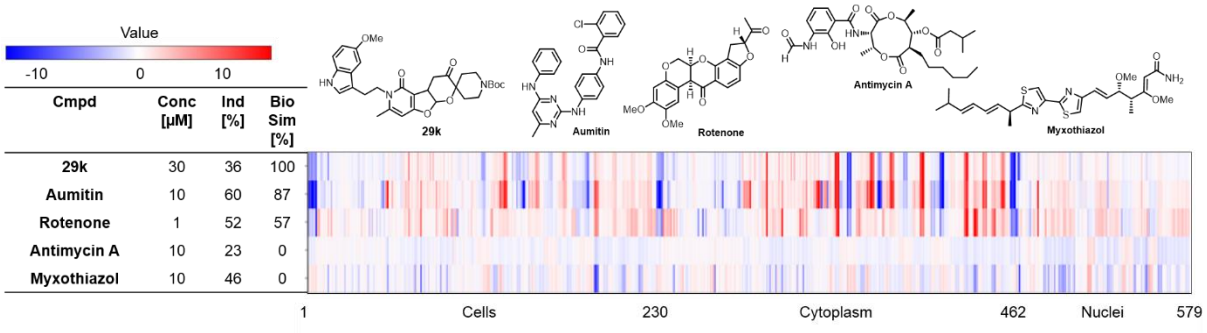

Cmpd	Conc [µM]	Ind [%]	Bio Sim [%]
29k	30	36	100
Aumitin	10	60	87
Rotenone	1	52	57
Antimycin A	10	23	0
Myxothiazol	10	46	0

Figure 16. Fingerprint comparison between **29k** and known complex I and III inhibitors; The top line is set as reference fingerprint (100% BioSim) to which subjacent fingerprints are compared, respectively; blue indicates a decreased value of a specific parameter compared to the DMSO control; red indicates an increased value of a specific parameter compared to the DMSO control. Cmpd = compound, Conc = concentration, Ind = induction, BioSim = biological similarity.

3.6.7. General Activity Trends

To evaluate the distribution of compounds exhibiting activity in the cell painting assay according to their core scaffold, a structure-induction relationship analysis was performed. Therefore, the whole cell painting data set for 162 PFPs was filtered for induction between 5 and 85%. Structural analysis of all active compounds at 10, 30 and 50 µM revealed that general scaffold **C** seems to be privileged in terms of ability to induce phenotypic changes since at 50 µM significantly more active compounds of substructure class **C** were found compared to general scaffolds **A** and **B** (Figure 17). Noteworthy, for monopodal connected isomers no activity was observed even at the highest screened concentration of 50 µM.

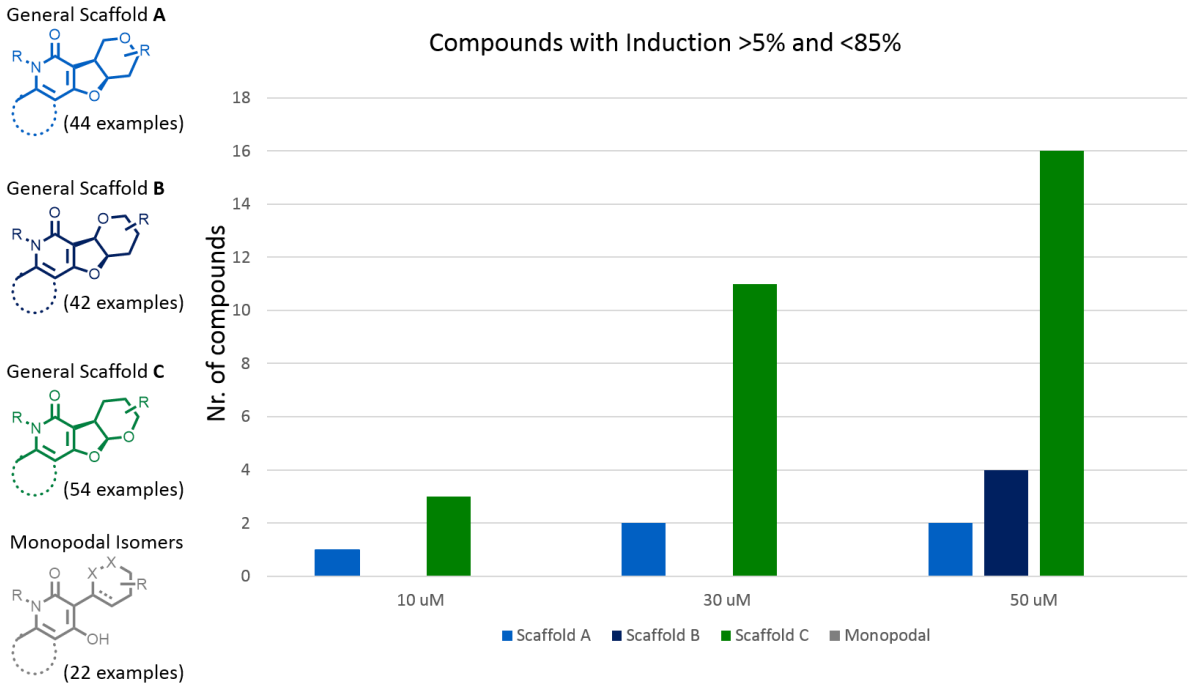

Figure 17. Structure-induction relationship. Number of compounds per general scaffold with induction > 5% and < 85%. () indicates the number of compounds per general scaffold submitted for biological testing in the cell painting assay.

Interestingly, the most potent compounds in the cell painting assay **29k** and **30k** (see 3.6.1. and 3.6.2), for which also a target hypothesis was derived and validated (see 3.6.3.; 3.6.4.; 3.6.5.) belong obviously to substructure class **C**. Hence, it was speculated if substructure class **C** is not only privileged in terms of general activity in the cell painting assay but if the found compounds are also structurally related and if they induce similar morphological fingerprints. Therefore, all PFP pseudo NPs of general scaffold **C** with induction > 5 % and < 85% at all concentrations (10, 30 and 50 µM) were clustered (see the Experimental Part 5.3.2.) yielding a 16-membered cluster of structurally related compounds with biosimilarities > 82% (Table 9). With the active compounds of substructure class **C** being chemically related while eliciting similar phenotypic changes, a structure phenotype relationship analysis was performed as described in chapter 3.6.8.

Entry	Compound Nr.	Structure	Induction [%]	Cluster	BioSim [%]	Chem Sim
1	**30k**	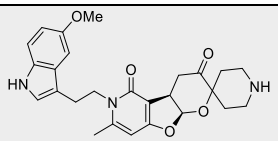	80 (at 50 µM)	1	-	-
2	**30k**	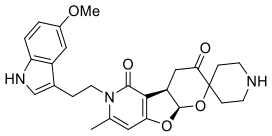	69 (at 30 µM)	1	98	1.00
3	**29d**	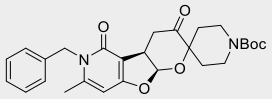	28 (at 50 µM)	1	93	0.44
4	**29f**	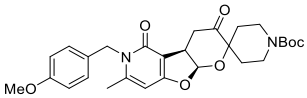	40 (at 50 µM)	1	93	0.49
5	**29e**	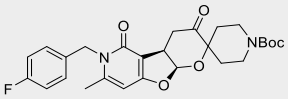	34 (at 50 µM)	1	92	0.45
6	**29g**	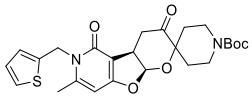	47 (at 50 µM)	1	90	0.43
7	**29f**	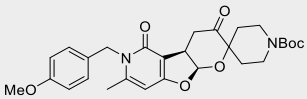	27 (at 30 µM)	1	89	0.49
8	**29e**	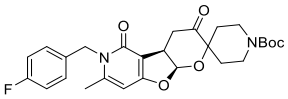	17 (at 30 µM)	1	89	0.45
9	**29k**	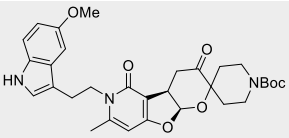	36 (at 30 µM)	1	88	0.72
10	**29c**	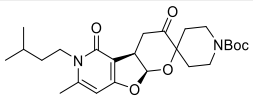	39 (at 50 µM)	1	87	0.42
11	**29k**	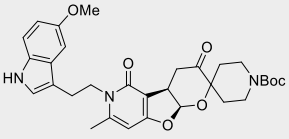	35 (at 50 µM)	1	86	0.72
12	**29l**	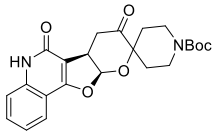	25 (at 50 µM)	1	85	0.36

13	**29g**	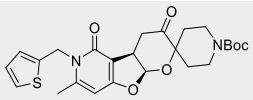	34 (at 30 µM)	1	85	0.43
14	**29d**	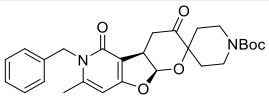	16 (at 30 µM)	1	85	0.44
15	**29k**	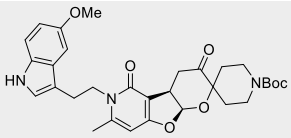	29 (at 10 µM)	1	84	0.72
16	**28f**	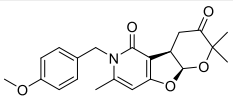	29 (at 50 µM)	1	82	0.48

Table 9. Cluster of all active compounds belonging to general scaffold **C**. Induction cut-off filter < 5%, > 85% for PFPs with general structure **C** measured at 10, 30 and 50 µM. Only compounds belonging to cluster 1 are listed. Biological similarity (BioSim) was compared to entry 1. ChemSim = chemical similarity.

3.6.8. Comparison of SPR to SAR

The MitoSOX Red assay was performed by Aylin Binici and Julian Wilke

To assess whether the multiparametric cell painting assay may guide identification of qualitative trends in structure phenotype relationship (SPR), all fingerprints of the obtained 16-membered cluster (see. 3.6.7.) and profiles of structurally related compounds were analyzed and the derived trends in SPR were compared to trends of the structure-activity relationship (SAR) determined by means of a MitoSOX Red assay (see the Experimental Part 5.3.6.). This live-cell fluorescence-based assay monitors the production of mitochondrial superoxide upon inhibition of the mitochondrial respiratory system.[75] Given the fact that inhibition of mitochondrial complexes I and III induces formation of superoxide[81-82], concentration dependent formation of mitochondrial superoxide employing the fluorogenic indicator MitoSOX Red[99] was assayed.

Since **29k** displayed the highest induction at 10 µM and it was a member of the substructure class **C** cluster (see. 3.6.7., Table 9, entry 15), its morphological profile at 10 µM was set as a reference phenotype to which all other cluster profiles and fingerprints of structurally related compounds were compared (Table 10). The comparison was preferably performed in an induction range of 20-40% to avoid that the similarity calculations are negatively affected by larger differences in fingerprint richness. In analogy to SAR-studies, only structural changes on specific parts of the molecule while keeping the structure otherwise constant were investigated

in terms of changes in induction values as a measure for bioactivity, and changes in profile similarity to the reference fingerprint.

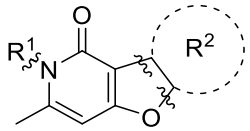

Entry	Nr.	R^1 =	R^2 =	Induction [%]	BioSim [%]	EC_{50} [µM]
1	**29b**		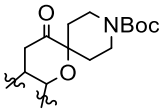	2 (50 µM)	n.c.	>30
2	**29c**		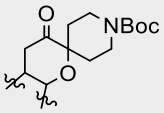	39 (50 µM)	92	>30
3	**29k**	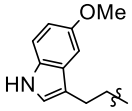	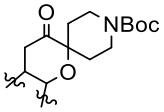	29 (30 µM)	100	3.7 ± 0.9
4	**29d**		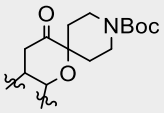	28 (50 µM)	87	9.2 ± 2.4
5	**29f**	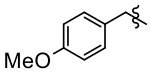	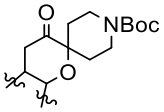	27 (30 µM)	85	6.8 ± 0.7
6	**29e**	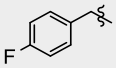	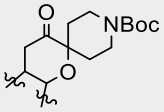	34 (50 µM)	87	15.7 ± 6.6
7	**29g**		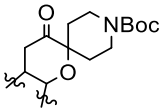	34 (30 µM)	90	13.4 ± 2.6
8	**29i**		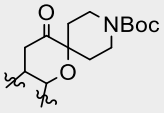	3 (50 µM)	n.c.	>30
9	**29h**	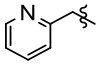	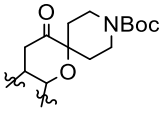	10 (50 µM)	n.c.	25.3 ± 6.2
10	**29j**	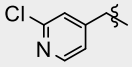	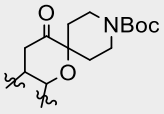	24 (50 µM)	90	9.7 ± 1.8
11	**29n**	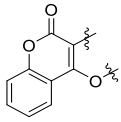	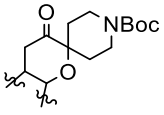	3 (50 µM)	n.c.	>30

12	**29l**	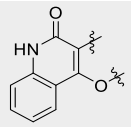	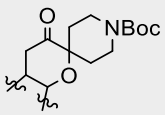	25 (50 µM)	90	13.5 ± 1.2
13	**30k**	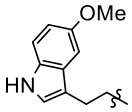	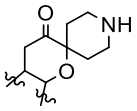	23 (10 µM)	84	10.7 ± 3.6
14	**20h**	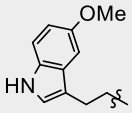		15 (50 µM)	37	>30
15	**25k**	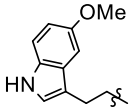	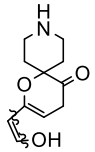	3 (50 µM)	n.c.	>30
16	**28f**	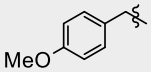	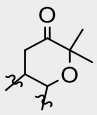	28 (30 µM)	62[a]	>30
17	**26d**	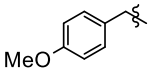	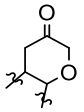	6 (50 µM)	n.c.	>30
18	**22e**	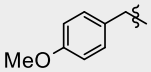	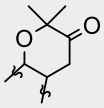	3 (50 µM)	n.c.	>30
19	**26a**		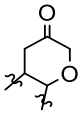	1 (50 µM)	n.c.	>30

Table 10. Establishment of a structure-phenotype relationship (SPR) for the PFPs by means of the induction delineated from the cell painting assay, and comparison with the activity in the MitoSOX Red assay; EC_{50} determined in HeLa cells (n = 3); Biosimilarity (BioSim) was compared to **29k** if not indicated differently; n.c. = biosimilarity was not calculated because induction was out of 20-40% comparison window. [a] Biosimilarty was compared to **29f**.

For the investigation of pyridone *N*-substituents of **29k** (Table 10, R^1), the right-hand side (Table 10, R^2) was kept unchanged. Substitution of the indolyl moiety in **29k** by a small methyl group was not tolerated with respect to induction (compare entry 1 with 3) while isopentyl, benzyl, substituted benzyl groups and thiophenyl as R^1 led to high induction at comparable profile similarities (compare entry 3 with entries 2 and 4-7). Replacement of the methoxy-indolyl by basic 4- and 2-pyridinyl was detrimental for induction (compare entry 3 with entries 8 and 9). Bioactivity and biosimilarity were reestablished by introduction of a chlorine next to the basic nitrogen of the 4-pyridinyl substituent, thereby reducing the basicity (entry 10). Furthermore, when the whole *N*-substituted pyridone was replaced by an aromatic bicycle, a quinolinone was preferred over a coumarine subscaffold to ensure induction and high profile

similarity to **29k** (compare entry 3 with entries 11 and 12). Collectively, these observations indicate that variation of the pyridone *N*-substituent while remaining high induction values at retained bioactivity is possible if the substituent is not too small or too polar. Therefore, for R^1 a lipophilic residue at a distance to the fused ring system appears to be advantageous, and a quinolinone as the pyridone unit is preferred over a coumarine subscaffold.

The left-hand side of **29k** (Table 10, R^1) remained unchanged to study the influence on induction and biosimilarity of structural changes to the right-hand side and the core (Table 10, R^2). Removal of the Boc group in **29k** slightly decreased the induction while the profile shape was conserved (compare entry 3 with 13). When the R^2 substituent was further minimized to a dimethyl derivative induction remained high but the profile similarity declined to 62% (entry 16). Further simplification to a R^2-unsubstituted derivative (entry 17) and other structural changes on the cyclic acetal core unit (entries 15 and 18) were not tolerated with **20h** (entry 14) representing a borderline case in which the 15% induction value is close to the 20% cut-off for comparison. Consequently, for R^2 a bipodal-fused and α,α-disubstituted ketone substructure with the quaternary carbon next to the cyclic acetal is beneficial for induction at high biological similarity to **29k**.

Compounds representing the general trends in SPR were then subjected to dose-response analysis (EC_{50} determination) in a MitoSOX Red assay (see the Experimental Part 5.3.6.). Altogether, the EC_{50} values reflected qualitatively the trends observed for the SPR analysis as described above with some exceptions. Consistent with the trends in the SPR, compound **29k** was identified as the most potent PFP pseudo NP with an EC_{50} value of 3.7 ± 0.9 µM (Table 10, entry 3). The majority of the compounds with induction >20% and profile similarity >80% to **29k** induced mitochondrial superoxide formation (entries 3-7, 10, 12, 13). In fact, only a few exceptions (entries 2, 14 and 16) were notable indicating that the SPR-SAR correlation cannot be regarded as entirely parallel. Indeed, compound **29c** deviated from the SPR-SAR correlation as it exhibited activity in the cell painting assay and a high profile similarity to **29k** but for which no activity could be observed in the MitoSOX Red assay (entry 2). Compound **20h** and **28f** must also be regarded as exceptions from the general trends as they both elicited induction but no MitoSOX Red signal (entries 14 and 16). However, for both compounds decreased profile similarities of 37 and 62% were observed, respectively, indicating that the morphological changes might be induced through different modes of action. Noteworthy, although the central cyclic acetal scaffold was observed to be privileged for activity in the cell painting assay (see 3.6.6.), the scaffold on its own was not sufficient to establish the observed

kind of bioactivity (entry 19) indicating that both, R^1 and R^2 have a significant impact on the overall bioactivity and that they must be decorated as outlined above simultaneously.

Another point to evaluate concerned the biological activity of fragments that PFPs consist of. By comparing the profile similarity of PFP **29k** to its building blocks respectively as well as the activity of the fragments in the MitoSOX Red assay, it was analyzed if the identified activity of pseudo NP **29k** as a mitochondrial superoxide inducer can be attributed to one or both of the fragments.

In the cell painting assay, fragments of **29k** were either not active at the highest measured concentration (Table 11, entries 1 and 3) or had low biological similarity to **29k** (entry 2). Consistent with the SPR analysis outlined above, fragments of **29k** that were not active in the cell painting assay did also not elicit a MitoSOX Red signal. Noteworthy, although fragment **4d** has a profile similarity of only 9% to **29k** it was also determined to be active in the MitoSOX Red assay with an EC_{50} of 3.4 ± 0.1 µM (Table 11, entry 2). However, this compound decreased the cell count to 50% at 10 µM. Toxicity further increased at higher concentrations (cell count = 37% at 30 µM and 7% at 50 µM; see Appendix 8.2., Figures 24-26). Thus, the activity of **4d** in the MitoSOX Red assay must be caused by a different mode of action since **29k** was non-toxic at all measured concentrations (see Appendix 8.2., Figures 21-23).

Entry	Compound Nr.	Fragment	Induction [%]	BioSim [%]	EC_{50} [µM]
1	**2s**	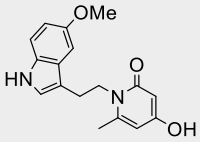	2 (50 µM)	n.c.	>30
2	**4d**	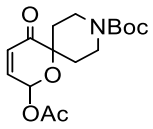	27 (10 µM)	9	3.4 ± 0.1
3	**4e**[a]	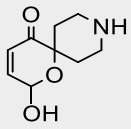	1 (50 µM)	n.c.	>30

Table 11. Biological evaluation of fragments of PFP **29k** by means of the induction delineated from the cell painting assay, and comparison with the activity in the MitoSOX Red assay; EC_{50} determined in HeLa cells (n = 3); Biosimilarity (BioSim) was compared to **29k** if not indicated differently; n.c. = biosimilarity was not calculated because induction was out of 20-40% comparison window.
[a] Synthesis is described in the Experimental Part.

In summary, for the PFP pseudo NP library general scaffold **C** as a privileged structural subclass was identified, for which general trends in the SPR correlated with the SAR studies in the MitoSOX Red assay with only a few exceptions. It was determined that R^1 should be a bulky aromatic residue which is not too polar while for R^2, removal of the Boc group, no substituent on the cyclic acetal core, and a regio-isomeric connection pattern was detrimental for activity. Further consistent with the SPR, the fragments of **29k** were not active in the MitoSox assay. Altogether, target-agnostic qualitative SPR analysis based on morphological profiling has the potential to inform hit expansion efforts through synthesis of additional compounds or predict suitable linker attachment sites for target identification efforts e.g. by affinity-based proteomics. Nevertheless, PFPs represent unoptimized hits that may have multiple targets which even may differ among the library members and still, different modes of action can result in a similar phenotype. Although data obtained from such phenotypic analysis should be viewed with caution to avoid over-interpretation, general trends pointing towards a distinct biological activity and qualitative structure-phenotype relationship, as is the case for the herein discussed PFPs, should be investigated in more detail.

3.6.9. Additivity of Morphological Fingerprints

Finally, the question of profile additivity was addressed and if it is possible to predict the profile of a pseudo NP from the fingerprint combination of its consisting fragments. Therefore, the morphological profiles of fragments **2p** and **4d** were determined and added mathematically to generate an artificial profile **29j-art.** representing the *in silico* combination of the two fragments (Figure 18). Comparison of the artificial profile with the profile of the synthesized PFP pseudo NP **29j** showed only 4% similarity, demonstrating that the synthetic combination of NP-fragments to pseudo NPs generates novel scaffolds endowed with specific properties that are more than merely the sum of topologic characteristics of the individual fragments. However, this analysis should be regarded with caution because on the one hand fragment **2p** is very low inducing (6%) so that the artificial profile is dominated by the contributions of fragment **4d**. To balance this, an example would be needed in which the pyridone fragment itself is sufficiently inducing morphological changes. Unfortunately, **2p** is already the highest inducing fragment synthesized and tested in the cell painting assay during this project. On the other hand, fragments **2p** and **4d** are the building blocks for PFP **29j** and not the actual fragments thereof. Hence, the analysis as outlined above would have to be repeated with the actual fragments which would be, for example, the phenol methylated derivative of **2p** and an anomeric O-

methylated instead of O-acetylated **4d** fragment. In summary, the prediction of pseudo NP profiles by mathematical addition of fragment profiles was not successful for the analyzed example.

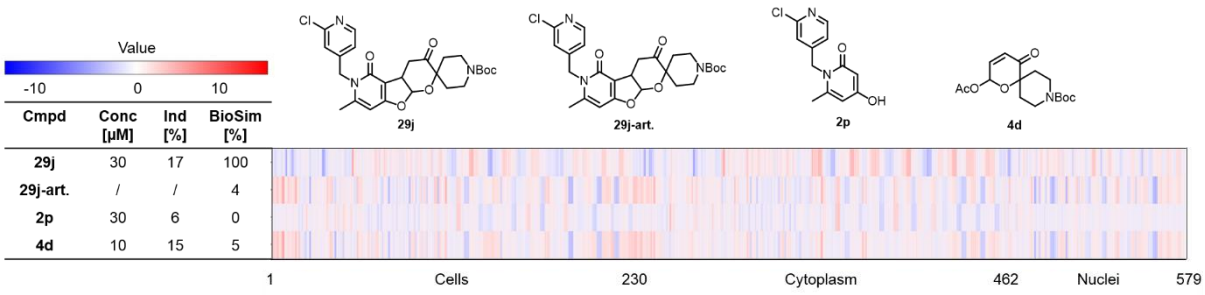

Figure 18. Evaluation of additivity of profiles. The top line is set as reference fingerprint (100% BioSim) to which subjacent fingerprints are compared, respectively; blue indicates a decreased value of a specific parameter compared to the DMSO control; red indicates an increased value of a specific parameter compared to the DMSO control. Cmpd = compound, Conc = concentration, Ind = induction, BioSim = biological similarity.

3.6.10. Summary of Cell Painting Data Analysis and Biological Results

While the cell painting assay was previously applied as a general indicator for biological activity[36] and as a tool for compound prioritization and library design[42], this thesis extends its application and marks the first demonstration of the cell painting assay as a tool for target hypothesis generation and structure-phenotype relationship determination. Hence, exemplified on the data analysis performed for this project, a suggested general work-flow model is depicted in Figure 19.

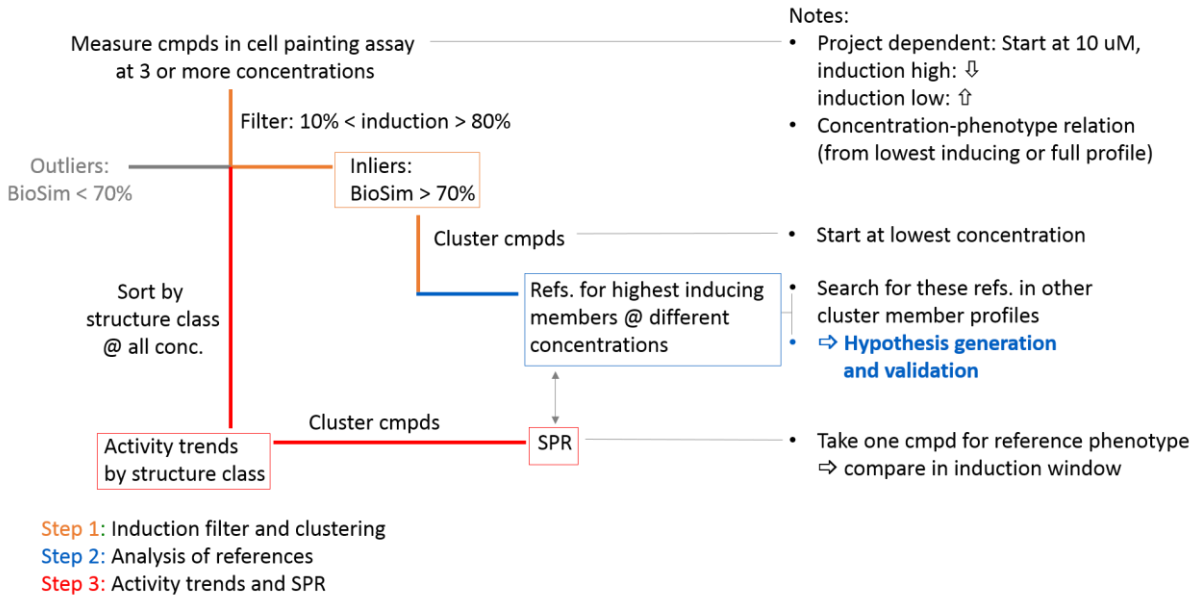

Figure 19. Summary of cell painting data analysis and suggestion for a generalized work-flow model. BioSim = biological similarity, Conc. = concentration, Refs. = references with annotated biological activity, Cmpds = compounds, SPR = structure-phenotype relationship.

Before starting with the actual analysis, sufficient amount of meaningful data needs to be generated by measuring all compounds of interest in at least three different concentrations in the cell painting assay. For the PFP pseudo NP library the screening of compounds commenced at 10 µM resulting in only few compounds with induction > 10%. Therefore, additional testing at 30 and 50 µM were carried out to increase the number of compounds exhibiting an induction value of > 10%. For highly active compounds that tend to elicit an over activation (induction > 85%) at 10 µM, additional assays should be carried out at lower concentrations. With sufficient data suitable for analysis at hand, the analysis workflow can be divided into three major steps as outlined for the analysis of the PFP library (Figure 19, orange, blue, red).

Step 1: The generated data set was filtered applying an induction cut-off of < 10% and > 80% and a biosimilarity threshold of 70% to any of the reference compounds to identify all "inliers" (Figure 19, orange). In case of PFPs, initially the data set of the 10 µM screen was filtered and clustered to identify **29k** and **30k** as the most active compounds. For these compounds a concentration-induction-phenotype dependency was verified by either using the full profiles or only parameters from the lowest inducing profile for comparison. This step is crucial because the kind of biological activity i.e. the shape of the fingerprint should not change drastically with changes in concentration and induction. All active compounds that are below the biosimilarity threshold of 70% are termed "outliers" (Figure 19, grey), as these compounds elicit morphological profiles that are not similar to any of the fingerprints of the reference compounds

with annotated bioactivity. Outliers could potentially lead to compounds with entirely novel modes of action. However, for the PFP library no outliers were observed.

Step 2: For the most active compounds, i.e. the highest inducing compounds, common references occurring at all measured concentrations were identified and analyzed to generate a mode-of-action hypothesis. For the PFP pseudo NPs **29k** and **30k**, a potential activity as modulators of mitochondrial respiration was deduced (Figure 19, blue). This hypothesis was subsequently validated by demonstrating an inhibitory effect of **29k** on mitochondrial respiration and activity was traced to inhibition of mitochondrial complex I as at least one responsible molecular target.

Step 3: An activity analysis of all substructure classes revealed PFP general structure **C** as a privileged scaffold (Figure 19, red). Clustering of all active compounds of substructure class **C** indicated structural and fingerprint relatedness to PFP **29k**. Hence, a structure-phenotype-relationship (SPR) analysis was carried out setting the fingerprint of **29k** as a reference phenotype. The derived trends in SPR were then compared to structure-activity-relationship (SAR) trends employing a MitoSOX Red assay for determination of EC_{50} values. In general, trends in SPR correlated in parallel to trends in SAR identifying **29k** as the most active PFP pseudo NP with an EC_{50} value of 3.7± 0.9 µM.

4. Summary of the Thesis

Rarely related natural product (NP) fragments 2-pyridones and dihydropyrans were synthesized and functionalized for combination to pyrano-furo-pyridones (PFPs) defining a new class of pseudo natural products (pseudo NPs). The fusion of the two fragments was carried out in three different regioisomeric arrangements of a bipodal connection employing a palladium-catalyzed allylic alkylation cascade (Tsuji-Trost cascade) to derive general scaffold **A**, a Tsuji-Trost oxa-Michael addition cascade to derive general scaffold **B** and a quinine mediated Michael transacetalization cascade to derive general scaffold **C** (Figure 20). Monopodal connection isomers could be isolated in some examples from the corresponding reaction mixtures as well. Cheminformatic analyses disclosed that PFPs exhibit favorable drug-like features and their unprecedented scaffolds reside in an area of NP-like chemical space which is not covered by NPs reflecting that pseudo NPs are not accessible by biosynthesis.

Comparison of morphological fingerprints generated for pyrano-furo-pyridones to those determined for references with annotated biological activity pointed towards activity as modulators of mitochondrial respiration. This hypothesis could be verified in further experiments demonstrating an inhibitory effect of PFP **29k** on mitochondrial respiration. Eventually, the activity could be traced to inhibition of mitochondrial complex I, thereby causing induction of reactive oxygen species (Figure 20). In addition, the cell painting data indicated a correlation of molecular architecture and biological phenotype which was subsequently validated in structure-activity relationship studies employing the formation of mitochondrial superoxide as a readout. Hence, PFP **29k** was identified as the most potent compound investigated with an EC_{50} value of 3.7± 0.9 µM.

These results provide a proof-of-principle for the validity of the pseudo NP concept for the *de novo* design and synthesis of novel biologically relevant compound classes. In addition, they demonstrate that target agnostic morphological profiling has the potential to determine bioactivity, provide mode of action hypothesis and provide qualitative information about structure-phenotype relation even in the absence of a proven target. These insights might inspire further hit expansion or determine suitable attachment points for reporter groups and linkers, which will enable subsequent target identification. Established methods for target identification frequently fail if the target protein is expressed only on a very low level or if it is a membrane protein. In such cases information derived from morphological profiling will be particularly valuable to guide mode-of-action hypothesis generation and subsequent targeted assays.

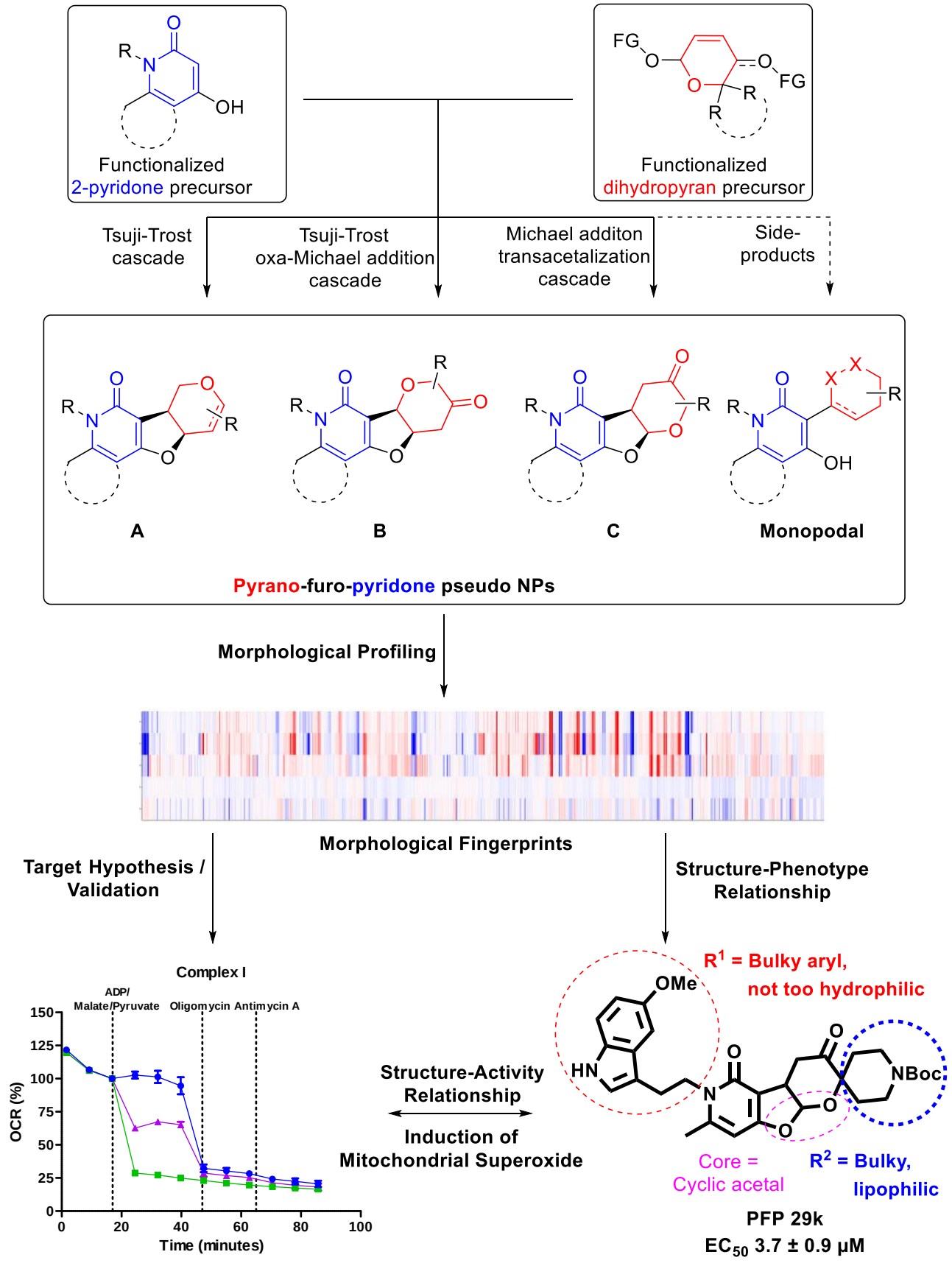

Figure 20. Summary of the thesis.

5. Experimental

5.1. Chemistry

5.1.1 General Remarks

All reactions were performed in oven dried glassware and under inert Argon atmosphere if not indicated differently. Dry solvents were purchased from Fischer Scientific and/or Acros and used without further treatment. Oxygen and/or moisture sensitive solutions were transferred using syringes and cannulas.

Thin layer chromatography was performed on silica coated aluminium plates (Merck 60 F_{254}) and visualization was achieved under UV irradiation (254 nm), potassium permanganate stain (1.5 g KMnO4, 10 g K_2CO_3, 1.25 mL of 10% aqueous NaOH solution and 200 mL of water) or *p*-anisaldehyde stain (0.7 mL *p*-anisaldehyde, 9.5 mL conc. H_2SO_4, 2.7 mL of acetic acid and 250 mL of EtOH).

Analytical UHPLC-MS and LC-MS was performed on an Agilent 1290 Infinity system equipped with a mass detector (column: Zorbax Eclipse C18 Rapid Resolution 2.1x50 mm 1.8µm) and on a Thermo Scientific fleet station (column: Nuleodur C18 gravity EC 50/3, 1.8 µm). Appropriate gradient systems were applied by mixing water (+ 0.1% TFA) and acetonitrile (+ 0.1%).

Purification of crude products was achieved through flash column chromatography (FC, silica gel 60, 0.035-0.070 mm) or automated medium pressure liquid chromatography (MPLC, Grace Reveleris X2) using the indicated solvents. Challenging separations were carried out on an Agilent 1100 preparative HPLC system equipped with a mass detector (columns: Nuleodur C18 gravity VP 125/10 5 µm, Nucleodur C18 gravity VP 125/21 5 µm, Nucleodur C4 gravity VP 125/10 5 µm). Appropriate gradient systems were applied by mixing water (+ 0.1% TFA) and acetonitrile (+ 0.1%).

NMR spectra were recorded on Bruker AV 400 Avance III HD (NanoBay), Agilent Technologies DD2, Bruker AV 500 Avance III HD (Prodigy), Bruker AV 600 Avance III HD (CryoProbe) or Bruker AV 700 Avance III HD (CryoProbe) spectrometers. Data is reported in ppm with reference to the used deuterated solvent ($CDCl_3$: 7.26 ppm, 77.16 ppm; DMSO-d_6: 2.50 ppm, 39.52 ppm; CD_2Cl_2: 5.32 ppm, 53.84 ppm; MeOH-d_4: 3.31 ppm, 49.00 ppm; Acetone-d_6: 2.05 ppm, 29.84 ppm, 206.26 ppm).[100] Signals were assigned to their

corresponding Hydrogens or Carbons based on 2D NMR correlations ($^{1}H/^{1}H$ COSY, $^{1}H/^{1}H$ NOESY, $^{1}H/^{13}C$ HSQC, $^{1}H/^{13}C$ HMBC).

High-resolution mass spectrometry (HRMS) was performed on a LTQ Orbitrap mass spectrometer coupled to an Accela HPLC-System (HPLC column: Hypersyl GOLD, 50 mm x 1 mm, particle size 1.9 µm, ionization method: electron spray ionization (ESI)).

Microwave reactions were carried out in a CEM Discover SP Activent machine.

First generation photoreactor consisted of an 8 mL tube vial, magnetic stirrer and 34W blue LEDs (Kessil H150-Blue LED Lamp). Ventilation was achieved by a cooling fan.

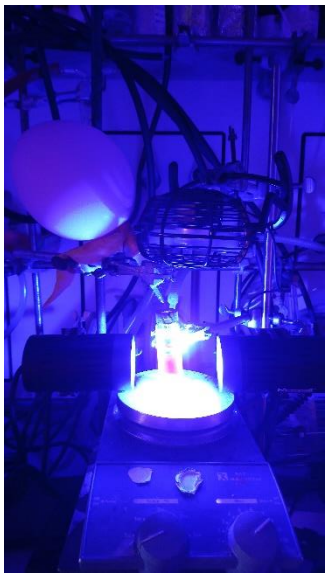

Second generation photoreactor consisted of a 250 mL or 500 mL schlenck flask, magnetic stirrer and two 34W blue LEDs (Kessil H150-Blue LED Lamp). The schlenck flask was placed in a dewar vessel of appropriate size. The dewar vessel was filled with iso-propanol and a constant flow of compressed air over the iso-propanol surface was adjusted. This cooling system maintained a bath temperature between 23-26 °C while irradiating the schlenck flask with two blue LEDs in a 45 °C angle.[54]

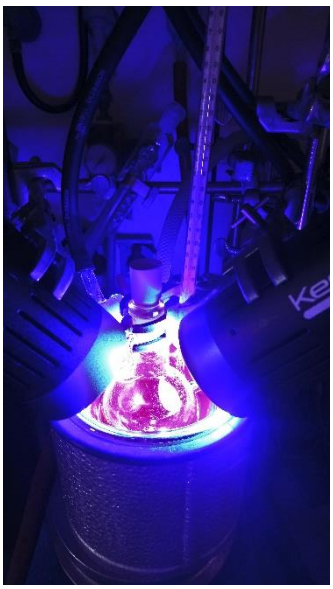

5.1.2. Synthesis of 2-Pyridones

General procedure 1:[65]

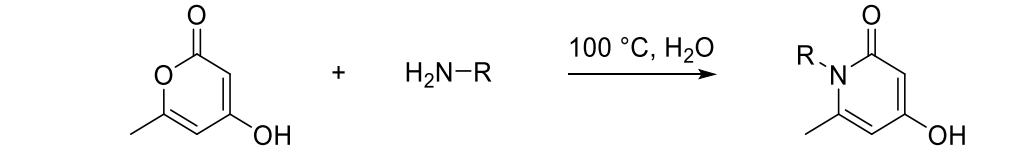

4-Hydroxy-6-methyl-2-pyrone (**1a**) 4-Hydroxy-2-pyridones (**2**)

4-Hydroxy-6-mehtyl-pyrone (**1**) (1.00 g, 7.93 mmol) was suspended in H_2O (0.5 M) and amine (1 equiv) was added at room temperature. The mixture was stirred in a sealed vial at 100 °C overnight. Upon cooling to 0 °C a white precipitate formed which was filtered off and washed with cold H_2O. The remaining filter residue was triturated with EtOH and drying in vacuo afforded the corresponding pyridones as white to off-white solids.

4-hydroxy-6-methylpyridin-2(1H)-one (2a)[101]

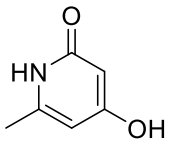

0.54 g, 54%. **^{1}H-NMR** (400 MHz, DMSO-d_6): δ 10.89 (s, 1H), 10.29 (s, 1H), 5.58 (dd, *J* = 2.2 Hz, 0.8 Hz, 1H), 5.32 (d, 2.2 Hz 1H), 2.07 (s, 3H). **LCMS**-ESI (m/z): 125.97 $[M + H]^+$.

4-hydroxy-1,6-dimethylpyridin-2(1H)-one (2b)[102]

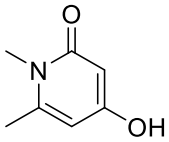

0.67 g, 61%. **^{1}H-NMR** (400 MHz, DMSO-d_6): δ 10.28 (s, 1H), 5.75 (dd, *J* = 2.2 Hz, 0.6 Hz, 1H), 5.48 (d, *J* = 2.2 Hz 1H), 3.29 (s, 3H), 2.26 (s, 3H). **LCMS**-ESI (m/z): 140.03 $[M + H]^+$.

cyclobutyl-4-hydroxy-6-methylpyridin-2(1H)-one (2c)

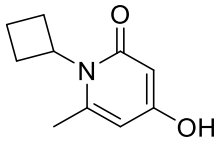

0.62 g, 56%. **^{1}H-NMR** (700 MHz, DMSO-d_6): 10.26 (s, 1H), 5.66 (d, *J* = 2.5 Hz, 1H), 5.40 (d, *J* = 2.5 Hz, 1H), 4.68 (p, *J* = 8.8 Hz, 1H), 3.12 (m, 2H), 2.26 (s, 3H), 2.13-2.07 (m, 2H), 1.77 (q, *J* = 10.3 Hz, 1H), 1.64 (dq, *J* = 18.4, 9.4 Hz, 1H). **^{13}C-NMR** (176 MHz, DMSO-d_6) δ 165.4, 165.1, 147.05, 100.5, 97.5, 51.2, 26.91, 20.9, 14.1. **HRMS**-ESI (m/z): $[M + H]^+$ calculated for $C_{10}H_{14}O_2N^+$, 180.1019; found, 180.1018.

4-hydroxy-1-isopentyl-6-methylpyridin-2(1H)-one (2d)[103]

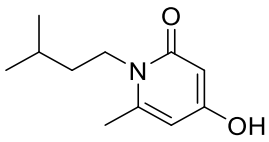

0.76 g, 50%. **^{1}H-NMR** (700 MHz, DMSO-d_6): δ 5.73 (dd, *J* = 2.7, 1.0 Hz, 1H), 5.46 (d, *J* = 2.7 Hz, 1H), 3.84-3.81 (m, 2H), 2.29 (s, 3H), 1.60 (dt, *J* = 13.3, 6.7 Hz, 1H), 1.37 (dt, *J* = 9.6, 6.8 Hz, 2H), 0.91 (d, *J* = 6.7 Hz, 6H). **^{13}C-NMR** (176 MHz, DMSO-d_6): δ 165.6, 163.7, 146.9, 100.4, 96.0, 41.4, 37.1, 26.0, 22.3, 19.7. **HRMS**-ESI (m/z): $[M + H]^+$ calculated for $C_{11}H_{18}NO_2^+$, 196.1332; found, 196.1330.

4-hydroxy-6-methyl-1-((tetrahydrofuran-2-yl)methyl)pyridin-2(1H)-one (2e)[104]

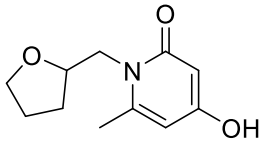

1.29 g, 80%. **^{1}H-NMR** (700 MHz, DMSO-d_6): δ 10.36 (s, 1H), 5.72 (s, 1H), 5.48 (s, 1H), 4.08 (dd, *J* = 13.9, 3.2 Hz, 1H), 4.05-4.01 (m, 1H), 3.75 (ddd, *J* = 8.3, 7.2, 6.2 Hz, 1H), 3.67 (dd, *J* = 13.9, 8.3 Hz, 1H), 3.59 (td, *J* = 7.8, 6.1 Hz, 1H), 2.31 (s, 3H), 1.93 (dddd, *J* = 12.2, 8.5, 6.9, 5.2 Hz, 1H), 1.85 (dddd, *J* = 18.6, 8.7, 7.1, 5.7 Hz, 1H), 1.78 (ddtd, *J* = 12.0, 8.5, 7.3, 6.2 Hz, 1H), 1.55 (ddt, *J* = 12.2, 8.7, 7.1 Hz, 1H). **^{13}C-NMR** (176 MHz, DMSO-d_6): δ 166.1, 164.3, 148.5, 100.5, 96.3, 77.2, 67.6, 47.6, 29.2, 25.6, 21.0. **HRMS**-ESI (m/z): $[M + H]^+$ calculated for C11H16NO3$^+$, 210.1125; found, 210.1121.

4-hydroxy-6-methyl-1-(tetrahydro-2H-pyran-4-yl)pyridin-2(1H)-one (2f)

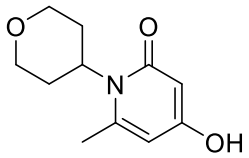

0.35 g, 22%. **^{1}H-NMR** (700 MHz, DMSO-d_6): δ 10.26 (s, 1H), 5.70 (bd, *J* = 1.6 Hz, 1H), 5.40 (s, 1H), 3.89 (dd, *J* = 11.5, 4.2 Hz, 2H), 3.35 (d, *J* = 11.5 Hz, 2H), 2.95-2.85 (bm, 2H), 2.32 (s, 3H), 1.44 (d, *J* = 11.5 Hz, 1H). **^{13}C-NMR** (176 MHz, DMSO-d_6): δ 165.2, 164.6, 147.2, 100.8, 97.9, 67.0, 52.0, 28.2, 21.0. **HRMS**-ESI (m/z): $[M + H]^+$ calculated for $C_{11}H_{16}O_3N^+$, 210.1125; found, 210.1126.

1-benzyl-4-hydroxy-6-methylpyridin-2(1H)-one (2g)[101]

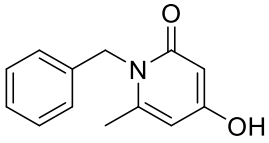

0.35 g, 62%. **^{1}H-NMR** (500 MHz, DMSO-d_6): δ 10.47 (s, 1H), 7.32 (t, *J* = 7.4 Hz, 2H), 7.24 (t, *J* = 7.4 Hz, 1H), 7.08 (d, *J* = 7.4 Hz, 2H), 5.79 (dd, 2.2 Hz, 1H), 5.59 (d, 2.2 Hz 1H), 5.18 (bs, 2H), 2.16 (s, 3H). **HRMS**-ESI (m/z): $[M + H]^+$ calculated for $C_{13}H_{14}O_2N^+$, 216.1019; found, 216.1017.

1-(4-fluorobenzyl)-4-hydroxy-6-methylpyridin-2(1H)-one (2h)[105]

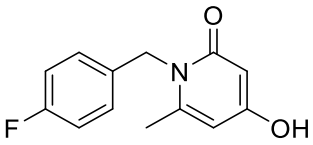

0.50 g**,** 28%. **^{1}H-NMR** (600 MHz, DMSO-d_6): δ 10.51 (s, 1H), 7.15 (d, *J* = 7.3 Hz, 4H), 5.79 (d, *J* = 2.3Hz, 1H), 5.59 (d, *J* = 2.3 Hz, 1H), 5.16 Hz (s, 2H), 2.17 (s, 3H). **^{13}C-NMR** (151 MHz, DMSO-d_6): δ 165.9, 164.0, 162.0, 160.3, 147.5, 133.9, 128.3, 128.2, 115.4, 115.3, 100.5, 95.9, 44.7, 19.9. **HRMS**-ESI (m/z): $[M + H]^+$ calculated for $C_{13}H_{13}O_2NF^+$, 234.0925; found, 234.0920.

1-(2-chlorobenzyl)-4-hydroxy-6-methylpyridin-2(1H)-one (2i)[104]

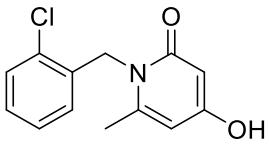

0.47 g, 24%. **^{1}H-NMR** (500 MHz, DMSO-d_6): δ 10.60 (s, 1H), 7.50 (dd, *J* = 7.2, 2.0 Hz, 1H), 7.32-7.26 (m, 2H), 6.59 (dd, *J* = 7.1, 2.2 Hz, 1H), 5.88 (d, *J* = 2.6 Hz, 1H), 5.60 (d, *J* = 2.6 Hz, 1H), 5.17 (s, 2H), 2.13 (s, 3H). **^{13}C-NMR** (126MHz, DMSO-d_6): δ 166.2, 163.7, 147.5, 134.7, 131.3, 129.4, 128.7, 127.7, 125.9, 100.8, 95.8, 43.8, 19.8. **HRMS**-ESI (m/z): $[M + H]^+$ calculated for $C_{13}H_{13}O_2NCl^+$, 250.0629; found, 250.0631.

1-(3,5-dimethylbenzyl)-4-hydroxy-6-methylpyridin-2(1H)-one (2j)

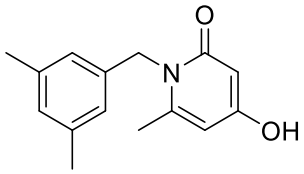

0.18 g, 10%. **^{1}H-NMR** (500 MHz, MeOH-d_4-d_4): δ 6.90 (s, 1H), 6.70 (s, 2H), 5.97 (d, *J* = 6.3 Hz, 1H), 5.82 (d, *J* = 2.6 Hz, 1H), 5.25 (s, 2H), 2.25 (s, 6H), 2.24 (s, 3H). **HRMS**-ESI (m/z): $[M + H]^+$ calculated for $C_{15}H_{18}O_2N^+$, 244.1332; found, 244.1331.

4-hydroxy-1-(4-methoxybenzyl)-6-methylpyridin-2(1H)-one (2k)[101]

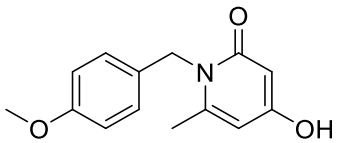

Using 500.0 mg (3.89 mmol) 4-Hydroxy-6-mehtyl-pyrone. Purification by MPLC (DCM/MeOH 1:0 to 4:1) afforded the desired product as a white solid (0.38 g, 40%). **^{1}H-NMR** (700 MHz, DMSO-d_6): δ 10.50 (s, 1H), 7.05 (d, *J* = 8.6 Hz, 2H), 6.87 (d, *J* = 8.6 Hz, 2H), 5.77 (d, 2.2 Hz, 1H), 5.59 (d, 2.2 Hz 1H), 5.11 (bs, 2H, CH_2), 3.71 (s, 1H), 2.17 (s, 3H). **^{13}C-NMR** (176 MHz, DMSO-d_6): δ 165.8, 164.1, 158.3, 147.6, 129.7, 127.6, 114.0, 100.4, 96.0, 55.1, 44.7, 20.0. **HRMS**-ESI (m/z): $[M + H]^+$ calculated for $C_{14}H_{16}O_3N^+$, 246.1125; found, 246.1123.

4-hydroxy-6-methyl-1-(thiophen-2-ylmethyl)pyridin-2(1H)-one (2l)

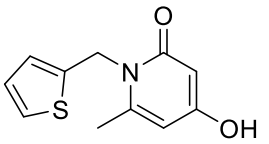

1.00 g, 60%. **^{1}H-NMR** (500 MHz, DMSO-d_6): δ 10.52 (s, 1H), 7.39 (dd, *J* = 5.1, 1.0 Hz, 1H), 7.03 (d, *J* = 3.1 Hz, 1H), 6.94 (dd, *J* = 5.1, 3.1 Hz, 1H), 5.76 (s, 1H), 5.56 (s, 1H), 5.26 (s, 2H), 2.32 (s, 3H). **^{13}C-NMR** (126 MHz, DMSO-d_6): δ 166.0, 163.6, 148.0, 140.0, 126.5, 126.5, 126.0, 100.5, 95.9, 41.2, 19.9. **HRMS**-ESI (m/z): $[M + H]^+$ calculated for $C_{11}H_{12}O_2NS^+$, 222.0583; found, 222.0582.

4-hydroxy-6-methyl-1-(pyridin-2-ylmethyl)pyridin-2(1H)-one) (2m)[106]

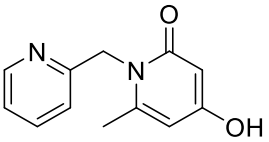

1.09 g, 64%. **^{1}H-NMR** (600 MHz, DMSO-d_6): δ 10.46 (s, 1H), 8.48 (ddd, *J* = 4.9, 1.9, 0.9 Hz, 1H), 7.74 (td, *J* = 7.8, 7.6, 1.9 Hz, 1H), 7.26 (ddd, *J* = 7.6, 4.9, 1.2 Hz, 1H), 7.10 (d, *J* = 7.8 Hz, 1H), 5.81 (dd, *J* = 2.6, 1.0 Hz, 1H), 5.53 (d, *J* = 2.6 Hz, 1H), 3.34 (s, 2H), 2.23 (s, 3H). **^{13}C-NMR** (151 MHz, DMSO-d_6): δ 165.9, 163.8, 156.9, 149.0, 147.9, 136.9, 122.3, 120.9, 100.3, 95.8, 47.4, 39.9, 39.8, 39.7, 39.5, 39.4, 39.2, 39.1, 20.2. **HRMS**-ESI (m/z): $[M + H]^+$ calculated for $C_{12}H_{13}O_2N_2^+$, 217.0972; found, 217.0972.

4-hydroxy-6-methyl-1-(pyridin-4-ylmethyl)pyridin-2(1H)-one (2n)[106]

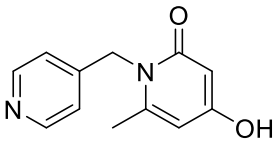

1.34 g, 80%. **^{1}H-NMR** (500 MHz, DMSO-d_6): δ 10.49 (bs, 1H), 8.49 (d, *J* = 6.0 Hz, 2H), 7.05 (d, *J* = 6.0 Hz, 2H), 5.84 (d, *J* = 2.3 Hz, 1H), 5.59 (d, *J* = 2.3 Hz, 1H), 5.20 (s, 2H), 2.14 (s, 3H). **^{13}C-NMR** (126 MHz, DMSO-d_6): δ 166.2, 163.9, 149.9, 147.4, 146.9, 121.2, 100.7, 95.8, 44.7, 19.9. **HRMS**-ESI (m/z): $[M + H]^+$ calculated for $C_{12}H_{13}O_2N_2^+$, 217.0972; found, 217.0970.

4-hydroxy-6-methyl-1-((3-methylpyridin-4-yl)methyl)pyridin-2(1H)-one (2o)

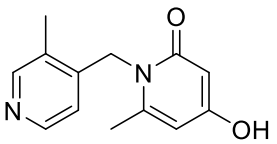

0.73 g, 41%. **^{1}H-NMR** (700 MHz, DMSO-d_6): δ 10.6 (s, 1H), 8.37 (s, 1H), 8.29 (d, *J* = 5.0 Hz, 1H), 6.42 (d, *J* = 5.0 Hz, 1H), 5.88 (d, *J* = 2.6 Hz, 1H), 5.60 (d, *J* = 2.6 Hz, 1H), 5.13 (s, 2H), 2.33 (s, 3H), 2.11 (s, 3H). **^{13}C-NMR** (176 MHz, DMSO-d_6): δ 166.1, 163.7, 150.1, 147.7, 147.4, 144.8, 130.4, 118.4, 100.7, 95.8, 43.0, 19.6, 15.3. **HRMS**-ESI (m/z): $[M + H]^+$ calculated for $C_{13}H_{15}O_2N_2^+$, 231.1128; found, 231.1124.

1-((2-chloropyridin-4-yl)methyl)-4-hydroxy-6-methylpyridin-2(1H)-one (2p)

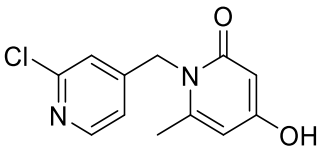

0.90 g, 50%. **^{1}H-NMR** (500 MHz, DMSO-d_6): δ 10.65 (s, 1H), 8.34 (d, *J* = 5.1 Hz, 1H), 7.17 (s, 1H), 7.07 (d, *J* = 5.1 Hz, 1H), 5.86 (d, *J* = 2.2 Hz, 1H), 5.59 (d, *J* = 2.2 Hz, 1H), 5.20 (s, 2H), 2.16 (s, 3H). **^{13}C-NMR** (126 MHz, DMSO-d_6): δ 166.3, 163.8, 151.2, 150.6, 150.3, 147.4, 121.5, 120.7, 100.9, 95.8, 44.6, 20.0. **HRMS**-ESI (m/z): $[M + H]^+$ calculated for $C_{112}H_{12}O_2N_2Cl^+$, 251.0582; found, 251.0581.

4-hydroxy-1-(4-methoxyphenyl)-6-methylpyridin-2(1H)-one (2q)[107]

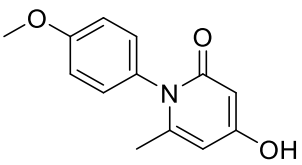

0.62 g, 35%. **^{1}H-NMR** (700 MHz, DMSO-d_6): δ 10.51 (s, 1H), 7.08 (d, *J* = 8.6 Hz, 2H), 7.01 (d, *J* = 8.6 Hz, 2H), 5.85 (s, 1H), 5.52 (s, 1H), 3.79 (s, 3H), 1.83 (s, 3H). **^{13}C-NMR** (176 MHz, DMSO-d_6): δ 166.3, 164.2, 158.7, 147.4, 131.5, 129.6, 114.3, 99.8, 96.0, 55.3, 20.8. **HRMS**-ESI (m/z): $[M + H]^+$ calculated for $C_{13}H_{14}O_3N^+$, 232.0895; found, 232.0969.

4-hydroxy-6-methyl-1-(4-morpholinophenyl)pyridin-2(1H)-one (2r)

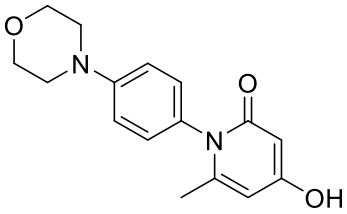

Using 500.0 mg (3.89 mmol) 4-Hydroxy-6-mehtyl-pyrone. 0.50 g, 45%. **^{1}H-NMR** (700 MHz, DMSO-d_6): δ 10.48 (s, 1H), 7.00 (s, 4H), 5.84 (d, *J* = 2.1 Hz, 1H), 5.52 (d, *J* = 2.1 Hz, 1H), 3.76-3.73 (m, 4H), 3.16-3.14 (m, 4H), 1.84 (s, 3H). **^{13}C-NMR** (176 MHz, DMSO-d_6): δ 166.6, 164.79, 150.9, 148.0, 130.4, 129.4, 115.6, 100.2, 96.5, 66.6, 48.6, 21.7. **HRMS**-ESI (m/z): $[M + H]^+$ calculated for $C_{16}H_{19}O_3N_2^+$, 287.1390; found, 287.1393.

4-hydroxy-1-(2-(5-methoxy-1H-indol-3-yl)ethyl)-6-methylpyridin-2(1H)-one (2s)

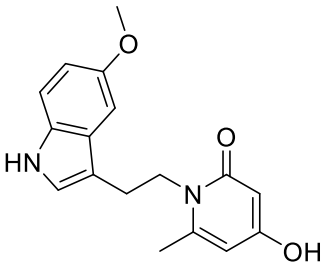

Using 500.0 mg (3.89 mmol) 4-Hydroxy-6-mehtyl-pyrone. 0.41 g, 36%. **^{1}H-NMR** (400 MHz, DMSO-d_6): δ 10.69 (s, 1H), 10.33 (s, 1H), 7.22 (d, *J* = 8.7 Hz, 1H), 7.10 (dd, *J* = 5.8, 2.5 Hz, 2H), 6.70 (dd, *J* = 8.7, 2.5 Hz, 1H), 5.68 (d, *J* = 2.6 Hz, 1H), 5.56 (d, *J* = 2.6 Hz, 1H), 4.10-4.02 (m, 2H), 3.74 (s, 3H), 2.94-2.89 (m, 2H), 2.16 (s, 3H). **^{13}C-NMR** (100 MHz, DMSO-d_6): δ 165.5, 163.8, 153.0, 147.3, 131.3, 127.6, 123.6, 112.0, 111.2, 111.0, 100.1. 99.9, 96.1, 55.2, 44.0, 24.1, 19.8. **HRMS**-ESI (m/z): $[M + H]^+$ calculated for $C_{17}H_{19}O_3N_2^+$, 299.1390; found, 299.1389.

1-(2-(1H-imidazol-4-yl)ethyl)-4-hydroxy-6-methylpyridin-2(1H)-one (2t)[105]

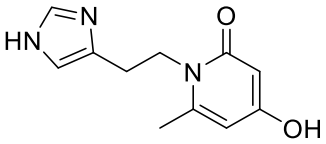

Using 500.0 mg (3.89 mmol) 4-Hydroxy-6-mehtyl-pyrone. 0.56 g, 66%. **^{1}H-NMR** (400 MHz, DMSO-d_6): δ 11.85 (s, 1H), 10.39 (s, 1H), 7.55 (s, 1H), 6.78 (s, 1H), 5.69 (d, *J* = 2.6 Hz, 1H), 5.50 (d , *J* = 2.6 Hz, 1H), 4.01 (dd, *J* = 8.25, 7.0 Hz, 2H), 2.74 (dd, *J* = 8.25, 7.0 Hz, 2H), 2.17 (s, 3H). **^{13}C-NMR** (100 MHz, DMSO-d_6): δ 165.6, 163.6, 147.3, 135.1, 134.9, 134.2, 100.0, 96.0, 43.3, 26.0, 19.8. **HRMS**-ESI (m/z): $[M + H]^+$ calculated for $C_{11}H_{14}O_2N_3^+$, 220.1081; found, 220.1076.

7-hydroxy-5-oxo-1,2,3,5-tetrahydroindolizine-8-carboxylic acid (2zb)[108]

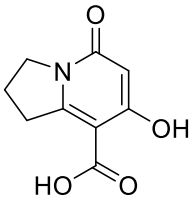

To a solution of methyl 7-hydroxy-5-oxo-1,2,3,5-tetrahydroindolizine-8-carboxylate (**2za**) (0.16 g, 0.76 mmol) in MeOH/THF/H2O (3:2:2) was added LiOH (91.6 mg, 3.82 mmol) and the mixture was stirred at room temperature overnight. The mixture was then concentrated, and the residual mixture was diluted with water and acidified to pH 5. The precipitated solid was filtered off, washed with cold H2O and dried in vacuo to afford the product as a white solid (0.12 g, 82%). **^{1}H-NMR** (500 MHz, DMSO-d_6): δ 5.55 (s, 1H), 3.96 (t, *J* = 7.5 Hz, 1H), 3.43 (t, *J* = 7.8 Hz, 1H), 2.08 (p, *J* = 7.8 Hz, 1H). **^{13}C-NMR** (126 MHz, DMSO-d_6): δ 171.4, 169.0, 161.5, 160.7, 96.4, 96.1, 49.3, 35.3, 20.2. **HRMS**-ESI (m/z): $[M + H]^+$ calculated for $C_9H_{10}O_4N^+$, 196.0604; found, 196.0601.

5.1.3. Synthesis of Dihydropyrans

(±) 6-hydroxy-2H-pyran-3(6H)-one (6a)[50]

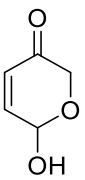

To a solution of furfuryl alcohol (**5a**) (5.00 g, 50.97 mmol) in dichloromethane (100 mL) at 0 °C was added *m*CPBA (13.19 g, 76.45 mmol, 1.5 equiv) in 3 portions over 45 minutes. The reaction mixture was allowed to slowly warm to ambient temperature and stirring was continued for 3 h. The reaction was then cooled to -20 °C and stirred for 15 minutes before removal of insoluble m-chlorobenzoic acid (white precipitate) by filtration. The filtrate was concentrated *in vacuo* and purified by flash column chromatography (EtOAc/Pet. Ether 1:3 to 2:3 to 1:1). The compound was isolated as a white crystalline solid (2.82 g, 48%). **^{1}H-NMR** (400 MHz, $CDCl_3$): δ 6.95 (dd, *J* = 10.4 Hz, 2.9 Hz, 1H), 6.17 (d, *J* =

10.4 Hz, 1H), 5.64 (d, *J* = 2.9 Hz, 1H), 4.58 (d, *J* = 16.9 Hz, 1H), 4.14 (d, *J* = 16.9 Hz, 1H), 3.00 (s, 1H).

(±) 6-((tert-butyldimethylsilyl)oxy)-2H-pyran-3(6H)-one (7a)[50]

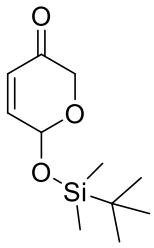

To a solution of **6a** (2.80 g, 24.50 mmol) in THF (25 mL) was added $AgNO_3$ (5.00 g, 29.41 mmol, 1.2 equiv) and pyridine (8.78 mL, 0.11 mol, 4.44 equiv). The suspension was stirred for 20 minutes to allow the dissolution of any large lumps of solid. TBSCl (4.80 g, 31.86 mmol, 1.3 equiv) was added at 0 °C and precipitation of a white solid resulted. The reaction was stirred overnight at room temperature, after which the reaction mixture was filtered through celite and concentrated in vacuo. The resulting crude product was subjected to flash column chromatography (5% EtOAc/Pet. Ether) to afford the desired product as a white crystalline solid (5.33 g, 95%). **^{1}H-NMR** (400 MHz, $CDCl_3$): δ 6.86 (dd, *J* = 10.3 Hz, 3.1 Hz, 1H), 6.08 (d, *J* = 10.3 Hz, 1H), 5.53 (d, *J* = 3.1 Hz, 1H), 4.50 (d, *J* = 16.8 Hz, 1H), 4.07 (d, *J* = 16.8 Hz, 1H), 0.92 (s, 9H), 0.17 (s, 6H).

(±) *Cis* 6-((tert-butyldimethylsilyl)oxy)-3,6-dihydro-2H-pyran-3-ol (8a)[50]

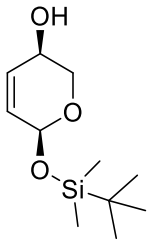

To a cooled (- 20 °C) solution of **7a** (8.20 g, 35.91 mmol) in methanol (34 mL) was added $CeCl_3$ x $7H_2O$ (16.05 g, 43.09 mmol, 1.2 equiv). The reaction mixture was kept at -20 °C and sodium borohydride (1.63 g, 43.09 mmol, 1.2 equiv) was added portionwise over 45 minutes. The reaction was stirred at -20 °C for 3 h before quenching with 35 mL of acetone. The reaction mixture was warmed to room temperature, filtered through celite and concentrated in vacuo. The crude was diluted with water (150 mL) and dichloromethane (150 mL) and filtered through celite. The filtrate was then extracted with dichloromethane (3 x 100 mL) and the combined organic phases were washed with brine (200 mL), dried over $MgSO_4$, filtered and concentrated in vacuo. The crude product was purified by flash column chromatography (Pet. Ether/EtOAc 95:5 to 9:1 to 4:1). The product was isolated as a racemic mixture of the *cis*-isomer as a clear colourless oil (5.074 g, 61%). A mixed fraction of racemic *cis*- and *trans* isomer was isolated as well (*cis:trans* = 0.5:1, 36.7 mg, 0.5%). Overall dr *cis:trans* = 1:0.005. **^{1}H-NMR** *cis*-isomer (400 MHz, $CDCl_3$): δ 5.94 (dd, *J* = 10.3 Hz, 2.7 Hz, 1H), 5.75 (ddd, *J* = 10.3 Hz, 2.3 Hz, 1.7 Hz, 1H), 5.25 (m, 1H), 4.13 (m, 1H), 3.77 (m, 2H), 1.57 (bs, 1H), 0.91 (s, 9H), 0.13 (s, 6H).

(±) *Cis* 6-((tert-butyldimethylsilyl)oxy)-3,6-dihydro-2H-pyran-3-yl methyl carbonate (3a)[50]

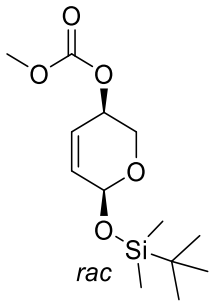

To a solution of **8a** (4.179 g, 18.14 mmol) in degassed DCM (40 mL) was added DMAP (2.770 g, 22.67 mmol, 1.25 equiv), followed by methyl chloroformate (1.750 mL, 22.67 mmol, 1.25 equiv). The reaction was stirred for 1 d at room temperature before concentrating in vacuo and purification by flash column chromatography (5% EtOAc/Pet. Ether). The desired product was isolated as a clear colourless oil (4.191 g, 82% yield). **^{1}H-NMR** (600 MHz, $CDCl_3$): δ 5.91 (dd, *J* = 10.3 Hz, 2.2 Hz, 1H), 5.84 (dt, *J* = 10.3 Hz, 2.0 Hz, 1H), 5.27 (bs, 1H), 5.14-5.09 (m, 1H), 3.92-3.85 (m, 2H), 3.79 (s, 3H), 0.90 (s, 9H), 0.13 (s, 3H), 0.12 (s, 3H). **^{13}C-NMR** (151 MHz, $CDCl_3$): δ 155.4, 132.3, 126.5, 89.3, 68.5, 60.2, 55.0, 25.8, -3.5, -4.3, -5.1.

(±) 6-hydroxy-2-methyl-2H-pyran-3(6H)-one (6b)[53]

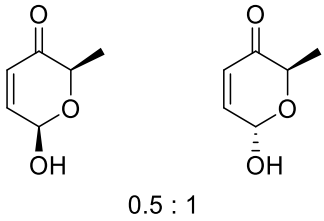

A 250 mL schlenck-flask was evacuated and backfilled with argon. $Na_2S_2O_8$ (11.1 g, 46.82 mmol) and $Ru(bpy)_3Cl_2$ x 6 H_2O (66.8 mg, 0.2 mol%) were added and dissolved in water (85 mL), followed by (±) 1-(2-furyl)-ethanol (**5b**) (5.00 g, 44.59 mmol, 1.0 equiv) in acetonitrile/DMSO (85 mL, 1:1). The reaction mixture was kept in the dark while argon was bubbled through it for 15 minutes. Then the reaction mixture was irradiated in the batch photoreactor with rapid stirring for 4 hours at 25 °C. After completion of reaction the mixture was diluted with brine (60 mL) and extracted with EtOAc (3 x 200 mL). The combined organic phases were dried over $MgSO_4$, filtered and concentrated in vacuo. The crude product was plugged through a short pad of silica and dried in vacuo to afford the product as a mixture of *trans/cis* isomer (1:0.5, 3.85 g, 67%). **^{1}H-NMR** *trans*-isomer (600 MHz, $CDCl_3$): δ 6.89 (dd, *J* = 10.2 Hz, 3.3 Hz, 1H), 6.11 (d, *J* = 10.2 Hz, 1H), 5.63 (d, *J* = 3.3 Hz, 1H), 4.71 (q, *J* = 6.8 Hz, 6.8 Hz, 6.8 Hz, 1H), 3.00 (bs, 1H), 1.39 (d, *J* = 6.8 Hz, 3H). **^{13}C-NMR** *trans*-isomer (151 MHz, $CDCl_3$): δ 196.9, 144.4, 127.3, 87.7, 70.4, 15.3. **^{1}H-NMR** *cis*-isomer (600 MHz, $CDCl_3$): δ 6.94 (dd, *J* = 10.3 Hz, 1.3 Hz, 1H), 6.15 (dd, *J* = 10.3 Hz, 1.5 Hz, 1H), 5.68 (bd, *J* = 1.3 Hz, 1H), 4.23 (qd, *J* = 6.8 Hz, 6.8 Hz, 6.8 Hz, 1.1 Hz, 1H), 1.65 (bs, 1H), 1.46 (d, *J* = 6.8 Hz, 3H). **^{13}C-NMR** *cis*-isomer (151 MHz, $CDCl_3$): δ 196.4, 148.0, 128.6, 91.0, 75.3, 16.3.

(±) 6-((*Tert*-butyldimethylsilyl)oxy)-2-methyl-3,6-dihydro-2H-pyran-3-yl methyl carbonate (3b)

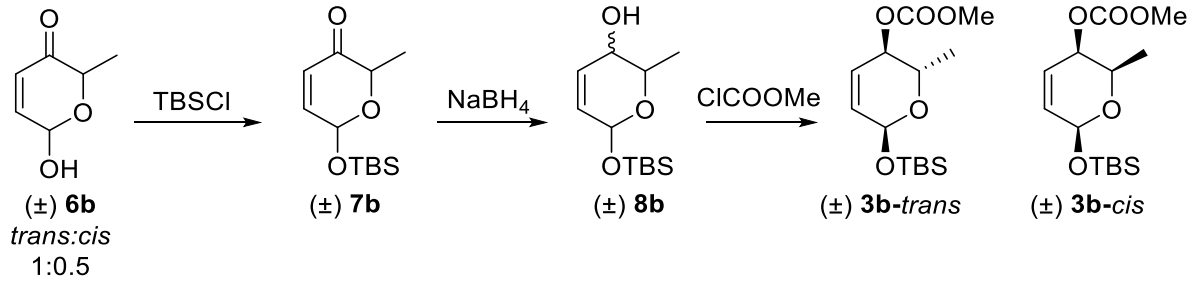

To a solution of **6b** (3.85 g, 30.0 mmol) in THF (140 mL) was added $AgNO_3$ (7.65 g, 45.0 mmol, 1.5 equiv) and pyridine (10.8 mL, 133.2 mmol, 4.44 equiv). The suspension was stirred for 20 minutes to allow the dissolution of any large lumps of solid. TBSCl (6.79 g, 45.0 mmol, 1.5 equiv) was added at 0 °C and precipitation of a white solid resulted. The reaction was stirred overnight and filtered through celite. After dilution with with EtOAc (150 mL) the mixture was washed with saturated $NaHCO_3$ solution (200 mL) and the aqueous phase was extracted with EtOAc (3 x 100 mL). The combined organic phases were washed with brine (200 mL), dried over $MgSO_4$ and concentrated in vacuo. The resulting crude product was plugged through a short pad of silica and the pad was flushed with DCM. Solvents were removed under reduced pressure and the crude was dried under high vacuum overnight to afford the desired product. The crude was dissolved in anhydrous DCM (200 mL) and $CeCl_3$ x 7 H_2O (2.45 g, 6.58 mmol, 0.22 equiv) in MeOH (12 mL) was added at -78 °C, followed by addition of $NaBH_4$ (1.36 g, 35.89 mmol, 1.3 equiv). The reaction was stirred for 4 hours at-78 °C after which it was quenched by addition of Acetone (2.1 mL) and saturated $NaHCO_3$ solution (200 mL). The layers were separated and the aqueous phase was extracted with DCM (3 x 100 mL). The combined organic phases were washed with brine (200 mL), dried over $MgSO_4$ and concentrated in vacuo. The crude was dissolved in anhydrous DCM (200 mL) and cooled to 0 °C. DMAP (0.36 g, 2.99 mmol, 0.1 equiv), pyridine (14.5 mL, 179.21 mmol, 6 equiv) and methyl chloroformate (13.9 mL, 179.21 mmol, 6 equiv) was added and the reaction was allowed to stir overnight at room temperature. The reaction mixture was quenched with saturated $NaHCO_3$ solution (200 mL), extracted with DCM (5 x 50 mL), dried over $MgSO_4$ and concentrated in vacuo. The crude was purified by flash chromatography (Pet. Ether/Tol 9:1 + 1% NEt_3) to afford the desired *trans*-product as a colorless oil (5.86 g, 65%). The *cis*-isomer was isolated in a separated fraction (2.93 g, 32%). **^{1}H-NMR** *trans*-isomer (400 MHz, $CDCl_3$): δ 5.83 (bd, *J* = 10.3 Hz, 1H), 5.78 (ddd, *J* = 10.3 Hz, 2.7 Hz, 1.9 Hz 1H), 5.31 (d, *J* = 1.9 Hz, 1H), 4.85 (ddd, *J* = 9.2 Hz, 2.7 Hz, 1.6 Hz, 1H), 4.04 (dd, *J* = 9.2 Hz, 6.3 Hz, 1H), 3.81 (s, 3H),

1.25 (d, *J* = 6.3 Hz, 1H), 0.90 (s, 9H), 0.12 (s, 6H). **^{13}C-NMR** *trans*-isomer (100 MHz, $CDCl_3$): δ 155.2, 130.8, 127.3, 89.2, 74.9, 64.4, 55.1, 25.8, 18.2, 18.1, -5.2. **^{1}H-NMR** *cis*-isomer (400 MHz, $CDCl_3$): δ 6.01-5.94 (m, 2H), 5.31 (bs, 1H), 4.80-4.78 (m, 1H), 3.85 (ddd, *J* = 6.5 Hz, 6.5 Hz, 2.8 Hz, 1H), 3.78 (s, 3H), 1.27 (d, *J* = 6.5 Hz, 1H), 0.90 (s, 9H), 0.12 (s, 6H). **^{13}C-NMR** *cis*-isomer (100 MHz, $CDCl_3$): δ 155.9, 136.3, 124.2, 92.8, 69.8, 69.6, 55.0, 25.9, 18.3, 16.5, -3.7, -4.5.

(±) 6-hydroxy-2,2-dimethyl-2H-pyran-3(6H)-one (6c)[109]

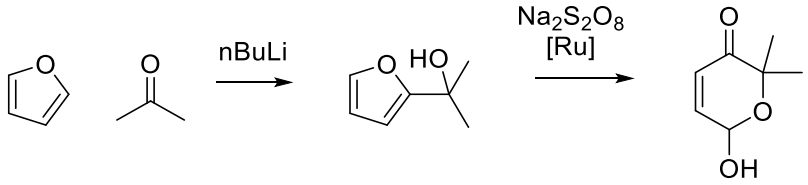

(±) **5c** (±) **6c**

An oven dried flask was evacuated and filled with argon three times. To this flask was added dry THF (160 mL), followed by freshly distilled furan (8.70 mL, 120 mmol, 1.5 equiv). The solution was stirred and cooled to 0° C, and then n-BuLi (38.4 mL, 1.2 equiv, 2.5 M solution in hexanes) was added slowly. The reaction mixture was allowed to stir at 0° C for 1 hour at which point the reaction mixture was cooled to -78° C. Freshly distilled acetone (5.88 mml, 80.0 mmol) was added slowly and the reaction mixture was allowed to stir and warm to room temperature over 18 hours. The resulting reaction mixture was quenched under inert atmosphere via slow addition of saturated saturated NH_4Cl (50 mL) followed by brine (50 mL). The aqueous phase was extracted with EtOAc (3 x 100 mL). The combined organic phases were dried over $MgSO_4$ and concentrated via rotary evaporator. The resulting crude product was dissolved in acetonitrile/DMSO (160 mL, 1:1) and loaded into a 500 mL oven dried schlenck- flask under argon. $Na_2S_2O_8$ (20.0 g, 84.00 mmol, 1.05 equiv) and $Ru(bpy)_3Cl_2$ x 6 H_2O (149.7 mg, 0.2 mol%) dissolved in water (160 mL) were added to the mixture and argon was bubbled through it for 15 minutes in the dark. Then the reaction mixture was irradiated in the batch photoreactor with rapid stirring for 5 hours at 25 °C. After completion of reaction the mixture was diluted with brine (100 mL) and extracted with EtOAc (3 x 200 mL). The combined organic phases were dried over $MgSO_4$, filtered and concentrated in vacuo. The crude product was plugged through a short pad of silica and dried in vacuo to afford the product as colorless oil (5.69 g, 50%). **^{1}H-NMR** (400 MHz, $CDCl_3$): δ 6.87 (dd, *J* = 10.3, 2.1 Hz, 1H), 6.03 (dd, *J* = 10.3, 1.4 Hz, 1H), 5.70 (dd, *J* = 2.1, 1.4 Hz, 1H), 4.63 (d, *J* = 5.9 Hz, 1H), 1.47 (s, 3H), 1.38 (s, 3H).

(±) 6-((tert-butyldimethylsilyl)oxy)-2,2-dimethyl-2H-pyran-3(6H)-one (**7c**)

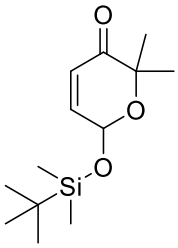

To a solution of **6c** (2.84 g, 20.0 mmol) in THF (200 mL) was added $AgNO_3$ (4.08 g, 24.0 mmol, 1.2 equiv) and pyridine (7.2 mL, 88.8 mmol, 4.44 equiv). The suspension was stirred for 20 minutes to allow the dissolution of any large lumps of solid. TBSCl (6.03 g, 40.0 mmol, 2 equiv) was added at 0 °C and precipitation of a white solid resulted. The reaction was stirred overnight and filtered through celite. After dilution with with EtOAc (150 mL) the mixture was washed with saturated $NaHCO_3$ solution (200 mL) and the aqueous phase was extracted with EtOAc (3 x 100 mL). The combined organic phases were washed with brine (200 mL), dried over $MgSO_4$ and concentrated in vacuo. The resulting crude product was plugged through a short pad of silica and the pad was flushed with DCM. Solvents were removed under reduced pressure to give the product as a colorless oil (5.08 g, 99%). **^{1}H-NMR** (500 MHz, $CDCl_3$): δ δ 6.77 (dd, *J* = 10.3, 2.4 Hz, 1H), 5.99 (dd, *J* = 10.3, 1.2 Hz, 1H), 5.64 (dd, *J* = 2.4, 1.2 Hz, 1H), 1.47 (s, 3H), 1.37 (s, 3H), 0.92 (s, 9H), 0.17 (s, 6H). **^{13}C-NMR** (126 MHz, $CDCl_3$): δ 199.7, 147.4, 125.3, 88.2, 79.3, 27.1, 25.8, 24.1, 18.1, -3.8, -5.0.

(±) 6-((tert-butyldimethylsilyl)oxy)-2,2-dimethyl-3,6-dihydro-2H-pyran-3-yl methyl carbonate (**3c**)

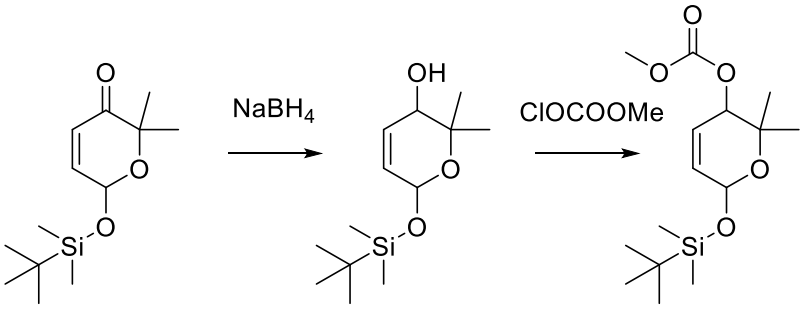

7c (5.05 g, 19.69 mmol) was dissolved in anhydrous DCM (200 mL) and $CeCl_3$ x 7 H_2O (1.61 g, 4.33 mmol, 0.22 equiv) in MeOH (8.5 mL) was added at -78 °C, followed by addition of $NaBH_4$ (0.89 g, 23.63 mmol, 1.2 equiv). The reaction was stirred for 4 hours at-78 °C after which it was quenched by addition of Acetone (10 mL) and saturated $NaHCO_3$ solution (100 mL). The layers were separated and the aqueous phase was extracted with DCM (5 x 50 mL). The combined organic phases were washed with brine (200 mL), dried over $MgSO_4$ and concentrated in vacuo. The crude was dissolved in anhydrous DCM (200 mL) and cooled to 0 °C. DMAP (0.24 g, 1.97 mmol, 0.1 equiv), pyridine (9.5 mL, 118.14 mmol, 6 equiv) and methyl

chloroformate (9.2 mL, 118.14 mmol, 6 equiv) was added and the reaction was allowed to stir overnight at room temperature. The reaction mixture was quenched with saturated $NaHCO_3$ solution (200 mL), extracted with DCM (5 x 50 mL), dried over $MgSO_4$ and concentrated in vacuo. The crude was purified by flash chromatography (Pet. Ether/Tol 9:1 + 1% NEt_3) to give the desired *trans*-product as a white oil (4.20 g, 67%). **^{1}H-NMR** (500 MHz, $CDCl_3$): δ 5.78-5.77 (m, 2H), 5.36-5.34 (m, 1H), 4.94-4.92 (m, 1H), 3.81 (s, 3H), 1.26 (s, 6H), 0.90 (s, 9H), 0.13 (s, 3H), 0.12 (s, 3H). **^{13}C-NMR** (126 MHz, $CDCl_3$): δ 155.8, 131.2, 125.4, 89.0, 75.9, 71.7, 55.1, 26.9, 25.9, 22.4, 18.2, -3.8, -5.0.

(±) 5-oxo-5,6-dihydro-2H-pyran-2-yl acetate (4a)[110]

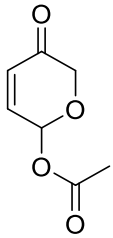

To **6a** (1.75 g, 15.31 mmol) in DCM (150 mL) was added pyridine (1.85 mL, 22.97 mmol, 1.5 equiv) and acetic anhydride (2.17 mL, 22.97 mmol, 1.5 equiv) at 0 °C. The mixture was allowed to warm to room temperature and kept stirring for 2 days. The reaction was quenched by addition of saturated $NaHCO_3$ solution (50 mL) and the layers were separated. The aqueous layer was extracted with EtOAc (3 x 50 mL). The combined organic layers were washed with brine (150 mL), dried over $MgSO_4$ and concentrated in vacuo. Flash chromatography (Pet. Ether/EtOAc 9:1 + 1% NEt_3) afforded the product as a colorless oil (1.77 g, 74%). **^{1}H-NMR** (400 MHz, $CDCl_3$): δ 6.92 (dd, *J* = 10.4, 3.6 Hz, 1H), 6.49 (dd, *J* = 3.6, 0.8 Hz, 1H), 6.27 (d, *J* = 10.4 Hz, 1H), 4.51 (d, *J* = 17.0 Hz, 1H), 4.23 (dd, *J* = 17.0, 0.5 Hz, 1H), 2.14 (s, 3H). **^{13}C-NMR** (100 MHz, $CDCl_3$): δ 193.5, 169.7, 142.4, 128.9, 86.8, 67.5, 21.1.

(±) *Trans*-6-methyl-5-oxo-5,6-dihydro-2H-pyran-2-yl acetate (4b)[111]

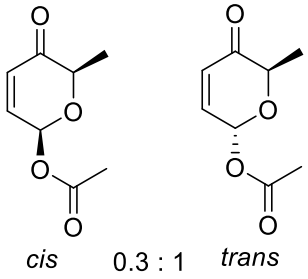

To **6b** (500 mg, 3.90 mmol) in DCM (40 mL) was added pyridine (0.38 mL, 4.68 mmol, 1.2 equiv) and acetic anhydride (0.44 mL, 4.68 mmol, 1.2 equiv) at 0 °C. The mixture was allowed to warm to room temperature and kept stirring for 2 days. The reaction was quenched by addition of saturated $NaHCO_3$ solution (50 mL) and the layers were separated. The aqueous layer was extracted with EtOAc (3 x 50 mL). The combined organic layers were washed with brine (150 mL), dried over $MgSO_4$ and concentrated in vacuo. Flash chromatography (Pet. Ether/EtOAc 1:0 to 4:1) afforded two separated fractions of the racemic *cis*- and desired *trans* isomer (0.3: 1, 595 mg, 90%). **^{1}H-NMR** *trans-isomer* (700 MHz, $CDCl_3$): δ 6.87 (dd, *J* = 10.2 Hz, 3.6 Hz, 1H), 6.48 (d, *J* = 3.6 Hz, 1H), 6.21 (d, *J* = 10.2 Hz, 1H), 4.60 (q, *J* = 6.7 Hz, 6.7 Hz, 6.7 Hz, 1H), 2.14 (s, 3H), 1.41

(d, *J* = 6.7 Hz, 3H). **^{13}C-NMR** *trans*-isomer (176 MHz, $CDCl_3$): δ 196.0, 169.6, 141.8, 128.4, 87.1, 72.5, 21.0, 15.4. **^{1}H-NMR** *cis*-isomer (700 MHz, $CDCl_3$): δ 6.87 (dd, *J* = 10.3 Hz, 3.6 Hz, 1H), 6.55 (bs, 1H), 6.22 (d, *J* = 10.3 Hz, 1H), 4.37 (q, *J* = 7.0 Hz, 7.0 Hz, 7.0 Hz, 1H), 2.15 (s, 3H), 1.49 (d, *J* = 7.0 Hz, 3H). **^{13}C-NMR** *cis*-isomer (176 MHz, $CDCl_3$): δ 195.7, 169.2, 143.7, 128.5, 88.0, 76.0, 21.2, 18.3.

(±) 6,6-dimethyl-5-oxo-5,6-dihydro-2H-pyran-2-yl acetate (4c)[112]

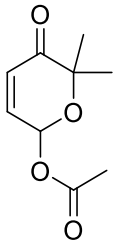

To **6c** (2.84 g, 20.0 mmol) in DCM (200 mL) was added pyridine (4.03 mL, 50.0 mmol, 2.5 equiv) and acetic anhydride (3.77 mL, 40.0 mmol, 2 equiv) at 0 °C. The mixture was allowed to warm to room temperature and kept stirring overnight. The reaction was quenched by addition of saturated $NaHCO_3$ solution (100 mL) and the layers were separated. The aqueous layer was extracted with DCM (3 x 100 mL). The combined organic layers were washed with brine (250 mL), dried over $MgSO_4$ and concentrated in vacuo. Flash chromatography (Pet. Ether/EtOAc 1:0 to 4:1) provided the desired product as a yellow oil (2.06 g, 56%). **^{1}H-NMR** (700 MHz, $CDCl_3$): δ 6.82 (dd, *J* = 10.3, 3.2 Hz, 1H), 6.56 (dd, *J* = 3.2, 1.1 Hz, 1H), 6.16 (dd, *J* = 10.3, 1.1 Hz, 1H), 2.12 (s, 3H), 1.49 (s, 3H), 1.42 (s, 3H). **^{13}C-NMR** (176 MHz, $CDCl_3$): δ 198.4, 169.7, 141.7, 127.1, 86.9, 80.2, 27.2, 21.4.

(±) *Tert*-butyl 2-acetoxy-5-oxo-1-oxa-9-azaspiro[5.5]undec-3-ene-9-carboxylate (4d)

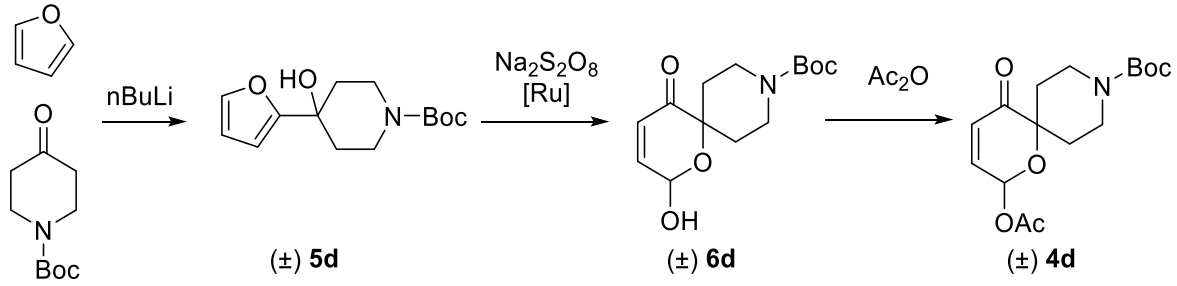

An oven dried flask was evacuated and filled with argon three times. To this flask was added dry THF (125 mL), followed by freshly distilled furan (2.91 mL, 40.15 mmol, 1.6 equiv). The solution was stirred and cooled to 0° C, and then n-BuLi (16.5 mL, 1.05 equiv, 1.6 M solution in hexanes) was added slowly. The reaction mixture was allowed to stir at 0° C for 1 hour at which point the reaction mixture was cooled to -78° C. Tert-butyl 4-oxopiperidine-1-carboxylate (5.00 g, 25.09 mmol) was added slowly and the reaction mixture was allowed to stir and warm to room temperature over 18 hours. The resulting reaction mixture was quenched under inert atmosphere via slow addition of saturated NH_4Cl (50 mL) followed by brine (50

mL). The aqueous phase was extracted with EtOAc (3 x 100 mL). The combined organic phases were dried over $MgSO_4$ and concentrated via rotary evaporator. The resulting crude product was dissolved in acetonitrile/DMSO (50 mL, 1:1) and loaded into a 250 mL oven dried schlenck- flask under argon. $Na_2S_2O_8$ (6.27 g, 26.3 mmol, 1.05 equiv) and $Ru(bpy)_3Cl_2$ x 6 H_2O (37.6 mg, 0.2 mol%) dissolved in water (50 mL) were added to the mixture and argon was bubbled through it for 15 minutes in the dark. Then the reaction mixture was irradiated in the batch photoreactor with rapid stirring for 5 hours at 25 °C. After completion of reaction the mixture was diluted with brine (100 mL) and extracted with EtOAc (3 x 200 mL). The combined organic phases were dried over $MgSO_4$, filtered and concentrated in vacuo. The crude product was plugged through a short pad of silica and dried in vacuo to afford the product as colorless oil (5.90 g, 83%). This was dissolved in DCM (200 mL). Pyridine (4.19 mL, 52.1 mmol, 2.5 equiv) and acetic anhydride (2.36 mL, 25.0 mmol, 1.2 equiv) were then added at 0 °C. The mixture was allowed to warm to room temperature and kept stirring overnight. The reaction was quenched by addition of saturated $NaHCO_3$ solution (100 mL) and the layers were separated. The aqueous layer was extracted with DCM (3 x 100 mL). The combined organic layers were washed with brine (250 mL), dried over $MgSO_4$ and concentrated in vacuo. Flash chromatography (Pet. Ether/EtOAc 1:0 to 9:1) provided the desired product as a yellow solid (6.00 g, 89%). **^{1}H-NMR** (500 MHz, $CDCl_3$): δ 6.83 (dd, *J* = 10.3, 3.2 Hz, 1H), 6.61 (dd, *J* = 3.2, 1.1 Hz, 1H), 6.19 (dd, *J* = 10.3, 1.1 Hz, 1H), 4.07-3.86 (m, 2H), 3.20-2.98 (m, 2H), 2.12 (s, 3H), 2.05-1.99 (m, 2H), 1.76 (td, *J* = 13.1, 4.7 Hz, 1H)1.68-1.61 (m, 1H), 1.46 (s, 9H). **^{13}C-NMR** (126 MHz, $CDCl_3$): δ 196.9, 169.6, 147.0, 141.3, 127.3, 86.7, 79.9, 79.2, 38.1, 31.6, 28,6, 21.2. **HRMS**-ESI (m/z): $[M + H]^+$ calculated for $C_{16}H_{24}NO_6^+$, 326.1598; found, 326.1600.

(±) 2-hydroxy-1-oxa-9-azaspiro[5.5]undec-3-en-5-one (4e)

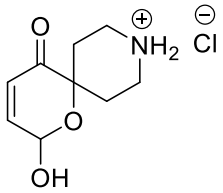

4d (22.0 mg, 0.07 mmol) was treated with HCl in dioaxen (4 M, 1 mL) at room temperature overnight. Diethyl ether (10 mL) and 1 M aqueous HCl (10 mL) were added and the phases were separated. The aqueous phase was concentrated and triturated with diethyl ether. The white precipitate was filtered off and dried in vacuo to afford the desired product (14.7 mg, 99%). **^{1}H-NMR** (500 MHz, DMSO-d_6): δ 8.24 (d, *J* = 5.6 Hz, 1H), 6.47 (d, *J* = 5.6 Hz, 1H), 3.21-3.11 (m, 5H), 3.07-2.97 (m, 1H), 2.73 (dt, *J* = 11.8, 6.0 Hz, 4H). **^{13}C-NMR** (126 MHz, DMSO-d_6): δ 169.6, 145.1, 141.7, 120.9, 119.4, 43.5, 42.9, 24.4, 24.3.

5.1.4. Synthesis of Pyrano-Furo-Pyridones

General procedure 2 (GP2): An oven-dried microwave vial was loaded with 5 mol% superstable Pd(0) catalyst[55] ($Pd[P[3,5\text{-}(CF_3)_2C_6H_3]_3]_3$) and the bis-electrophile under Argon atmosphere. THF (0.2 M) was added and the vial was sealed. After stirring for 10 minutes the bis-nucleophile was added (for pyridones: DMF was added subsequently to afford a 3:1 mixture of THF/DMF with a final concentration of 0.1 M). The sealed vial was then subjected for microwave irradiation (200 W, 100 to 110 °C, 30 to 60 minutes). The reaction mixture was concentrated in vacuo, immobilized on isolute and purified by FC or MPLC.

General procedure 3 (GP3):[50] An oven-dried schlenck-tube was filled with Argon, charged with 10 mol% $Pd(Ph_3)_4$, evacuated and then back-filled with Argon. The bis-electrophile was dissolved in toluene (0.1 M) in a separate vessel under Argon atmosphere and then added to the Pd-catalyst and allowed to stir for 20 min before the bis-nucleophile was added (for pyridones: DMF was added subsequently to afford a 3:1 mixture of toluene/DMF with a final concentration of 0.05 M). After stirring for 3-6 h at room temperature, additional 10 mol% Pd-catalyst were added to the reaction mixture. The mixture was then allowed to stir at room temperature overnight, filtered through celite and concentrated in vacuo. The crude was immobilized on isolute and purified by FC or MPLC.

General procedure 4 (GP4): The glycal substrate was dissolved in DMF (0.1 M) and $Pd(OAc)_2$ together with boronic acid were added. The mixture was stirred overnight, filtered through a short pad of silica and concentrated under reduced pressure. The crude was purified by MPLC.

General procedure 5 (GP5): The glycal substrate was dissolved in acetonitrile/H_2O (1:1, 0.075 M) and NBS (1.5 eq.) was added at room temperature. The mixture was stirred overnight before being quenched by the addition of saturated $NaHCO_3$ and diluted with EtOAc. The layers were separated and the aqueous phase was extracted with EtOAc three times. The combined organic layers were washed with brine, dried over $MgSO_4$ and concentrated in vacuo. The crude was immobilized on isolute and purified by FC or MPLC. The hydrobromination product was dissolved in MeOH (0.1 M) and cooled to 0 °C. $NaBH_4$ (1.2 eq) was added and the reaction mixture was stirred at 0 °C for 30 minutes. The reaction was quenched by addition of acetone (1 mL) and the solvents were removed in vacuo. The crude was immobilized on isolute and purified by MPLC or prep. HPLC.

General procedure 6 (GP6):[112] An oven-dried schlenck-tube was filled with Argon, charged with 5 mol% $Pd(Ph_3)_4$, evacuated and then back-filled with Argon. The bis-electrophile was

dissolved in THF (0.15 M) in a separate vessel under Argon atmosphere and then added to the Pd-catalyst and allowed to stir for 20 min before the bis-nucleophile was added as a solution in DMF (0.4 M) and triethylamine (1 equiv). The mixture was then allowed to stir at room temperature overnight, before being quenched by addition of saturated $NaHCO_3$ solution. The mixture was diluted with EtOAc, the phases were separated, and the aqueous phase was extracted with EtOAc three times. The combined organic layers were washed with brine, dried over $MgSO_4$ and concentrated in vacuo. The crude was immobilized on isolute and purified by FC or MPLC.

General procedure 7 (GP7):[112] To a stirred solution of the bis-electrophile in dry DCM (0.075 M) was added the bis-nucleophile and quinine (1 equiv). After stirring at 60 °C in a sealed vial for 18 h, the solvent was removed under reduced pressure and the crude was purified by MPLC.

5.1.4.1. Synthesis of General Scaffold A Isomers

(±) 3-methyl-5a,9a-dihydro-1H,9H-furo[3,2-c:4,5-c']dipyran-1-one (9a)[50]

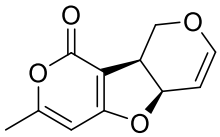

According to GP2, **3a** (200.0 mg, 0.69 mmol) was reacted with 4-hydroxy-6-methyl-pyrone (**1a**) (86.9 mg, 0.69 mmol) at 100 °C for 1 hour. Purification by MPLC (cyclohexane/EtOAc) afforded the product as a white solid (122.4 mg, 86%). **^{1}H-NMR** (600 MHz, DMSO-d_6): δ 6.86 (d, *J* = 6.2 Hz, 1H,), 6.31 (s, 1H,), 5.24 (dd, *J* = 8.3 Hz, 4.3 Hz, 1H), 5.18 (dd, 6.2 Hz, 4.3 Hz, 1H), 4.14 (dd, 10.9 Hz, 4.7 Hz, 1H), 3.55 (dd 10.9 Hz, 9.0 Hz, 1H), 3.44 (td, 9.0 Hz, 8.3 Hz, 4.7 Hz, 1H), 2.22 (s, 3H). **HRMS**-ESI (m/z): $[M + H]^+$ calculated for $C_{11}H_{11}O_4^+$, 207.0652; found, 207.0653.

(±) 3-methyl-5a,6,9,9a-tetrahydro-1H,7H-furo[3,2-c:4,5-c']dipyran-1-one (10a); (±) 4-hydroxy-6-methyl-3-(tetrahydro-2H-pyran-3-yl)-2H-pyran-2-one (11a);

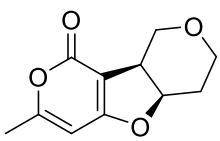

10a

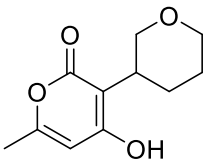

11a

A suspension of **9a** (13.5 mg, 0.07 mmol) and Pd/C (1.3 mg, 10 wt%) in toluene (0.7 mL) was hydrogenated at 20 °C for 7 hours using a H_2-balloon. The catalyst was filtered off and the solvent removed in vacuo. The crude was purified by prep. HPLC to afford the product **11a** (5.0 mg, 37%) and **10a** (7.6 mg, 55%) in separated fractions. **^{1}H-NMR** product **10a** (700 MHz, $CDCl_3$): δ 5.96 (s, 1H), 4.99-4.95 (bm, 1H), 4.05 (dd, *J* = 11.8 Hz, 5.7 Hz, 1H), 3.81 (m, 1H), 3.65 (dd, *J* = 10.9 Hz, 10.9 Hz 1H), 3.54 (dd, *J* = 11.8 Hz, 7.4 Hz, 1H), 3.35 (dd, *J* = 13.4 Hz,

6.7 Hz, 1H), 2.27 (s, 3H) 2.21-2.09 (m, 2H).**^{13}C-NMR** product **10a** (176 MHz, $CDCl_3$): δ 172.5, 166.0, 162.1, 102.4, 96.1, 82.9, 66.6, 62.7, 37.1, 26.7, 20.6. **HRMS**-ESI (m/z) product **10a**: $[M + H]^+$ calculated for $C_{11}H_{13}O_4^+$, 209.0808; found, 209.0807. **^{1}H-NMR** product **11a** (600 MHz, $CDCl_3$): δ 11.50 (s, 1H), 5.83 (s, 1H), 4.16 (bdd, *J* = 11.9 Hz, 4.3 Hz, 1H), 4.09 (bd, *J* = 12.3 Hz, 1H), 3.89 (dd, *J* = 12.3 Hz, 3.3 Hz, 1H), 3.64 (td, *J* = 12.7 Hz, 11.9 Hz, 2.4 Hz, 1H), 3.24 (m, 1H), 2.19 (s, 3H) 1.95 (bd, *J* = 13.9 Hz, 1H), 1.85 (tt, *J* = 13.9 Hz, 13.7 Hz, 4.4 Hz, 4.3 Hz, 1H), 1.69 (ddt, *J* = 20.3 Hz, 12.7 Hz, 4.3 Hz, 4.3 Hz, 1H), 1.56 (bd, *J* = 20.3 Hz, 1H). **^{13}C-NMR** product **11a** (151 MHz, $CDCl_3$): δ 166.5, 166.2, 159.7, 102.8, 102.2, 70.2, 69.7, 33.0, 28.2, 23.0, 19.7. **HRMS**-ESI (m/z) product **11a**: $[M + H]^+$ calculated for $C_{11}H_{15}O_4^+$, 211.0965; found, 211.0965.

(±) 6b,9,10,10a-tetrahydro-6H,7H-pyrano[3',4':4,5]furo[3,2-c]chromen-6-one (10b); (±) 4-hydroxy-3-(tetrahydro-2H-pyran-3-yl)-2H-chromen-2-one (11b)

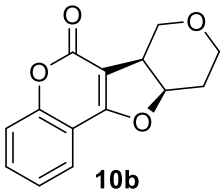

10b

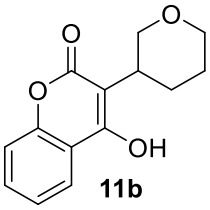

11b

According to GP3, **3a** (50.0 mg, 0.17 mmol) was reacted with **1b** (28.1 mg, 0.17 mmol). Purification by MPLC (cyclohexane/EtOAc 1:0 to 0:1) afforded the product (22.4 mg, 53%). The product was directly suspended with Pd/C (2.5 mg, 10 wt%) in toluene (1.5 mL) and was hydrogenated at 20 °C for 4 hours using a H_2-balloon. The catalyst was filtered off and the solvent removed in vacuo. The crude was purified by prep. HPLC to afford the product **10b** (7.5 mg, 33%) and **11b** (5.4 mg, 28%) in separated fractions. **^{1}H-NMR** product **10b** (700 MHz, $CDCl_3$): δ 7.68 (dd, *J* = 7.9 Hz, 1.5 Hz, 1H) 7.58 (ddd, *J* = 8.5 Hz, 7.7 Hz, 1.5 Hz, 1H), 7.39 (d, *J* = 8.5 Hz, 1H), 7.30 (dd, *J* = 7.9 Hz, 7.7 Hz, 1H), 5.17 (dt, *J* = 10.9 Hz, 4.3 Hz, 4.3 Hz, 1H), 4.13 (dd, *J* = 12.1 Hz, 5.9 Hz, 1H), 3.87 (ddd, *J* = 11.3 Hz, 5.5 Hz, 4.0 Hz, 1H), 3.72 (ddd, *J* = 11.3 Hz, 10.4 Hz, 4.3 Hz, 1H), 3.65 (dd, *J* = 12.1 Hz, 7.4 Hz, 1H) 3.51 (dd, *J* = 10.9 Hz, 7.4 Hz, 1H), 2.30-2.21 (m, 2H). **^{13}C-NMR** product **10b** (176 MHz, CD_2Cl_2): 167.9, 160.7, 155.2, 132.8, 124.2, 122.9, 117.3, 112.8, 105.2, 83.6, 66.5, 62.7, 38.2, 26.7. **HRMS**-ESI (m/z) product **10b**: $[M + H]^+$ calculated for $C_{14}H_{13}O_4^+$, 245.0814; found, 245.0808. **^{1}H-NMR** product **11b** (700 MHz, $CDCl_3$): δ 12.14 (s, 1H), 7.95 (dd, *J* = 7.9 Hz, 1.3 Hz, 1H) 7.52 (dd, *J* = 8.5 Hz, 8.5 Hz, 1H), 7.32-7.28 (m, 2H), 4.25 (dd, *J* = 11.6 Hz, 4.2 Hz, 1H), 4.22 (d, *J* = 12.5 Hz, 1H), 3.98 (d, *J* = 12.5 Hz, 3.2 Hz, 1H), 3.74-3.69 (m, 1H), 3.44-3.40 (m, 1H), 2.03 (d, *J* = 14.1 Hz, 1H), 1.98-1.92 (m, 1H), 1.77 (ddd, *J* = 14 Hz, 4.2 Hz, 4.2 Hz, 1H), 1.61 (bd, *J* = 14.0 Hz, 1H). **^{13}C-NMR** product **11b** (176 MHz, CD_2Cl_2): 167.8, 161.8, 152.4, 131.8, 124.0, 123.9, 117.2, 116.3, 105.2, 70.2, 69.8, 33.5, 28.3, 22.9. **HRMS**-ESI (m/z) product **11b**: $[M + H]^+$ calculated for $C_{14}H_{15}O_4^+$, 247.0965; found, 247.0967.

(±) 7,8-dimethyl-8,9b-dihydro-1H-pyrano[3',4':4,5]furo[3,2-c]pyridin-9(4aH)-one (9c)

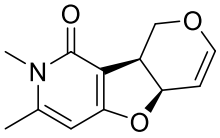

According to GP2, **3a** (1.00 g, 3.47 mmol) was reacted with **2b** (0.48 g, 3.47 mmol) at 110 °C for 1 hour. Purification by MPLC (DCM/MeOH 1:0 to 95:5) afforded the product (0.50 g, 66%). **^{1}H-NMR** (700 MHz, DMSO-d_6): δ 6.81 (d, *J* = 6.2 Hz, 1H), 6.00 (s, 1H), 5.16 (dd, *J* = 6.2 Hz, 4.3 Hz, 1H), 5.04 (dd, *J* = 7.7 Hz, 4.3 Hz, 1H), 4.16 (dd, *J* = 10.7 Hz, 4.8 Hz, 1H), 3.47 (dd, *J* = 10.2 Hz, 10.2 Hz, 1H), 3.39-3.32 (m, 4H), 2.32 (s, 3H). **^{13}C-NMR** (176 MHz, DMSO-d_6): δ 166.4, 160.7, 150.0, 149.5, 105.1, 99.7, 94.3, 76.2, 64.2, 37.5, 29.8, 20.7. **LCMS**-ESI (m/z): 220.16 $[M + H]^+$.

(±) 7,8-dimethyl-4,4a,8,9b-tetrahydro-1H-pyrano[3',4':4,5]furo[3,2-c]pyridin-9(3H)-one (10c)

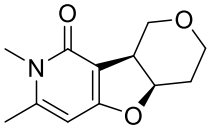

According to GP2, **3a** (50.0 mg, 0.17 mmol) was reacted with **2b** (24.1 mg, 0.17 mmol) at 110 °C for 1 hour. After filtration over celite the crude product was directly suspended with Pd/C (5 mg, 10 wt%) in toluene (1.5 mL) and was hydrogenated at 20 °C for 6 hours using a H_2-balloon. The catalyst was filtered off and the filtrate was diluted with EtOAc (10 mL) and washed with saturated Na_2CO_3 solution (15 mL). The aqueous phase was extracted with EtOAc (3 x 10 mL) and the combined organic layers were washed with brine (50 mL), dried over $MgSO_4$ and concentrated in vacuo. The crude was purified by MPLC (DCM/MeOH 1:0 to 95:5) to afford the product (8.3 mg, 21%). **^{1}H-NMR** (700 MHz, $CDCl_3$): δ 5.88 (s. 1H), 4.87-4.83 (m, 1H), 4.13 (dd, *J* = 11.4, 6.0 Hz, 1H), 3.84-3.80 (m, 1H), 3.63 (td, *J* = 11.4, 3.6 Hz, 1H), 3.50-3.44 (m, 4H), 3.41 (dd, *J* = 14.2, 7.2 Hz, 1H), 2.33 (s, 3H), 2.15 (ddd, *J* = 20.7, 10.6, 5.2 Hz, 1H), 2.08 (dq, *J* = 15.0, 3.3 Hz, 1H). **^{13}C-NMR** (176 MHz, $CDCl_3$): δ 167.5, 161.9, 148.5, 109.1, 95.7, 81.6, 67.4, 62.9, 38.2, 30.7, 27.0, 21.8. **HRMS**-ESI (m/z): $[M + H]^+$ calculated for $C_{12}H_{16}NO_3^+$, 222.1125; found, 222.1124.

(±) 7-methyl-8,9b-dihydro-1H-pyrano[3',4':4,5]furo[3,2-c]pyridin-9(4aH)-one (9d)

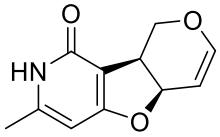

According to GP2, **3a** (20.0 mg, 0.07 mmol) was reacted with **2a** (8.68 mg, 0.07 mmol) at 110 °C for 1 hour. Purification by FC (DCM/MeOH 1:0 to 9:1) afforded the product (15.2 mg, 98%). **^{1}H-NMR** (700 MHz, CD_2Cl_2): δ 6.77 (d, *J* = 6.2 Hz, 1H), 5.95 (s, 1H), 5.33 (s, 1H), 5.20 (dd, *J* = 6.2 Hz, 4.4 Hz, 1H), 5.01 (dd, *J* = 7.0 Hz, 4.4 Hz, 1H), 4.32 (dd, *J* = 10.4 Hz, 4.5 Hz, 1H), 3.55 (dd, *J* = 10.3 Hz, 10.3 Hz, 1H), 3.52-3.49 (m, 1H), 2.31 (s, 3H). **^{13}C-NMR** (176 MHz, CD_2Cl_2): δ 171.5, 162.1, 150.5, 149.0, 106.9, 99.3, 96.8, 78.3, 65.0, 37.5, 19.6. **HRMS**-ESI (m/z): $[M + H]^+$ calculated for $C_{11}H_{12}O_3N^+$, 206.0812; found, 206.0821.

(±) 7-methyl-4,4a,8,9b-tetrahydro-1H-pyrano[3',4':4,5]furo[3,2-c]pyridin-9(3H)-one (10d)

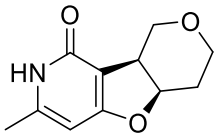

According to GP2, **3a** (50.0 mg, 0.17 mmol) was reacted with **2a** (22.0 mg, 0.17 mmol) at 110 °C for 1 hour. After filtration over celite the crude was purified by FC (EtOAc/MeOH 1:0 to 9:1) and the product was directly suspended with Pd/C (5 mg, 10 wt%) in toluene (2 mL) and was hydrogenated at 20 °C for 6 hours using a H_2-balloon. The catalyst was filtered off and the solvent removed in vacuo. The crude was purified by MPLC (EtOAc/MeOH 1:0 to 9:1) to afford the product (3.6 mg, 10%). **^{1}H-NMR** (700 MHz, CD_2Cl_2): δ 11.80 (s, 1H), 5.82 (s, 1H), 4.89-4.85 (m, 1H), 4.01 (dd, *J* = 11.8, 6.0 Hz, 1H), 3.77-3.73 (m, 1H), 3.61 (td, *J* = 10.9, 3.8 Hz, 1H), 3.52 (dd, *J* = 11.8, 7.5 Hz, 1H), 3.34 (dd, *J* = 13.8, 7.5 Hz, 1H), 2.27 (s, 3H), 2.12 (ddt, *J* = 15.2, 10.3, 5.2 Hz, 1H), 2.04 (dq, *J* = 14.9, 3.8 Hz, 1H). **^{13}C-NMR** (176 MHz, CD_2Cl_2): δ 170.7, 163.5, 148.2, 109.0, 95.0, 82.0, 67.2, 63.2, 38.0, 27.5, 19.5. **HRMS**-ESI (m/z): $[M + H]^+$ calculated for $C_{11}H_{14}NO_3^+$, 208.0968; found, 208.0970.

(±) 8-cyclobutyl-7-methyl-8,9b-dihydro-1H-pyrano[3',4':4,5]furo[3,2-c]pyridin-9(4aH)-one (9e)

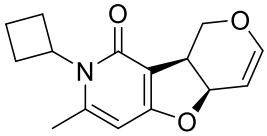

According to GP2, **3a** (50.0 mg, 0.17 mmol) was reacted with **2c** (31.1 mg, 0.17 mmol) at 110 °C for 30 minutes. Purification by MPLC (Pet. Ether/EtOAc 1:0 to 0:1) afforded the product (33.4 mg, 74%). **^{1}H-NMR** (700 MHz, CD_2Cl_2): δ 6.75 (d, *J* = 6.2 Hz, 1H),5.74 (s, 1H), 5.17 (dd, *J* = 6.2, 4.5 Hz, 1H), 4.96 (dd, *J* = 7.5, 4.5 Hz, 1H), 4.72 (p, *J* = 8.8 Hz, 1H), 4.34 (dd, *J* = 10.6, 5.0 Hz, 1H), 3.51 (t, *J* = 10.6 Hz, 1H), 3.45-3.40 (m, 1H), 3.26-3.19 (m, 2H), 2.28-2.18 1.73 (m, 2H), 1.96-1.90 (m, 1H), 1.73 (dq, *J* = 18.3, 9.2 Hz, 1H). **^{13}C-NMR** (176 MHz, CD_2Cl_2): δ 167.2, 163.5, 150.2, 149.1, 108.2, 99.7, 96.1, 77.2, 65.4, 53.2, 38.6, 28.4, 28.1, 22.5, 15.1. **LC-MS**-ESI (m/z): 260.16 $[M + H]^+$.

(±) 8-cyclobutyl-7-methyl-4,4a,8,9b-tetrahydro-1H-pyrano[3',4':4,5]furo[3,2-c]pyridin-9(3H)-one (10e)

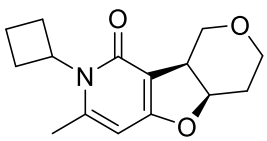

A suspension of **9e** (10.0 mg, 0.04 mmol) and Pd/C (1.0 mg, 10 wt%) in toluene (0.5 mL) was hydrogenated at 20 °C for 6 hours using a H_2-balloon. The catalyst was filtered off and the solvent removed in vacuo. The crude was purified by prep. HPLC to afford product (2.3 mg, 23%). **^{1}H-NMR** A (700 MHz, $CDCl_3$): δ 6.01 (s, 1H), 4.93 (s,10H), 4.81-4.76 (m, 1H), 4.15 (dd, *J* = 11.9, 6.0 Hz, 1H), 3.89-

3.84 (m, 1H), 3.67-3.60 (m, 2H), 3.43 (dd, *J* = 11.9, 7.8 Hz, 1H), 3.20 (dp, *J* = 14.8, 9.9 Hz, 2H), 2.40 (s, 3H), 2.37-2.27 (m, 4H), 2.18 (ddd, *J* = 15.8, 10.5, 5.0 Hz, 1H), 2.11 (dd, *J* = 15.2, 2.6 Hz, 1H), 2.01 (q, *J* = 11.1 Hz, 1H), 1.76 (dt, *J* = 19.2, 9.4 Hz, 2H). **HRMS**-ESI (m/z): $[M + H]^+$ calculated for $C_{15}H_{20}NO_3^+$, 262.1438; found, 262.1439.

(±) 7-methyl-8-(tetrahydro-2H-pyran-4-yl)-4,4a,8,9b-tetrahydro-1H-pyrano[3',4':4,5]furo[3,2-c]pyridin-9(3H)-one (10f)

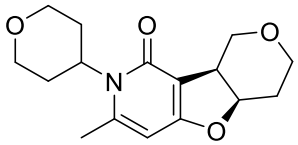

According to GP2, **3a** (75.0 mg, 0.26 mmol) was reacted with **2f** (40.8 mg, 0.20 mmol) at 100 °C for 1 hour. After purification by FC (Hep/EtOAc 1:0 to 1:1) the product was directly suspended with Pd/C (5 mg, 10 wt%) in THF (1.5 mL) and was hydrogenated at 20 °C for 2 hours using a H_2-balloon. The catalyst was filtered off and the solvent removed in vacuo. The crude was purified by FC (EtOAc/MeOH 1:0 to 9:1) to afford the product (7.4 mg, 10%). **^{1}H-NMR** (700 MHz, CD_2Cl_2): δ 5.81 (s, 1H), 4.84-4.81 (m, 1H), 4.03 (dd, *J* = 11.5, 4.6 Hz, 2H), 3.99 (dd, *J* = 11.8, 5.9 Hz, 1H), 3.75-3.71 (m, 1H), 3.61 (td, *J* = 10.5, 3.8 Hz, 1H), 3.54 (dd, *J* = 11.8, 7.5 Hz, 1H), 3.42-3.37 (m, 2H), 3.31 (dd, *J* = 13.7, 7.5 Hz, 1H), 2.37 (s, 3H), 2.10 (ddt, *J* = 15.2, 10.5, 5.2 Hz, 1H), 2.06.1.99 (m, 2H), 1.54-1.45 (m, 2H), 1.34-1.25 (m, 2H). **^{13}C-NMR** (176 MHz, CD_2Cl_2): δ 167.2, 162.8, 148.3, 96.7, 81.8, 68.4, 67.1, 63.1, 39.0, 29.4, 27.5, 22.6. **HRMS**-ESI (m/z): $[M + H]^+$ calculated for $C_{16}H_{22}NO_4^+$, 292.1543; found, 292.1547.

(±) 7-methyl-8-(4-morpholinophenyl)-8,9b-dihydro-1H-pyrano[3',4':4,5]furo[3,2-c]pyridin-9(4aH)-one (9g)

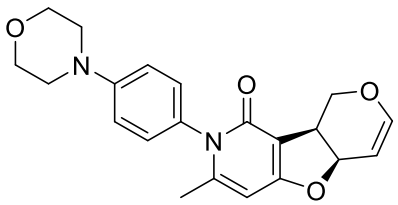

According to GP2, **3a** (50.0 mg, 0.17 mmol) was reacted with **2r** (49.6 mg, 0.17 mmol) at 110 °C for 30 minutes. Purification by FC (Pet. Ether/EtOAc 1:0 to 95:5 + 1% NEt_3) afforded the product (21.0 mg, 33%). **^{1}H-NMR** (700 MHz, CD_2Cl_2): δ 7.07-6.97 (m, 4H), 6.78 (d, *J* = 6.2 Hz, 1H), 5.91 (s, 1H), 5.21 (dd, *J* = 6.2, 4.5 Hz, 1H), 5.04 (dd, *J* = 7.6, 4.5 Hz, 1H), 4.33 (dd, *J* = 10.8, 4.9 Hz, 1H), 3.86-3.82 (m, 4H), 3.55 (t, *J* = 10.8 Hz, 1H), 3.47 (ddd, *J* = 10.8, 7.6, 5.1 Hz, 1H), 3.22-3.19 (m, 4H), 1.94 (s, 1H). **^{13}C-NMR** (176 MHz, CD_2Cl_2): δ 168.2, 162.5, 151.7, 150.3, 150.2, 130.8, 129.3, 129.2, 116.1, 106.9, 99.6, 95.5, 77.5, 67.2, 65.4, 49.3, 38.5, 22.5. **HRMS**-ESI (m/z): $[M + H]^+$ calculated for $C_{21}H_{23}N_2O_4^+$, 367.1652; found, 367.1649.

(±) 7-methyl-8-(4-morpholinophenyl)-4,4a,8,9b-tetrahydro-1H-pyrano[3',4':4,5]furo[3,2-c]pyridin-9(3H)-one (10g)

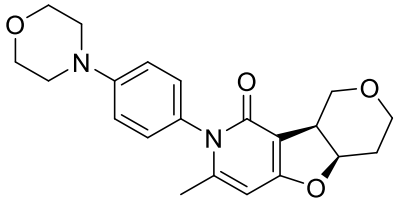

According to GP2, **3a** (50.0 mg, 0.17 mmol) was reacted with **2r** (49.6 mg, 0.17 mmol) at 110 °C for 1 hour. After filtration over celite the crude was purified by FC (Hep/EtOAc 1:0 to 0:1) and the product was directly suspended with Pd/C (5 mg, 10 wt%) in toluene (2 mL) and was hydrogenated at 20 °C for 6 hours using a H_2-balloon. The catalyst was filtered off and the filtrate was diluted with EtOAc (10 mL) and washed with saturated Na_2CO_3 solution (15 mL). The aqueous phase was extracted with EtOAc (3 x 10 mL) and the combined organic layers were washed with brine (50 mL), dried over $MgSO_4$ and concentrated in vacuo. The crude was purified by MPLC (EtOAc/MeOH 1:0 to 9:1 + 0.1% DIPEA) to afford the product (2.0 mg, 3%). **^{1}H-NMR** (700 MHz, CD_2Cl_2): δ 7.07-6.97 (m 4H), 5.93 (s, 1H), 4.92-4.89 (m, 1H), 4.00 (dd, *J* = 11.8, 5.9 Hz, 1H), 3.86-3.82 (m, 4H), 3.78-3.74 (m, 1H), 3.66 (td, *J* = 10.8, 3.9 Hz, 1H), 3.58 (dd, *J* = 11.8, 7.4 Hz, 1H), 3.35 (dd, *J* = 13.6, 7.4 Hz, 1H), 3.21-3.19 (m, 4H), 2.17-2.11 (m, 1H), 2.06 (dq, *J* = 14.9, 3.9 Hz, 1H), 1.94 (s, 1H). **^{13}C-NMR** (176 MHz, CD_2Cl_2): δ 168.4, 162.6, 151.6, 149.8, 131.0, 129.4, 129.2, 116.1, 116.1, 109.2, 95.4, 82.0, 67.2, 67.1, 63.2, 49.3, 38.8, 27.5, 22.5. **HRMS**-ESI (m/z): $[M + H]^+$ calculated for $C_{21}H_{25}N_2O_4^+$, 369.1809; found, 369.1816.

(±) 8-benzyl-7-methyl-8,9b-dihydro-1H-pyrano[3',4':4,5]furo[3,2-c]pyridin-9(4aH)-one (9h)[50]

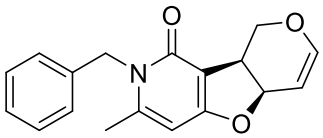

According to GP3, **3a** (50.0 mg, 0.17 mmol) was reacted with **2g** (37.3 mg, 0.17 mmol) in THF (2 mL + 24 µL NEt_3) for 2 days at room temperature. Purification by FC (Hep/EtOAc 4:1 to 1:1 + 1% NEt_3) afforded the product (24.1 mg, 48%). **^{1}H-NMR** (600 MHz, DMSO-d_6): δ 7.33 (t, *J* = 7.5 Hz, 2H), 7.25 (t, *J* = 7.5 Hz, 1H), 7.10 (d, *J* = 7.5 Hz, 2H), 6.84 (d, *J* = 6.2 Hz, 1H), 6.05 (s, 1H), 5.37 (d, *J* = 15.8 Hz, 1H), 5.19 (dd, *J* = 6.2 Hz, 4.3 Hz, 1H), 5.12 (d, *J* = 15.8 Hz, 1H), 5.10 (dd, *J* = 7.5 Hz, 4.3 Hz, 1H), 4.20 (dd, *J* = 10.5 Hz, 4.7 Hz, 1H), 3.52 (dd, *J* = 10.2 Hz, 10.2 Hz, 1H), 3.47-3.42 (m, 1H), 2.22 (s, 3H). **^{13}C-NMR** (151 MHz, DMSO-d_6): δ 166.8, 160.9, 149.8, 149.7, 137.4, 128.7, 127.0, 126.1, 105.3, 99.7, 95.2, 76.4, 64.2, 45.6, 37.6, 20.4. **LCMS**-ESI (m/z): 296.23 $[M + H]^+$.

(±) 8-benzyl-7-methyl-4,4a,8,9b-tetrahydro-1H-pyrano[3',4':4,5]furo[3,2-c]pyridin-9(3H)-one (10h)

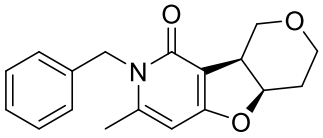

A suspension of **9h** (75.2 mg, 0.25 mmol) and Pd/C (7.5 mg, 10 wt%) in toluene (2 mL) was hydrogenated at 20 °C for 6 hours using a H_2-balloon. The catalyst was filtered off and the solvent removed in vacuo. The crude was purified by prep. HPLC to afford the product (37.0 mg, 49%). **^{1}H-NMR** (700 MHz, CD_2Cl_2): δ 7.33 (t, *J* = 7.5 Hz, 2H), 7.28 (t, *J* = 7.5 Hz, 1H), 7.11 (d, *J* = 7.5 Hz, 2H), 6.10 (s, 1H), 5.45 (d, *J* = 15.6 Hz, 1H), 5.25 (d, *J* = 15.6 Hz, 1H), 4.96 (dt, *J* = 7.3, 3.8 Hz, 1H), 4.09 (dd, *J* = 11.5, 5.8 Hz, 1H), 3.83 (ddd, *J* = 11.0, 5.6, 2.9 Hz, 1H), 3.63 (td, *J* = 11.0, 3.8 Hz, 1H), 3.47 (dd, *J* = 13.9, 7.3 Hz, 1H), 3.43 (dd, *J* = 11.5, 8.1 Hz, 1H), 2.31 (s, 3H), 2.18 (ddd, *J* = 21.1, 10.6, 5.2 Hz, 1H), 2.11 (dq, *J* = 15.1, 3.1 Hz, 1H). **^{13}C-NMR** (176 MHz, CD_2Cl_2): δ 169.7, 162.4, 150.3, 136.6, 129.2, 127.9, 126.6, 110.2, 98.4, 83.0, 67.1, 63.0, 47.8, 38.3, 26.9, 21.5. **HRMS**-ESI (m/z): $[M + H]^+$ calculated for $C_{18}H_{20}NO_3^+$, 298.1438; found, 298.1430.

(±) 8-(4-methoxybenzyl)-7-methyl-8,9b-dihydro-1H-pyrano[3',4':4,5]furo[3,2-c]pyridin-9(4aH)-one (9i)

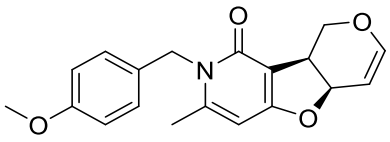

According to GP2, **3a** (28.0 mg, 0.10 mmol) was reacted with **2k** (23.8 mg, 0.10 mmol) at 100 °C for 1 hour. Purification by FC (Hep/EtOAc 1:0 to 1:1) afforded the product (24.3 mg, 77%). **^{1}H-NMR** (700 MHz, CD_2Cl_2): δ 7.07 (d, *J* = 8.7 Hz, 2H), 6.85 (d, *J* = 8.7 Hz, 2H), 6.79 (d, *J* = 6.2 Hz, 1H), 5.97 (s, 1H), 5.34 (d, *J* = 16.4 Hz, 1H), 5.22 (dd, *J* = 6.2 Hz, 4.3 Hz, 1H), 5.14 (d, *J* = 16.4 Hz, 1H), 5.06 (dd, *J* = 7.1 Hz, 4.3 Hz, 1H), 4.39 (dd, *J* = 9.9 Hz, 4.3 Hz, 1H), 3.55-3.47 (m, 2H), 2.29 (s, 3H). **^{13}C-NMR** (176 MHz, CD_2Cl_2): δ 168.7, 162.3, 159.4, 150.5, 150.2, 128.9, 128.1, 114.5, 107.5, 99.2, 97.5, 78.0, 65.2, 55.7, 46.9, 38.2, 21.5. **HRMS**-ESI (m/z): $[M + H]^+$ calculated for $C_{19}H_{20}O_4N^+$, 326.1387; found, 326.1387.

(±) 8-(4-methoxybenzyl)-7-methyl-4,4a,8,9b-tetrahydro-1H-pyrano[3',4':4,5]furo[3,2-c]pyridin-9(3H)-one (10i)

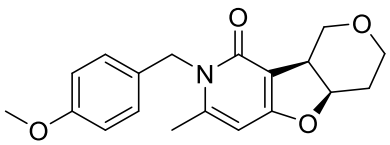

According to GP2, **3a** (50.0 mg, 0.17 mmol) was reacted with **2k** (42.5 mg, 0.17 mmol) at 110 °C for 1 hour. After filtration over celite the crude was suspended with Pd/C (5 mg, 10 wt%) in toluene (1.7 mL) and was hydrogenated at 20 °C for 6 hours using a H_2-balloon. The catalyst was filtered off and the filtrate was diluted with EtOAc (10 mL) and washed with saturated

Na_2CO_3 solution (15 mL). The aqueous phase was extracted with EtOAc (3 x 10 mL) and the combined organic layers were washed with brine (50 mL), dried over $MgSO_4$ and concentrated in vacuo. The crude was purified by MPLC (cyclohexane/EtOAc 1:0 to 0:1) to afford the product (7.2 mg, 13%). **^{1}H-NMR** (600 MHz, CD_2Cl_2): δ 7.07 (d, *J* = 8.7 Hz, 2H), 6.84 (d, *J* = 8.7 Hz, 2H), 5.86 (s, 1H), 5.29 (d, *J* = 15.4 Hz, 1H), 5.07 (d, *J* = 15.4 Hz, 1H), 4.91-4.87 (m, 1H), 4.05 (dd, *J* = 11.7, 5.9 Hz, 1H), 3.79-3.75 (m, 4H), 3.63 (td, *J* = 10.9, 3.7 Hz, 1H), 3.54 (dd, *J* = 11.7, 7.5 Hz, 1H), 3.39 (dd, *J* = 13.7, 7.5 Hz, 1H), 2.25 (s, 3H), 2.17-2.11 (m, 1H), 2.08-2.02 (m, 1H). **^{13}C-NMR** (151 MHz, CD_2Cl_2): δ 170.0, 162.1, 159.2, 149.3, 129.6, 128.1, 114.4, 109.2, 96.1, 82.0, 67.3, 63.1, 55.6, 46.3, 38.7, 27.5, 21.5. **HRMS**-ESI (m/z): $[M + H]^+$ calculated for $C_{19}H_{22}NO_4^+$, 328.1543; found, 328.1544.

(±) 8-(4-fluorobenzyl)-7-methyl-4,4a,8,9b-tetrahydro-1H-pyrano[3',4':4,5]furo[3,2-c]pyridin-9(3H)-one (10j)

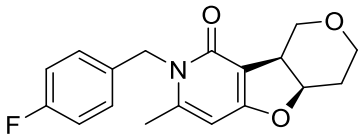

According to GP2, **3a** (75.9 mg, 0.26 mmol) was reacted with **2h** (45.0 mg, 0.20 mmol) at 100 °C for 1 hour. After filtration over celite the crude was purified by FC (Hep/EtOAc 1:0 to 1:1) and the product was directly suspended with Pd/C (5 mg, 10 wt%) in toluene (2 mL) and was hydrogenated at 20 °C for 9 hours using a H_2-balloon. The catalyst was filtered off and the solvent removed in vacuo. The crude was purified by MPLC (EtOAc/MeOH 1:0 to 9:1 + 0.1% DIPEA) to afford the product (24.7 mg, 40%). **^{1}H-NMR** (600 MHz, CD_2Cl_2): δ 7.13 (dd, *J* = 8.7, 5.4 Hz, 2H), 7.01 (t, *J* = 8.7 Hz, 2H), 5.88 (s, 1H), 5.35 (d, *J* = 15.4 Hz, 1H), 5.11 (d, *J* = 15.4 Hz, 1H), 4.92-4.88 (m, 1H), 4.04 (dd, *J* = 11.7, 5.9 Hz, 1H), 3.79-3.74 (m, 1H), 3.63 (td, *J* = 10.8, 3.8 Hz, 1H), 3.56 (dd, *J* = 11.7, 7.5 Hz, 1H), 3.39 (dd, *J* = 13.7, 7.5 Hz, 1H), 2.24 (s, 3H), 2.14 (ddd, *J* = 20.5, 10.3, 5.2 Hz, 1H), 2.05 (dq, *J* = 15.0, 3.8 Hz, 1H). **^{13}C-NMR** (151 MHz, CD_2Cl_2): δ 168.1, 163.2, 161.5, 161.9, 149.1, 133.6, 128.6, 128.5, 115.9, 115.8, 109.3, 96.3, 82.0, 67.2, 63.1, 46.1, 38.8, 27.4, 21.4. **HRMS**-ESI (m/z): $[M + H]^+$ calculated for $C_{18}H_{19}FNO_3^+$, 316.1344; found, 316.1348.

(±) 7-methyl-8-(thiophen-2-ylmethyl)-4,4a,8,9b-tetrahydro-1H-pyrano[3',4':4,5]furo[3,2-c]pyridin-9(3H)-one (10k)

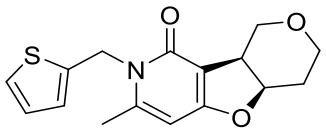

According to GP2, **3a** (50.0 mg, 0.17 mmol) was reacted with **2l** (43.2 mg, 0.17 mmol) at 100 °C for 1 hour. After filtration over celite the crude was purified by FC (Hep/EtOAc 1:0 to 1:1) and the product was directly suspended with Pd/C (5 mg, 10 wt%) in toluene (2 mL) and was

hydrogenated at 20 °C for 14 hours using a H_2-balloon. The catalyst was filtered off and the solvent removed in vacuo. The crude was purified by MPLC (cyclohexane/EtOAc 1:0 to 0:1) to afford the product (9.7 mg, 16%). **^{1}H-NMR** (700 MHz, CD_2Cl_2): δ 7.22 (dd, *J* = 5.1, 1.0 Hz, 1H), 6.97 (dd, *J* = 3.4, 1.0 Hz, 1H), 6.93 (dd, *J* = 5.1, 3.4 Hz, 1H), 5.85 (s, 1H), 5.43 (d, *J* = 15.4 Hz, 1H), 5.24 (d, *J* = 15.4 Hz, 1H), 4.89-4.85 (m, 1H), 4.04 (dd, *J* = 11.8, 5.9 Hz, 1H), 3.78-3.73 (m, 1H), 3.61 (td, *J* = 10.6, 3.8 Hz, 1H), 3.55 (dd, *J* = 11.8, 7.5 Hz, 1H), 3.38 (dd, *J* = 13.7, 7.5 Hz, 1H), 2.40 (s, 3H), 2.12 (ddt, *J* = 15.2, 10.6, 5.2 Hz, 1H), 2.05-2.00 (m, 1H). **^{13}C-NMR** (176 MHz, CD_2Cl_2): δ 168.3, 161.7, 148.7, 140.2, 126.9, 126.6, 125.8, 109.3, 96.2, 82.0, 67.1, 63.1, 42.5, 38.7, 27.4, 21.2. **HRMS**-ESI (m/z): $[M + H]^+$ calculated for $C_{16}H_{18}NO_3S^+$, 304.1002; found, 304.1003.

(±) 7-methyl-8-(pyridin-2-ylmethyl)-4,4a,8,9b-tetrahydro-1H-pyrano[3',4':4,5]furo[3,2-c]pyridin-9(3H)-one (10l)

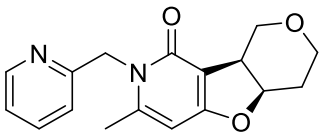

According to GP2, **3a** (63.5 mg, 0.22 mmol) was reacted with **2m** (43.2 mg, 0.20 mmol) at 100 °C for 18 hours. After filtration over celite the crude was purified by MPLC (cyclohexane/EtOAc 1:0 to 0:1 + 0.1% NEt_3) and an aliquot of the product (10 mg, 0.03 mmol) was directly suspended with Pd/C (5 mg, 10 wt%) in toluene (2 mL) and was hydrogenated at 20 °C for 24 hours using a H_2-balloon. The catalyst was filtered off and the solvent removed in vacuo and the crude was purified by prep. HPLC to afford the product (3.8 mg, 38%). **^{1}H-NMR** (600 MHz, $CDCl_3$): δ 8.73 (dt, *J* = 5.5, 1.6 Hz, 1H), 8.05 (td, *J* = 7.8, 1.6 Hz, 1H), 7.57 (ddd, *J* = 7.8, 5.5, 1.2 Hz, 1H), 7.44 (d, *J* = 7.8 Hz, 1H), 6.06 (s, 1H), 5.70 (d, *J* = 16.7 Hz, 1H), 5.60 (d, *J* = 16.7 Hz, 1H), 4.97 (dt, *J* = 7.5, 3.8 Hz, 1H), 4.11 (dd, *J* = 11.3, 5.4 Hz, 1H), 3.86 (ddd, *J* = 11.3, 5.8, 3.2 Hz, 1H), 3.67 (td, *J* = 11.3, 3.8 Hz, 1H), 3.54-3.45 (m, 2H), 2.36 (s, 3H), 2.20 (dddd, *J* = 15.2, 10.5, 5.8, 4.5 Hz, 1H), 2.13 (dq, *J* = 15.2, 3.8 Hz, 1H). **^{13}C-NMR** (151 MHz, $CDCl_3$): δ 169.5, 161.9, 154.3, 149.2, 145.0, 142.4, 124.5, 123.9, 109.8, 98.2, 82.5, 66.7, 62.7, 46.4, 38.0, 26.7, 21.6. **HRMS**-ESI (m/z): $[M + H]^+$ calculated for $C_{17}H_{19}N_2O_3^+$, 299.1390; found, 299.1392.

(±) 7-methyl-8-(pyridin-4-ylmethyl)-4,4a,8,9b-tetrahydro-1H-pyrano[3',4':4,5]furo[3,2-c]pyridin-9(3H)-one and (±) 4-hydroxy-6-methyl-1-(pyridin-4-ylmethyl)-3-(tetrahydro-2H-pyran-3-yl)pyridin-2(1H)-one (10ma+10mab)

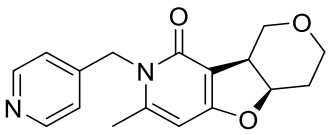

10ma

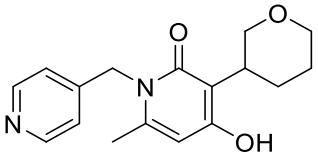

10mb

According to GP2, **3a** (50.0 mg, 0.17 mmol) was reacted with **2n** (37.5 mg, 0.17 mmol) at 110 °C for 1 hour. After filtration over celite the crude was purified by FC (Hep/EtOAc 1:0 to 1:1) and the product was directly suspended with Pd/C (5 mg, 10 wt%) in toluene (2 mL) and was hydrogenated at 20 °C for 12 hours using a H_2-balloon. The catalyst was filtered off and the solvent removed in vacuo. The crude was purified by MPLC (EtOAc/MeOH 1:0 to 4:1 + 0.1% DIPEA) to afford an inseparable mixture of products a and b (ratio of 2:1 by NMR, 15.0 mg, 30%). **^{1}H-NMR** product **10ma** (500 MHz, $CDCl_3$): δ 8.51 (d, *J* = 6.0 Hz, 2H), 7.06 (d, *J* = 6.0 Hz, 2H), 6.13 (s, 1H), 5.35 (d, *J* = 17.0 Hz, 1H), 5.17 (d, *J* = 17.0 Hz, 2H), 4.99-4.95 (m, 1H), 3.85 (dd, *J* = 11.5, 5.6 Hz, 1H), 3.67 (dt, *J* = 10.1, 4.9 Hz, 1H), 3.53 (dd, *J* = 11.5, 6.6 Hz, 1H), 3.51-3.48 (m, 1H), 3.30 (dd, *J* = 13.6, 6.6 Hz, 1H), 2.21 (s, 3H), 2.09-2.05 (m, 1H), 1.92 (dq, *J* = 12.8, 4.1 Hz, 1H). **^{13}C-NMR** product **10ma** (126 MHz, $CDCl_3$): δ 167.3, 160.7, 149.8, 149.2, 146.7, 121.2, 107.7, 95.6, 81.0, 65.5, 62.0, 44.9, 37.9, 26.5, 20.5. **HRMS**-ESI (m/z) product **10ma**: $[M + H]^+$ calculated for $C_{17}H_{19}N_2O_3^+$, 299.1390, found, 299.1391. **^{1}H-NMR** product **10mb** (500 MHz, $CDCl_3$): δ 10.35 (s, 1H), 8.50-8.48 (m, 2H), 7.03 (d, *J* = 6.0 Hz, 2H), 5.86 (s, 1H), 5.20-5.16 (m, 2H), 3.91 (d, *J* = 10.8 Hz, 1H), 3.82-3.77 (m, 1H), 3.56-3.49 (m, 1H), 3.29-3.24 (m, 1H), 3.22-3.15 (m, 1H), 2.34-2.27 (m, 1H), 2.10 (s, 3H), 1.57-1.50 (m, 3H). **UHPCL-MS**-ESI (m/z) product **10mb**: 301.0 $[M + H]^+$.

(±) 7-methyl-8-((3-methylpyridin-4-yl)methyl)-8,9b-dihydro-1H-pyrano[3',4':4,5]furo[3,2-c]pyridin-9(4aH)-one (9n)

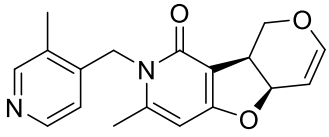

According to GP2, **3a** (95.2 mg, 0.33 mmol) was reacted with **2o** (69.1 mg, 0.30 mmol) at 100 °C for 18 hours. Purification by MPLC (cyclohexane/EtOAc 1:0 to 0:1) afforded the product (68.6 mg, 74%). **^{1}H-NMR** (600 MHz, CD_2Cl_2): δ 8.38 (s, 1H), 8.30 (d, *J* = 5.1 Hz, 1H), 6.78 (d, *J* = 5.8 Hz, 1H), 6.51 (d, *J* = 5.1 Hz, 1H), 5.94 (s, 1H), 5.29 (d, *J* = 17.3 Hz, 1H), 5.22 (dd, *J* = 5.8, 4.3 Hz, 1H), 5.09-5.04 (m, 2H), 4.34 (dd, *J* = 10.4, 4.7 Hz, 1H), 3.57 (t, *J* = 10.4 Hz, 1H), 3.53-3.50 (m, 1H), 2.36 (s, 3H), 2.16 (s, 3H). **^{13}C-NMR** (151 MHz, CD_2Cl_2): δ 167.8, 161.4, 150.8,

150.1, 148.3, 148.2, 144.3, 130.5, 118.8, 106.6, 99.3, 96.3, 77.4, 65.0, 43.7, 38.2, 20.9, 15.8. **HRMS**-ESI (m/z): $[M + H]^+$ calculated for $C_{18}H_{19}O_3N_2$, 311.1390; found, 311.1390.

(±) 8-(2-(5-methoxy-1H-indol-3-yl)ethyl)-7-methyl-4,4a,8,9b-tetrahydro-1H-pyrano[3',4':4,5]furo[3,2-c]pyridin-9(3H)-one (10o)

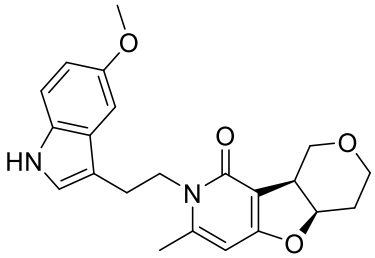

According to GP2, **3a** (63.5 mg, 0.22 mmol) was reacted with **2s** (59.7 mg, 0.20 mmol) at 110 °C for 1 hour. After filtration over celite the crude was purified by MPLC (cyclohexane/EtOAc 1:0 to 0:1 + 0.1% NEt_3) and the product was directly suspended with Pd/C (5 mg, 10 wt%) in toluene (2 mL) and was hydrogenated at 20 °C for 24 hours using a H_2-balloon. The catalyst was filtered off and the solvent removed in vacuo and the crude was purified by prep. HPLC to afford the product (17.4 mg, 23%). **^{1}H-NMR** (500 MHz, $CDCl_3$): δ 8.02 (s, 1H), 7.24 (d, *J* = 8.7, 1H), 7.08 (d, *J* = 2.4 Hz, 1H), 6.98 (d, *J* = 2.3 Hz, 1H), 6.86 (dd, *J* = 8.7, 2.4 Hz, 1H), 5.96 (s, 1H), 4.92 (dt, *J* = 7.6, 3.6 Hz, 1H), 4.35 (dt, *J* = 14.6, 7.5 Hz, 1H), 4.21 (dd, *J* = 14.6, 6.7 Hz, 1H), 4.16 (dd, *J* = 11.8, 5.9 Hz, 1H), 3.64 (td, *J* = 11.2, 3.9 Hz, 1H), 3.52 (td, *J* = 7.6, 5.9 Hz, 1H), 3.44 (dd, *J* = 11.8, 8.1 Hz, 1H), 3.13 (t, *J* = 7.5 Hz, 2H), 2.23 (s, 3H), 2.21-2.15 (m, 1H), 2.12 (dq, *J* = 15.0, 3.6 Hz, 1H). **^{13}C-NMR** (126 MHz, $CDCl_3$): δ 168.9, 161.9, 154.3, 149.0, 131.4, 127.8, 123.2, 112.6, 112.1, 110.3, 100.4, 97.8, 82.4, 67.1, 62.7, 56.0, 46.0, 37.9, 26.7. **HRMS**-ESI (m/z): $[M + H]^+$ calculated for $C_{22}H_{25}N_2O_4^+$, 381.1809; found, 381.1807.

(±) 1,2,3,4,5b,8,9,9a-octahydro-5H,6H-cyclopenta[b]pyrano[3',4':4,5]furo[2,3-d]pyridin-5-one (10p)

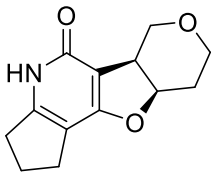

According to GP2, **3a** (67.5 mg, 0.23 mmol) was reacted with **2x** (29.5 mg, 0.20 mmol) at 110 °C for 1 hour. After filtration over celite the crude was purified by FC (cyclohexane/EtOAc 1:0 to 0:1) and the product was directly suspended with Pd/C (5 mg, 10 wt%) in toluene (2 mL) and was hydrogenated at 20 °C for 12 hours using a H_2-balloon. The catalyst was filtered off and the solvent removed in vacuo. The crude was purified by MPLC (EtOAc/MeOH 1:0 to 9:1) to afford the product (15.5 mg, 32%). **^{1}H-NMR** (600 MHz, $CDCl_3$): δ 5.00-4.96 (m, 1H), 4.13-4.07 (m, 1H), 3.85 (ddd, *J* = 11.3, 5.7, 3.4 Hz, 1H), 3.66 (td, *J* = 11.3, 4.0 Hz, 1H), 3.49-3.44 (m, 2H), 2.93 (t, *J* = 7.7 Hz, 2H), 2.80-2.76 (m, 2H), 2.23-2.12 (m, 4H). **^{13}C-NMR** (151 MHz, $CDCl_3$): δ 169.0, 161.5, 153.9, 111.3, 109.0, 83.0, 62.8, 37.1, 31.3, 26.7, 26.7, 23.2. **HRMS**-ESI (m/z): $[M + H]^+$ calculated for $C_{13}H_{16}NO_3^+$, 234.1125; found, 234.1127.

(±) 11-oxo-4a,7,8,9,11,11b-hexahydro-1H-pyrano[3',4':4,5]furo[3,2-f]indolizine-6-carboxylic acid (9q)

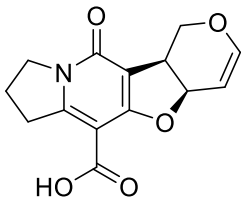

According to GP2, **3a** (63.5 mg, 0.22 mmol) was reacted with **2zb** (39.0 mg, 0.20 mmol) at 110 °C for 1 hour. After filtration over celite the crude was purified by FC (cyclohexane/EtOAc 1:0 to 0:1 + 0.1% acetic acid) and repurified by prep. HPLC to afford the product (4.0 mg, 7%). **^{1}H-NMR** (700 MHz, Acetone): δ 9.59 (d, *J* = 8.0 Hz, 1H), 7.87 (dd, *J* = 15.4, 11.4 Hz, 1H), 7.41 (ddd, *J* = 15.0, 11.4, 0.8 Hz, 1H), 7.34 (d, *J* = 15.4 Hz, 1H), 6.13 (dd, *J* = 15.0, 8.0 Hz, 1H), 4.17-4.12 (m, 2H), 3.64 (t, *J* = 7.9 Hz, 2H), 2.24 (p, *J* = 7.9 Hz, 2H), 2.07-2.06 (m, 2H). **^{13}C-NMR** (176 MHz, Acetone): δ 193.7, 172.5, 160.9, 160.9, 156.4, 135.0, 130.3, 127.6, 105.6, 95.9, 95.9, 50.4, 36.3, 20.5. **HRMS**-ESI (m/z): $[M + H]^+$ calculated for $C_{14}H_{14}NO_5^+$, 276.0867; found, 276.0874.

(±) 6b,9,10,10a-tetrahydro-7H-pyrano[3',4':4,5]furo[3,2-c]quinolin-6(5H)-one (10r)

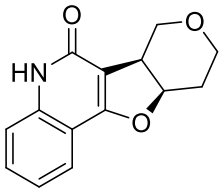

According to GP2, **3a** (75.9 mg, 0.26 mmol) was reacted with **2u** (31.4 mg, 0.20 mmol) at 100 °C for 1 hour. After filtration over celite the crude was purified by FC (cyclohexane/EtOAc 1:0 to 1:1) and the product was directly suspended with Pd/C (5 mg, 10 wt%) in toluene (2 mL) and was hydrogenated at 20 °C for 48 hours using a H_2-balloon. The catalyst was filtered off and the solvent removed in vacuo. The crude was purified by MPLC (EtOAc/MeOH 1:0 to 95:5) to afford the product (4.5 mg, 10%). **^{1}H-NMR** (500 MHz, CD_2Cl_2): δ 11.30 (s, 1H), 7.72 (dd, *J* = 8.3, 1.0 Hz, 1H), 7.53 (ddd, *J* = 8.3, 7.7, 1.4 Hz, 1H), 7.36 (d, *J* = 8.3 Hz, 1H), 7.22 (dd, *J* = 8.3, 7.7 Hz, 1H), 5.13-5.09 (m, 1H), 4.14 (dd, *J* = 11.7, 5.9 Hz, 1H), 3.86-3.80 (m, 1H), 3.69 (ddd, *J* = 11.7, 10.1, 4.5 Hz, 1H), 3.64 (dd, *J* = 11.7, 7.7 Hz, 1H), 3.55 (dd, *J* = 13.6, 7.7 Hz, 1H), 2.28-2.15 (m, 2H). **^{13}C-NMR** (126 MHz, CD_2Cl_2): δ 165.8, 163.1, 140.0, 131.4, 122.7, 122.4, 116.3, 112.3, 111.4, 82.9, 67.3, 63.2, 38.8, 27.4. **HRMS**-ESI (m/z): $[M + H]^+$ calculated for $C_{14}H_{14}NO_3^+$, 244.0968; found, 244.0970.

(±) 5-methyl-6b,9,10,10a-tetrahydro-7H-pyrano[3',4':4,5]furo[3,2-c]quinolin-6(5H)-one (10s)

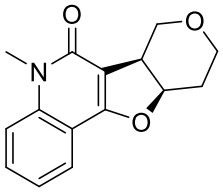

According to GP2, **3a** (75.9 mg, 0.26 mmol) was reacted with **2w** (34.2 mg, 0.20 mmol) at 100 °C for 1 hour. After filtration over celite the crude was purified by FC (cyclohexane/EtOAc 1:0 to 1:1) and the product was directly suspended with Pd/C (5 mg, 10 wt%) in toluene (2 mL) and was

hydrogenated at 20 °C for 6 hours using a H_2-balloon. The catalyst was filtered off and the solvent removed in vacuo. The crude was purified by MPLC (cyclohexane/EtOAc 1:0 to 0:1) to afford the product (26.1 mg, 52%). **^{1}H-NMR** (500 MHz, $CDCl_3$): δ 7.78 (dd, *J* = 7.5, 1.4 Hz, 1H), 7.60 (ddd, *J* = 8.7, 7.3, 1.4 Hz, 1H), 7.38 (d, *J* = 8.7 Hz, 1H), 7.25 (dd, *J* = 7.5, 7.3 Hz, 2H), 5.07-5.03 (m, 1H), 4.25-4.17 (m, 1H), 3.88 (dt, *J* = 11.4, 4.5 Hz, 1H), 3.72-3.66 (m, 4H), 3.60-3.53 (m, 2H), 2.27-2.20 (m, 2H). **^{13}C-NMR** (126 MHz, $CDCl_3$): δ 163.6, 161.3, 140.9, 131.4, 123.3, 121.8, 114.7, 112.9, 111.3, 82.2, 67.5, 63.0, 39.0, 29.2, 27.1. **HRMS**-ESI (m/z): $[M + H]^+$ calculated for $C_{15}H_{16}NO_3^+$, 258.1125; found, 258.1125.

(±) 1,3,4,5,6b,9,10,10a-octahydro-7H-pyrano[3',4':4,5]furo[3,2-c]quinolin-6(2H)-one (10t); (±) 4-hydroxy-3-(tetrahydro-2H-pyran-3-yl)-5,6,7,8-tetrahydroquinolin-2(1H)-one (11c)

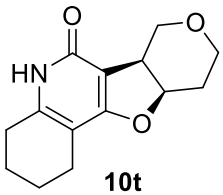

10t

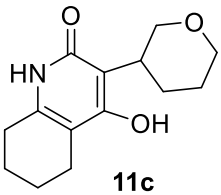

11c

According to GP2, **3a** (73.3 mg, 0.25 mmol) was reacted with **2v** (35.0 mg, 0.21 mmol) at 110 °C for 1 hour. After filtration over celite the crude was purified by MPLC (cyclohexane/EtOAc 1:0 to 0:1) and the product was directly suspended with Pd/C (5 mg, 10 wt%) in toluene (2 mL) and was hydrogenated at 20 °C for 12 hours using a H_2-balloon. The catalyst was filtered off and the solvent removed in vacuo. The crude was purified by MPLC (EtOAc/MeOH 1:0 to 9:1 + 0.1% DIPEA) to afford a mixture of products a and b. The product mixture was subjected for separation by prep. HPLC to afford pure product **10t** (2.3 mg, 4%) and **11c** (1.1 mg, 2%). **^{1}H-NMR** product **10t** (700 MHz, CD_2Cl_2): δ 14.5 (bs, 1H), 5.07 (dt, *J* = 7.7, 4.3 Hz, 1H), 4.02 (dd, *J* = 11.3, 5.1 Hz, 1H), 3.79 (ddd, *J* = 11.5, 5.7, 3.8 Hz, 1H), 3.65 (ddd, *J* = 11.5, 10.3, 4.0 Hz, 1H), 3.56-3.49 (m, 2H), 2.75 (t, *J* = 6.3 Hz, 2H), 2.51 (t, *J* = 6.4 Hz, 2H), 2.22-2.17 (m, 1H), 2.13-2.09 (m, 1H), 1.87-1.83 (m, 2H), 1.81-1.77 (m, 2H). **^{13}C-NMR** product **10t** (176 MHz, CD_2Cl_2): δ 172.8, 164.9, 158.8, 148.0, 108.7, 83.8, 66.0, 62.5, 37.2, 26.6, 26.6, 21.2, 21.2, 20.7. **HRMS**-ESI (m/z) product **10t**: $[M + H]^+$ calculated for $C_{14}H_{18}NO_3^+$, 248.1281; found, 248.1282. **^{1}H-NMR** product **11c** (700 MHz, CD_2Cl_2): δ 14.5 (bs, 1H), 12.2 (s, 1H), 4.21 (dd, *J* = 11.6, 4.5 Hz, 1H), 4.14 (d, *J* = 12.8 Hz, 1H), 3.96 (dd, *J* = 12.8, 3.4 Hz, 1H), 3.70 (ddd, *J* = 12.6, 11.6, 2.5 Hz, 1H), 3.43-3.40 (m, 1H), 2.73 (t, *J* = 6.2 Hz, 2H), 2.54 (t, *J* = 6.4 Hz, 1H), 2.00-1.90 (m, 2H), 1.84-1.77 (m, 4H), 1.70-1.57 (m, 2H). **UPHLC-MS**-ESI (m/z) product **11c**: 250.0 $[M + H]^+$.

(±) (5aR,9S,9aS)-3,9-dimethyl-5a,9a-dihydro-1H,9H-furo[3,2-c:4,5-c']dipyran-1-one (12a)

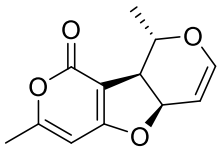

A reaction vessel was charged with 4-Hydroxy-6-methyl-2-pyron (**1a**) (27.1 mg, 0.21 mmol, 1.0 eq), evacuated and back-filled with argon. Toluene (1.5 mL) and Triethylamine (30.0 µL, 0.21 mmol, 1.0 equiv) were added to the reaction vessel. A separate reaction vessel was charged with $Pd(PPh_3)_4$ (5 mol%), evacuated and back-filled with argon, then charged with toluene (0.5 mL) followed by **3b**-*trans* (65.0 mg, 0.17 mmol, 1.0 equiv) The contents of this flask were stirred for approximately 20 min. before being added via syringe to the bis-nucleophile solution. The reaction was stirred for one day at room temperature before being concentrated in vacuo and purified by flash column chromatography (Heptane/EtOAc 9:1 to 4:1 to 7:3 + 1% NEt_3) to afford the product (69% yield). **^{1}H-NMR** (500 MHz, DMSO-d_6): δ 6.88 (d, *J* = 6.2 Hz, 1H), 6.31 (s, 1H), 5.29 (dd, *J* = 6.2 Hz, 4.7 Hz, 1H), 5.11 (ddd, *J* = 7.2 Hz, 4.7 Hz, 1.0 Hz, 1H), 3.39 (dd, *J* = 10.8 Hz, 6.2 Hz, 1H), 2.92 (dd, *J* = 10.8 Hz, 7.2 Hz, 1H), 2.22 (s, 3H), 1.35 (d, *J* = 6.2 Hz, 3H). **^{13}C-NMR** (126 MHz, DMSO-d_6): δ 172.2, 166.5, 161.2, 149.8, 99.7, 97.9, 95.8, 79.5, 72.5, 41.7, 20.0, 19.1. **HRMS**-ESI (m/z): $[M + H]^+$ calculated for $C_{12}H_{13}O_4^+$, 221.0808; found, 221.0807.

(±) 3,9-dimethyl-5a,6,9,9a-tetrahydro-1H,7H-furo[3,2-c:4,5-c']dipyran-1-one (13a); (±) 4-hydroxy-6-methyl-3-(2-methyltetrahydro-2H-pyran-3-yl)-2H-pyran-2-one (14a)

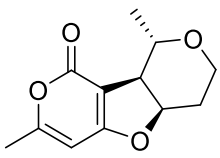

13a

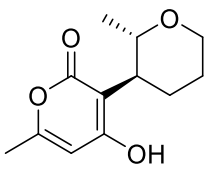

14a

A suspension of **12a** (16.3 mg, 0.07 mmol) and Pd/C (1.6 mg, 10 wt%) in toluene (0.7 mL) was hydrogenated at 20 °C for 20 hours using a H_2-balloon. The catalyst was filtered off and the solvent removed in vacuo. The crude was purified by prep. HPLC to afford product **13a** (3.7 mg, 22%) and **14a** (5.4 mg, 33%) in separated fractions. **^{1}H-NMR** product **13a** (500 MHz, $CDCl_3$): δ 5.97 (s, 1H), 4.88-4.81 (m, 1H), 3.97-3.92 (m, 1H), 3.58 (td, *J* = 11.6, 4.0 Hz, 1H), 3.17 (dq, *J* = 9.9, 6.1 Hz, 1H), 2.83 (dd, *J* = 9.8, 6.5 Hz, 1H), 2.27 (s, 3H), 2.12-2.07 (m, 2H), 1.41 (d, *J* = 6.2 Hz, 3H). **^{13}C-NMR** product **13a** (126 MHz, $CDCl_3$): δ 166.4, 162.3, 147.0, 103.6, 96.2, 84.8, 63.1, 43.1, 23.8, 21.4, 20.7. **HRMS**-ESI (m/z) product **13a**: $[M + H]^+$ calculated for $C_{12}H_{15}O_4^+$, 223.0965; found, 223.0964. **^{1}H-NMR** product **14b** (500 MHz, $CDCl_3$): δ 11.86 (s, 1H), 5.86 (s, 1H), 4.37-4.26 (m, 1H), 3.93 (td, *J* = 11.3, 10.8, 3.1 Hz, 1H), 3.88-3.76 (m, 1H), 2.19 (s, 3H), 2.12-2.00 (m, 1H), 1.78-1.61 (m, 2H), 1.57-1.43 (m, 2H). **HRMS**-ESI (m/z) product **14b**: $[M + H]^+$ calculated for $C_{12}H_{17}O_4^+$, 225.1121; found, 225.1120.

(±) 5,7-dimethyl-6b,9,10,10a-tetrahydro-7H-pyrano[3',4':4,5]furo[3,2-c]quinolin-6(5H)-one (13b); (±) 4-hydroxy-1-methyl-3-(2-methyltetrahydro-2H-pyran-3-yl)quinolin-2(1H)-one (14b)

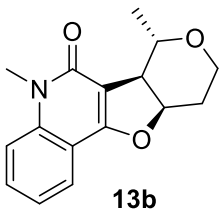

13b

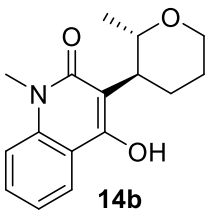

14b

According to GP3, **3b**-*trans* (66.5 mg, 0.22 mmol) was reacted with **2w** (35.0 mg, 0.20 mmol). After purification by MPLC (cyclohexane/EtOAc 1:0 to 0:1), the product was directly suspended with Pd/C (5 mg, 10 wt%) in toluene (2 mL) and was hydrogenated at 20 °C for 48 hours using a H_2-balloon. The catalyst was filtered off and the solvent removed in vacuo. The crude was purified by prep. HPLC to afford product **13b** (3.6 mg, 7%) and **14b** (3.6 mg, 7%) in separated fractions. **^{1}H-NMR** product **13b** (500 MHz, CD_2Cl_2): δ 7.80 (dd, *J* = 8.0, 1.6 Hz, 1H), 7.63 (ddd, *J* = 8.7, 7.6, 1.6 Hz, 1H), 7.43 (d, *J* = 8.7 Hz, 1H), 7.27 (dd, *J* = 8.0, 7.6 Hz, 1H), 4.93 (m, 1H), 3.94 (ddt, *J* = 12.0, 5.9, 1.3 Hz, 1H), 3.69 (s, 3H), 3.64 (td, *J* = 12.0, 2.7 Hz, 1H), 3.21 (dq, *J* = 9.9, 6.1 Hz, 1H), 3.00 (dd, *J* = 9.9, 6.4 Hz, 1H), 2.27 (dq, *J* = 15.4, 2.2 Hz, 1H), 2.16 (dddd, *J* = 15.4, 12.8, 5.9, 4.3 Hz, 1H), 1.39 (d, *J* = 6.1 Hz, 3H). **^{13}C-NMR** product **13b** (126 MHz, CD_2Cl_2): δ 164.6, 161.5, 141.0, 131.8, 123.4, 122.1, 115.1, 113.1, 112.6, 84.7, 77.3, 63.3, 45.3, 29.6, 27.4, 21.6. **HRMS**-ESI (m/z) product **13b**: $[M + H]^+$ calculated for $C_{16}H_{18}NO_3^+$, 272.1261; found, 272.1278. **^{1}H-NMR** product **14b** (500 MHz, MeOH-d_4): δ 8.07-7.06 (m, 1H), 7.65-7.58 (m, 1H), 7.57-7.48 (m, 1H), 7.34-7.26 (m, 1H), 4.54-4.38 (m, 1H), 4.02-3.95 (m, 1H), 3.72-3.62 (m, 4H), 3.07-2.93 (m 1H), 2.53-2.39 (m, 1H), 1.86-1.58 (m, 3H), 1.01 (bs, 3H). **^{13}C-NMR** product **14b** (126 MHz, MeOH-d_4): δ 159.5, 159.4, 140.0, 131.9, 124.7, 123.1, 118.0, 115.4, 113.5, 76.4, 69.4, 43.1, 29.7, 27.8, 27.7, 20.2. **HRMS**-ESI (m/z) product **14b**: $[M + H]^+$ calculated for $C_{16}H_{20}NO_3^+$, 274.1438; found, 274.1445.

(±) 1-methyl-4,4a,6,7,8,9b-hexahydro-1H-pyrano[3',4':4,5]furo[3,2-c]pyridin-9(3H)-one (13c)

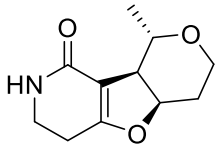

According to GP3, **3b**-*trans* (66.5 mg, 0.22 mmol) was reacted with **2y** (22.6 mg, 0.20 mmol). After purification by MPLC (cyclohexane/EtOAc 1:0 to 0:1), the product was directly suspended with Pd/C (5 mg, 10 wt%) in toluene (2 mL) and was hydrogenated at 20 °C for 48 hours using a H_2-balloon. The catalyst was filtered off and the solvent removed in vacuo. The crude was purified by prep. HPLC to afford the product (8.8 mg, 21%). **^{1}H-NMR** (600 MHz, CD_2Cl_2): δ 5.72 (s, 1H), 4.74-4.71 (m, 1H), 3.90-3.85 (m, 1H), 3.55 (td, *J* = 11.5, 4.2 Hz, 1H), 3.52-3.42 (m, 2H), 3.13 (dt, *J* = 12.3, 6.1 Hz, 1H), 2.62-2.59 (m, 1H), 2.58-2.54 (m, 1H), 2.49 (dt, *J* = 17.3, 6.4 Hz, 1H), 2.08-2.03

(m, 1H), 1.28 (d, *J* = 6.1 Hz, 3H). **^{13}C-NMR** (151 MHz, CD_2Cl_2): δ 171.9, 168.3, 110.0, 84.7, 78.0, 63.2, 43.9, 39.7, 27.4, 23.8, 21.1. **HRMS**-ESI (m/z): $[M + H]^+$ calculated for $C_{11}H_{16}NO_3^+$, 210.1125; found, 210.1122.

(±) 1,7,8-trimethyl-8,9b-dihydro-1H-pyrano[3',4':4,5]furo[3,2-c]pyridin-9(4aH)-one (12d)

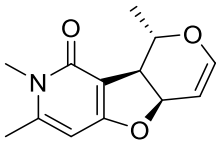

According to GP3, **3b**-*trans* (100.0 mg, 0.33 mmol) was reacted with **2b** (46.0 mg, 0.33 mmol). Purification by FC (Hep/EtOAc 7:3 to 1:1 + 1% NEt_3) afforded the product (37 mg, 48%). **^{1}H-NMR** (700 MHz DMSO-d_6): δ 6.82 (d, *J* = 6.1 Hz, 1H) 6.01 (s, 1H), 5.24 (dd, *J* = 6.1 Hz, 5.0 Hz, 1H), 4.92 (dd, *J* = 6.7 Hz, 5.0 Hz, 1H), 3.37 (s, 3H), 3.34 (dd, *J* = 10.7 Hz, 6.2 Hz, 1H), 2.88 (dd, *J* = 10.7 Hz, 6.7 Hz, 1H), 2.32 (s, 3H), 1.37 (d, *J* = 6.2 Hz, 3H). **^{13}C-NMR** (176 MHz, DMSO-d_6): δ 167.3, 161.3, 150.7, 149.5, 106.3, 99.0, 94.7, 78.2, 73.4, 43.5, 30.6, 21.5, 19.9. **HRMS**-ESI (m/z): $[M + H]^+$ calculated for $C_{13}H_{16}O_3N^+$, 234.1125; found, 234.1124.

(±) 1,7,8-trimethyl-4,4a,8,9b-tetrahydro-1H-pyrano[3',4':4,5]furo[3,2-c]pyridin-9(3H)-one (13d); (±) 4-hydroxy-1,6-dimethyl-3-(2-methyltetrahydro-2H-pyran-3-yl)pyridin-2(1H)-one (14d)

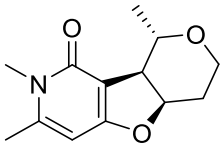

13d

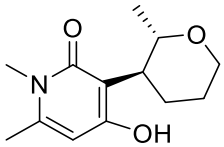

14d

According to GP3, **3b**-*trans* (69.6 mg, 0.23 mmol) was reacted with **2b** (27.8 mg, 0.20 mmol). After purification by MPLC (cyclohexane/EtOAc 1:0 to 0:1), the product was directly suspended with Pd/C (5 mg, 10 wt%) in toluene (2 mL) and was hydrogenated at 20 °C for 48 hours using a H_2-balloon. The catalyst was filtered off and the solvent removed in vacuo. The crude was purified by prep. HPLC to afford product **13d** (3.8 mg, 8%) and **14d** (16.0 mg, 34%) in separated fractions. **^{1}H-NMR** product **13d** (500 MHz, $CDCl_3$): δ 6.01 (s, 1H), 4.75 (dt, *J* = 6.2, 3.3 Hz, 1H), 3.96-3.91 (m, 1H), 3.61 (td, *J* = 11.2, 4.9 Hz, 1H), 3.54 (s, 3H), 3.15 (dq, *J* = 9.9, 6.2 Hz, 1H), 2.95 (dd, *J* = 9.9, 6.2 Hz, 1H), 2.38 (s, 3H), 2.12 (ddd, *J* = 11.2, 5.4, 3.3 Hz, 2H), 1.41 (d, *J* = 6.2 Hz, 3H). **^{13}C-NMR** product **13d** (126 MHz, $CDCl_3$): δ 168.8, 162.1, 149.0, 110.9, 97.2, 83.9, 77.0, 63.1, 44.1, 31.6, 27.0, 22.0, 21.5. **HRMS**-ESI (m/z) product **13d**: $[M + H]^+$ calculated for $C_{13}H_{18}NO_3^+$, 236.1281; found, 236.1286. **^{1}H-NMR** product **14d** (500 MHz, CD_2Cl_2): δ 5.90 (s, 1H), 4.34-4.21 (m, 1H), 3.97-3.89 (m, 1H), 3.75-3.68 (m, 1H), 3.19-3.11 (m, 1H), 2.32 (s, 3H), 1.97-1.88 (m, 1H), 1.85-1.76 (m, 1H), 1.67-1.57 (m, 2H), 1.33-1.29 (bs, 3H). **^{13}C-NMR** product **14d** (126 MHz, CD_2Cl_2): δ 165.4, 164.2, 144.9, 111.0, 103.6, 73.3, 63.8, 38.5, 32.2, 24.6, 24.4,

20.9, 18.0. **HRMS**-ESI (m/z) product **14d**: $[M + H]^+$ calculated for $C_{13}H_{20}NO_3^+$, 238.1438; found, 238.1443.

(±) 8-benzyl-1,7-dimethyl-8,9b-dihydro-1H-pyrano[3',4':4,5]furo[3,2-c]pyridin-9(4aH)-one (12e)

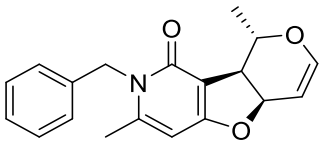

According to GP3, **3b**-*trans* (100.0 mg, 0.33 mmol) was reacted with **2g** (71.2 mg, 0.33 mmol). Purification by FC (Hep/EtOAc 7:3 to 1:1 + 1% NEt_3) afforded the product (36 mg, 35%). **^{1}H-NMR** (700 MHz DMSO-d_6): δ 7.33 (dd, *J* = 7.5 Hz, 7.4 Hz, 2H), 7.25 (dd, *J* = 7.4 Hz, 7.4 Hz, 1H), 7.10 (d, *J* = 7.5 Hz, 2H), 6.85 (d, *J* = 6.2 Hz, 1H) 6.07 (s, 1H), 5.37 (d, *J* = 15.2 Hz, 1H), 5.27 (dd, *J* = 6.2 Hz, 4.8 Hz, 1H), 5.16 (d, *J* = 15.2 Hz, 1H), 5.00 (m, 1H), 3.44-3.39 (m, 1H), 2.94 (dd, *J* = 10.7 Hz, 7.0 Hz, 1H), 2.23 (s, 3H), 1.39 (d, *J* = 6.3 Hz, 3H). **^{13}C-NMR** (176 MHz, DMSO-d_6): δ 167.7, 161.5, 150.5, 149.7, 137.9, 129.1, 127.5, 126.6, 106.8, 99.0, 95.6, 78.5, 73.5, 46.2, 43.4, 21.0, 19.9. **LCMS**-ESI (m/z): 310.28 $[M + H]^+$.

(±) 8-benzyl-1,7-dimethyl-4,4a,8,9b-tetrahydro-1H-pyrano[3',4':4,5]furo[3,2-c]pyridin-9(3H)-one (13e); (±) 1-benzyl-4-hydroxy-6-methyl-3-(2-methyltetrahydro-2H-pyran-3-yl)pyridin-2(1H)-one (14f)

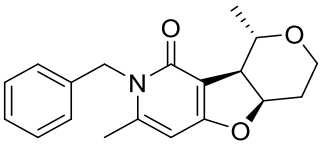

13e

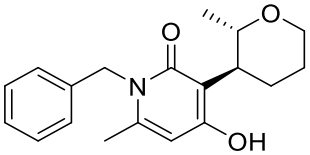

14f

A suspension of **12e** (13.9 mg, 0.04 mmol) and Pd/C (1.4 mg, 10 wt%) in toluene (0.5 mL) was hydrogenated at 20 °C for 24 hours using a H_2-balloon. The catalyst was filtered off and the solvent removed in vacuo. The crude was purified by prep. HPLC to afford product **13e** (5.0 mg, 36%) and **14f** (5 mg, 36%) in separated fractions. **^{1}H-NMR** product **13e** (600 MHz, $CDCl_3$): δ 7.34-7.21 (m, 3H), 7.13 (d, *J* = 7.0 Hz, 2H), 5.92 (s, 1H), 5.46 (d, *J* = 16.0 Hz, 1H), 5.19 (d, *J* = 16.0 Hz, 1H), 4.80-4.76 (m, 1H), 3.97-3.92 (m, 1H), 3.63 (td, *J* = 11.2, 4.9 Hz, 1H), 3.26-3.19 (m, 1H), 2.97 (dd, *J* = 9.8, 6.3 Hz, 1H), 2.28 (s, 3H), 2.16-2.09 (m, 2H), 1.46 (d, *J* = 6.2 Hz, 3H). **HRMS**-ESI (m/z) product **13e**: $[M + H]^+$ calculated for $C_{19}H_{22}NO_3^+$, 312.1594; found, 312.1599. **^{1}H-NMR** product **14f** (600 MHz, $CDCl_3$): δ 11.03 (s, 1H), 7.29 (t, *J* = 7.5 Hz, 2H), 7.23 (t, *J* = 7.5 Hz, 1H), 7.11 (d, *J* = 7.5 Hz, 2H), 5.86 (s, 1H), 5.38 (d, *J* = 16.1 Hz, 1H), 5.21 (d, *J* = 16.1 Hz, 1H), 4.42-4.34 (m, 1H), 3.93 (t, *J* = 11.7 Hz, 1H), 3.86-3.80 (m, 1H), 3.36-3.30 (m, 1H), 2.22 (s, 3H), 2.13-2.06 (m, 1H), 1.79-1.67 (m, 2H), 1.58-1.50 (m, 1H), 1.47 (d, *J* = 6.5 Hz, 3H). **^{13}C-NMR** product **14f** (151 MHz, $CDCl_3$): δ 165.2, 163.4, 144.0, 137.2, 129.9, 127.3, 126.4, 110.8, 103.4, 72.4, 61.9, 47.7, 36.9, 23.5, 23.2, 20.4,

17.2. **HRMS**-ESI (m/z) product **14f**: $[M + H]^+$ calculated for $C_{19}H_{24}NO_3^+$, 314.1751; found, 314.1751.

(±) 8-(4-methoxybenzyl)-1,7-dimethyl-8,9b-dihydro-1H-pyrano[3',4':4,5]furo[3,2-c]pyridin-9(4aH)-one (12f); (±) 6-(4-methoxybenzyl)-2,7-dimethyl-4a,9a-dihydro-2H-pyrano[3',2':4,5]furo[3,2-c]pyridin-5(6H)-one (15f)

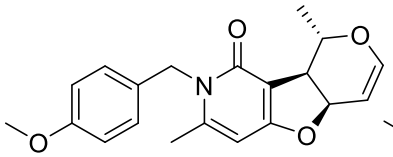

12f

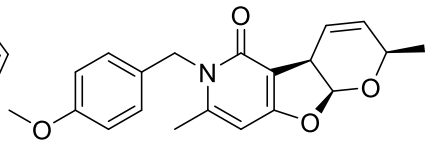

15f

According to GP3, **3b**-*trans* (50.0 mg, 0.17 mmol) was reacted with **2k** (35.0 mg, 0.15 mmol). Purification by FC (Hep/EtOAc 7:3 to 1:1 + 1% NEt_3) afforded the product **12f** (7.5 mg, 13%) and product **15f** (8.1 mg, 14%) in separated fractions. **^{1}H-NMR** product **12f** (500 MHz, CD_2Cl_2): δ 7.08 (d, *J* = 8.6 Hz, 2H), 6.84 (d, *J* = 8.6 Hz, 2H), 6.78 (d, *J* = 6.2 Hz, 1H), 5.84 (s, 1H), 5.28 (d, *J* = 15.7 Hz, 1H), 5.24 (dd, *J* = 6.2, 4.7 Hz, 1H), 5.13 (d, *J* = 15.7 Hz, 1H), 4.95 (ddd, *J* = 6.9, 4.7, 1.1 Hz, 1H), 3.76 (s, 3H), 3.51 (dq, *J* = 11.5, 6.3 Hz, 1H), 3.01 (dd, *J* = 11.5, 6.9 Hz, 1H), 2.25 (s, 3H), 1.48 (d, *J* = 6.3 Hz, 3H). **^{13}C-NMR** product **12f** (126 MHz, CD_2Cl_2): δ 168.1, 162.1, 159.2, 149.9, 149.7, 129.6, 128.1, 114.4, 107.6, 98.6, 95.4, 79.2, 74.0, 55.6, 46.4, 44.0, 21.5, 19.8. **UHPCL-MS**-ESI product **12f** (m/z): 340.0 $[M + H]^+$. **^{1}H-NMR** product **15f** (700 MHz, CD_2Cl_2): δ 7.07 (d, *J* = 8.7 Hz, 2H), 6.84 (d, *J* = 8.7 Hz, 2H), 6.26 (ddd, *J* = 10.3, 3.9, 2.0 Hz, 1H), 6.13 (d, *J* = 6.6 Hz, 1H), 5.92 (s, 1H), 5.88 (ddd, *J* = 10.3, 2.6, 1.9 Hz, 1H), 5.33 (m, 1H), 5.08 (d, *J* = 15.9 Hz, 1H), 4.36 (qq, *J* = 6.9, 2.6 Hz, 1H), 3.77-3.75 (m, 4H), 2.27 (s, 3H), 1.28 (d, *J* = 6.9 Hz, 1H). **^{13}C-NMR** product **15f** (176 MHz, CD_2Cl_2): δ 165.5, 161.8, 159.3, 149.6, 130.5, 129.3, 128.1, 122.1, 114.4, 109.0, 105.8, 96.4, 68.2, 55.6, 46.5, 38.4, 22.2, 21.5. **HRMS**-ESI (m/z) product **15f**: $[M + H]^+$ calculated for $C_{20}H_{22}NO_4^+$, 340.1543; found, 340.1545.

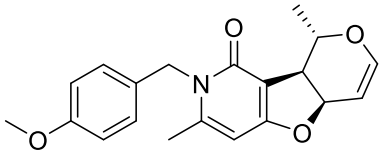

A reaction vessel was evacuated and back-filled with argon. Allyl-Pd-Cl dimer (1.37 mg, 2.5 mol%) and Xantphos (6.51 mg, 7.5 mol%) was loaded into the vessel and dissolved in THF (0.5 mL). After 5 min, **3b**-*trans* (50.0 mg, 0.17 mmol) dissolved in THF (0.65 mL) was added. A mixture of **2k** (35.0 mg, 0.15 mmol, 1 equiv) and NEt_3 (41 microL, 2 equiv) in DMF (0.35 mL) was added and the mixture was stirred at room temperature overnight. The mixture was diluted with EtOAc and concentrated in vacuo. The crude was dissolved in DCM and immobilized on isolute for purification by MPLC (cyclohexane/EtOAc 1:0 to 3:7 + 0.1% NEt_3) to afford the product (30.9 mg, 61%).

(±) 8-(4-methoxybenzyl)-1,7-dimethyl-4,4a,8,9b-tetrahydro-1H-pyrano[3',4':4,5]furo[3,2-c]pyridin-9(3H)-one (13f); (±) 4-hydroxy-1-(4-methoxybenzyl)-6-methyl-3-(2-methyltetrahydro-2H-pyran-3-yl)pyridin-2(1H)-one (14g)

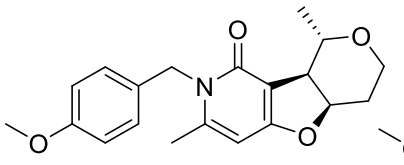

13f

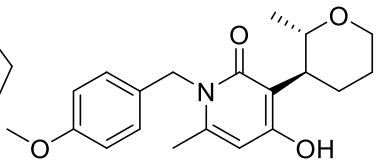

14g

12f (22.5 mg, 0.07 mmol) was suspended with Pd/C (2.5 mg, 10 wt%) in toluene (1 mL) and hydrogenated at 20 °C for 48 hours using a H_2-balloon. The catalyst was filtered off and the solvent removed in vacuo. The crude was purified by prep. HPLC to afford the product **13f** (7.6 mg, 34%) and **14g** (9.0 mg, 40%) in separated fractions. **^{1}H-NMR** product **13f** (500 MHz, CD_2Cl_2): δ 7.07 (d, *J* = 8.5 Hz, 2H), 6.85 (d, *J* = 8.5 Hz, 2H), 6.02 (s, 1H), 5.34 (d, , *J* = 15.6 Hz, 1H), 5.18 (d, *J* = 15.6 Hz, 1H), 4.79 (dt, *J* = 6.0, 2.9 Hz, 1H), 3.92-3.88 (m, 1H), 3.59 (td, *J* = 11.4, 4.4 Hz, 1H), 3.19-3.13 (m, 1H), 2.93 (dd, *J* = 9.8, 6.0 Hz, 1H), 2.31 (s, 3H), 2.15-2.08 (m, 2H), 1.36 (d, *J* = 6.2 Hz, 1H). **^{13}C-NMR** product **13f** (126 MHz, CD_2Cl_2): δ 169.5, 162.3, 159.4, 150.0, 128.9, 128.1, 114.5, 111.1, 97.8, 84.4, 77.2, 63.3, 55.6, 47.1, 44.5, 27.2, 21.6, 21.5. **HRMS**-ESI (m/z) product **13f**: $[M + H]^+$ calculated for $C_{20}H_{24}NO_4^+$, 342.1700; found, 342.1698. **^{1}H-NMR** product **14g** (400 MHz, MeOH-d_4): δ 7.01 (d, *J* = 8.6 Hz, 2H), 6.86 (d, *J* = 8.6 Hz, 2H), 5.86 (s, 1H), 5.31-5.21 (m, 2H), 4.36-4.18 (m, 1H), 3.93 (dd, *J* = 11.3, 4.3 Hz, 1H), 3.76 (bs, 4H), 3.56 (t, *J* = 11.3 Hz, 1H), 2.16 (s, 3H), 1.79-1.52 (m, 4H), 1.02 (d, *J* = 6.2 Hz, 3H). **^{13}C-NMR** product **14g** (126 MHz, MeOH-d_4): δ 164.8, 160.4, 160.3, 146.7, 130.3, 128.4, 115.2, 111.4, 101.0, 76.5 69.4, 55.7, 47.3, 40.1, 28.2, 28.1, 20.4. **HRMS**-ESI (m/z) product **14g**: $[M + H]^+$ calculated for $C_{20}H_{26}NO_4^+$, 344.1856; found, 344.1865.

(±) 8-(4-fluorobenzyl)-1,7-dimethyl-4,4a,8,9b-tetrahydro-1H-pyrano[3',4':4,5]furo[3,2-c]pyridin-9(3H)-one (13g); (±) 1-(4-fluorobenzyl)-4-hydroxy-6-methyl-3-(2-methyltetrahydro-2H-pyran-3-yl)pyridin-2(1H)-one (14h); (±) 6-(4-fluorobenzyl)-2,7-dimethyl-3,4,4a,9a-tetrahydro-2H-pyrano[3',2':4,5]furo[3,2-c]pyridin-5(6H)-one (16g);

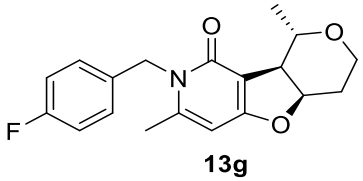

13g

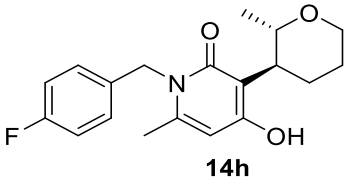

14h

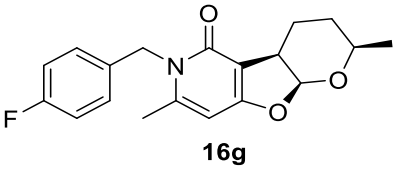

16g

According to GP3, **3b**-*trans* (69.6 mg, 0.23 mmol) was reacted with **2h** (46.6 mg, 0.20 mmol). After purification by MPLC (cyclohexane/EtOAc 1:0 to 0:1), the product was directly suspended with Pd/C (5 mg, 10 wt%) in toluene (2 mL) and was hydrogenated at 20 °C for 48

hours using a H_2-balloon. The catalyst was filtered off and the solvent removed in vacuo. The crude was purified by prep. HPLC to afford product **13g** (4.5 mg, 7%), **14h** (4.9 mg, 7%) and **16g** (3.0 mg, 5%) in separated fractions. **^{1}H-NMR** product **13g** (500 MHz, CD_2Cl_2): δ 7.13 (dd, *J* = 8.6, 5.4 Hz, 2H), 7.01 (t, *J* = 8.6 Hz, 2H), 5.91 (s, 1H), 5.36 (d, *J* = 14.4 Hz, 1H) 5.15 (d, *J* = 14.4 Hz, 1H), 4.76 (dt, *J* = 6.3, 3.0 Hz, 1H), 3.91-3.87 (m, 1H), 3.58 (td, *J* = 11.4, 4.2 Hz, 1H), 3.16 (dq, *J* = 9.8, 6.2 Hz, 1H), 2.87 (dd, *J* = 9.8, 6.3 Hz, 1H), 2.25 (s, 1H), 2.12-2.07 (m, 2H), 1.37 (d, *J* = 6.2 Hz, 3H). **^{13}C-NMR** product **13g** (126 MHz, CD_2Cl_2): δ 168.4, 162.9, 161.0, 161.6, 148.9, 133.1, 128.1, 115.5, 110.3, 96.3, 83.6, 77.0, 62.9, 46.1, 44.3, 27.0, 21.3, 21.2. **HRMS**-ESI (m/z) product **13g**: $[M + H]^+$ calculated for $C_{19}H_{21}FNO_3^+$, 330.1500; found, 330.1505. **^{1}H-NMR** product **14h** (600 MHz, CD_2Cl_2): δ 7.14-6.96 (m, 4H), 5.91 (s, 1H), 5.31-5.16 (m, 2H), 4.34-4.25 (m, 1H), 3.96-3.89 (m, 1H), 3.79-3.69 (m, 1H), 3.24-3.14 (m, 1H), 2.19 (s, 3H), 2.04-1.94 (m, 1H), 1.80-1.52 (m, 3H), 1.37 (bs, 3H). **^{13}C-NMR** product **14h** (151 MHz, CD_2Cl_2): δ 165.4, 164.1, 163.2, 161.6, 144.5, 133.3, 128.4, 115.9, 111.1, 103.8, 73.1, 63.3, 47.4, 38.1, 24.4, 24.1, 20.4, 17.8. **HRMS**-ESI (m/z) product **14h**: $[M + H]^+$ calculated for $C_{19}H_{23}FNO_3^+$, 332.1657; found, 332.1660. **^{1}H-NMR** product **16g** (500 MHz, CD_2Cl_2): δ 7.12 (dd, *J* = 8.6, 5.5 Hz, 2H), 7.01 (t, *J* = 8.6 Hz, 2H), 5.70 (s, 1H), 5.41 (d, *J* = 5.0 Hz, 1H), 5.27 (d, *J* = 15.8 Hz, 1H), 5.18 (d, *J* = 15.8 Hz, 1H), 4.46 (q, *J* = 6.6 Hz, 1H), 3.22-3.19 (s, 1H), 2.22-1.92 (m, 7H), 1.35 (d, *J* = 6.6 Hz, 3H). **^{13}C-NMR** product **16g** (126 MHz, CD_2Cl_2): δ 164.0, 163.4, 163.3, 144.9, 133.3, 128.4, 115.9, 114.3, 102.5, 98.1, 77.4, 47.1, 34.3, 28.2, 21.3, 20.6, 20.5. **HRMS**-ESI (m/z) product **16g**: $[M + H]^+$ calculated for $C_{19}H_{21}FNO_3^+$, 330.1500; found, 330.1506.

(±) 4-hydroxy-3-(2-methyltetrahydro-2H-pyran-3-yl)-5,6,7,8-tetrahydroquinolin-2(1H)-one (14c)

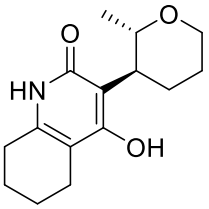

According to GP3, **3b**-*trans* (66.5 mg, 0.22 mmol) was reacted with **2v** (33.0 mg, 0.20 mmol). After purification by MPLC (cyclohexane/EtOAc 1:0 to 0:1), the product was directly suspended with Pd/C (5 mg, 10 wt%) in toluene (2 mL) and was hydrogenated at 20 °C for 48 hours using a H_2-balloon. The catalyst was filtered off and the solvent removed in vacuo. The crude was purified by prep. HPLC to afford the product (3.1 mg, 6%). **^{1}H-NMR** (600 MHz, CD_2Cl_2): δ 14.65 (s, 1H), 12.42 (s, 1H), 4.38 (q, *J* = 7.0 Hz, 1H), 3.97 (td, *J* = 12.2, 2.6 Hz, 1H), 3.89 (dd, *J* = 12.2, 4.5 Hz, 1H), 3.27-3.21 (m, 1H), 2.74 (t, *J* = 6.1 Hz, 2H), 2.53 (t, *J* = 5.9 Hz, 3H), 2.21-2.14 (m, 1H), 1.86-1.77 (m, 4H), 1.72 (bd, *J* = 14.3 Hz, 1H), 1.68-1.61 (m, 1H), 1.58-1.53 (m, 1H), 1.52 (d, *J* = 7.0 Hz, 3H). **^{13}C-NMR** (151 MHz, CD_2Cl_2): δ 167.9, 159.9, 143.5, 116.0, 109.2, 71.4, 61.4, 35.1,

26.3, 23.1, 22.3, 21.6, 21.4, 21.2, 16.5. **HRMS**-ESI (m/z): $[M + H]^+$ calculated for $C_{15}H_{22}NO_3^+$, 264.1594; found, 264.1597.

(±) 1-cyclobutyl-4-hydroxy-6-methyl-3-(2-methyltetrahydro-2H-pyran-3-yl)pyridin-2(1H)-one (14e)

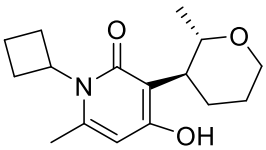

According to GP3, **3b**-*trans* (66.5 mg, 0.22 mmol) was reacted with **2c** (35.8 mg, 0.20 mmol). After purification by MPLC (cyclohexane/EtOAc 1:0 to 0:1), the product was directly suspended with Pd/C (5 mg, 10 wt%) in toluene (2 mL) and was hydrogenated at 20 °C for 48 hours using a H_2-balloon. The catalyst was filtered off and the solvent removed in vacuo. The crude was purified by prep. HPLC to afford the product (6.9 mg, 12%). **^{1}H-NMR** (500 MHz, MeOH-d_4): δ 5.68 (s, 1H), 4.81 (q, *J* = 8.7 Hz, 1H), 4.38-4.14 (m, 1H), 3.94-3.90 (m, 1H), 3.61-3.48 (m, 1H), 3.18-3.08 (m, 2H), 2.32-2.22 (m, 6H) 1.93 (qt, *J* = 10.4, 2.9 Hz, 1H), 1.82-1.74 (m, 1H), 1.72-1.59 (m, 2H), 0.98 (d, *J* = 6.2 Hz, 3H). **^{13}C-NMR** (126 MHz, MeOH-d_4): δ **HRMS**-ESI (m/z): $[M + H]^+$ calculated for $C_{16}H_{24}NO_3^+$, 278.1751; found, 278.1755.

(±) 1,7-dimethyl-8-(4-morpholinophenyl)-8,9b-dihydro-1H-pyrano[3',4':4,5]furo[3,2-c]pyridin-9(4aH)-one (12k)

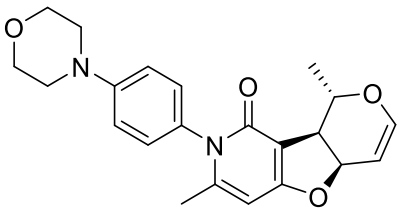

According to GP2, **3b**-*trans* (66.5 mg, 0.22 mmol) was reacted with **2r** (57.3 mg, 0.20 mmol) at 110 °C for 2 hours. The catalyst was filtered off and the filtrate was diluted with DCM (10 mL) and washed with saturated $NaHCO_3$ solution (15 mL). The aqueous phase was extracted with DCM (3 x 10 mL) and the combined organic layers were washed with brine (50 mL), dried over $MgSO_4$ and concentrated in vacuo. The crude was purified by MPLC (EtOAc/MeOH 1:0 to 9:1) to afford the product (3.3 mg, 4%). **^{1}H-NMR** (600 MHz, CD_2Cl_2): δ 7.06-6.97 (m 4H), 6.78 (d, *J* = 6.1 Hz, 1H), 5.92 (s, 1H), 5.25 (dd, *J* = 6.1, 4.9 Hz, 1H), 4.96 (dd, *J* = 6.7, 4.9 Hz, 1H), 3.86-3.83 (m, 5H), 3.55-3.50 (m, 1H), 3.21-3.19 (m, 4H), 2.99 (dd, *J* = 10.7, 6.7 Hz, 1H), 1.95 (s, 3H), 1.44 (d, *J* = 6.2 Hz, 3H). **^{13}C-NMR** (151 MHz, CD_2Cl_2): δ 168.6, 162.6, 151.6, 150.2, 149.9, 131.0, 129.3, 129.3, 116.1, 116.1, 107.6, 98.6, 95.3, 79.2, 74.0, 67.2, 54.2, 54.0, 53.8, 53.7, 53.5, 49.3, 44.0, 22.5, 19.8. **HRMS**-ESI (m/z): $[M + H]^+$ calculated for $C_{22}H_{25}N_2O_4^+$, 381.1809; found, 381.1810.

(±) 1,7-dimethyl-8-(tetrahydro-2H-pyran-4-yl)-8,9b-dihydro-1H-pyrano[3',4':4,5]furo[3,2-c]pyridin-9(4aH)-one (12l)

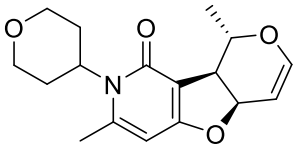

According to GP2, **3b**-*trans* (39.7 mg, 0.13 mmol) was reacted with **2f** (25.0 mg, 0.12 mmol) at 110 °C for 1 hour. The catalyst was filtered off and the filtrate was diluted with DCM (10 mL) and washed with saturated $NaHCO_3$ solution (15 mL). The aqueous phase was extracted with DCM (3 x 10 mL) and the combined organic layers were washed with brine (50 mL), dried over $MgSO_4$ and concentrated in vacuo. The crude was purified by MPLC (cyclohexane/EtOAc 1:0 to 1:1) to afford the product (9.6 mg, 27%). **^{1}H-NMR** (600 MHz, CD_2Cl_2): δ 6.76 (d, *J* = 6.2 Hz, 1H), 5.80 (s, 1H), 5.21 (dd, *J* = 6.2, 4.7 Hz, 1H), 4.89 (ddd, *J* = 6.9, 4.7, 1.1 Hz, 1H), 4.20-4.09 (bm, 1H), 4.04 (ddd, *J* = 11.7, 5.1, 1.5 Hz, 2H), 3.45 (dq, *J* = 10.7, 6.3 Hz, 1H), 3.42-3.36 (bm, 2H), 3.24-3.08 (bm, 2H), 2.94 (dd, *J* = 10.7, 6.9 Hz, 1H), 2.36 (s, 3H), 1.55-1.48 (bm, 2H), 1.45 (d, *J* = 6.3 Hz, 3H). **^{13}C-NMR** (151 MHz, CD_2Cl_2): δ 167.5, 162.7, 149.9, 148.8, 109.4, 98.6, 96.5, 79.2, 74.0, 68.3, 57.6, 44.0, 28.9, 22.7. 19.8. **HRMS**-ESI (m/z): $[M + H]^+$ calculated for $C_{17}H_{22}NO_4^+$, 304.1543; found, 304.1544.

(±) 1,7-dimethyl-8-(pyridin-4-ylmethyl)-8,9b-dihydro-1H-pyrano[3',4':4,5]furo[3,2-c]pyridin-9(4aH)-one (12m)

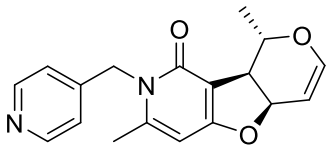

According to GP2, **3b**-*trans* (66.5 mg, 0.22 mmol) was reacted with **2n** (43.3 mg, 0.20 mmol) at 110 °C for 2 hours. The catalyst was filtered off and the filtrate was diluted with DCM (10 mL) and washed with saturated $NaHCO_3$ solution (15 mL). The aqueous phase was extracted with DCM (3 x 10 mL) and the combined organic layers were washed with brine (50 mL), dried over $MgSO_4$ and concentrated in vacuo. The crude was purified by MPLC (EtOAc/MeOH 1:0 to 9:1) to afford the product (2.9 mg, 5%). **^{1}H-NMR** (600 MHz, CD_2Cl_2): δ 8.75 (d, *J* = 6.5 Hz, 2H), 7.53 (d, *J* = 6.5 Hz, 2H), 6.80 (d, *J* = 6.1 Hz, 1H), 6.01 (s, 1H), 5.55 (d, *J* = 17.2 Hz, 1H), 5.34 (d, *J* = 17.2 Hz, 1H), 5.26 (dd, *J* = 6.1, 5.0 Hz, 1H), 5.02 (dd, *J* = 6.7, 5.0 Hz, 1H), 3.55-3.50 (m, 1H), 3.03 (dd, *J* = 10.7, 6.7 Hz, 1H), 2.25 (s, 3H), 1.43 (d, *J* = 6.3 Hz, 2H). **^{13}C-NMR** (151 MHz, CD_2Cl_2): δ 169.1, 161.7, 156.0, 150.2, 148.7, 143.6, 124.2, 108.0, 98.3, 97.5, 79.8, 73.7, 46.8, 43.9, 21.6, 19.7. **HRMS**-ESI (m/z): $[M + H]^+$ calculated for $C_{18}H_{19}N_2O_3^+$, 311.1317; found, 311.1390.

(±) 6-bromo-3-methyl-5a,9a-dihydro-1H,9H-furo[3,2-c:4,5-c']dipyran-1-one (17a)

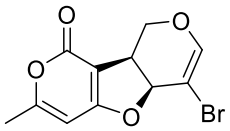

To a stirred solution of **9a** (70 mg, 0.34 mmol) in dry acetonitrile (3 mL) was added NBS (66.5 mg, 0.37 mmol, 1.1 equiv) and AgNO3 (115.3 mg, 0.68 mmol, 2 equiv) successively. The reaction tube was sealed and the mixture was stirred for 2 h at 80 °C. The reaction mixture was filtered and the filtrate was evaporated to afford a crude product which was purified by silica gel column chromatography (Pet. Ether/EtOAc 4:1). The product was obtained as an off-white powder (56.5 mg, 58%). **^{1}H-NMR** (700 MHz, $CDCl_3$): δ 7.01 (s, 1H), 6.01 (s, 1H), 5.15 (d, *J* = 7.4 Hz, 1H), 4.42-4.37 (m, 1H), 3.65-3.56 (m, 2H), 2.28 (s, 3H). **^{13}C-NMR** (176 MHz, $CDCl_3$): δ 171.8, 166.7, 161.6, 149.8, 99.7, 96.2, 96.1, 82.3, 65.0, 38.6, 20.7. **HRMS**-ESI (m/z): $[M + H]^+$ calculated for $C_{11}H_{10}O_4{}^{79}Br^+$, 284.9757; found, 284.9760; calculated for $C_{11}H_{10}O_4{}^{81}Br^+$, 286.9737; found, 286.9734.

(±) 3-methyl-6-phenyl-5a,9a-dihydro-1H,9H-furo[3,2-c:4,5-c']dipyran-1-one (17b)

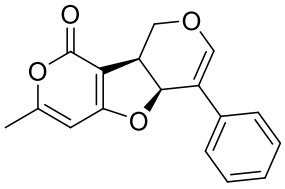

A microwave vial was flushed with Argon and loaded with **17a** (24.5 mg, 0.09 mmol), phenylboronic acid (21.0 mg, 0.17 mmol, 2 equiv), NaO^{t}Bu (16.5 mg, 0.17 mmol, 2 equiv), $Pd(OAc)_2$ (1.0 mg, 5 mol%), Xphos (4.1 mg, 10 mol%) and toluene (0.04 M). The mixture was irradiated at 100 °C for 5 minutes. After cooling back to room temperature the mixture was directly loaded on a silica column and eluted with Pet. Ether/EtOAc (9:1 to 7:3) to give the product (9.1 mg, 92%). **^{1}H-NMR** (700 MHz, $CDCl_3$): δ 7.41 (d, *J* = 7.6 Hz, 2H), 7.37 (t, *J* = 7.6 Hz, 2H), 7.28 (t, *J* = 7.6 Hz, 1H), 7.17 (s, 1H), 5.94 (s, 1H), 5.61 (d, *J* = 7.6 Hz, 1H), 4.46 (dd, *J* = 10.7, 4.9 Hz, 1H), 3.61-3.55 (m, 1H), 3.51 (t, *J* = 10.7 Hz, 1H), 2.26 (s, 3H). **^{13}C-NMR** (176 MHz, $CDCl_3$): δ 172.1, 166.2, 161.8, 147.7, 136.0, 128.9, 127.1, 125.1, 112.1, 99.8, 96.0, 79.9, 65.0, 36.8, 20.6. **UHPLC-MS**-ESI (m/z): 283.2 $[M + H]^+$.

(±) 6-(4-methoxyphenyl)-3-methyl-5a,9a-dihydro-1H,9H-furo[3,2-c:4,5-c']dipyran-1-one (17c)

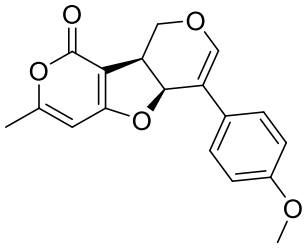

A microwave vial was flushed with Argon and loaded with **17a** (10.0 mg, 0.04 mmol), (4-methoxyphenyl)boronic acid (10.7 mg, 0.07 mmol, 2 equiv), NaO^{t}Bu (6.7 mg, 0.07 mmol, 2 equiv), $Pd(OAc)_2$ (0.4 mg, 5 mol%), Xphos (1.7 mg, 10 mol%) and toluene (0.04 M). The mixture was irradiated at 100 °C for 10 minutes. After cooling back to room temperature the mixture was directly loaded on a silica column and eluted with

Pet. Ether/EtOAc (9:1 to 7:3) to give the product (3.9 mg, 36%). The product decomposed quickly in acetonitrile/H_2O or DMSO/H_2O mixtures. **UHPLC-MS**-ESI (m/z): 313.3 $[M + H]^+$.

(±) 3-methyl-6-(4-(trifluoromethyl)phenyl)-5a,9a-dihydro-1H,9H-furo[3,2-c:4,5-c']dipyran-1-one (17d)

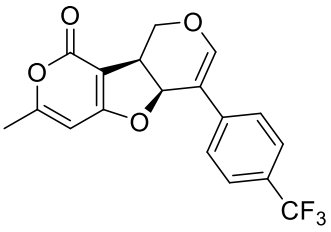

A microwave vial was flushed with Argon and loaded with **17a** (10.0 mg, 0.04 mmol), (4-(trifluoromethyl)phenyl)boronic acid (13.3 mg, 0.07 mmol, 2 equiv), NaO^tBu (6.7 mg, 0.07 mmol, 2 equiv), $Pd(OAc)_2$ (0.4 mg, 5 mol%), Xphos (1.7 mg, 10 mol%) and toluene (0.04 M). The mixture was irradiated at 130 °C for 40 minutes. After cooling back to room temperature the mixture was directly loaded on a silica column and eluted with Pet. Ether/EtOAc (9:1 to 7:3) and repurified by prep. HPLC to afford the product (6.1 mg, 50%). **^{1}H-NMR** (700 MHz DMSO-d_6): δ 7.73-7.70 (m, 4H), 7.63 (s, 1H), 6.33 (s, 1H), 5.93 (d, *J* = 7.5 Hz, 1H), 4.31 (dd, *J* = 10.2 Hz, 4.3 Hz, 1H), 3.62-3.58 (m, 1H), 3.56 (dd, *J* = 10.4 Hz, 10.2 Hz, 1H), 2.23 (s, 3H). **^{13}C-NMR** (176 MHz, DMSO-d_6): δ 172.1, 167.0, 161.1, 150.2, 140.9, 127.4, 125.9, 125.6, 124.1, 111.4, 99.4, 96.1, 79.0, 64.8, 36.4, 20.4. **UHPLC-MS**-ESI (m/z): 351.0 $[M + H]^+$.

(±) *Tert*-butyl (E)-3-(7-methyl-9-oxo-4a,9b-dihydro-1H,9H-furo[3,2-c:4,5-c']dipyran-4-yl)acrylate (17e)

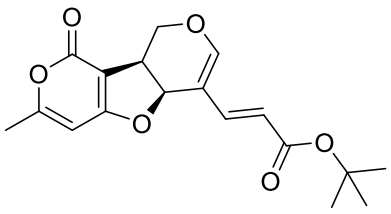

To a solution of **9a (**100 mg, 0.48 mmol) palladium diacetate (10.9 mg, 0.05 mmol) and copper trifluoromethanesulfonate (175.4 mg, 0.48 mmol) in dimethylacetamide (1 mL) and acetic acid (1 mL) underair bubbling at 70 °C, ethyl acrylate (0.14 ml, 0.97 mmol) was added dropwise. The mixture was allowed to stir at 70 °C for 3 hours. Then the mixture was diluted with ethyl acetate (20 mL), filtered, washed with water (20 mL) and brine (20 mL). The organic layer was dried over $MgSO_4$, evaporated and the residue was purified by flash column chromatography (Pet. Ether/EtOAc = 7/3) to afford the product as colorless oil (33.6 mg, 21%). **^{1}H-NMR** (700 MHz DMSO-d_6): δ 7.53 (s, 1H), 7.23 (d, 15.7 Hz, 1H) 6.39 (s, 1H), 5.84 (d, 15.7 Hz, 1H), 5.53 (d, 7.9 Hz, 1H), 4.25 (dd, 10.7 Hz, 4.7 Hz, 1H), 3.68 (dd, 10.7 Hz, 10.3 Hz, 1H), 3.57-3.52 (m, 1H), 2.23 (s, 3H), 1.44 (s, 9H). **^{13}C-NMR** (176 MHz, DMSO-d_6): δ 172.2, 167.0, 161.1, 166.1, 157.1, 141.4, 116.1, 111.5, 99.1, 96.1, 79.9, 77.5, 65.0, 35.8, 28.4, 20.1.

(±) 7,8-dimethyl-3-phenyl-4,8-dihydro-1H-pyrano[3',4':4,5]furo[3,2-c]pyridin-9(3H)-one (18a)

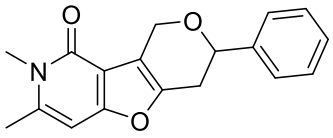

According to GP4, **9c** (40.0 mg, 0.18 mmol) was reacted with phenylboronic acid (44.5 mg, 0.36 mmol, 2 equiv) and $Pd(OAc)_2$ (20.5 mg, 0.09 mmol, 0.5 equiv) at room temperature for 18 hours. The crude was purified by MPLC (cyclohexane/EtOAc 1:0 to 0:1) to afford the product (35.0 mg, 64%). **^{1}H-NMR** (700 MHz DMSO-d_6): δ 7.47 (d, *J* = 7.4 Hz, 2H), 7.39 (t, *J* = 7.4 Hz, 2H), 7.32 (t, *J* = 7.4 Hz, 1H), 6.63 (d, *J* = 0.6 Hz, 1H), 4.96 (dd, *J* = 14.7, 1.8 Hz, 1H), 4.89 (dt, *J* = 14.7, 2.8 Hz, 1H), 4.79 (dd, *J* = 10.3, 3.5 Hz, 1H), 3.47 (s, 3H), 3.10-3.05 (m, 1H), 2.88 (ddt, *J* = 15.8, 10.3, 2.6 Hz, 1H), 2.43 (s, 3H). **^{13}C-NMR** (176 MHz, DMSO-d_6): δ 158.9, 158.1, 148.2, 143.6, 141.3, 128.3, 127.7, 126.0, 113.6, 110.4, 94.9, 75.3, 63.0, 31.2, 30.1, 20.9. **HRMS**-ESI (m/z): $[M + H]^+$ calculated for $C_{18}H_{18}NO_3^+$, 296.1281; found, 296.1291.

9c (30.0 mg, 0.14 mmol), phenylboronic acid (33.4 mg, 0.27 mmol), $Pd(OAc)_2$ (10 mol%), and $Cu(OAc)_2$ (49.7 mg, 0.27 mmol) were dissolved in DMF (3 mL) and stirred under O_2 atmosphere for 20 hours at room temperature. The reaction was quenched by addition of H_2O (20 mL) and extracted with a 1:1 mixture of methyl-*tert*-butyl ether and EtOAc (5 x 20 mL). The combined organic phases were washed with brine (100 mL), dried over $MgSO_4$ and concentrated in vacuo. The crude was purified by MPLC (cyclohexane/EtOAc 1:0 to 0:1) to afford the product (17.3 mg, 43%).

(±) 3-(4-methoxyphenyl)-7,8-dimethyl-4,8-dihydro-1H-pyrano[3',4':4,5]furo[3,2-c]pyridin-9(3H)-one (18b)

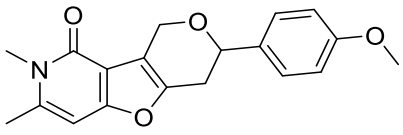

According to GP4, **9c** (40.0 mg, 0.18 mmol) was reacted with (4-methoxyphenyl)boronic acid (55.5 mg, 0.36 mmol, 2 equiv) and $Pd(OAc)_2$ (20.5 mg, 0.09 mmol, 0.5 equiv) at room temperature for 18 hours. The crude was purified by MPLC (cyclohexane/EtOAc 1:0 to 0:1) and repurified by prep. HPLC to afford the product (24.9 mg, 42%). **^{1}H-NMR** (700 MHz, $CDCl_3$): δ 7.37 (d, *J* = 8.5 Hz, 2H), 6.92 (d, *J* = 8.7 Hz, 2H), 6.41 (s, 1H), 5.18 (dd, *J* = 14.9, 2.0 Hz, 1H), 5.00 (dt, *J* = 14.9, 2.9 Hz, 1H), 4.70 (dd, *J* = 9.8, 3.8 Hz, 1H), 3.82 (s, 3H), 3.59 (s, 3H), 3.03-2.97 (m, 1H), 2.96-2.92 (m, 1H), 2.44 (s, 2H). **^{13}C-NMR** (176 MHz, $CDCl_3$): δ 160.4, 158.9, 159.5, 150.0, 142.1, 133.4, 127.6, 114.5, 114.1, 112.1, 96.6, 76.0, 64.0, 55.5, 31.9, 31.0, 21.8. **HRMS**-ESI (m/z): $[M + H]^+$ calculated for $C_{19}H_{20}NO_4^+$, 326.1387; found, 326.1397.

(±) 7,8-dimethyl-3-(4-(trifluoromethyl)phenyl)-4,8-dihydro-1H-pyrano[3',4':4,5]furo[3,2-c]pyridin-9(3H)-one (18c)

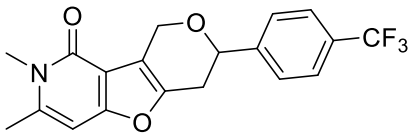

According to GP4, **9c** (20.0 mg, 0.09 mmol) was reacted with (4-(trifluoromethyl)phenyl)boronic acid (34.7 mg, 0.18 mmol, 2 equiv) and $Pd(OAc)_2$ (10.2 mg, 0.05 mmol, 0.5 equiv) at room temperature for 18 hours. The crude was purified by MPLC (cyclohexane/EtOAc 1:0 to 0:1) and repurified by prep. HPLC to afford the product (12.9 mg, 39%). **^{1}H-NMR** (500 MHz, $CDCl_3$): δ 7.65 (d, *J* = 8.2 Hz, 2H), 7.58 (d, *J* = 8.2 Hz, 2H), 6.39 (s, 1H), 5.25 (dd, *J* = 15.1, 2.0 Hz, 1H), 5.03 (dt, *J* = 15.1, 2.8 Hz, 1H), 4.81 (dd, *J* = 10.0, 3.8 Hz, 1H), 3.58 (s, 3H), 3.06-2.98 (m, 1H), 2.93 (ddt, *J* = 16.0, 10.0, 2.7 Hz, 1H), 2.44 (s, 3H). **^{13}C-NMR** (126 MHz, $CDCl_3$): δ 160.3, 158.9, 148.0, 145.3, 142.3, 130.4, 126.3, 125.7, 123.1, 114.6, 111.9, 96.2, 75.6, 64.2, 32.1, 30.8, 21.9. **HRMS**-ESI (m/z): $[M + H]^+$ calculated for $C_{19}H_{17}F_3NO_3^+$, 364.1155; found, 364.1155.

(±) 2-(7,8-dimethyl-9-oxo-3,4,8,9-tetrahydro-1H-pyrano[3',4':4,5]furo[3,2-c]pyridin-3-yl)benzonitrile (18d)

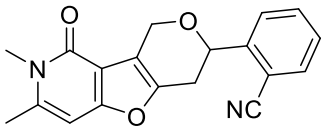

According to GP4, **9c** (25.0 mg, 0.11 mmol) was reacted with (2-cyanophenyl)boronic acid (33.5 mg, 0.23 mmol, 2 equiv) and $Pd(OAc)_2$ (12.8 mg, 0.06 mmol, 0.5 equiv) at 50 °C for 18 hours. The crude was purified by MPLC (cyclohexane/EtOAc 1:0 to 0:1) and repurified by prep. HPLC to afford the product (28.7 mg, 79%). **^{1}H-NMR** (700 MHz, $CDCl_3$): δ 7.77 (d, *J* = 8.0 Hz, 1H), 7.70-7.65 (m, 2H), 7.43 (td, *J* = 7.6, 1.2 Hz, 1H), 6.43 (s, 1H), 5.27 (dd, *J* = 15.0, 2.0 Hz, 1H), 5.10 (dd, *J* = 10.4, 3.6 Hz, 1H), 5.07 (ddd, *J* = 15.0, 3.3, 2.4 Hz, 1H), 3.60 (s, 3H), 3.16 (dt, *J* = 16.1, 3.0 Hz, 1H), 2.88 (dddt, *J* = 13.3, 10.4, 5.5, 2.3 Hz, 1H), 2.46 (s, 3H). **^{13}C-NMR** (176 MHz, $CDCl_3$): δ 160.4, 159.1, 147.9, 145.2, 142.4, 133.6, 132.9, 128.5, 126.7, 117.4, 114.4, 112.0, 110.3, 96.7, 74.1, 64.3, 31.7, 31.0, 21.8. **HRMS**-ESI (m/z): $[M + H]^+$ calculated for $C_{19}H_{17}N_2O_3^+$, 321.1234; found, 321.1235.

(±) 3-(1H-indol-5-yl)-7,8-dimethyl-4,8-dihydro-1H-pyrano[3',4':4,5]furo[3,2-c]pyridin-9(3H)-one (18e)

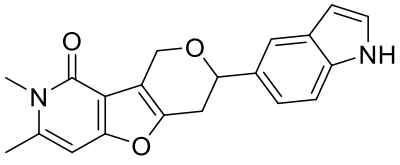

According to GP4, **9c** (25.0 mg, 0.11 mmol) was reacted with (1H-indol-5-yl)boronic acid (36.7 mg, 0.23 mmol, 2 equiv) and $Pd(OAc)_2$ (12.8 mg, 0.06 mmol, 0.5 equiv) at 50 °C for 18 hours. The crude was purified by MPLC (cyclohexane/EtOAc 1:0 to 0:1) and repurified by

prep. HPLC to afford the product (18.9 mg, 50%). **^{1}H-NMR** (500 MHz, $CDCl_3$): δ 8.23 (s, 1H),7.68 (s, 1H), 7.41 (d, *J* = 8.5 Hz, 1H), 7.30 (dd, *J* = 8.5, 1.7 Hz, 1H), 7.25-7.20 (m, 1H), 6.57-6.54 (m, 1H), 6.36 (s, 1H), 5.24 (dd, *J* = 15.0, 2.0 Hz, 1H), 5.06 (dt, *J* = 15.0, 2.8 Hz, 1H), 4.84 (dd, *J* = 10.0, 3.6 Hz, 1H), 3.54 (s, 3H), 3.16-3.08 (m, 1H), 3.00 (dt, *J* = 16.4, 3.1 Hz, 1H), 2.40 (s, 3H). **^{13}C-NMR** (126 MHz, $CDCl_3$): δ 160.4, 158.7, 149.1, 141.9, 135.7, 132.7, 128.0, 125.0, 120.6, 118.6, 114.6, 112.0, 111.3, 102.9, 96.3, 64.1, 32.4, 30.8, 21.8. **HRMS**-ESI (m/z): $[M + H]^+$ calculated for $C_{20}H_{19}N_2O_3^+$, 335.1390; found, 335.1391.

(±) 3-(6-fluoropyridin-3-yl)-7,8-dimethyl-4,8-dihydro-1H-pyrano[3',4':4,5]furo[3,2-c]pyridin-9(3H)-one (18f)

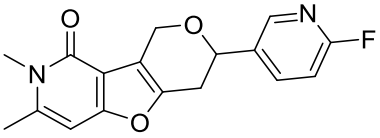

According to GP4, **9c** (40.0 mg, 0.18 mmol) was reacted with (6-fluoropyridin-3-yl)boronic acid (51.4 mg, 0.36 mmol, 2 equiv) and $Pd(OAc)_2$ (20.5 mg, 0.09 mmol, 0.5 equiv) at room temperature for 18 hours. The crude was purified by MPLC (cyclohexane/EtOAc 1:0 to 0:1) to afford the product (9.4 mg, 17%). **^{1}H-NMR** (500 MHz, $CDCl_3$): δ 8.27 (d, *J* = 2.5 Hz, 1H), 7.92 (td, *J* = 8.3, 2.5 Hz, 1H), 6.97 (dd, *J* = 8.3, 2.9 Hz, 1H), 6.39 (s, 1H), 5.22 (dd, *J* = 15.1, 1.9 Hz, 1H), 5.03 (dt, *J* = 15.1, 2.8 Hz, 1H), 4.80 (dd, *J* = 9.8, 4.1 Hz, 1H), 3.55 (s, 3H), 3.04-2.91 (m, 2H), 2.44 (s, 3H). **^{13}C-NMR** (126 MHz, $CDCl_3$): δ 164.3, 162.4, 160.1, 158.8, 147.4, 145.4, 142.3, 139.2, 135.4, 114.5, 111.7, 109.5, 95.1, 73.3, 31.9, 30.7, 21.7. **HRMS**-ESI (m/z): $[M + H]^+$ calculated for $C_{17}H_{16}FN_2O_3^+$, 315.1140; found, 315.1145.

(±) 7,8-dimethyl-3-(thiophen-3-yl)-4,8-dihydro-1H-pyrano[3',4':4,5]furo[3,2-c]pyridin-9(3H)-one (18g)

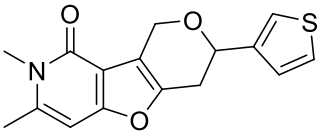

According to GP4, **9c** (35.0 mg, 0.16 mmol) was reacted with thiophen-3-ylboronic acid (40.9 mg, 0.32 mmol, 2 equiv) and $Pd(OAc)_2$ (17.9 mg, 0.08 mmol, 0.5 equiv) at room temperature for 18 hours. The crude was purified by MPLC (cyclohexane/EtOAc 1:0 to 0:1) to afford the product (2.6 mg, 5%). **^{1}H-NMR** (700 MHz, $CDCl_3$): δ 7.35 (dd, *J* = 5.0, 3.0 Hz, 1H), 7.34-7.30 (m, 1H), 7.17 (dd, *J* = 5.0, 1.3 Hz, 1H), 6.38 (s, 1H), 5.17 (dt, *J* = 14.9, 1.3 Hz, 1H), 5.02 (dt, *J* = 14.9, 2.8 Hz, 1H), 4.87 (dd, *J* = 8.7, 4.7 Hz, 1H), 3.57 (s, 3H), 3.08-3.01 (m, 2H), 2.43 (s, 3H). **HRMS**-ESI (m/z): $[M + H]^+$ calculated for $C_{16}H_{16}NO_3S^+$, 302.0845; found, 302.0847.

(±) 7,8-dimethyl-3-phenyl-4,4a,8,9b-tetrahydro-1H-pyrano[3',4':4,5]furo[3,2-c]pyridin-9(3H)-one (18h)

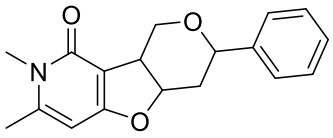

18a (16.0 mg, 0.05 mmol) was dissolved in EtOH (1 mL) and $Pd(OH)_2$ (1.6 mg, 20% on carbon) was added. The mixture was stirred under H_2 atmosphere at room temperature for 40 hours. The catalyst was filtered off and the solvent removed under reduced pressure. The crude was purified by prep. HPLC to afford the product (4.0 mg, 25%). **^{1}H-NMR** (700 MHz, $CDCl_3$): δ 7.31-7.29 (m, 4H), 7.25-7.22 (m, 1H), 5.90 (s, 1H), 5.20 (td, *J* = 8.8, 6.5 Hz, 1H), 4.81 (dd, *J* = 12.2, 3.3 Hz, 1H), 4.50 (dd, *J* = 10.5, 3.5 Hz, 1H), 4.00 (dd, *J* = 12.2, 4.6 Hz, 1H), 3.61 (dt, *J* = 8.8, 4.0 Hz, 1H), 3.52 (s, 3H), 2.37-2.31 (m, 4H), 1.93 (ddd, *J* = 14.0, 10.5, 8.9 Hz, 1H). **^{13}C-NMR** (176 MHz, $CDCl_3$): δ 167.5, 162.5, 148.8, 142.5, 128.5, 127.6, 125.9, 107.1, 96.5, 81.7, 74.9, 64.1, 39.7, 35.2, 30.9, 21.9. **HRMS**-ESI (m/z): $[M + H]^+$ calculated for $C_{18}H_{20}NO_3^+$, 298.1438; found, 298.1450.

(±) 3-(4-methoxyphenyl)-7-methyl-8-(thiophen-2-ylmethyl)-4,8-dihydro-1H-pyrano[3',4':4,5]furo[3,2-c]pyridin-9(3H)-one (18i)

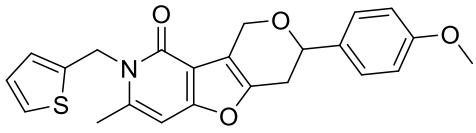

According to GP2, **3a** (100.0 mg, 0.35 mmol) was reacted with **2l** (70.0 mg, 0.32 mmol) at 100 °C for 1 hour. After filtration over celite the crude was purified by FC (Hep/EtOAc 1:0 to 1:1) and an aliquot of the product (35.0 mg, 0.12 mmol) was directly reacted according to GP4, (35.0 mg, 0.12 mmol) with (4-methoxyphenyl)boronic acid (35.3 mg, 0.23 mmol, 2 equiv), $Pd(OAc)_2$ (5.2 mg, 20 mol%) and $Cu(OAc)_2$ (42.2 mg, 0.23 mmol, 2 equiv) at 50 °C for 18 hours under O_2 atmosphere. The crude was purified by MPLC (cyclohexane/EtOAc 1:0 to 0:1) and repurified by prep. HPLC to afford the product (5.7 mg, 12%). **^{1}H-NMR** (700 MHz, $CDCl_3$): δ 7.38 (d, *J* = 8.5 Hz, 2H), 7.21 (d, *J* = 5.0 Hz, 1H), 7.00 (d, *J* = 3.1 Hz, 1H), 6.97-6.95 (m, 1H), 6.93 (d, *J* = 8.5 Hz, 2H), 6.33 (s, 1H), 5.52-5.40 (m, 2H), 3.80 (s, 3H), 5.22 (d, *J* = 15.0 Hz, 1H), 5.05-5.02 (m, 1H), 4.70 (dd, *J* = 9.8, 3.8 Hz, 1H), 3.03-2.98 (m, 1H), 2.96-2.93 (m, 1H), 2.50 (s, 3H). **^{13}C-NMR** (176 MHz, $CDCl_3$): δ 160.0, 159.5, 159.0, 148.9, 141.6, 139.5, 133.4, 127.6, 126.8, 126.5, 125.6, 114.4, 114.1, 112.4, 96.9, 76.0, 64.4, 55.5, 42.9, 32.2, 21.3. **HRMS**-ESI (m/z): $[M + H]^+$ calculated for $C_{23}H_{22}NO_4S^+$, 408.1191; found, 408.1264.

(±) 3-(hydroxymethyl)-6-methyl-1,3,3a,8b-tetrahydro-8H-furo[3',4':4,5]furo[3,2-c]pyran-8-one (19a)

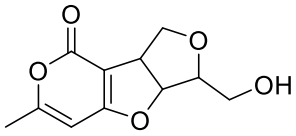

9a (50.0 mg, 0.24 mmol) was reacted according to GP5 and purified by MPLC (DCM/MeOH 1:0 to 9:1) to give the product (14.7 mg, 70% over two steps). **^{1}H-NMR** (700 MHz, $CDCl_3$): 5.94 (s, 1H), 5.30 (dd, *J* = 8.6, 2.7 Hz, 1H), 4.20 (dd, *J* = 9.0, 6.6 Hz, 1H), 4.17 (ddd, *J* = 6.7, 4.3, 2.7 Hz, 1H), 4.01-3.96 (m, 2H), 3.80-3.73 (m, 2H), 2.26 (s, 3H). **^{13}C-NMR** (176 MHz, $CDCl_3$): δ 171.3, 166.1, 162.0, 101.6, 95.8, 91.3, 85.3, 72.6, 61.6, 45.0, 20.6. **HRMS**-ESI (m/z): $[M + H]^+$ calculated for $C_{11}H_{13}O_5^+$, 225.0758; found, 225.0760.

(±) 3-(hydroxymethyl)-6,7-dimethyl-3,3a,7,8b-tetrahydrofuro[3',4':4,5]furo[3,2-c]pyridin-8(1H)-one (19b)

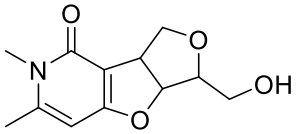

9c (70.0 mg, 0.32 mmol) was reacted according to GP5 and purified by MPLC (DCM/MeOH 1:0 to 9:1) to give the product (16.9 mg, 29% over two steps). **^{1}H-NMR** (700 MHz, MeOH-d_4): δ 6.08 (s, 1H), 5.31 (dd, *J* = 8.9, 2.1 Hz, 1H), 4.18 (dd, *J* = 9.0, 6.9 Hz, 1H), 4.10 (td, *J* = 5.6, 2.1 Hz, 1H), 4.00 (ddd, *J* = 8.9, 6.9, 3.1 Hz, 1H), 3.89 (dd, *J* = 9.0, 3.1 Hz, 1H), 3.69-3.62 (m, 2H), 3.51 (s, 3H), 2.41 (s, 3H). **^{13}C-NMR** (176 MHz, MeOH-d_4): δ 169.1, 163.5, 151.5, 109.5, 96.9, 92.2, 87.2, 73.5, 62.1, 47.0, 31.3, 21.4. **HRMS**-ESI (m/z): $[M + H]^+$ calculated for $C_{12}H_{16}NO_4^+$, 238.1074; found, 238.1072.

(±) 7-(4-fluorobenzyl)-3-(hydroxymethyl)-6-methyl-3,3a,7,8b-tetrahydrofuro[3',4':4,5]furo[3,2-c]pyridin-8(1H)-one (19c)

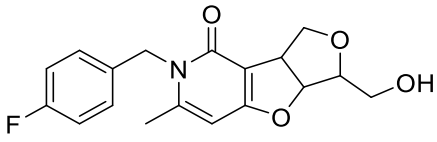

According to GP2, **3a** (47.6 mg, 0.17 mmol) was reacted with **2h** (35.0 mg, 0.15 mmol) at 100 °C for 18 hours. Purification by MPLC (cyclohexane/EtOAc 1:0 to 0:1) afforded the corresponding glycal (25.6 mg, 55%), which was directly reacted according to GP5 and purified by prep. HPLC to give the product (7.2 mg, 28% over two steps). **^{1}H-NMR** (700 MHz, $CDCl_3$): δ 7.13 (dd, *J* = 8.4, 5.2 Hz, 2H), 7.01 (td, *J* = 8.4, 1.3 Hz, 2H), 5.95 (s, 1H), 5.35 (d, *J* = 15.3 Hz, 1H), 5.26 (dd, *J* = 8.9, 2.8 Hz, 1H), 5.22 (d, *J* = 15.3 Hz, 1H), 4.28-4.25 (m, 1H), 4.20-4.17 (m, 1H), 4.13-4.09 (m, 1H), 4.04 (dd, *J* = 9.2, 3.7 Hz, 1H), 3.82-3.74 (m, 2H), 2.29 (s, 3H). **^{13}C-NMR** (176 MHz, $CDCl_3$): δ 167.7, 163.0, 162.0, 149.2, 132.3, 128.4, 116.0, 108.8, 96.9, 90.4, 85.5, 72.8, 61.6, 46.6, 46.1, 21.4. **HRMS**-ESI (m/z): $[M + H]^+$ calculated for $C_{18}H_{19}FNO_4^+$, 332.1293; found, 332.1295.

(±) 7-((2-chloropyridin-4-yl)methyl)-3-(hydroxymethyl)-6-methyl-3,3a,7,8b-tetrahydrofuro[3',4':4,5]furo[3,2-c]pyridin-8(1H)-one (19d)

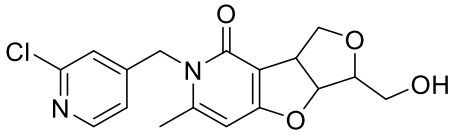

According to GP2, **3a** (95.2 mg, 0.33 mmol) was reacted with **2p** (75.2 mg, 0.30 mmol) at 100 °C for 18 hours. Purification by MPLC (cyclohexane/EtOAc 1:0 to 0:1) afforded the corresponding glycal (25.0 mg, 25%), which was directly reacted according to GP5 and purified by prep. HPLC to give the product (2.5 mg, 10% over two steps). **^{1}H-NMR** (700 MHz, $CDCl_3$): δ 8.33 (d, *J* = 5.2 Hz, 1H), 7.07 (s, 1H), 6.99 (d, *J* = 5.2 Hz, 1H), 5.94 (s, 1H), 5.27-5.25 (m, 1H), 4.29-4.26 (m, 1H), 4.21-4.17 (m, 1H), 4.12-4.08 (m, 1H), 4.05-4.01 (m, 1H), 3.83-3.75 (m, 2H), 2.25 (s, 3H). **HRMS**-ESI (m/z): $[M + H]^+$ calculated for $C_{17}H_{18}ClN_2O_4^+$, 349.0950; found, 349.0952.

(±) 3-(hydroxymethyl)-6-methyl-7-(pyridin-2-ylmethyl)-3,3a,7,8b-tetrahydrofuro[3,4-b]benzofuran-8(1H)-one (19e)

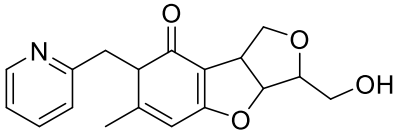

According to GP2, **3a** (63.5 mg, 0.22 mmol) was reacted with **2m** (43.3 mg, 0.20 mmol) at 100 °C for 18 hours. Purification by MPLC (cyclohexane/EtOAc 1:0 to 0:1) afforded the corresponding glycal (43.0 mg, 75%), which was directly reacted according to GP5 and purified by prep. HPLC to give the product (7.1 mg, 11% over two steps). **^{1}H-NMR** (700 MHz, $CDCl_3$): δ 8.78-8.66 (m, 1H), 8.06-7.97 (m, 1H), 7.58-7.50 (m, 1H), 7.44-7.36 (m 1H), 6.04-5.94 (s, 1H), 5.72-5.56 (m, 2H), 5.31-5.26 (m, 1H), 4.30-4.18 (m, 2H), 4.15-3.99 (m, 2H), 3.84-3.75 (m, 2H),2.37 (s, 1H). **HRMS**-ESI (m/z): $[M + H]^+$ calculated for $C_{17}H_{19}O_4N_2^+$, 315.1339; found, 315.1342.

(±) 3-(hydroxymethyl)-6-methyl-7-(thiophen-2-ylmethyl)-3,3a,7,8b-tetrahydrofuro[3',4':4,5]furo[3,2-c]pyridin-8(1H)-one (19f)

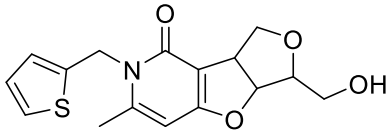

According to GP2, **3a** (100.0 mg, 0.35 mmol) was reacted with **2l** (70.0 mg, 0.32 mmol) at 100 °C for 18 hours. Purification by MPLC (cyclohexane/EtOAc 1:0 to 0:1) afforded the corresponding glycal (35.0 mg, 38%) which was directly reacted according to GP5 and purified by MPLC (DCM/MeOH 1:0 to 4:1) to give the product (8.0 mg, 17% over two steps). **^{1}H-NMR** (600 MHz, $CDCl_3$): δ 7.22 (dd, *J* = 5.1, 1.2 Hz, 1H), 7.01 (dd, *J* = 3.5, 1.2 Hz, 1H), 6.93 (dd, *J* = 5.1, 3.5 Hz, 1H), 5.90 (s, 1H), 5.46 (d, *J* = 15.4 Hz, 1H), 5.32 (d, *J* = 15.4 Hz, 1H), 5.22 (dd, *J* = 9.5, 2.9 Hz, 1H), 4.27 (dd, *J* = 9.2, 7.0 Hz, 1H), 4.15 (ddd, *J* = 6.8, 4.1, 2.9 Hz, 1H), 4.10

(ddd, *J* = 9.5, 7.0, 3.8 Hz, 1H), 4.02 (dd, *J* = 9.2, 3.8 Hz, 1H), 3.82-3.73 (m, 2H), 2.46 (s, 3H). **^{13}C-NMR** (151 MHz, $CDCl_3$): δ 167.5, 161.6, 148.6, 138.8, 126.9, 126.7, 125.9, 108.8, 96.7, 90.3, 85.5, 72.8, 61.5, 46.0, 42.7, 21.4. **HRMS**-ESI (m/z): $[M + H]^+$ calculated for $C_{16}H_{18}NSO_4^+$, 320.0951; found, 320.0948.

(±) 9-(hydroxymethyl)-5-methyl-6b,7,9,9a-tetrahydrofuro[3',4':4,5]furo[3,2-c]quinolin-6(5H)-one (19g)

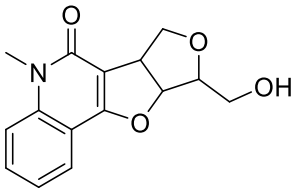

According to GP2, **3a** (75.9 mg, 0.26 mmol) was reacted with **2w** (34.2 mg, 0.20 mmol) at 100 °C for 1 hour. Purification by MPLC (cyclohexane/EtOAc 1:0 to 0:1) afforded the corresponding glycal (31.9 mg, 60%), which was directly reacted according to GP5 and purified by prep. HPLC to give the product (2.9 mg, 9% over two steps). **^{1}H-NMR** (700 MHz, $CDCl_3$): δ 7.75 (d, *J* = 7.9 Hz, 1H), 7.61 (dd, *J* = 8.7, 7.1 Hz, 1H), 7.40 (d, *J* = 8.7 Hz, 1H), 7.27 (dd, *J* = 7.9, 7.1 Hz, 1H), 5.55 (dd, *J* = 8.1, 4.1, 1H), 4.32 (d, *J* = 9.5 Hz, 1H), 4.25 (ddd, *J* = 8.1, 6.3, 1.5 Hz, 1H), 4.07 (ddd, *J* = 11.8, 4.6, 1.3 Hz, 1H), 4.00 (ddd, *J* = 11.8, 7.0, 1.3 Hz, 1H), 3.97-3.94 (m, 1H), 3.86 (ddd, *J* = 9.5, 6.3, 1.3 Hz, 1H), 3.71 (s, 3H). **^{13}C-NMR** (176 MHz, $CDCl_3$): δ 163.3, 161.2, 140.9, 131.6, 123.3, 122.2, 114.9, 112.2, 109.6, 89.7, 84.3, 72.0, 61.3, 47.6, 29.3. **HRMS**-ESI (m/z): $[M + H]^+$ calculated for $C_{15}H_{16}NO_4^+$, 274.1074; found, 274.1073.

5.1.4.2. Synthesis of General Scaffold B Isomers

(±) 7,8-dimethyl-4,4a,8,9b-tetrahydro-2H-pyrano[2',3':4,5]furo[3,2-c]pyridine-3,9-dione (20a)

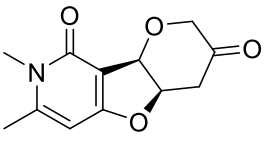

According to GP6, **4a** (50.0 mg, 0.32 mmol) was reacted with **2b** (44.5 mg, 0.32 mmol) employing allylpalladium(II) chloride dimer (2.5 mol%) and Xantphos (7.5 mol%) as catalyst. Purification by MPLC (cyclohexane/EtOAc 1:0 to 0:1) afforded the product (49.5 mg, 66%). **^{1}H NMR** (700 MHz, $CDCl_3$): δ 5.85 (s, 1H), 5.60 (d, *J* = 7.4 Hz, 1H), 5.20 (dt, *J* = 7.4, 3.9 Hz, 1H), 4.02 (d, *J* = 18.4 Hz, 1H), 3.71 (d, *J* = 18.4 Hz, 1H), 3.51 (s, 3H), 3.07 (dd, *J* = 16.1, 3.9 Hz, 1H), 2.96 (dd, *J* = 16.1, 3.9 Hz, 1H), 2.37 (s, 3H). **^{13}C NMR** (176 MHz, $CDCl_3$): δ 207.7, 169.2, 161.7, 151.6, 102.8, 94.6, 82.0, 74.8, 68.9, 39.7, 30.8, 22.1. **HRMS**-ESI (m/z): $[M + H]^+$ calculated for $C_{12}H_{14}O_4N^+$,236.09173; found, 236.09173.

(±) 8-benzyl-7-methyl-4,4a,8,9b-tetrahydro-2H-pyrano[2',3':4,5]furo[3,2-c]pyridine-3,9-dione (20b)

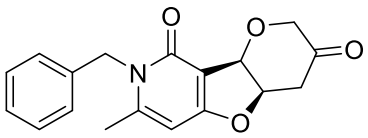

According to GP6, **4a** (50.0 mg, 0.32 mmol) was reacted with **2g** (68.9 mg, 0.32 mmol) employing allylpalladium(II) chloride dimer (2.5 mol%) and Xantphos (7.5 mol%) as catalyst. Purification by MPLC (cyclohexane/EtOAc 1:0 to 0:1) afforded the product (73.0 mg, 73%). **^{1}H NMR** (600 MHz, $CDCl_3$): δ 7.32 (t, *J* = 7.4 Hz, 2H), 7.28 (d, *J* = 7.4 Hz, 1H), 7.14 (d, *J* = 7.4 Hz, 2H), 5.96 (s, 1H), 5.68 (d, *J* = 7.4 Hz, 1H, 5.49 (d, *J* = 15.7 Hz, 1H), 5.28 (dt, *J* = 7.4, 3.9 Hz, 1H), 5.24 (d, *J* = 15.7 Hz, 1H), 4.05 (d, *J* = 18.4 Hz, 1H), 3.75 (d, *J* = 18.4 Hz, 1H), 3.10 (dd, *J* = 16.1, 3.9 Hz, 1H), 3.00 (dd, *J* = 16.1, 3.9 Hz, 1H), 2.33 (s, 1H). **^{13}C NMR** (151 MHz, $CDCl_3$): δ 207.2, 169.8, 162.1, 152.1, 135.9, 128.9, 127.6, 126.3, 103.3, 96.2, 82.4, 74.3, 68.8, 47.1, 39.5, 21.5. **HRMS**-ESI (m/z): $[M + H]^+$ calculated for $C_{18}H_{18}O_4N^+$,312.12303; found, 312.12330.

(±) 8-(4-fluorobenzyl)-7-methyl-4,4a,8,9b-tetrahydro-2H-pyrano[2',3':4,5]furo[3,2-c]pyridine-3,9-dione (20c)

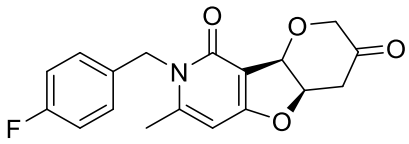

According to GP6, **4a** (50.0 mg, 0.32 mmol) was reacted with **2h** (74.7 mg, 0.32 mmol) employing allylpalladium(II) chloride dimer (2.5 mol%) and Xantphos (7.5 mol%) as catalyst. Purification by MPLC (cyclohexane/EtOAc 1:0 to 0:1) afforded the product (72.5 mg, 69%). **^{1}H NMR** (500 MHz, Chloroform-d): δ 7.16 (m, 2H), 7.00 (m, 2H), 5.86 (d, *J* = 1.1 Hz, 1H), 5.64 (d, *J* = 7.4 Hz, 1H), 5.42 (d, *J* = 15.7 Hz, 1H), 5.25 (dt, *J* = 7.4, 3.9 Hz, 1H), 5.15 (d, *J* = 15.7 Hz, 1H), 4.07 (d, *J* = 18.3 Hz, 1H), 3.76 (d, *J* = 18.3 Hz, 1H), 3.10 (dd, *J* = 16.1, 3.9 Hz, 1H), 2.99 (dd, *J* = 16.1, 3.9 Hz, 1H), 2.30 (s, 3H). **^{13}C NMR** (126 MHz, $CDCl_3$): δ 207.7, 169.5, 163. 2, 161. 7, 151.8, 132.4, 116.0, 115.8, 103.1, 95.4, 82.2, 74.8, 69.0, 46.2, 39.7, 21.7. **HRMS**-ESI (m/z): $[M + H]^+$ calculated for $C_{18}H_{17}O_4NF^+$,330.11361; found, 330.11400.

(±) 8-(2-chlorobenzyl)-7-methyl-4,4a,8,9b-tetrahydro-2H-pyrano[2',3':4,5]furo[3,2-c]pyridine-3,9-dione (20d)

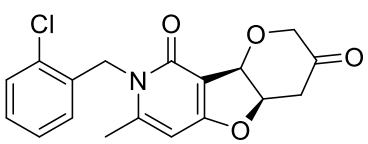

According to GP6, **4a** (50.0 mg, 0.32 mmol) was reacted with **2i** (79.9 mg, 0.32 mmol) employing allylpalladium(II) chloride dimer (2.5 mol%) and Xantphos (7.5 mol%) as catalyst. Purification by MPLC (cyclohexane/EtOAc 1:0 to 0:1) afforded the product (96.8 mg, 87%). **^{1}H NMR** (500 MHz, $CDCl_3$): δ 7.39 (dd, *J* = 7.6, 1.6 Hz, 1H), 7.19 (dtd, *J* = 16.7, 7.6, 1.6 Hz,

2H), 6.78 (dd, *J* = 7.6, 1.6 Hz, 1H), 5.90 (s, 1H), 5.66 (d, *J* = 7.4 Hz, 1H), 5.51 (d, *J* = 17.3 Hz, 1H), 5.31 (d, *J* = 17.3 Hz, 1H), 5.27 (m, 1H), 4.08 (d, *J* = 18.3 Hz, 1H), 3.78 (d, *J* = 18.3 Hz, 1H), 3.11 (dd, *J* = 16.1, 3.9 Hz, 1H), 3.01 (dd, *J* = 16.1, 3.9 Hz, 1H), 2.24 (s, 3H). **^{13}C NMR** (126 MHz, $CDCl_3$): δ 207.7, 169.7, 161.6, 151.9, 133.9, 132.5, 129.7, 128.7, 127.6, 126.5, 102.9, 95.5, 82.3, 74.8, 69.0, 44.4, 39.8, 21.4. **HRMS**-ESI (m/z): $[M + H]^+$ calculated for $C_{18}H_{17}O_4NCl^+$,346.08406; found, 346.08453.

(±) 7-methyl-8-(pyridin-2-ylmethyl)-4,4a,8,9b-tetrahydro-2H-pyrano[2',3':4,5]furo[3,2-c]pyridine-3,9-dione (20e)

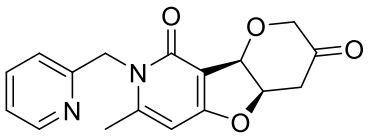

According to GP6, **4a** (50.0 mg, 0.32 mmol) was reacted with **2m** (69.2 mg, 0.32 mmol) employing allylpalladium(II) chloride dimer (2.5 mol%) and Xantphos (7.5 mol%) as catalyst. Purification by MPLC (cyclohexane/EtOAc 1:0 to 0:1) afforded the product (71.6 mg, 72%). **^{1}H NMR** (700 MHz, $CDCl_3$): δ 8.51 (d, *J* = 4.1 Hz, 1H), 7.63 (td, *J* = 7.6, 1.5 Hz, 1H), 7.27 (d, *J* = 4.8 Hz, 1H), 7.18 (ddd, *J* = 7.6, 4.8, 1.5 Hz, 1H), 5.88 (s, 1H), 5.61 (d, *J* = 7.4 Hz, 1H), 5.49 (d, *J* = 16.0 Hz, 1H), 5.28 (d, *J* = 16.0 Hz, 1H), 5.23 (dt, *J* = 7.4, 3.9 Hz, 1H), 4.03 (d, *J* = 18.3 Hz, 1H), 3.75 (d, *J* = 18.3 Hz, 1H), 3.07 (dd, *J* = 16.1, 3.9 Hz, 1H), 2.97 (dd, *J* = 16.1, 3.9 Hz, 1H), 2.43 (s, 3H). **^{13}C NMR** (176 MHz, $CDCl_3$) δ 207.6, 169.6, 161.5, 156.3, 152.5, 149.4, 137.1, 122.7, 122.2, 102.8, 95.2, 82.1, 77.3, 77.2, 76.9, 74.7, 68.9, 60.5, 48.7, 39.7, 22.1, 14.3. **HRMS**-ESI (m/z): $[M + H]^+$ calculated for $C_{17}H_{17}O_4N_2^+$,313.11828; found, 313.11845.

(±) 8-((2-chloropyridin-4-yl)methyl)-7-methyl-4,4a,8,9b-tetrahydro-2H-pyrano[2',3':4,5]furo[3,2-c]pyridine-3,9-dione (20f)

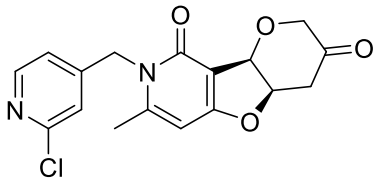

According to GP6, **4a** (50.0 mg, 0.32 mmol) was reacted with **2p** (80.3 mg, 0.32 mmol) employing allylpalladium(II) chloride dimer (2.5 mol%) and Xantphos (7.5 mol%) as catalyst. Purification by MPLC (cyclohexane/EtOAc 1:0 to 0:1) afforded the product (81.2 mg, 73%). **^{1}H NMR** (600 MHz, $CDCl_3$): δ 8.37 (d, *J* = 5.2 Hz, 1H), 7.09 (s, 1H), 7.04 (d, *J* = 5.2 Hz, 1H), 6.02 (s, 1H), 5.64 (d, *J* = 7.4 Hz, 1H), 5.50 (d, *J* = 15.9 Hz, 1H), 5.30 (dt, *J* = 7.4, 4.0 Hz, 1H), 5.15 (d, *J* = 15.9 Hz, 1H), 4.04 (d, *J* = 18.3 Hz, 1H), 3.73 (d, *J* = 18.3 Hz, 1H), 3.10 (dd, *J* = 16.1, 4.0 Hz, 1H), 3.01 (dd, *J* = 16.1, 4.0 Hz, 1H), 2.31 (s, 3H). **^{13}C NMR** (151 MHz, $CDCl_3$): δ 207.0, 170.3, 161.8, 152.2, 151.3, 150.0, 149.4, 122.1, 120.4, 103.7, 97.0, 82.8, 74.4, 69.1, 46.0, 39.6, 21.7. **HRMS**-ESI (m/z): $[M + H]^+$ calculated for $C_{17}H_{16}O_4N_2Cl^+$,347.07931; found, 347.07978.

(±) 7-methyl-8-((3-methylpyridin-4-yl)methyl)-4,4a,8,9b-tetrahydro-2H-pyrano[2',3':4,5]furo[3,2-c]pyridine-3,9-dione (20g)

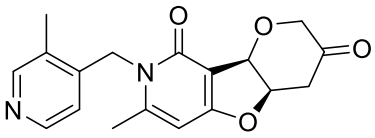

According to GP6, **4a** (50.0 mg, 0.32 mmol) was reacted with **2o** (104.3 mg, 0.32 mmol) employing allylpalladium(II) chloride dimer (2.5 mol%) and Xantphos (7.5 mol%) as catalyst. Purification by MPLC (cyclohexane/EtOAc 1:0 to 0:1) afforded the product (58.0 mg, 56%). **^{1}H NMR** (500 MHz, $CDCl_3$): δ 8.69 (s, 1H), 8.53 (d, *J* = 5.8 Hz, 1H), 7.02 (d, *J* = 5.8 Hz, 1H), 6.04 (s, 1H), 5.61 (d, *J* = 7.6 Hz, 1H), 5.52 (d, *J* = 17.7 Hz, 1H), 5.31 (dt, *J* = 7.6, 4.0 Hz, 1H), 5.16 (d, *J* = 17.7 Hz, 1H), 4.07 (d, *J* = 18.3 Hz, 1H), 3.76 (d, *J* = 18.3 Hz, 1H), 3.12 (dd, *J* = 16.1, 4.0 Hz, 1H), 3.03 (dd, *J* = 16.1, 4.0 Hz, 1H), 2.58 (s, 3H), 2.28 (s, 3H). **^{13}C NMR** (176 MHz, $CDCl_3$): δ 207.1, 170.0, 161.1, 152.8, 150.2, 143.7, 142.1, 134.2, 121.7, 96.26, 82.63, 74.62, 69.15, 41.14, 39.67, 31.08, 21.49, 14.27. **HRMS**-ESI (m/z): $[M + H]^+$ calculated for $C_{18}H_{19}O_4N_2^+$,327.13393; found, 327.13412.

(±) 8-(2-(5-methoxy-1H-indol-3-yl)ethyl)-7-methyl-4,4a,8,9b-tetrahydro-2H-pyrano[2',3':4,5]furo[3,2-c]pyridine-3,9-dione (20h)

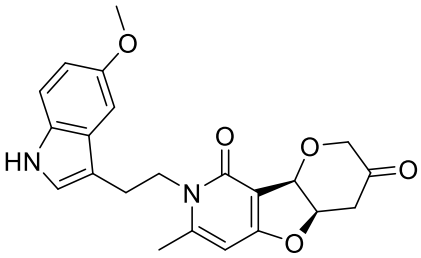

According to GP6, **4a** (12.5 mg, 0.08 mmol) was reacted with **2s** (23.8 mg, 0.08 mmol) employing allylpalladium(II) chloride dimer (2.5 mol%) and Xantphos (7.5 mol%) as catalyst. Purification by MPLC (cyclohexane/EtOAc 1:0 to 0:1) afforded the product (23.7 mg, 75%). **^{1}H NMR** (700 MHz, $CDCl_3$): δ 8.15 (s, 1H), 7.25 (s, 1H), 7.12 (d, *J* = 2.4 Hz, 1H), 6.97 (d, *J* = 2.4 Hz, 1H), 6.85 (dd, *J* = 8.8, 2.4 Hz, 1H), 5.76 (s, 1H), 5.64 (d, *J* = 7.4 Hz, 1H), 5.21 (dt, *J* = 7.4, 3.9 Hz, 1H), 4.26 (ddt, *J* = 28.7, 13.8, 6.9 Hz, 2H), 4.05 (d, *J* = 18.4 Hz, 1H), 3.86 (s, 3H), 3.75 (d, *J* = 18.4 Hz, 1H), 3.14 (t, *J* = 7.6 Hz, 2H), 3.08 (dd, *J* = 16.2, 4.0 Hz, 1H), 2.98 (dd, *J* = 16.2, 4.0 Hz, 1H), 2.19 (s, 3H). **^{13}C NMR** (176 MHz, $CDCl_3$) δ 207.7, 169.3, 161.6, 154.3, 151.6, 131.6, 127.9, 123.2, 112.5, 112.3, 112.1, 103.2, 100.8, 94.8, 82.1, 74.8, 69.0, 56.1, 45.4, 39.7, 24.6, 21.6. **HRMS**-ESI (m/z): $[M + H]^+$ calculated for $C_{22}H_{23}O_5N_2^+$,395.16015; found, 395.15963.

(±) 2,7-dimethyl-4,4a,8,9b-tetrahydro-2H-pyrano[2',3':4,5]furo[3,2-c]pyridine-3,9-dione (21a)

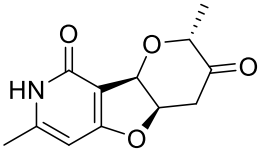

According to GP6, **4b** (25.5 mg, 0.15 mmol) was reacted with **2a** (18.8 mg, 0.15 mmol). Purification by MPLC (cyclohexane/EtOAc 1:0 to 0:1) afforded the product (19.7 mg, 56%). **^{1}H-NMR** (700 MHz, CD_2Cl_2): δ

11.83 (s, 1H), 5.81 (s, 1H), 5.55 (d, *J* = 7.2 Hz, 1H), 5.24 (dt, *J* = 7.2, 3.2 Hz, 1H), 3.64 (q, *J* = 6.8 Hz, 1H), 3.05 (dd, *J* = 16.5, 3.4 Hz, 1H), 2.89 (dd, *J* = 16.5, 3.1 Hz, 1H), 2.33 (s, 3H), 1.25 (d, *J* = 6.8 Hz, 3H). **^{13}C-NMR** (176 MHz, CD_2Cl_2): δ 209.6, 172.3, 163.4, 151.1, 103.5, 94.1, 83.1, 73.9, 73.5, 39.1, 19.8, 15.9. **HRMS**-ESI (m/z): $[M + H]^+$ calculated for $C_{12}H_{14}NO_4^+$, 236.0917; found, 236.0916.

(±) 2,7,8-trimethyl-4,4a,8,9b-tetrahydro-2H-pyrano[2',3':4,5]furo[3,2-c]pyridine-3,9-dione (21b)

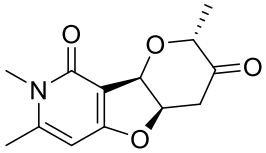

According to GP6, **4b** (24.0 mg, 0.14 mmol) was reacted with **2b** (19.6 mg, 0.14 mmol). Purification by MPLC (cyclohexane/EtOAc 1:0 to 0:1) afforded the product (19.3 mg, 55%). **^{1}H-NMR** (700 MHz, CD_2Cl_2): δ 5.82 (s, 1H), 5.53 (d, *J* = 7.4 Hz, 1H), 5.20 (dt, *J* = 7.4, 3.2 Hz, 1H), 3.60 (q, *J* = 6.8 Hz, 1H), 3.45 (s, 3H), 3.04 (ddd, *J* = 16.3, 3.2, 0.6 Hz, 1H), 2.85 (ddd, *J* = 16.3, 3.2, 0.6 Hz, 1H), 2.33 (s, 3H), 1.24 (d, *J* = 6.8 Hz, 3H). **^{13}C-NMR** (176 MHz, CD_2Cl_2): δ 209.9, 169.4, 161.7, 152.1, 103.2, 94.4, 82.9, 74.8, 73.5, 39.2, 30.8, 22.1, 15.9. **HRMS**-ESI (m/z): $[M + H]^+$ calculated for $C_{13}H_{16}NO_4^+$, 250.1074; found, 250.1071.

(±) 8-cyclobutyl-2,7-dimethyl-4,4a,8,9b-tetrahydro-2H-pyrano[2',3':4,5]furo[3,2-c]pyridine-3,9-dione (21c)

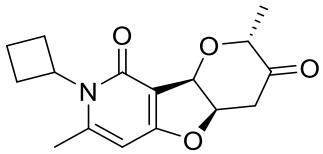

According to GP6, **4b** (25.5 mg, 0.15 mmol) was reacted with **2c** (26.8 mg, 0.15 mmol). Purification by MPLC (cyclohexane/EtOAc 1:0 to 0:1) afforded the product (19.0 mg, 44%). **^{1}H-NMR** (700 MHz, CD_2Cl_2): δ 5.84 (s, 1H), 5.57 (d, *J* = 7.5 Hz, 1H), 5.22 (dt, *J* = 7.5, 3.3 Hz, 1H), 4.77 (p, *J* = 9.3 Hz, 1H), 3.60 (q, *J* = 6.9 Hz, 1H), 3.27-3.14 (m, 2H), 3.04 (dd, *J* = 16.4, 3.5 Hz, 1H), 2.86 (dd, *J* = 16.4, 3.1 Hz, 1H), 2.36 (s, 3H), 2.33-2.25 (m, 2H), 2.00-1.94 (m, 1H), 1.80-1.73 (m, 1H), 1.24 (d, *J* = 6.9 Hz, 3H). **^{13}C-NMR** (176 MHz, CD_2Cl_2): δ 209.8, 169.6, 163.8, 152.3, 105.2, 96.3, 83.3, 74.5, 73.6, 53.8, 39.1, 28.5, 22.8, 15.8, 15.1. **HRMS**-ESI (m/z): $[M + H]^+$ calculated for $C_{16}H_{20}NO_4^+$, 290.1387; found, 290.1386.

(±) 8-methyl-1,2,3,4,5,6b,10,10a-octahydro-6H-pyrano[2',3':4,5]furo[3,2-c]quinoline-6,9(8H)-dione (21d)

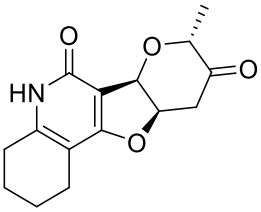

According to GP6, **4b** (25.5 mg, 0.15 mmol) was reacted with **2v** (24.8 mg, 0.15 mmol). Purification by MPLC (cyclohexane/EtOAc 1:0 to 0:1) afforded the product (13.0 mg, 31%). **^{1}H-NMR** (700 MHz, CD_2Cl_2): δ 11.76, 5.55 (d, *J* = 7.2 Hz, 1H), 5.23 (dt, *J* = 7.2, 3.2 Hz, 1H), 3.65 (q, *J* = 6.8 Hz, 1H), 3.05 (dd, *J* = 16.5, 3.4 Hz, 1H), 2.91 (dd, *J* = 16.5, 3.1 Hz, 1H), 2.63 (t, *J* = 6.4 Hz, 2H), 2.34 (t, *J* = 6.3 Hz, 2H), 1.79 (p, *J* = 5.9 Hz, 2H), 1.74-1.69 (m, 2H), 1.25 (d, *J* = 6.8 Hz, 3H). **^{13}C-NMR** (176 MHz, CD_2Cl_2): δ 209.8, 171.0, 162.6, 148.2, 103.5, 103.1, 82.9, 74.3, 73.4, 39.2, 27.3, 22.1, 22.0, 20.9, 15.8. **HRMS**-ESI (m/z): $[M + H]^+$ calculated for $C_{15}H_{18}NO_4^+$, 276.1230; found. 276.1233.

(±) 8-(4-fluorobenzyl)-2,7-dimethyl-4,4a,8,9b-tetrahydro-2H-pyrano[2',3':4,5]furo[3,2-c]pyridine-3,9-dione (21e)

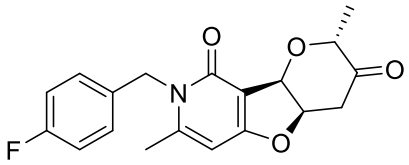

According to GP6, **4b** (25.5 mg, 0.15 mmol) was reacted with **2h** (35.0 mg, 0.15 mmol). Purification by MPLC (cyclohexane/EtOAc 1:0 to 0:1) afforded the product (56.1 mg, 90%). **^{1}H-NMR** (700 MHz, CD_2Cl_2): δ 7.14 (dd, *J* = 8.6, 5.4 Hz, 2H), 7.02 (t, *J* = 8.6 Hz, 2H), 5.85 (s, 1H), 5.59 (d, *J* = 7.5 Hz, 1H), 5.43 (d, *J* = 15.7 Hz, 1H), 5.26 (dt, *J* = 7.5, 3.2 Hz, 1H), 5.08 (d, *J* = 15.7 Hz, 1H), 3.66 (q, *J* = 6.9 Hz, 1H), 3.07 (dd, *J* = 16.3, 3.4 Hz, 1H), 2.88 (dd, *J* = 16.3, 3.1 Hz, 1H), 2.26 (s, 3H), 1.27 (d, *J* = 6.9 Hz, 3H). **^{13}C-NMR** (176 MHz, CD_2Cl_2): δ 209.8, 169.7, 163.1, 161.7, 161.6, 152.2, 133.2, 128.6, 116.0, 103.6, 95.2, 83.1, 74.8, 73.6, 46.2, 39.1, 21.7, 15.9. **HRMS**-ESI (m/z): $[M + H]^+$ calculated for $C_{19}H_{19}FNO_4^+$, 344.1293; found, 344.1293.

(±) 8-(2-chlorobenzyl)-2,7-dimethyl-4,4a,8,9b-tetrahydro-2H-pyrano[2',3':4,5]furo[3,2-c]pyridine-3,9-dione (21f)

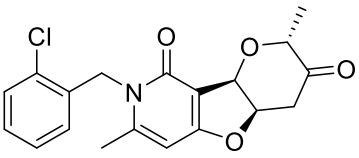

According to GP6, **4b** (25.5 mg, 0.15 mmol) was reacted with **2i** (37.5 mg, 0.15 mmol). Purification by MPLC (cyclohexane/EtOAc 1:0 to 0:1) afforded the product (27.5 mg, 51%). **^{1}H-NMR** (700 MHz, CD_2Cl_2): δ 7.43 (dd, *J* = 7.9, 1.4 Hz, 1H), 7.26-7.23 (m, 1H), 7.20 (td, *J* = 7.6, 1.4 Hz, 1H), 6.72 (dd, *J* = 7.6, 1.7 Hz, 1H), 5.91 (s, 1H), 5.62 (d, *J* = 7.5 Hz, 1H), 5.50 (d, *J* = 16.1 Hz, 1H), 5.29 (dt, *J* = 7.5, 3.2 Hz, 1H), 5.21 (d, *J* = 16.9 Hz, 1H), 3.68 (q, *J* = 6.8 Hz, 1H), 3.08 (dd, *J* = 16.3, 3.4 Hz, 1H), 2.90 (dd, *J* = 16.3, 3.1 Hz, 1H), 2.21 (s, 3H), 1.28

(d, *J* = 6.8 Hz, 3H). **^{13}C-NMR** (176 MHz, CD_2Cl_2): δ 209.8, 169.9, 161.7, 152.2, 134.4, 132.7, 130.0, 129.0, 127.7, 126.5, 103.6, 95.3, 83.2, 74.7, 73.6, 44.7. 39.1, 21.4, 15.9. **HRMS**-ESI (m/z): $[M + H]^+$ calculated for $C_{19}H_{19}ClNO_4^+$, 360.0997; found, 360.0999.

(±) 8-(4-methoxybenzyl)-2,7-dimethyl-4,4a,8,9b-tetrahydro-2H-pyrano[2',3':4,5]furo[3,2-c]pyridine-3,9-dione (21g)

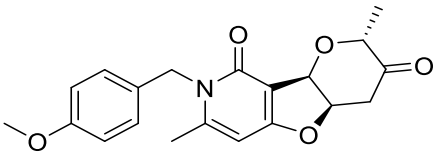

According to GP6, **4b** (50.0 mg, 0.29 mmol) was reacted with **2k** (72.1 mg, 0.29 mmol). Purification by MPLC (cyclohexane/EtOAc 1:0 to 0:1) afforded the product (44.0 mg, 42%). **^{1}H-NMR** (500 MHz, CD_2Cl_2): δ 7.08 (d, *J* = 8.7 Hz, 2H), 6.86 (d, *J* = 8.7 Hz, 2H), 5.95 (s, 1H), 5.64 (d, *J* = 7.6 Hz, 1H), 5.45 (d, *J* = 15.7 Hz, 1H), 5.29 (dt, *J* = 7.6, 3.4 Hz, 1H), 5.08 (d, *J* = 15.7 Hz, 1H), 3.77 (s, 3H), 3.63 (q, *J* = 6.8 Hz, 1H), 3.08 (dd, *J* = 16.4, 3.4 Hz, 1H), 2.89 (dd, *J* = 16.4, 3.1 Hz, 1H), 2.32 (s, 3H), 1.26 (d, *J* = 6.8 Hz, 3H). **^{13}C-NMR** (126 MHz, CD_2Cl_2): δ 209.6, 170.1, 162.4, 159.4, 152.7, 128.6, 128.1, 114.5, 104.0, 96.4, 83.4, 74.4, 73.6, 55.6, 46.9, 39.1, 21.8, 15.8. **HRMS**-ESI (m/z): $[M + H]^+$ calculated for $C_{20}H_{22}NO_4^+$, 356.1493; found, 356.1498.

(±) 2,7-dimethyl-8-(pyridin-4-ylmethyl)-4,4a,8,9b-tetrahydro-2H-pyrano[2',3':4,5]furo[3,2-c]pyridine-3,9-dione (21h)

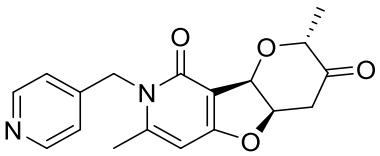

According to GP6, **4b** (25.5 mg, 0.15 mmol) was reacted with **2n** (32.4 mg, 0.15 mmol). Purification by MPLC (EtOAc/MeOH 1:0 to 4:1) afforded the product (18.7 mg, 32%). **^{1}H-NMR** (700 MHz, $CDCl_3$): δ 8.57 (m, 2H), 7.07 (d, *J* = 5.0 Hz, 2H), 5.89 (s, 1H), 5.67 (d, *J* = 7.1 Hz, 1H), 5.54 (d, *J* = 16.0 Hz, 1H), 5.28 (dt, *J* = 7.1, 3.2 Hz, 1H), 5.11 (d, *J* = 16.0 Hz, 1H), 3.69 (q, *J* = 6.7 Hz, 1H), 3.08 (dd, *J* = 16.2, 3.4 Hz, 1H), 2.94 (dd, *J* = 16.2, 3.1 Hz, 1H), 2.26 (s, 1H), 1.33 (d, *J* = 6.7 Hz, 3H). **^{13}C-NMR** (176 MHz, $CDCl_3$): δ 209.7, 169.6, 161.4, 151.2, 150.1, 146.3, 121.6, 103.6, 95.7, 82.9, 74.4, 73.6, 45.9, 38.9, 21.6, 16.0. **HRMS**-ESI (m/z): $[M + H]^+$ calculated for $C_{18}H_{19}N_2O_4^+$, 327.1339; found, 327.1339.

(±) 8-((2-chloropyridin-4-yl)methyl)-2,7-dimethyl-4,4a,8,9b-tetrahydro-2H-pyrano[2',3':4,5]furo[3,2-c]pyridine-3,9-dione (21i)

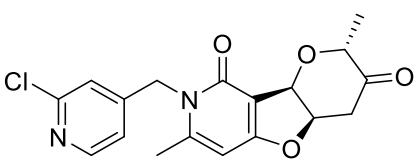

According to GP6, **4b** (25.5 mg, 0.15 mmol) was reacted with **2p** (37.6 mg, 0.15 mmol). Purification by MPLC (cyclohexane/EtOAc 1:0 to 0:1) afforded the product (17.3

mg, 32%). **^{1}H-NMR** (700 MHz, CD_2Cl_2): δ 8.31 (d, *J* = 5.2 Hz, 1H), 7.04 (s, 1H), 7.02 (dd, *J* = 5.2, 1.5 Hz, 1H), 5.90 (s, 1H), 5.59 (d, *J* = 7.5 Hz, 1H), 5.49-5.46 (m, 1H), 5.29 (dt, *J* = 7.5, 3.2 Hz, 1H), 5.07 (d, *J* = 16.4 Hz, 1H), 3.65 (q, *J* = 6.8 Hz, 1H), 3.08 (dd, *J* = 16.3, 3.4 Hz, 1H), 2.90 (dd, *J* = 16.3, 3.1 Hz, 1H), 2.23 (s, 3H), 1.28 (d, *J* = 6.8 Hz, 3H). **^{13}C-NMR** (176 MHz, CD_2Cl_2): δ 209.6, 170.0, 161.3, 152.5, 151.6, 150.5, 149.9, 122.0, 120.7, 103.7, 95.8, 83.3, 74.7, 73.6, 45.7, 39.1, 21.7, 15.9. **HRMS**-ESI (m/z): $[M + H]^+$ calculated for $C_{18}H_{18}ClN_2O_4^+$, 361.0945; found, 361.0951.

(±) 2,2,7,8-tetramethyl-4,4a,8,9b-tetrahydro-2H-pyrano[2',3':4,5]furo[3,2-c]pyridine-3,9-dione (22a)

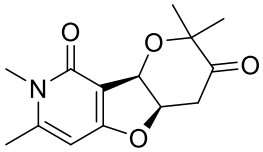

According to GP6, **4c** (27.6 mg, 0.15 mmol) was reacted with **2b** (20.9 mg, 0.15 mmol). Purification by MPLC (cyclohexane/EtOAc 1:0 to 0:1) afforded the product (6.3 mg, 16%). **^{1}H-NMR** (700 MHz, CD_2Cl_2): δ 5.99 (s, 1H), 5.37 (d, *J* = 6.6 Hz, 1H), 5.01 (dt, *J* = 7.7, 6.6 Hz, 1H), 3.51 (s, 3H), 3.06 (dd, *J* = 13.8, 7.7 Hz, 1H), 2.98 (dd, *J* = 13.8, 6.9 Hz, 1H), 2.38 (s, 3H), 1.38 (s, 3H), 1.24 (s, 3H). **^{13}C-NMR** (176 MHz, CD_2Cl_2): δ 212.4, 169.3, 162.1, 152.2, 106.4, 96.2, 84.3, 81.7, 71.6, 40.0, 31.4, 25.6, 22.1, 21.5. **HRMS**-ESI (m/z): $[M + H]^+$ calculated for $C_{14}H_{18}NO_4^+$, 264.1230; found, 264.1230.

(±) 8-benzyl-2,2,7-trimethyl-4,4a,8,9b-tetrahydro-2H-pyrano[2',3':4,5]furo[3,2-c]pyridine-3,9-dione (22b)

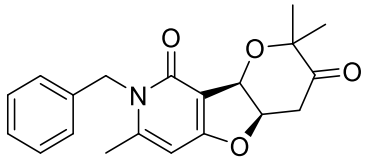

According to GP6, **4c** (50.0 mg, 0.32 mmol) was reacted with **2g** (58.4 mg, 0.32 mmol) employing allylpalladium(II) chloride dimer (2.5 mol%) and Xantphos (7.5 mol%) as catalyst. Purification by MPLC (cyclohexane/EtOAc 1:0 to 0:1) afforded the product (48.0 mg 52%). **^{1}H NMR** (500 MHz, $CDCl_3$): δ 7.31 (m, 2H), 7.16 (d, *J* = 6.7 Hz, 2H), 5.96 (s, 1H), 5.55 (d, *J* = 15.7 Hz, 1H), 5.44 (d, *J* = 6.7 Hz, 1H), 5.14 (d, *J* = 15.7 Hz, 1H), 5.03 (dt, *J* = 7.9, 6.7 Hz, 1H), 3.14 (dd, *J* = 13.7, 7.3 Hz, 1H), 3.02 (dd, *J* = 13.7, 7.3 Hz, 1H), 2.32 (s, 1H), 1.43 (s, 3H), 1.31 (s, 3H). **^{13}C NMR** (126 MHz, $CDCl_3$): δ 212.7, 169.1, 161.9, 151.6, 136.2, 128.9, 127.5, 126.6, 106.4, 96.4, 83.9, 81.5, 71.3, 47.1, 39.7, 25.5, 21.6, 21.2. **HRMS**-ESI (m/z): $[M + H]^+$ calculated for $C_{20}H_{22}O_4N^+$,340.15433; found, 340.15470.

(±) 8-(4-fluorobenzyl)-2,2,7-trimethyl-4,4a,8,9b-tetrahydro-2H-pyrano[2',3':4,5]furo[3,2-c]pyridine-3,9-dione (22c)

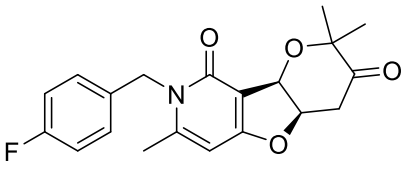

According to GP6, **4c** (50.0 mg, 0.27 mmol) was reacted with **2h** (63.3 mg, 0.27 mmol). Purification by MPLC (cyclohexane/EtOAc 1:0 to 0:1) afforded the product (23.7 mg, 24%). **^{1}H-NMR** (600 MHz, $CDCl_3$): δ δ 7.18-7.15 (m, 2H), 7.01 (dd, *J* = 10.6, 6.0 Hz, 2H), 5.97 (s, 1H), 5.48 (d, *J* = 16.0 Hz, 1H), 5.44 (d, *J* = 6.3 Hz, 1H), 5.14-5.10 (m, 1H), 5.05-5.00 (m, 1H), 3.13 (dd, *J* = 13.7, 7.2 Hz, 1H), 3.02 (dd, *J* = 13.7, 6.0 Hz, 1H), 2.33 (s, 3H), 1.43 (s, 3H), 1.31 (s, 3H). **^{13}C-NMR** (151 MHz, $CDCl_3$): δ 212.6, 169.3, 163.1, 161.5, 162.0, 151.5, 132.1, 128.6, 115.9, 106.6, 96.8, 84.2, 81.7, 71.4, 46.8, 39.8, 25.6, 21.8, 21.4. **HRMS**-ESI (m/z): $[M + H]^+$ calculated for $C_{20}H_{21}NO_4F^+$, 358.1449; found, 358.1466.

(±) 8-(2-chlorobenzyl)-2,2,7-trimethyl-4,4a,8,9b-tetrahydro-2H-pyrano[2',3':4,5]furo[3,2-c]pyridine-3,9-dione (22d)

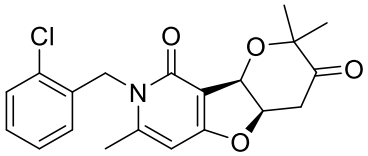

According to GP6, **4c** (50.0 mg, 0.27 mmol) was reacted with **2i** (67.8 mg, 0.27 mmol). Purification by MPLC (cyclohexane/EtOAc 1:0 to 0:1) afforded the product (5.8 mg, 6%). **^{1}H-NMR** (600 MHz, CD_2Cl_2): δ 7.43 (dd, *J* = 7.7, 1.4 Hz, 1H), 7.24 (td, *J* = 7.7, 1.7 Hz, 1H), 7.20 (td, *J* = 7.7, 1.4 Hz, 1H), 6.75 (dd, *J* = 7.7, 1.7 Hz, 1H), 5.99 (s, 1H), 5.44 (d, *J* = 16.9 Hz, 1H), 5.41 (d, *J* = 6.6 Hz, 1H), 5.29 (d, *J* = 16.9 Hz, 1H), 5.11-5.04 (m, 1H), 3.10 (dd, *J* = 13.8, 7.5 Hz, 1H), 3.02 (dd, *J* = 13.8, 6.7 Hz, 1H), 2.23 (s, 3H), 1.40 (s, 3H), 1.28 (s, 3H). **^{13}C-NMR** (151 MHz, CD_2Cl_2): δ 212.5, 169.5, 161.8, 152.0, 134.3, 132.7, 130.0, 129.0, 127.7, 126.6, 106.5, 96.4, 84.4, 81.7, 71.8, 44.9, 40.0, 25.5, 22.0. 21.4. **HRMS**-ESI (m/z): $[M + H]^+$ calculated for $C_{20}H_{21}NO_4Cl^+$, 374.1154; found, 374.1167.

(±) 8-(4-methoxybenzyl)-2,2,7-trimethyl-4,4a,8,9b-tetrahydro-2H-pyrano[2',3':4,5]furo[3,2-c]pyridine-3,9-dione (22e)

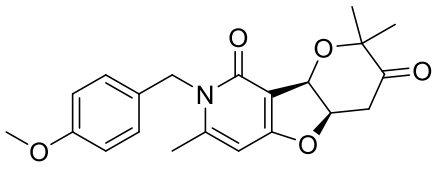

According to GP6, **4c** (27.7 mg, 0.15 mmol) was reacted with **2k** (55.2 mg, 0.15 mmol). Purification by MPLC (cyclohexane/EtOAc 1:0 to 0:1) afforded the product (10.1 mg, 18%). **^{1}H-NMR** (600 MHz, $CDCl_3$): δ 7.10 (d, *J* = 8.8 Hz, 2H), 6.81 (d, *J* = 8.8 Hz, 2H), 5.88 (s, 1H), 5.42 (d, *J* = 15.4 Hz, 1H), 5.40 (d, *J* = 6.6 Hz, 1H), 5.03 (d, *J* = 15.4 Hz, 1H), 4.98 (dt, *J* = 7.9, 6.6 Hz, 1H), 3.74 (s, 3H), 3.10 (dd, *J* = 13.6,

7.9 Hz, 1H), 2.98 (dd, *J* = 13.6, 6.9 Hz, 1H), 2.29 (s, 3H), 1.40 (s, 3H), 1.28 (s, 3H). **^{13}C-NMR** (151 MHz, $CDCl_3$): δ 212.9, 169.0, 161.9, 159.1, 151.6, 128.6, 128.2, 114.3, 106.4, 96.1, 84.0, 81.6, 71.6, 55.4, 46.6, 39.8, 21.7, 21.5. **HRMS**-ESI (m/z): $[M + H]^+$ calculated for $C_{21}H_{24}NO_5^+$, 370.1649; found, 370.1637.

(±) 2,2,7-trimethyl-8-(pyridin-4-ylmethyl)-4,4a,8,9b-tetrahydro-2H-pyrano[2',3':4,5]furo[3,2-c]pyridine-3,9-dione (22f)

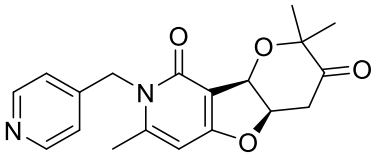

According to GP6, **4c** (27.7 mg, 0.15 mmol) was reacted with **2n** (32.2 mg, 0.15 mmol). Purification by MPLC (cyclohexane/EtOAc 1:0 to 0:1 then EtOAc/MeOH 1:0 to 9:1) afforded the product (11.5 mg, 23%). **^{1}H-NMR** (700 MHz, CD_2Cl_2): δ 8.53-8.51 (m, 2H), 7.05-7.04 (m, 2H), 5.93 (s, 1H), 5.38 (d, *J* = 6.7 Hz, 1H), 5.37 (d, *J* = 16.0 Hz, 1H), 5.16 (d, *J* = 16.0 Hz, 1H), 5.05 (dt, *J* = 7.5, 6.7 Hz, 1H), 3.09 (dd, *J* = 13.8, 7.5 Hz, 1H), 3.01 (dd, *J* = 13.8, 6.7 Hz, 1H), 2.24 (s, 3H), 1.40 (s, 3H), 1.28 (s, 3H). **^{13}C-NMR** (176 MHz, CD_2Cl_2): δ 212.6, 169.2, 161.3, 151.5, 150.5, 146.5, 121.6, 106.4, 95.8, 84.3, 81.6, 72.0, 46.1, 40.0, 25.4, 22.1, 21.7. **HRMS**-ESI (m/z): $[M + H]^+$ calculated for $C_{19}H_{21}N_2O_4^+$, 341.1496; found, 341.1493.

(±) 8-((2-chloropyridin-4-yl)methyl)-2,2,7-trimethyl-4,4a,8,9b-tetrahydro-2H-pyrano[2',3':4,5]furo[3,2-c]pyridine-3,9-dione (22g)

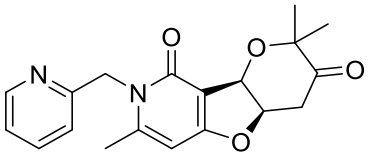

According to GP6, **4c** (50.0 mg, 0.32 mmol) was reacted with **2m** (58.7 mg, 0.32 mmol) employing allylpalladium(II) chloride dimer (2.5 mol%) and Xantphos (7.5 mol%) as catalyst. Purification by MPLC (cyclohexane/EtOAc 1:0 to 0:1) afforded the product (17.8 mg, 19%). ^{1}H NMR (700 MHz, $CDCl_3$): δ 8.70 (d, *J* = 4.5 Hz, 1H), 7.99 (td, *J* = 7.9, 1.7 Hz, 1H), 7.52 (m, 1H), 7.49 (d, *J* = 7.9 Hz, 1H), 6.04 (s, 1H), 5.69 (d, *J* = 16.5 Hz, 1H), 5.55 (d, *J* = 16.5 Hz, 1H), 5.40 (d, *J* = 6.5 Hz, 1H), 5.03 (m, 1H), 3.13 (dd, *J* = 13.7, 7.5 Hz, 1H), 3.02 (dd, *J* = 13.7, 7.5 Hz, 1H), 2.41 (s, 3H), 1.42 (s, 3H), 1.30 (s, 3H). **^{13}C NMR** (176 MHz, $CDCl_3$): δ 212.3, 169.8, 161.8, 154.4, 151.7, 145.6, 141.6, 124.3, 123.9, 106.5, 97.3, 84.2, 81.7, 71.2, 46.8, 39.7, 25.6, 21.9, 21.2. **HRMS**-ESI (m/z): $[M + H]^+$ calculated for $C_{19}H_{21}O_4N_2^+$,341.14958; found, 341.14984

(±) 8-((2-chloropyridin-4-yl)methyl)-2,2,7-trimethyl-4,4a,8,9b-tetrahydro-2H-pyrano[2',3':4,5]furo[3,2-c]pyridine-3,9-dione (22h)

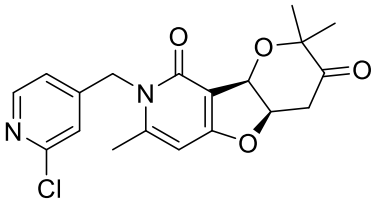

According to GP6, **4c** (27.7 mg, 0.15 mmol) was reacted with **2p** (37.3 mg, 0.15 mmol). Purification by MPLC (cyclohexane/EtOAc 1:0 to 0:1) afforded the product (35.2 mg, 63%). **^{1}H-NMR** (700 MHz, CD_2Cl_2): δ 8.31 (dd, *J* = 5.1, 0.8 Hz, 1H), 7.06 (dd, *J* = 1.6, 0.8 Hz, 1H), 7.03-7.02 (m, 1H), 5.94 (s, 1H), 5.38 (d, *J* = 6.7 Hz, 1H), 5.37 (d, *J* = 15.2 Hz, 1H), 5.13 (d, *J* = 15.2 Hz, 1H), 5.07 (dt, *J* = 7.5, 6.7 Hz, 1H), 3.09 (dd, *J* = 13.8, 7.5 Hz, 1H), 3.02 (dd, *J* = 13.8, 6.7 Hz, 1H), 2.24 (s, 3H), 1.39 (s, 3H), 1.28 (s, 3H). **^{13}C-NMR** (176 MHz, CD_2Cl_2): δ 212.4, 169.3, 161.2, 152.5, 151.2, 150.4, 150.0, 122.0, 120.7, 106.4, 96.1, 84.4, 81.6, 71.9, 45.8, 39.9, 25.5, 22.2, 21.7. **HRMS**-ESI (m/z): $[M + H]^+$ calculated for $C_{19}H_{20}ClN_2O_4^+$, 375.1106; found, 375.1105.

(±) 2,2,7-trimethyl-8-((3-methylpyridin-4-yl)methyl)-4,4a,8,9b-tetrahydro-2H-pyrano[2',3':4,5]furo[3,2-c]pyridine-3,9-dione (22i)

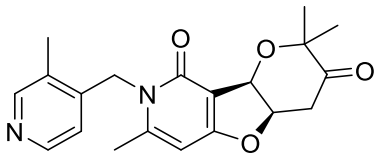

According to GP6, **4c** (50.0 mg, 0.32 mmol) was reacted with **2o** (35.4 mg, 0.32 mmol) employing Allylpalladium(II) chloride dimer (2.5 mol%) and Xantphos (7.5 mol%) as catalyst. Purification by MPLC (cyclohexane/EtOAc 1:0 to 0:1) afforded the product (4.7 mg, 5%). **^{1}H NMR** (700 MHz, $CDCl_3$): δ 8.71 (s, 1H), 8.57 (d, *J* = 5.7 Hz, 1H), 7.10 (d, *J* = 5.7 Hz, 1H), 6.11 (s, 1H), 5.48 (d, *J* = 17.6 Hz, 1H), 5.38 (d, *J* = 6.7 Hz, 1H), 5.23 (d, *J* = 17.6 Hz, 1H), 5.06 (dt, *J* = 8.1, 6.7 Hz, 1H), 3.15 (dd, *J* = 13.7, 7.6 Hz, 1H), 3.05 (dd, *J* = 13.7, 7.6 Hz, 1H), 2.60 (s, 3H), 2.30 (s, 3H), 1.41 (s, 3H), 1.31 (s, 3H). **^{13}C NMR** (176 MHz, $CDCl_3$): δ 212.1, 169.8, 161.2, 154.0, 150.0, 142.8, 140.9, 134.9, 121.8, 106.9, 97.5, 84.4, 81.8, 77.3, 77.2, 77.0, 71.1, 44.8, 39.7, 25.7, 21.5, 21.2, 16.6. **HRMS**-ESI (m/z): $[M + H]^+$ calculated for $C_{20}H_{23}O_4N_2^+$,355.16523; found, 355.16537.

(±) 5,8,8-trimethyl-5,6b,10,10a-tetrahydro-6H-pyrano[2',3':4,5]furo[3,2-c]quinoline-6,9(8H)-dione (22j)

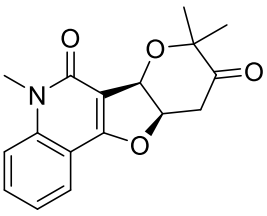

According to GP6, **4c** (27.7 mg, 0.15 mmol) was reacted with **2w** (26.3 mg, 0.15 mmol). Purification by MPLC (cyclohexane/EtOAc 1:0 to 0:1) and repurification by prep. HPLC afforded the product (2.1 mg, 5%). **^{1}H-NMR** (500 MHz, $CDCl_3$): δ 7.82 (dd, *J* = 8.0, 1.7 Hz, 1H), 7.68 (ddd, *J* = 8.7, 7.2, 1.7 Hz, 1H), 7.43 (d, *J* = 8.7 Hz, 1H), 7.30 (ddd, *J* = 8.0, 7.2, 0.9 Hz, 1H), 5.54 (d,

J = 6.7 Hz, 1H), 5.18 (dt, *J* = 8.0, 6.7 Hz, 1H), 3.74 (s, 3H), 3.24 (dd, *J* = 13.7, 8.0 Hz, 1H), 3.12 (dd, *J* = 13.7, 7.0 Hz, 1H), 1.48 (s, 3H), 1.32 (s, 3H). **^{13}C-NMR** (126 MHz, $CDCl_3$): δ 212.5, 161.1, 158.4, 141.7, 132.8, 124.0, 122.4, 115.1, 112.2, 107.7, 84.3, 81.9, 72.0, 39.8, 29.5, 25.5. 21.3. **HRMS**-ESI (m/z): $[M + H]^+$ calculated for $C_{17}H_{18}NO_4^+$, 300.1230; found, 300.1234.

(±) 2,2,7-trimethyl-4a,9b-dihydro-2H,9H-furo[3,2-b:4,5-c']dipyran-3,9(4H)-dione (22k)[112]

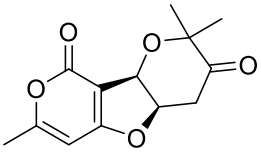

According to GP6, **4c** (27.6 mg, 0.15 mmol) was reacted with 4-hydroxy-6-methyl-2H-pyran-2-one (**1a**) (18.9 mg, 0.15 mmol). Purification by MPLC (cyclohexane/EtOAc 1:0 to 0:1) afforded the product (1.4 mg, 4%). **^{1}H-NMR** (700 MHz, CD_2Cl_2): δ 5.98 (s, 1H), 5.28 (d, *J* = 6.7 Hz, 1H), 5.07 (dt, *J* = 7.8, 6.7 Hz, 1H), 3.08 (dd, *J* = 13.8, 7.8 Hz, 1H), 3.01 (dd, *J* = 13.8, 6.8 Hz, 1H), 2.27 (s, 3H), 1.39 (s, 3H), 1.29 (s, 3H).). **HRMS**-ESI (m/z): $[M + H]^+$ calculated for $C_{13}H_{15}O_5^+$, 251.0914; found, 251.0915.

(±) *Tert*-butyl-7',8'-dimethyl-3',9'-dioxo-3',4',4a',8',9',9b'-hexahydrospiro[piperidine-4,2'-pyrano[2',3':4,5]furo[3,2-c]pyridine]-1-carboxylate (23a)

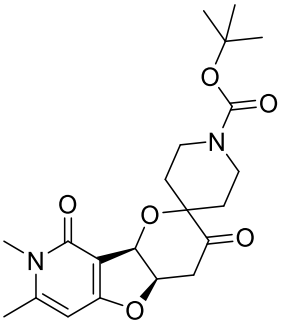

According to GP6, **4d** (50.0 mg, 0.15 mmol) was reacted with **2b** (21.4 mg, 0.15 mmol). Purification by MPLC (cyclohexane/EtOAc 1:0 to 0:1) afforded the product (56.1 mg, 90%). **^{1}H-NMR** (700 MHz, CD_2Cl_2): δ 5.85 (s, 1H), 5.35 (d, *J* = 6.7 Hz, 1H), 5.03 (q, *J* = 6.7 Hz, 1H), 3.98-3.73 (m 2H), 3.45 (s, 3H), 3.26-2.98 (m, 4H), 2.34 (s, 3H), 1.88 (d, *J* = 14.1 Hz, 1H), 1.72 (ddd, *J* = 13.8, 12.1, 4.5 Hz, 1H), 1.65-1.59 (m, 1H), 1.53-1.48 (m, 1H), 1.47 (m, 9H). **^{13}C-NMR** (176 MHz, CD_2Cl_2): δ 211.5; 168.6, 161.4, 154.8, 152.1, 105.7, 94.6, 83.9, 81.0, 79.5, 71.1, 40.1, 39.5, 38.6, 33.1, 30.7, 29.6, 28.5. **HRMS**-ESI (m/z): $[M + H]^+$ calculated for $C_{21}H_{29}N_2O_6^+$, 405.2020; found, 405.2015.

(±) 7',8'-dimethyl-3',9'-dioxo-3',4',4a',8',9',9b'-hexahydrospiro[piperidine-4,2'-pyrano[2',3':4,5]furo[3,2-c]pyridin]-1-ium triflate (24a)

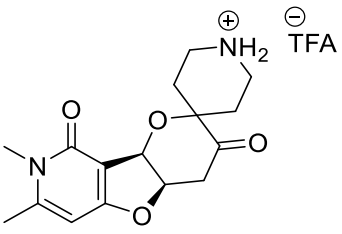

23a (35.0 mg, 0.09 mmol) was dissolved in DCM (1 mL) and cooled to 0 °C. A mixture of TMSOTf (0.16 mL, 10 equiv) and 2,6-lutidine (0.15 mL, 15 equiv) in DCM (0.1 mL) was added slowly and the mixture was stirred at 0 °C for 1 hour and at room temperature for 30 min. The reaction was quenched by slow

addition of saturated Na_2CO_3 solution at 0 °C and dilution with EtOAc (10 mL). The layers were separated and the aqueous phase was extracted with EtOAc (3 x 10 mL). The combined organic layers were washed with brine (20 mL), dried over $MgSO_4$ and concentrated in vacuo. Purification by prep. HPLC afforded the product (8.2 mg, 31%). **^{1}H-NMR** (500 MHz, DMSO): δ 8.56 (d, *J* = 11.2 Hz, 1H), 8.42 (d, *J* = 13.7 Hz, 1H), 6.07 (s, 1H), 5.33 (d, *J* = 6.5 Hz, 1H), 5.18 (q, *J* = 6.5 Hz, 1H), 3.34 (s, 3H), 3.21-2.91 (m, 6H), 2.36 (s, 3H), 1.87-1.57 (m, 4H). **^{13}C-NMR** (126 MHz, DMSO): δ 210.9, 168.2, 160.8, 153.2, 104.7, 94.1, 83.6, 77.7, 71.6, 40.5, 39.2, 30.4, 29.6, 26.5, 21.6. **HRMS**-ESI (m/z): $[M + H]^+$ calculated for $C_{16}H_{21}N_2O_4^+$, 305.1496; found, 305.1487.

(±) *Tert*-butyl 8'-cyclobutyl-7'-methyl-3',9'-dioxo-3',4',4a',8',9',9b'-hexahydrospiro[piperidine-4,2'-pyrano[2',3':4,5]furo[3,2-c]pyridine]-1-carboxylate (23b)

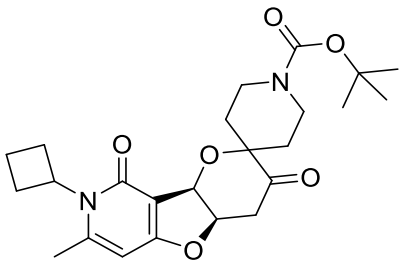

According to GP6, **4d** (48.8 mg, 0.15 mmol) was reacted with **2c** (26.9 mg, 0.15 mmol). Purification by MPLC (cyclohexane/EtOAc 1:0 to 0:1) afforded the product (47.7 mg, 72%). **^{1}H-NMR** (500 MHz, CD_2Cl_2): δ 5.76 (s, 1H), 5.36 (d, *J* = 6.8 Hz, 1H), 5.03 (q, *J* = 6.8 Hz, 1H), 4.72 (p, *J* = 8.9 Hz, 1H), 3.99-3.71 (m, 2H), 3.29-2.99 (m, 6H), 2.33 (s, 3H), 2.23 (ddd, *J* = 11.4, 7.9, 2.9 Hz, 2H), 1.99-1.47 (m, 6H), 1.42 (s, 9H). **^{13}C-NMR** (126 MHz, CD_2Cl_2): δ 211.6, 168.2, 162.9, 154.8, 151.7, 107.2, 95.3, 83.9, 81.0, 79.5, 72.1, 53.3, 40.2, 38.6, 38.5, 32.9, 30.1, 28.5, 28.1, 22.7, 15.0. **HRMS**-ESI (m/z): $[M + H]^+$ calculated for $C_{24}H_{33}N_2O_6^+$, 445.2333; found, 445.2328.

(±) 8'-benzyl-7'-methyl-3',9'-dioxo-3',4',4a',8',9',9b'-hexahydrospiro[piperidine-4,2'-pyrano[2',3':4,5]furo[3,2-c]pyridin]-1-ium triflate (24c)

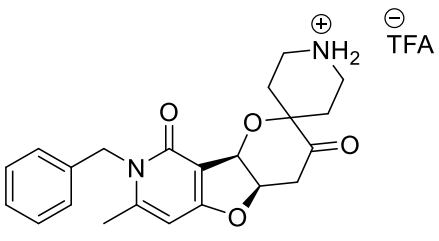

According to GP6, **4d** (39.0 mg, 0.12 mmol) was reacted with **2g** (25.8 mg, 0.12 mmol). Purification by MPLC (cyclohexane/EtOAc 1:0 to 0:1) afforded the product which was directly dissolved in DCM (1 mL) and cooled to 0 °C. A mixture of TMSOTf (0.21 mL, 10 equiv) and 2,6-lutidine (0.21 mL, 15 equiv) in DCM (0.1 mL) was added slowly and the mixture was stirred at 0 °C for 30 min. The reaction was quenched by slow addition of saturated Na_2CO_3 solution at 0 °C and dilution with EtOAc (10 mL). The layers were separated and the aqueous phase was

extracted with EtOAc (3 x 10 mL). The combined organic layers were washed with brine (20 mL), dried over $MgSO_4$ and concentrated in vacuo. Purification by prep. HPLC afforded the product (7.3 mg, 17% over two steps). **^{1}H-NMR** (700 MHz, DMSO): δ 8.56 (s, 1H), 8.45 (s, 1H), 7.37-7.32 (m, 2H), 7.27 (t, *J* = 7.4 Hz, 1H), 7.10 (d, *J* = 7.7 Hz, 2H), 6.13 (s, 1H), 5.42 (d, *J* = 6.7 Hz, 1H), 5.32 (d, *J* = 16.0 Hz, 1H), 5.28 (q, *J* = 6.4 Hz, 1H), 5.22 (d, *J* = 13.8 Hz, 1H), 3.29-3.23 (m, 1H), 3.18-3.14 (m, 1H), 3.10-3.00 (m, 3H), 2.97-2.93 (m, 1H), 2.28 (s, 3H), 1.86-1.78 (m, 2H), 1.73-1.68 (m, 1H), 1.66-1.61 (m, 1H). **^{13}C-NMR** (176 MHz, DMSO): δ 210.5,168.1, 160.1, 152.4, 137.7, 129.2, 127.6, 126.5, 104.9, 94.9, 83.9, 77.5, 71.4, 45.6, 38.8, 28.4, 26.7, 24.4, 20.7. **HRMS**-ESI (m/z): $[M + H]^+$ calculated for $C_{22}H_{25}N_2O_4^+$, 381.1809; found, 381.1810.

(±) *Tert*-butyl-8'-(4-fluorobenzyl)-7'-methyl-3',9'-dioxo-3',4',4a',8',9',9b'-hexahydrospiro[piperidine-4,2'-pyrano[2',3':4,5]furo[3,2-c]pyridine]-1-carboxylate (23d)

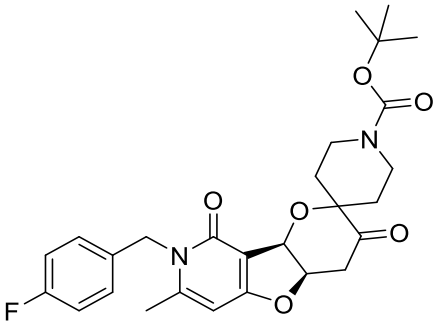

According to GP6, **4d** (48.8 mg, 0.15 mmol) was reacted with **2h** (35.0 mg, 0.15 mmol). Purification by MPLC (cyclohexane/EtOAc 1:0 to 0:1) afforded the product (55.2 mg, 74%). **^{1}H-NMR** (700 MHz, CD_2Cl_2): δ 7.15 (dd, *J* = 8.6, 5.3 Hz, 2H), 7.03 (t, *J* = 8.6 Hz, 2H), 5.88 (s, 1H), 5.47-5.38 (m, 1H), 5.27-5.07 (m, 3H), 3.99-3.70 (m, 2H), 3.25-3.05 (m, 4H), 2.28 (s, 3H), 1.87 (dq, *J* = 13.9, 2.9 Hz, 1H), 1.76-1.63 (m, 2H), 1.55-1.49 (m, 1H), 1.42 (s, 9H). **^{13}C-NMR** (176 MHz, CD_2Cl_2): δ 211.3, 168.9, 163.2, 161.8, 161.5, 154.8, 152.1, 133.2, 128.6, 116.0, 106.2, 95.5, 84.3, 81.2, 79.6, 72.1, 46.3, 40.0, 39.6, 38.6, 32.9, 30.1, 28.5, 21.8. **HRMS**-ESI (m/z): $[M + H]^+$ calculated for $C_{27}H_{32}FN_2O_6^+$, 499.2239; found, 499.2230.

(±) 8'-(4-fluorobenzyl)-7'-methyl-3',9'-dioxo-3',4',4a',8',9',9b'-hexahydrospiro[piperidine-4,2'-pyrano[2',3':4,5]furo[3,2-c]pyridin]-1-ium triflate (24d)

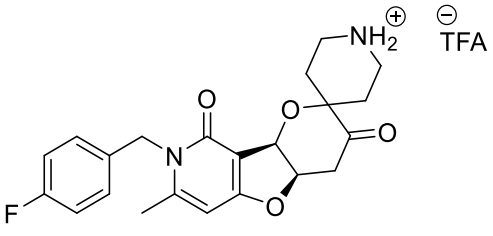

According to GP6, **4d** (97.6 mg, 0.30 mmol) was reacted with **2h** (70.0 mg, 0.30 mmol). Purification by MPLC (cyclohexane/EtOAc 1:0 to 0:1) afforded the product which was directly dissolved in DCM (1 mL) and cooled to 0 °C. A mixture of TMSOTf (0.13 mL, 10 equiv) and 2,6-lutidine (0.13 mL, 15 equiv) in DCM (0.1 mL) was added slowly and the

mixture was stirred at 0 °C for 1 hour and at room temperature overnight. The reaction was quenched by slow addition of saturated Na_2CO_3 solution at 0 °C and dilution with EtOAc (10 mL). The layers were separated and the aqueous phase was extracted with EtOAc (3 x 10 mL). The combined organic layers were washed with brine (20 mL), dried over $MgSO_4$ and concentrated in vacuo. Purification by prep. HPLC afforded the product (3.8 mg, 3% over two steps). **^{1}H-NMR** (700 MHz, DMSO): δ 8.51 (s, 1H), 8.43 (s, 1H), 7.24-7.13 (m, 4H), 6.13 (s, 1H), 5.41 (d, *J* = 6.7 Hz, 1H), 5.31-5.24 (m, 2H), 5.20 (d, , *J* = 12.7 Hz, 1H), 3.28-3.24 (m, 1H), 3.16 (dd, *J* = 14.4, 6.4 Hz, 1H), 3.11-3.07 (m, 1H), 3.03-3.00 (m, 1H), 2.96-2.92 (m, 1H), 3.05 (dd, *J* = 14.4, 6.2 Hz, 1H), 2.30 (s, 3H), 2.23-2.20 (m, 1H), 1.86-1.76 (m, 2H), 1.72-1.68 (m, 1H). **^{13}C-NMR** (176 MHz, DMSO): δ 210.3, 168.1, 161.9, 160.6, 160.4, 152.4, 133.4, 128.2, 115.4, 104.8, 94.6, 83.5, 77.4, 71.2, 45.0, 40.0, 38.8, 28.9, 26.7, 20.7. **HRMS**-ESI (m/z): $[M + H]^+$ calculated for $C_{22}H_{24}FN_2O_4^+$, 399.1715; found, 399.1713.

(±) 8'-(4-methoxybenzyl)-7'-methyl-3',9'-dioxo-3',4',4a',8',9',9b'-hexahydrospiro[piperidine-4,2'-pyrano[2',3':4,5]furo[3,2-c]pyridin]-1-ium triflate (24e)

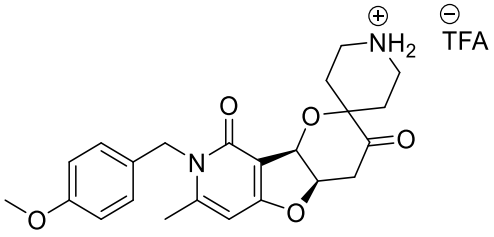

According to GP6, **4d** (97.6 mg, 0.30 mmol) was reacted with **2k** (76.6 mg, 0.30 mmol). Purification by MPLC (cyclohexane/EtOAc 1:0 to 0:1) afforded the product which was directly dissolved in DCM (1 mL) and cooled to 0 °C. A mixture of TMSOTf (0.20 mL, 10 equiv) and 2,6-lutidine (0.20 mL, 15 equiv) in DCM (0.1 mL) was added slowly and the mixture was stirred at 0 °C for 1 hour and at room temperature for 30 min. The reaction was quenched by slow addition of saturated Na_2CO_3 solution at 0 °C and dilution with EtOAc (10 mL). The layers were separated and the aqueous phase was extracted with EtOAc (3 x 10 mL). The combined organic layers were washed with brine (20 mL), dried over $MgSO_4$ and concentrated in vacuo. Purification by prep. HPLC afforded the product (5.2 mg, 4% over two steps). **^{1}H-NMR** (700 MHz, DMSO): δ 8.54 (s, 1H), 8.43 (s, 1H), 7.06 (d, *J* = 8.5 Hz, 2H), 6.90 (d, *J* = 8.5 Hz, 2H), 6.10 (s, 1H), 5.41 (d, *J* = 6.5 Hz, 1H), 5.27 (q, *J* = 6.5 Hz, 1H), 5.24-5.11 (m, 2H), 3.72 (s, 3H), 3.29-3.24 (m, 1H), 3.15 (dd, *J* = 14.4, 6.5 Hz, 1H), 3.11-3.07 (m, 1H), 3.06-3.01 (m, 2H), 2.99-2.93 (m, 1H), 2.29 (s, 3H), 2.24-2.20 (m, 1H), 1.86-1.77 (m, 2H), 1.72-1.66 (m, 1H). **^{13}C-NMR** (176 MHz, DMSO): δ 210.4, 168.0, 160.5, 1588.3, 152.5, 129.1, 127.6, 114.1, 104.8, 94.5, 83.4, 77.4, 71.3, 55.1, 45.1, 40.0, 38.8, 28.9, 26.7, 20.7. **HRMS**-ESI (m/z): $[M + H]^+$ calculated for $C_{23}H_{27}N_2O_5^+$, 411.1915; found, 411.1908.

(±) 7'-methyl-3',9'-dioxo-8'-(thiophen-2-ylmethyl)-3',4',4a',8',9',9b'-hexahydrospiro[piperidine-4,2'-pyrano[2',3':4,5]furo[3,2-c]pyridin]-1-ium triflate (24f)

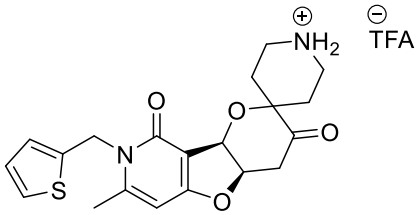

According to GP6, **4d** (48.8 mg, 0.15 mmol) was reacted with **2l** (33.2 mg, 0.15 mmol). Purification by MPLC (cyclohexane/EtOAc 1:0 to 0:1) afforded the product which was directly dissolved in DCM (1 mL) and cooled to 0 °C. A mixture of TMSOTf (0.21 mL, 10 equiv) and 2,6-lutidine (0.20 mL, 15 equiv) in DCM (0.1 mL) was added slowly and the mixture was stirred at 0 °C for 30 min. The reaction was quenched by slow addition of saturated Na_2CO_3 solution at 0 °C and dilution with EtOAc (10 mL). The layers were separated and the aqueous phase was extracted with EtOAc (3 x 10 mL). The combined organic layers were washed with brine (20 mL), dried over $MgSO_4$ and concentrated in vacuo. Purification by prep. HPLC afforded the product (3.6 mg, 6% over two steps). **^{1}H-NMR** (700 MHz, DMSO): δ 8.50 (s, 1H), 8.34 (s, 1H), 7.42 (d, *J* = 5.1 Hz, 1H), 7.07 (d, *J* = 3.7 Hz, 1H), 6.98 (dd, *J* = 5.1, 3.7 Hz, 1H), 6.09 (s, 1H), 5.42 (d, *J* = 6.6 Hz, 1H), 5.38 (d, *J* = 15.5 Hz, 1H), 5.33 (d, *J* = 15.5 Hz, 1H), 5.26 (q, *J* = 6.6 Hz, 1H), 3.17-2.99 (m, 6H), 2.44 (s, 3H), 2.25-2.21 (m, 1H), 1.85-1.75 (m, 2H), 1.69-1.65 (m, 1H). **^{13}C-NMR** (176 MHz, DMSO): δ 210.5, 168.1, 160.1, 152.0, 139.5, 126.7, 126.6, 126.1, 104.8, 94.6, 83.6, 77.4, 71.3, 41.5, 38.9, 38.8, 28.8, 26.8, 20.7. **HRMS**-ESI (m/z): $[M + H]^+$ calculated for $C_{20}H_{23}N_2O_4S^+$, 387.1373; found, 387.1374.

(±) *Tert*-butyl-7'-methyl-3',9'-dioxo-8'-(pyridin-4-ylmethyl)-3',4',4a',8',9',9b'-hexahydrospiro[piperidine-4,2'-pyrano[2',3':4,5]furo[3,2-c]pyridine]-1-carboxylate (23g)

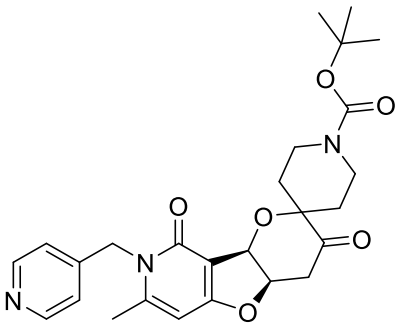

According to GP6, **4d** (48.8 mg, 0.15 mmol) was reacted with **2n** (32.4 mg, 0.15 mmol). Purification by MPLC (cyclohexane/EtOAc 1:0 to 0:1 then EtOAc/MeOH 1:0 to 9:1) afforded the product (43.9 mg, 61%). **^{1}H-NMR** (700 MHz, $CDCl_3$): δ 8.53 (d, *J* = 6.1 Hz, 2H), 7.04 (d, *J* = 6.1 Hz, 2H), 5.93 (s, 1H), 5.53-5.31 (m, 2H), 5.22-4.99 (m, 2H), 4.01-3.71 (m, 2H), 3.27-3.01 (m, 2H), 2.26 (s, 3H), 1.91-1.51 (m, 4H), 1.41 (s, 9H). **^{13}C-NMR** (176 MHz, $CDCl_3$): δ 211.2, 173.7, 171.2, 161.2, 151.1, 150.2, 146.0, 121.3, 106.0, 96.0, 83.9, 79.6, 71.2, 60.5, 45.9, 39.8, 39.2, 38.2, 33.2, 33.0, 28.5, 21.6. **HRMS**-ESI (m/z): $[M + H]^+$ calculated for $C_{26}H_{32}N_3O_6^+$, 482.2286; found, 482.2279.

(±) 7'-methyl-3',9'-dioxo-8'-(pyridin-2-ylmethyl)-3',4',4a',8',9',9b'-hexahydrospiro[piperidine-4,2'-pyrano[2',3':4,5]furo[3,2-c]pyridin]-1-ium triflate (24h)

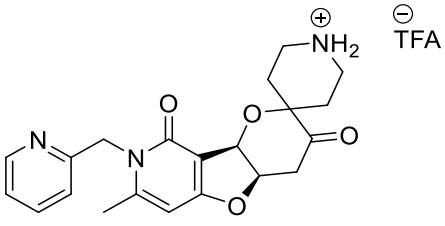

According to GP6, **4d** (48.8 mg, 0.15 mmol) was reacted with **2m** (32.4 mg, 0.15 mmol). Purification by MPLC (cyclohexane/EtOAc 1:0 to 0:1) afforded the product which was directly dissolved in DCM (1 mL) and cooled to 0 °C. A mixture of TMSOTf (0.12 mL, 10 equiv) and 2,6-lutidine (0.12 mL, 15 equiv) in DCM (0.1 mL) was added slowly and the mixture was stirred at 0 °C for 30 min. The reaction was quenched by slow addition of saturated Na_2CO_3 solution at 0 °C and dilution with EtOAc (10 mL). The layers were separated and the aqueous phase was extracted with EtOAc (3 x 10 mL). The combined organic layers were washed with brine (20 mL), dried over $MgSO_4$ and concentrated in vacuo. Purification by prep. HPLC afforded the product (1.0 mg, 1% over two steps). **^{1}H-NMR** (700 MHz, DMSO): δ 8.47 (d, *J* = 5.2 Hz, 2H), 8.40 (s, 1H), 8.27 (s, 1H), 7.79-7.77 (m, 1H), 7.29 (dd, *J* = 7.8, 4.9 Hz, 1H), 7.23 (d, *J* = 7.8 Hz, 1H), 6.13 (s, 1H), 5.40 (d, *J* = 6.9 Hz, 1H), 5.33-5.27 (m, 3H), 3.27-3.22 (m, 1H), 3.17 (dd, *J* = 14.4, 6.2 Hz, 1H), 3.01 (dd, *J* = 14.4, 5.9 Hz, 1H), 2.99-2.94 (m, 2H), 2.92-2.87 (m, 1H), 2.33 (s, 1H), 2.19-2.15 (m, 1H), 1.82-1.75 (m, 2H), 1.69-1.65 (m, 1H). **^{13}C-NMR** (176 MHz, DMSO): δ 210.4, 168.1, 160.3, 158.1, 157.9, 149.1, 137.0, 122.5, 121.3, 104.5, 94.2, 83.4, 77.4, 71.4, 47.4, 39.2, 38.8, 28.6, 27.1, 21.1. **HRMS**-ESI (m/z): $[M + H]^+$ calculated for $C_{21}H_{24}N_3O_4^+$, 382.1761; found, 382.1763.

(±) *Tert*-butyl-8'-((2-chloropyridin-4-yl)methyl)-7'-methyl-3',9'-dioxo-3',4',4a',8',9',9b'-hexahydrospiro[piperidine-4,2'-pyrano[2',3':4,5]furo[3,2-c]pyridine]-1-carboxylate (23i)

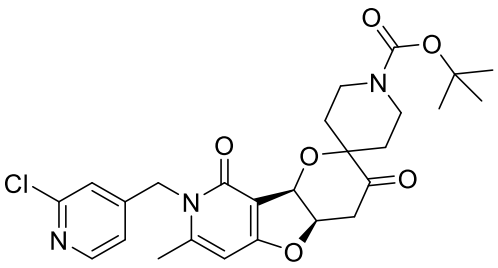

According to GP6, **4d** (48.8 mg, 0.15 mmol) was reacted with **2p** (37.6 mg, 0.15 mmol). Purification by MPLC (cyclohexane/EtOAc 1:0 to 0:1) afforded the product (54.1 mg, 70%). **^{1}H-NMR** (500 MHz, CD_2Cl_2): δ 8.31 (d, *J* = 5.2 Hz, 1H), 7.05 (s, 1H), 7.02 (dd, *J* = 5.2, 1.5 Hz, 1H), 5.95 (s, 1H), 5.46-5.46 (m, 2H), 5.22-5.09 (m, 2H), 3.94-3.73 (m, 2H), 3.23-3.00 (m, 4H), 2.25 (s, 3H), 1.91-1.85 (m, 1H), 1.69 (dtd, *J* = 30.4, 12.2, 4.5 Hz, 2H), 1.54 (dt, *J* = 15.1, 4.7 Hz, 1H), 1.41 (s, 9H). **^{13}C-NMR** (126 MHz, CD_2Cl_2): δ 211.2, 169.3, 161.2, 154.8, 152.4, 151.5, 150.4, 149.9, 121.9, 120.6, 106.3, 96.2, 84.4, 81.1, 79.6, 71.8, 45.8, 40.0, 39.5, 38.6, 33.1, 28.5, 21.7. **HRMS**-ESI (m/z): $[M + H]^+$ calculated for $C_{26}H_{31}ClN_3O_6^+$, 516.1896; found, 516.1892.

(±) 8'-((2-chloropyridin-4-yl)methyl)-7'-methyl-3',9'-dioxo-3',4',4a',8',9',9b'-hexahydrospiro[piperidine-4,2'-pyrano[2',3':4,5]furo[3,2-c]pyridin]-1-ium triflate (24i)

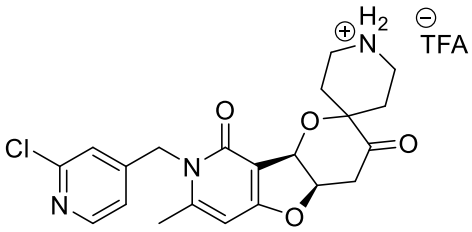

23h (42.1 mg, 0.08 mmol) was dissolved in DCM (1 mL) and cooled to 0 °C. A mixture of TMSOTf (0.15 mL, 10 equiv) and 2,6-lutidine (0.14 mL, 15 equiv) in DCM (0.1 mL) was added slowly and the mixture was stirred at 0 °C for 1 hour and at room temperature for 30 min. The reaction was quenched by slow addition of saturated Na_2CO_3 solution at 0 °C and dilution with EtOAc (10 mL). The layers were separated and the aqueous phase was extracted with EtOAc (3 x 10 mL). The combined organic layers were washed with brine (20 mL), dried over $MgSO_4$ and concentrated in vacuo. Purification by prep. HPLC afforded the product (3.5 mg, 10%). **^{1}H-NMR** (700 MHz, DMSO): δ 8.47 (s, 1H), 8.41-8.32 (m, 2H), 7.21 (s, 1H), 7.09 (d, *J* = 5.2 Hz, 1H), 6.20 (s, 1H), 5.42 (d, *J* = 6.8 Hz, 1H), 5.33-5.23 (m, 3H), 3.27-3.14 (m, 2H), 3.10-3.04 (m, 2H), 3.01-2.96 (m, 1H), 2.94-2.87 (m, 1H), 2.28 (s, 3H), 2.23-2.19 (m, 1H), 1.85-1.78 (m, 2H), 1.71 (dd, *J* = 14.4, 3.1 Hz, 1H). **^{13}C-NMR** (176 MHz, DMSO): δ 210.6, 168.9, 160.7, 152.8, 151.2, 151.1, 150.1, 122.0, 121.0, 105.3, 95.5, 84.1, 77.9, 71.5, 45.4, 39.4, 39.3, 29.4, 27.1, 21.4. **HRMS**-ESI (m/z): $[M + H]^+$ calculated for $C_{21}H_{23}ClN_3O_4^+$, 416.1372; found, 416.1369.

(±) 6',9'-dioxo-5',6',6b',9',10',10a'-hexahydrospiro[piperidine-4,8'-pyrano[2',3':4,5]furo[3,2-c]quinolin]-1-ium triflate (24j)

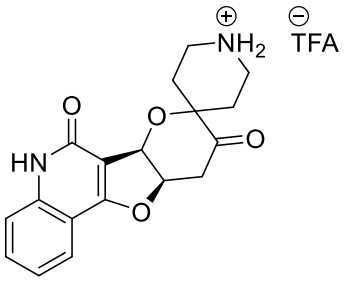

According to GP6, **4d** (50.0 mg, 0.15 mmol) was reacted with **2u** (24.8 mg, 0.15 mmol). Purification by MPLC (cyclohexane/EtOAc 1:0 to 0:1) afforded the product which was directly dissolved in HCl/dioxane (0.5 mL, 4M) at 0 °C and stirred at room temperature for 90 min. The reaction mixture was diluted by addition of DCM (10 mL) and 1 M HCl (10 mL). The layers were separated and the organic phase was extracted with 1 M HCl (3 x 10 mL). The combined aqueous layers were concentrated in vacuo and purified by prep. HPLC to afford the product (2.6 mg, 4% over two steps). **^{1}H-NMR** (500 MHz, MeOH-d_4): δ 7.80 (dd, *J* = 8.1, 1.4 Hz, 1H), 7.66 (ddd, *J* = 8.5, 8.1, 1.4 Hz, 1H), 7.43 (d, *J* = 8.5 Hz, 1H), 7.31 (t, *J* = 8.1 Hz, 1H), 5.61 (d, *J* = 6.8 Hz, 1H), 5.43 (qd, *J* = 6.8, 2.5 Hz, 1H), 3.43 (td, *J* = 13.0, 3.2 Hz, 1H), 3.37-3.31 (m, 2H), 3.28-3.18 (m, 3H), 2.37 (dq, *J* = 15.2, 3.1 Hz, 1H), 2.04 (ddd, *J* = 15.2, 13.0, 4.5 Hz, 1H), 1.94 (ddd, *J* = 14.8, 12.9, 4.5 Hz, 1H), 1.84 (dq, *J* = 14.8, 3.2 Hz, 1H). **^{13}C-NMR** (126 MHz,

MeOH-d_4): δ 210.3, 168.3, 163.5, 141.9, 133.9, 124.1, 124.0, 117.2, 112.3, 108.7, 86.0, 79.3, 72.9, 40.5, 40.4, 40.1, 31.0, 27.4. **HRMS**-ESI (m/z): $[M + H]^+$ calculated for $C_{18}H_{19}N_2O_4^+$, 327.1339; found, 327.1342.

(±) 5'-methyl-6',9'-dioxo-5',6',6b',9',10',10a'-hexahydrospiro[piperidine-4,8'-pyrano[2',3':4,5]furo[3,2-c]quinolin]-1-ium triflate (24k)

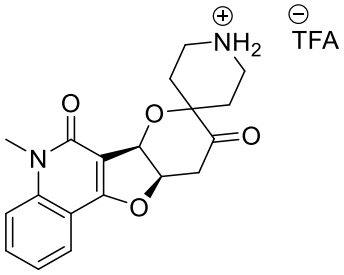

According to GP6, **4d** (97.6 mg, 0.30 mmol) was reacted with **2w** (52.6 mg, 0.30 mmol). Purification by MPLC (cyclohexane/EtOAc 1:0 to 0:1) afforded the product which was directly dissolved in DCM (1 mL) and cooled to 0 °C. A mixture of TMSOTf (0.34 mL, 10 equiv) and 2,6-lutidine (0.32 mL, 15 equiv) in DCM (0.1 mL) was added slowly and the mixture was stirred at 0 °C for 30 min. The reaction was quenched by slow addition of saturated Na_2CO_3 solution at 0 °C and dilution with EtOAc (10 mL). The layers were separated and the aqueous phase was extracted with EtOAc (3 x 10 mL). The combined organic layers were washed with brine (20 mL), dried over $MgSO_4$ and concentrated in vacuo. Purification by prep. HPLC afforded the product (2.6 mg, 3% over two steps). **^{1}H-NMR** (700 MHz, DMSO): δ 8.52 (s, 1H), 8.39 (s, 1H), 7.76 (m, 2H), 7.63 (d, *J* = 8.9 Hz, 1H), 7.34 (t, *J* = 7.5 Hz, 1H), 5.50 (d, *J* = 6.7 Hz, 1H), 5.43 (q, *J* = 6.7 Hz, 1H), 3.62 (s, 3H), 3.32-3.29 (m, 1H), 3.22 (d, *J* = 6.7 Hz, 2H), 3.15 (d, *J* = 12.6 Hz, 1H), 3.10-3.03 (m, 1H), 2.99-2.92 (m, 1H), 2.32 (dd, *J* = 14.9, 3.0 Hz, 1H), 1.90-1.85 (m, 1H), 1.81-1.72 (m, 2H). **^{13}C-NMR** (176 MHz, DMSO): δ 210.0, 163.9, 159.5, 141.3, 132.8, 123.1, 122.1, 115.6, 110.9, 107.1, 84.1, 77.6, 71.5, 40.0, 38.9, 38.8, 29.3, 28.7, 25.8. **HRMS**-ESI (m/z): $[M + H]^+$ calculated for $C_{19}H_{21}N_2O_4^+$, 341.1496; found, 341.1500.

2-(4-hydroxy-1,6-dimethyl-2-oxo-1,2-dihydropyridin-3-yl)-5-oxo-1-oxa-9-azaspiro[5.5]undec-2-en-9-ium triflate (25a)

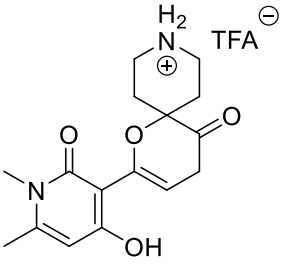

23a (30.0 mg, 0.07 mmol) was dissolved in dioxane (0.5 mL) and cooled to 0 °C. HCl in dioxane (0.18 mL, 4 M, 10 equiv) was added slowly and the mixture was stirred at 0 °C for 1 hour and at room temperature for 30 min. The reaction was quenched by slow addition of saturated Na_2CO_3 solution at 0 °C and diluted with EtOAc (10 mL). The layers were seperated and the aqueous phase was extracted with EtOAc (3 x 10 mL). The combined organic layers were washed with brine (20 mL), dried over $MgSO_4$ and concentrated

in vacuo. The crude was purified by prep. HPLC to afford the product (2.7 mg, 11%). **^{1}H-NMR** (700 MHz, DMSO): δ 8.77 (s, 1H), 8.51 (s, 1H), 6.65 (s, 1H), 6.58 (s, 1H), 4.25 (bs, 2H), 3.47 (s, 3H), 2.41 (s, 3H), 3.21 (dt, *J* = 12.7, 3.4 Hz, 1H), 3.12-3.06 (m, 1H), 1.92 (td, *J* = 13.6, 4.4 Hz, 1H), 1.80-1.76 (m, 1H). **^{13}C-NMR** (176 MHz, DMSO): δ 209.3, 158.9, 158.6, 149.6, 143.5, 113.2, 105.4, 94.6, 73.8, 39.0, 35.6, 30.3, 29.5, 20.9. **HRMS**-ESI (m/z): $[M + H]^+$ calculated for $C_{16}H_{21}O_4N_2^+$, 305.1496; found, 305.1491.

2-(1-cyclobutyl-4-hydroxy-6-methyl-2-oxo-1,2-dihydropyridin-3-yl)-5-oxo-1-oxa-9-azaspiro[5.5]undec-2-en-9-ium triflate (25b)

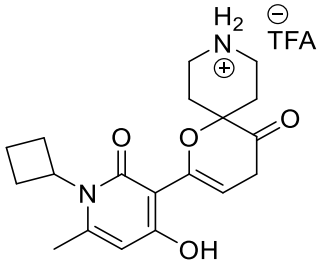

23b (46.0 mg, 0.10 mmol) was dissolved in dioxane (1 mL) and cooled to 0 °C. HCl in dioxane (0.26 mL, 4 M, 10 equiv) was added slowly and the mixture was stirred at 0 °C for 1 hour and at room temperature for 30 min. The reaction was evaporated to dryness and treated with Et_2O. The precipitate was filtered off and dried in vacuo. The crude was purified by prep. HPLC to afford the product (39.4 mg, 83%). **^{1}H-NMR** (700 MHz, DMSO): δ 8.76 (s, 1H), 8.48 (s, 1H), 6.61 (s, 1H), 6.50 (s, 1H), 4.86 (p, *J* = 8.8 Hz, 1H), 4.25 (bs, 2H), 3.24-3.14 (m, 4H), 3.10 (p, *J* = 12.3, 11.1 Hz, 2H), 2.41 (s, 3H), 2.19 (qt, *J* = 8.6, 2.6 Hz, 2H), 1.92 (td, *J* = 13.9, 4.1 Hz, 2H), 1.88-1.82 (m, 1H), 1.78 (d, *J* = 13.7 Hz, 2H), 1.74-1.68 (m, 1H). **^{13}C-NMR** (176 MHz, DMSO): δ 209.3, 160.3, 158.3, 149.6, 142.9, 115.1, 105.4, 95.4, 73.7, 51.9, 39.0, 35.5, 29.5, 26.9, 21.5, 14.1. **HRMS**-ESI (m/z): $[M + H]^+$ calculated for $C_{19}H_{25}N_2O_4^+$, 345.1801; found, 345.1808.

2-(1-benzyl-4-hydroxy-6-methyl-2-oxo-1,2-dihydropyridin-3-yl)-5-oxo-1-oxa-9-azaspiro[5.5]undec-2-en-9-ium (25c)

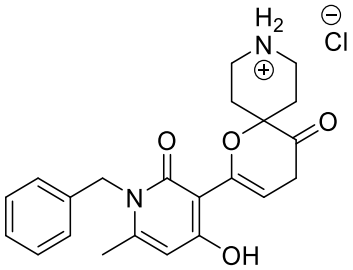

According to GP6, **4d** (50.0 mg, 0.15 mmol) was reacted with **2g** (33.1 mg, 0.15 mmol). Purification by MPLC (cyclohexane/EtOAc 1:0 to 0:1) afforded the product which was directly dissolved in HCl/dioxane (0.5 mL, 4M) at 0 °C and stirred at room temperature for 90 min. The reaction mixture was diluted by addition of DCM (10 mL) and 1 M HCl (10 mL). The layers were separated and the organic phase was extracted with 1 M HCl (3 x 10 mL). The combined aqueous layers were concentrated in vacuo to afford the product (22.0 mg, 35% over two steps). **^{1}H-NMR** (400 MHz, MeOH-d_4): δ 7.31 (t, *J* = 7.5 Hz, 2H), 7.25 (d, *J* = 7.5 Hz, 1H), 7.10 (d, *J* = 7.5 Hz, 2H), 6.80 (s, 1H), 6.67 (s, 1H), 5.48 (s, 2H), 4.30-4.28 (m, 2H), 3.36-3.29 (m, 4H), 2.40 (s, 3H),

2.20-2.09 (m, 2H), 1.98-1.90 (m, 2H). **^{13}C-NMR** (400 MHz, MeOH-d_4): δ 210.0, 161.9, 161.4, 152.2, 145.0, 138.0, 129.9, 128.4, 127.1, 115.5, 106.3, 98.5, 75.3, 48.2, 40.8, 36.7, 31.1, 21.1. **HRMS**-ESI (m/z): $[M + H]^+$ calculated for $C_{22}H_{25}N_2O_4^+$, 381.1809; found, 381.1810.

2-(1-(4-fluorobenzyl)-4-hydroxy-6-methyl-2-oxo-1,2-dihydropyridin-3-yl)-5-oxo-1-oxa-9-azaspiro[5.5]undec-2-en-9-ium triflate (**25d**)

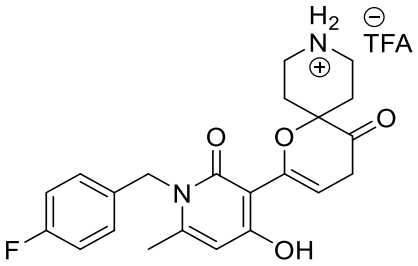

23d (40.0 mg, 0.08 mmol) was dissolved in dioxane (1 mL) and cooled to 0 °C. HCl in dioxane (0.20 mL, 4 M, 10 equiv) was added slowly and the mixture was stirred at 0 °C for 1 hour and at room temperature for 30 min. The reaction was quenched by slow addition of saturated Na_2CO_3 solution at 0 °C and diluted with EtOAc (10 mL). The layers were seperated and the aqueous phase was extracted with EtOAc (3 x 10 mL). The combined organic layers were washed with brine (20 mL), dried over $MgSO_4$ and concentrated in vacuo. The crude was purified by prep. HPLC to afford the product (11.1 mg, 35%). **^{1}H-NMR** (700 MHz, MeOH-d_4): δ 7.15 (dd, *J* = 8.6, 5.4 Hz, 2H), 7.05 (t, *J* = 8.6 Hz, 2H), 6.77 (s, 1H), 6.64 (s, 1H), 5.45 (bs, 2H), 4.28 (bs, 2H), 3.35-3.32 (m, 4H), 2.41 (s, 3H), 2.14-2.08 (m, 2H), 1.95-1.90 (m, 2H). **^{13}C-NMR** (126 MHz, CD_2Cl_2): δ 210.0, 164.1, 162.7, 162.1, 161.3, 151.9, 144.7, 134.2, 129.2, 116.5, 115.6, 106.4, 98.2, 75.2, 47.4, 40.8, 36.6, 31.1, 21.1. **HRMS**-ESI (m/z): $[M + H]^+$ calculated for $C_{22}H_{24}N_2O_4F^+$, 399.1715; found, 399.1705.

2-(4-hydroxy-1-(4-methoxybenzyl)-6-methyl-2-oxo-1,2-dihydropyridin-3-yl)-5-oxo-1-oxa-9-azaspiro[5.5]undec-2-en-9-ium triflate (25e)

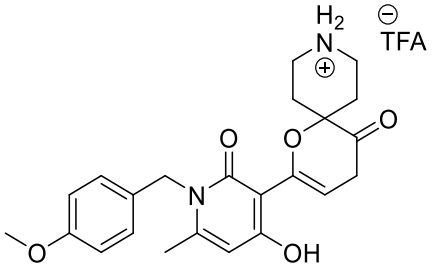

According to GP6, **4d** (50.0 mg, 0.15 mmol) was reacted with **2k** (37.7 mg, 0.15 mmol). Purification by MPLC (cyclohexane/EtOAc 1:0 to 0:1) afforded the product which was directly dissolved in HCl/dioxane (0.5 mL, 4M) at 0 °C and stirred at room temperature for 90 min. The reaction mixture was diluted by addition of DCM (10 mL) and 1 M HCl (10 mL). The layers were separated and the organic phase was extracted with 1 M HCl (3 x 10 mL). The combined aqueous layers were concentrated in vacuo and purified by prep. HPLC to afford the product (7.7 mg, 10% over two steps). **^{1}H-NMR** (700 MHz, MeOH-d_4): δ 7.06 (d, *J* = 8.8 Hz, 2H), 6.87 (d, *J* = 8.8 Hz, 2H), 6.77 (s, 1H), 6.61 (s, 1H), 5.43-5.38 (m, 2H), 4.28 (s, 2H), 3.76 (s, 3H), 3.33 (dd, *J* = 7.4, 2.9 Hz, 4H), 2.41 (s, 3H), 2.11 (dt, *J* = 14.3, 8.7 Hz, 2H), 1.92 (dq, *J* = 15.0,

2.8 Hz, 2H). **^{13}C-NMR** (176 MHz, MeOH-d_4): δ 210.0, 162.1, 161.3, 160.5, 151.7, 144.9, 130.1, 128.6, 115.6, 115.2, 106.4, 98.0, 75.2, 55.7, 47.5, 40.8, 36.6, 31.2, 21.1. **HRMS**-ESI (m/z): $[M + H]^+$ calculated for $C_{23}H_{27}N_2O_5^+$, 411.1915; found, 411.1933.

2-(4-hydroxy-6-methyl-2-oxo-1-(thiophen-2-ylmethyl)-1,2-dihydropyridin-3-yl)-5-oxo-1-oxa-9-azaspiro[5.5]undec-2-en-9-ium chloride (25f)

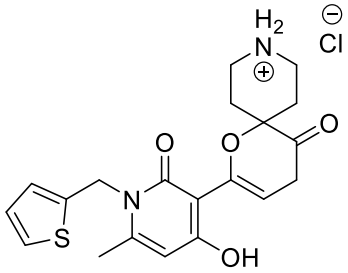

According to GP6, **4d** (50.0 mg, 0.15 mmol) was reacted with **2l** (34.0 mg, 0.15 mmol). Purification by MPLC (cyclohexane/EtOAc 1:0 to 0:1) afforded the product which was directly dissolved in HCl/dioxane (0.5 mL, 4M) at 0 °C and stirred at room temperature for 90 min. The reaction mixture was diluted by addition of DCM (10 mL) and 1 M HCl (10 mL). The layers were separated and the organic phase was extracted with 1 M HCl (3 x 10 mL). The combined aqueous layers were concentrated in vacuo to afford the product (10.1 mg, 16% over two steps). **^{1}H-NMR** (500 MHz, MeOH-d_4): δ 7.31 (d, *J* = 5.2 Hz, 1H), 7.05 (d, *J* = 3.6 Hz, 1H), 6.95 (dd, *J* = 5.2, 3.6 Hz, 1H), 6.78 (s, 1H), 6.62 (s, 1H), 4.30-4.28 (m, 2H), 3.36-3.30 (m, 4H), 2.56 (s, 3H), 2.16-2.08 (m, 2H), 1.95-1.89 (m, 2H). **^{13}C-NMR** (126 MHz, MeOH-d_4): δ 210.0, 161.6, 161.4, 152.0, 144.4, 140.5, 127.7, 127.6, 126.7, 115.5, 106.3, 98.4, 75.2, 43.9, 40.8, 36.7, 31.1, 21.0. **HRMS**-ESI (m/z): $[M + H]^+$ calculated for $C_{20}H_{23}N_2O_4S^+$, 387.1373; found, 387.1371.

(±) 7'-methyl-3',9'-dioxo-8'-(pyridin-4-ylmethyl)-3',4',4a',8',9',9b'-hexahydrospiro[piperidine-4,2'-pyrano[2',3':4,5]furo[3,2-c]pyridin]-1-ium chloride (25g)

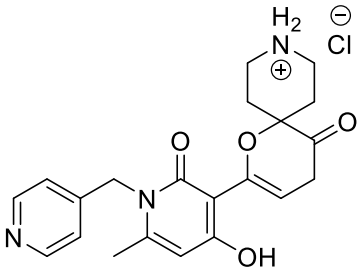

23g (37.3 mg, 0.08 mmol) was dissolved in dioxane (1 mL) and cooled to 0 °C. HCl in dioxane (0.19 mL, 4 M, 10 equiv) was added slowly and the mixture was stirred at 0 °C for 1 hour and at room temperature for 30 min. The reaction was evaporated to dryness and treated with Et_2O. The precipitate was filtered off and dried in vacuo to afford the product (29.5 mg, quant.). **^{1}H-NMR** (500 MHz, MeOH-d_4): δ 8.78 (bs, 2H), 7.81 (bs, 2H), 6.77 (bs, 2H), 5.69 (bs, 2H), 4.28 (bs, 2H), 3.61 (bs, 1H), 3.31-3.25 (m, 4H), 2.40 (s, 3H), 2.15-2.07 (m, 2H), 1.94-1.86 (m, 2H). **^{13}C-NMR** (126 MHz, MeOH-d_4): δ 210, 161.6, 161.0, 152.6, 144.1, 142.9, 125.9, 115.6, 109.0, 106.4, 98.8. 75.3, 68.1, 49.5, 40.8, 31.0. **HRMS**-ESI (m/z): $[M + H]^+$ calculated for $C_{21}H_{24}N_3O_4^+$, 382.1761; found, 382.1760.

2-(4-hydroxy-6-methyl-2-oxo-1-(pyridin-2-ylmethyl)-1,2-dihydropyridin-3-yl)-5-oxo-1-oxa-9-azaspiro[5.5]undec-2-en-9-ium chloride (25h)

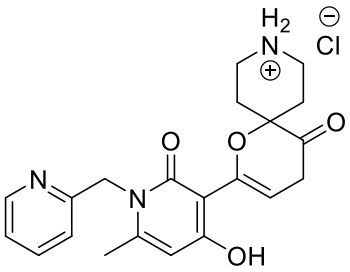

According to GP6, **4d** (50.0 mg, 0.23 mmol) was reacted with **2m** (33.2 mg, 0.23 mmol). Purification by MPLC (cyclohexane/EtOAc 1:0 to 0:1) afforded the product which was directly dissolved in HCl/dioxane (0.5 mL, 4M) at 0 °C and stirred at room temperature for 90 min. The reaction mixture was diluted by addition of DCM (10 mL) and 1 M HCl (10 mL). The layers were separated and the organic phase was extracted with 1 M HCl (3 x 10 mL). The combined aqueous layers were concentrated in vacuo and freeze-dried to afford the product (19.7 mg, 20 % over two steps).**^{1}H NMR** (500 MHz, MeOH-d_4): δ 8.79 (d, *J* = 5.7 Hz, 1H), 8.52 (t, *J* = 7.9 Hz, 1H), 7.97 (t, *J* = 6.6 Hz, 1H), 7.70 (d, *J* = 7.9 Hz, 1H), 6.74 (s, 1H), 6.68 (s, 1H), 5.68 (s, 1H), 4.25 (s, 1H), 3.28 (dd, *J* = 7.2, 3.4 Hz, 2H), 2.52 (s, 2H), 2.08 (ddd, *J* = 14.6, 10.7, 6.6 Hz, 1H), 1.87 (d, *J* = 14.6 Hz, 1H). **^{13}C NMR** (126 MHz, MeOH-d_4): δ 210.0, 161.8, 154.1, 152.5, 148.8, 144.1, 142.8, 127.2, 126.2, 115.6, 106.2, 99.0, 75.3, 49.5, 49.3, 49.2, 49.0, 48.8, 48.7, 48.5, 46.9, 40.8, 36.7, 31.0, 21.4. **HRMS**-ESI (m/z): $[M + H]^+$ calculated for $C_{21}H_{24}O_4N_3^+$,382.17613; found, 382.17593.

2-(4-hydroxy-6-methyl-1-((3-methylpyridin-4-yl)methyl)-2-oxo-1,2-dihydropyridin-3-yl)-5-oxo-1-oxa-9-azaspiro[5.5]undec-2-en-9-ium chloride (25i)

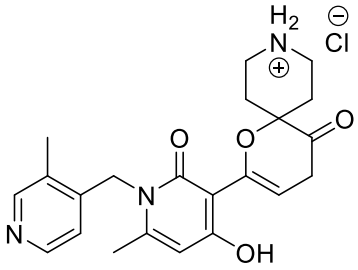

According to GP6, **4d** (50.0 mg, 0.23 mmol) was reacted with **2o** (62.5 mg, 0.23 mmol). Purification by MPLC (cyclohexane/EtOAc 1:0 to 0:1) afforded the product which was directly dissolved in HCl/dioxane (0.5 mL, 4M) at 0 °C and stirred at room temperature for 90 min. The reaction mixture was diluted by addition of DCM (10 mL) and 1 M HCl (10 mL). The layers were separated and the organic phase was extracted with 1 M HCl (3 x 10 mL). The combined aqueous layers were concentrated in vacuo and freeze-dried to afford the product (13.1 mg, 13% over two steps). **^{1}H NMR** (500 MHz, Methanol-d4): δ 8.74 (s, 1H), 8.54 (d, J = 5.5 Hz, 1H), 7.17 (d, J = 5.4 Hz, 1H), 6.77 (s, 1H), 6.73 (s, 1H), 5.60 (s, 2H), 4.29 (s, 2H), 3.30 (s, 4H), 2.65 (s, 2H), 2.41 (s, 2H), 2.11 (m, 2H), 1.90 (d, J = 14.4 Hz, 2H). **^{13}C NMR** (126 MHz, MeOH-d_4): δ 208.6, 160.3, 157.5, 151.1, 142.8, 140.8, 139.4, 136.6, 122.1, 114.2, 105.0, 98.0, 74.0, 48.1, 48.0, 48.0, 47.6, 47.5, 47.3, 47.1, 45.5, 39.4, 35.3, 29.7, 19.8, 15.0. **HRMS**-ESI (m/z): $[M + H]^+$ calculated for $C_{22}H_{26}O_4N_3^+$,396.19178; found, 396.19155.

2-(1-((2-chloropyridin-1-ium-4-yl)methyl)-4-hydroxy-6-methyl-2-oxo-1,2-dihydropyridin-3-yl)-5-oxo-1-oxa-9-azaspiro[5.5]undecan-9-ium chloride (25j)

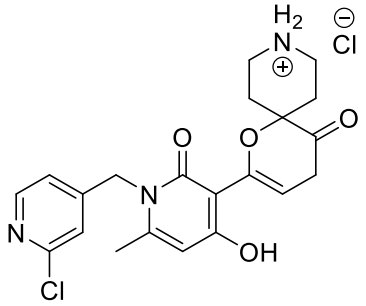

23i (33.2 mg, 0.06 mmol) was dissolved in dioxane (1 mL) and cooled to 0 °C. HCl in dioxane (0.16 mL, 4 M, 10 equiv) was added slowly and the mixture was stirred at 0 °C for 1 hour and at room temperature for 30 min. The reaction was evaporated to dryness and treated with Et_2O. The precipitate was filtered off and dried in vacuo to afford the product (29.1 mg, 99%). **^{1}H-NMR** (700 MHz, DMSO): δ 9.06 (s, 1H), 8.84 (s, 1H), 8.34 (d, *J* = 5.0 Hz, 1H), 7.21 (s, 1H), 7.06 (d, *J* = 5.0 Hz, 1H), 6.71 (bs, 2H), 5.38 (bs, 2H), 4.31 (bs, 2H), 3.21-3.15 (m, 2H), 3.10-3.04 (m, 2H), 2.31 (s, 3H), 2.01-1.95 (m, 2H), 1.84-1.79 (m 2H). **^{13}C-NMR** (176 MHz, DMSO): δ 209.3, 158.9, 158.8, 150.9, 150.6, 150.4, 150.3, 142.8, 121.5, 120.6, 113.5, 105.5, 95.8, 73.8, 45.1, 38.8, 35.6, 29.3, 20.5. **HRMS**-ESI (m/z): $[M + H]^+$ calculated for $C_{21}H_{23}ClN_3O_4^+$, 416.1372; found, 416.1362.

2-(4-hydroxy-1-(2-(5-methoxy-1H-indol-3-yl)ethyl)-6-methyl-2-oxo-1,2-dihydropyridin-3-yl)-5-oxo-1-oxa-9-azaspiro[5.5]undec-2-en-9-ium triflate (25k)

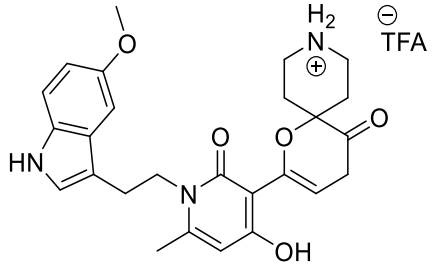

According to GP6, **4d** (50.0 mg, 0.15 mmol) was reacted with **2s** (45.8 mg, 0.15 mmol). Purification by MPLC (cyclohexane/EtOAc 1:0 to 0:1) afforded the product which was directly dissolved in HCl/dioxane (0.5 mL, 4M) at 0 °C and stirred at room temperature for 90 min. The reaction mixture was diluted by addition of DCM (10 mL) and 1 M HCl (10 mL). The layers were separated and the organic phase was extracted with 1 M HCl (3 x 10 mL). The combined aqueous layers were concentrated in vacuo and purified by prep. HPLC to afford the product (3.2 mg, 4% over two steps). **^{1}H-NMR** (500 MHz, MeOH-d_4): δ 7.20 (d, *J* = 9.0 Hz, 1H), 7.03 (s, 1H), 6.88 (d, *J* = 2.4 Hz, 1H), 6.80 (d, *J* = 0.8 Hz, 1H), 6.70 (dd, *J* = 9.0, 2.4 Hz, 1H), 6.43 (s, 1H), 4.39 (t, *J* = 7.1 Hz, 2H), 4.27 (s, 2H), 3.65 (s, 3H), 3.34 (dd, *J* = 7.1, 2.9 Hz, 4H), 3.17 (t, *J* = 7.1 Hz, 2H), 2.18 (s, 3H), 2.11 (ddd, *J* = 14.7, 9.7, 7.6 Hz, 2H), 1.95-1.89 (m, 2H). **^{13}C-NMR** (126 MHz, MeOH-d_4): δ 210.0, 161.9, 161.3, 155.1, 151.5, 144.9, 133.2, 129.1, 124.5, 115.7, 113.1, 113.0, 112.7, 106.3, 100.6, 97.6, 75.2, 56.1, 47.4, 40.8, 36.6, 31.1, 25.3, 21.1. **HRMS**-ESI (m/z): $[M + H]^+$ calculated for $C_{26}H_{30}N_3O_5^+$, 464.2180; found, 464.2177.

5.1.4.3. Synthesis of General Scaffold C Isomers

(±) 2,6,7-trimethyl-4a,9a-dihydro-2H-pyrano[3',2':4,5]furo[3,2-c]pyridin-5(6H)-one (15a)

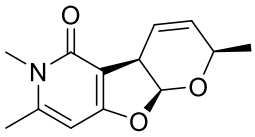

According to GP2, **3b**-*trans* (50.8 mg, 0.17 mmol) was reacted with **2b** (19.5 mg, 0.14 mmol) at 100 °C for 1 hour. After filtration over celite the crude was purified by FC (cyclohexane/EtOAc 1:0 to 0:1) to afford the product (19.4 mg, 59%). **^{1}H-NMR** (700 MHz, DMSO): δ δ 6.14 (d, *J* = 6.6 Hz, 1H), 6.10 (ddd, *J* = 10.3, 3.9, 2.0 Hz, 1H), 6.03 (s, 1H), 5.87 (ddd, *J* = 10.3, 2.8, 1.8 Hz, 1H), 4.34-4.30 (m, 1H), 3.66-3.63 (m, 1H), 2.32 (s, 3H), 1.16 (d, *J* = 6.8 Hz, 3H). **^{13}C-NMR** (176 MHz, DMSO): δ 163.9, 160.3, 149.8, 130.1, 121.6, 107.2, 104.5, 94.2, 66.9, 37.1, 29.9, 21.8, 20.9. **HRMS**-ESI (m/z): $[M + H]^+$ calculated for $C_{13}H_{16}NO_3^+$, 234.1125; found, 234.1124.

(±) 2,6,7-trimethyl-3,4,4a,9a-tetrahydro-2H-pyrano[3',2':4,5]furo[3,2-c]pyridin-5(6H)-one (16a)

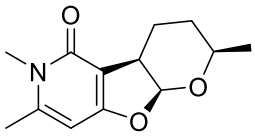

15a (19.4 mg, 0.08 mmol) was suspended with Pd/C (5 mg, 10 wt%) in toluene (2 mL) and was hydrogenated at 20 °C for 18 hours using a H_2-balloon. The catalyst was filtered off and the solvent removed in vacuo. The crude was purified by MPLC (EtOAc/MeOH 1:0 to 9:1 + 0.1% DIPEA) to afford the product (11.7 mg, 62%). **^{1}H-NMR** (700 MHz, CD_2Cl_2): δ 5.92 (d, *J* = 6.5 Hz, 1H), 5.32 (s, 1H), 3.82-3.77 (m, 1H), 3.43 (s, 3H), 3.34 (ddd, *J* = 8.0, 6.5, 2.3 Hz, 1H), 2.39 (dddd, *J* = 13.7, 4.5, 3.5, 2.3 Hz, 1H), 2.32 (s, 3H), 1.78 (dddd, *J* = 13.7, 13.0, 6.3, 3.7 Hz, 1H), 1.63-1.58 (m, 1H), 1.24-1.21 (m, 1H), 1.17 (d, *J* = 6.3 Hz, 3H). **^{13}C-NMR** (176 MHz, CD_2Cl_2): δ 165.9, 161.9, 149.1, 106.9, 106.5, 95.2, 70.8, 38.7, 30.6, 27.7, 23.2, 21.9, 20.3. **HRMS**-ESI (m/z): $[M + H]^+$ calculated for $C_{13}H_{18}NO_3^+$, 236.1281; found, 236.1284.

(±) 2,7-dimethyl-3,4,4a,9a-tetrahydro-2H-pyrano[3',2':4,5]furo[3,2-c]pyridin-5(6H)-one (16b)

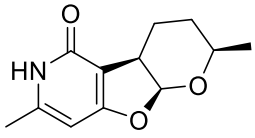

According to GP2, **3b**-*trans* (50.8 mg, 0.17 mmol) was reacted with **2a** (19.5 mg, 0.14 mmol) at 100 °C for 1 hour. After filtration over celite the crude was purified by FC (EtOAc/MeOH 1:0 to 9:1) and the product was directly suspended with Pd/C (5 mg, 10 wt%) in toluene (2 mL) and was hydrogenated at 20 °C for 18 hours using a H_2-balloon. The catalyst was filtered off and the solvent removed in vacuo. The crude was purified by MPLC (EtOAc/MeOH 1:0 to 9:1 + 0.1% DIPEA) to afford

the product (8.00 mg, 18%). **^{1}H-NMR** (600 MHz, CD_2Cl_2): δ 11.52 (s, 1H), 5.95 (d, *J* = 6.5 Hz, 1H), 5.84 (s, 1H), 3.81 (ttd, *J* = 10.5, 6.7, 6.2, 3.5 Hz, 1H), 3.35 (td, *J* = 6.5, 2.9 Hz, 1H), 2.39 (ddd, *J* = 13.6, 6.3, 2.9 Hz, 1H), 2.27 (s, 3H), 1.80 (tdd, *J* = 13.6, 6.3, 3.7 Hz, 1H), 1.65-1.60 (m, 1H), 1.28-1.24 (m, 1H), 1.17 (d, *J* = 6.3 Hz, 3H). **^{13}C-NMR** (151 MHz, CD_2Cl_2): δ 168.8, 163.3, 147.9, 107.2, 106.6, 94.7, 70.8, 37.9, 27.6, 23.2, 20.5, 19.6. **HRMS**-ESI (m/z): $[M + H]^+$ calculated for $C_{12}H_{16}NO_3^+$, 222.1125; found, 222.1130.

(±) 6-cyclobutyl-2,7-dimethyl-4a,9a-dihydro-2H-pyrano[3',2':4,5]furo[3,2-c]pyridin-5(6H)-one (15c)

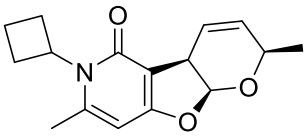

According to GP2, **3b**-*trans* (33.4 mg, 0.11 mmol) was reacted with **2c** (18.0 mg, 0.10 mmol) at 110 °C for 1 hour. The catalyst was filtered off and the filtrate was diluted with DCM (10 mL) and washed with saturated $NaHCO_3$ solution (15 mL). The aqueous phase was extracted with DCM (3 x 10 mL) and the combined organic layers were washed with brine (50 mL), dried over $MgSO_4$ and concentrated in vacuo. The crude was purified by MPLC (cyclohexane/EtOAc 1:0 to 1:1) to afford the product (3.4 mg, 12%). **^{1}H-NMR** (600 MHz, CD_2Cl_2): δ 6.26 (ddd, *J* = 10.3, 4.0, 2.0 Hz, 1H), 6.04 (d, *J* = 6.5 Hz, 1H), 5.84 (dt, *J* = 10.3, 2.4 Hz, 1H), 5.77 (s, 1H), 4.71 (p, *J* = 8.8 Hz, 1H), 4.31 (qq, *J* = 6.9, 2.4 Hz, 1H), 3.70-3.63 (m, 1H), 3.28-3.19 (m, 2H), 2.30 (s, 3H), 2.24-2.16 (m, 2H), 1.97-1.88 (m, 1H), 1.72 (dddd, *J* = 18.0, 11.0, 9.6, 8.5 Hz, 1H), 1.25 (d, *J* = 6.9 Hz, 3H). **^{13}C-NMR** (151 MHz, CD_2Cl_2): δ 164.6, 163.1, 148.9, 130.4, 122.5, 110.0, 105.4, 95.9, 68.0, 53.2, 38.8, 28.1, 22.5, 22.1, 15.1. **HRMS**-ESI (m/z): $[M + H]^+$ calculated for $C_{16}H_{10}NO_3^+$, 274.1438; found, 274.1439.

(±) 6-benzyl-2,7-dimethyl-3,4,4a,9a-tetrahydro-2H-pyrano[3',2':4,5]furo[3,2-c]pyridin-5(6H)-one (16d)

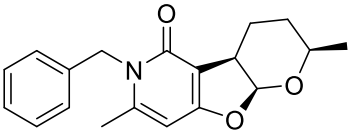

According to GP2, **3b**-*trans* (69.4 mg, 0.23 mmol) was reacted with **2k** (38.0 mg, 0.18 mmol) at 100 °C for 1 hour. After filtration over celite the crude was purified by FC (Hep/EtOAc 1:0 to 1:1) and the product was directly suspended with Pd/C (5 mg, 10 wt%) in toluene (2 mL) and was hydrogenated at 20 °C for 18 hours using a H_2-balloon. The catalyst was filtered off and the solvent removed in vacuo. The crude was purified by MPLC (EtOAc/MeOH 1:0 to 9:1 + 0.1% DIPEA) to afford the product (18.9 mg, 34%). **^{1}H-NMR** (500 MHz, $CDCl_3$): δ 7.30 (t, *J* = 7.4 Hz, 2H), 7.23 (t, *J* = 7.4 Hz, 1H), 7.13 (d, *J* = 7.4 Hz, 2H), 6.00 (d, *J* = 6.7 Hz, 1H), 5.93 (s, 1H), 5.46 (d, *J* = 15.9 Hz, 1H), 5.17 (d, *J* = 15.9 Hz, 1H), 3.87-3.79 (m, 1H), 3.47 (td, *J* = 6.7,

2.4 Hz, 1H), 2.54 (ddd, *J* = 13.6, 7.8, 2.4 Hz, 1H), 2.26 (s, 3H), 1.84 (tdd, *J* = 13.6, 6.2, 3.7 Hz, 1H), 1.64 (dq, *J* = 13.8, 3.7 Hz, 1H), 1.35 (tdd, *J* = 13.8, 10.4, 3.6 Hz, 1H), 1.23 (d, *J* = 6.3 Hz, 3H). **^{13}C-NMR** (126 MHz, $CDCl_3$): δ 166.2, 162.0, 148.8, 137.0, 128.9, 127.4, 126.5, 107.2, 106.2, 96.3, 70.6, 46.6, 38.5, 27.6, 23.1, 21.5, 20.1. **HRMS**-ESI (m/z): $[M + H]^+$ calculated for $C_{19}H_{22}NO_3^+$, 312.1594; found, 312.1592.

(±) 6-(3,5-dimethylbenzyl)-2,7-dimethyl-4a,9a-dihydro-2H-pyrano[3',2':4,5]furo[3,2-c]pyridin-5(6H)-one (15e)

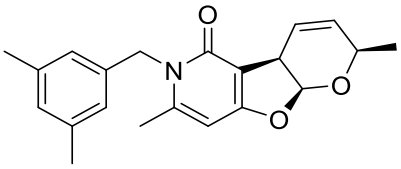

According to GP2, **3b**-*trans* (61.1 mg, 0.22 mmol) was reacted with **2j** (27.0 mg, 0.11 mmol) at 110 °C for 1 hour. The catalyst was filtered off and the filtrate was diluted with DCM (10 mL) and washed with saturated $NaHCO_3$ solution (15 mL). The aqueous phase was extracted with DCM (3 x 10 mL) and the combined organic layers were washed with brine (50 mL), dried over $MgSO_4$ and concentrated in vacuo. The crude was purified by prep. HPLC to afford the product (1.1 mg, 3%). **^{1}H-NMR** (600 MHz, CD_2Cl_2): δ 6.88 (s, 1H), 6.70 (s, 2H), 6.28 (ddd, *J* = 10.3, 3.9, 2.0 Hz, 1H), 6.12 (d, *J* = 6.5 Hz, 1H), 5.89 (s, 1H), 5.87 (dt, *J* = 10.3, 2.3 Hz, 1H), 5.36 (d, *J* = 15.9 Hz, 1H), 5.00 (d, *J* = 15.9 Hz, 1H), 4.35 (qq, *J* = 6.9, 2.3 Hz, 1H), 3.77-3.73 (bm, 1H), 2.26 (s, 6H), 2.24 (s, 3H), 1.28 (d, *J* = 6.9 Hz, 1H). **^{13}C-NMR** (151 MHz, CD_2Cl_2): δ 164.8, 161.2, 149.1, 138.3, 137.2, 130.0, 128.7, 123.8, 121.9, 108.4, 105.2, 95.5, 67.7, 46.3, 38.2, 21.7, 21.1. **HRMS**-ESI (m/z): $[M + H]^+$ calculated for $C_{21}H_{24}NO_3^+$, 338.1751; found, 338.1753.

(±) 6-(4-methoxybenzyl)-2,7-dimethyl-4a,9a-dihydro-2H-pyrano[3',2':4,5]furo[3,2-c]pyridin-5(6H)-one (15f)

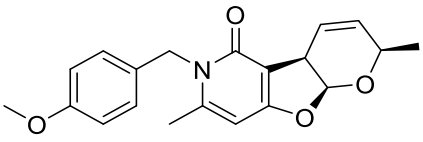

According to GP2, **3b**-*trans* (74.7 mg, 0.25 mmol) was reacted with **2k** (46.6 mg, 0.19 mmol) at 110 °C for 1 hour. After filtration over celite the crude was purified by FC (cyclohexane/EtOAc 1:0 to 1:1) to afford the product (23.2 mg, 36%). **^{1}H-NMR** (700 MHz, CD_2Cl_2): δ 7.07 (d, *J* = 8.7 Hz, 2H), 6.84 (d, *J* = 8.7 Hz, 2H), 6.26 (ddd, *J* = 10.3, 3.9, 2.0 Hz, 1H), 6.13 (d, *J* = 6.6 Hz, 1H), 5.92 (s, 1H), 5.88 (ddd, *J* = 10.3, 2.6, 1.9 Hz, 1H), 5.33 (m, 1H), 5.08 (d, *J* = 15.9 Hz, 1H), 4.36 (qq, *J* = 6.9, 2.6 Hz, 1H), 3.77-3.75 (m, 4H), 2.27 (s, 3H), 1.28 (d, *J* = 6.9 Hz, 1H). **^{13}C-NMR** (176 MHz, CD_2Cl_2): δ 165.5, 161.8, 159.3, 149.6, 130.5, 129.3, 128.1, 122.1, 114.4, 109.0, 105.8, 96.4, 68.2, 55.6, 46.5, 38.4, 22.2, 21.5. **HRMS**-ESI (m/z): $[M + H]^+$ calculated for $C_{20}H_{22}NO_4^+$, 340.1543; found, 340.1545.

(±) 6-(4-methoxybenzyl)-2,7-dimethyl-3,4,4a,9a-tetrahydro-2H-pyrano[3',2':4,5]furo[3,2-c]pyridin-5(6H)-one (16f); (±) 4-hydroxy-1-(4-methoxybenzyl)-6-methyl-3-(2-methyltetrahydro-2H-pyran-3-yl)pyridin-2(1H)-one (14g)

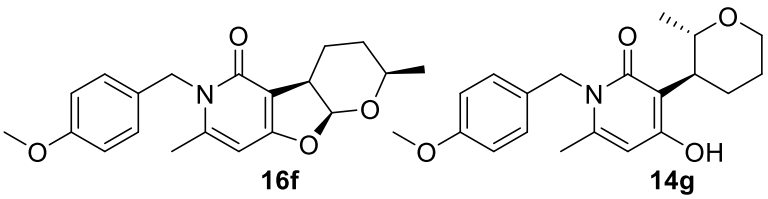

According to GP3, **3b**-*trans* (69.6 mg, 0.23 mmol) was reacted with **2k** (49.1 mg, 0.20 mmol). After purification by MPLC (cyclohexane/EtOAc 1:0 to 0:1), the product was directly suspended with Pd/C (5 mg, 10 wt%) in toluene (2 mL) and was hydrogenated at 20 °C for 48 hours using a H_2-balloon. The catalyst was filtered off and the solvent removed in vacuo. The crude was purified by prep. HPLC to afford product **16f** (5.9 mg, 9%) and **14g** (9.5 mg, 14%) in separated fractions. **^{1}H-NMR** product **16f** (600 MHz, CD_2Cl_2): δ 7.07 (d, *J* = 8.7 Hz, 2H), 6.84 (d, *J* = 8.7 Hz, 2H), 5.82 (s, 1H), 5.42 (d, *J* = 5.1 Hz, 1H), 5.26 (d, *J* = 15.5 Hz, 1H), 5.17 (d, *J* = 15.5 Hz, 1H), 4.46 (q, *J* = 6.5 Hz, 1H), 3.76 (s, 3H), 3.21 (bs, 1H), 2.24 (s, 3H), 2.21-2.10 (m, 3H), 1.99-1.94 (m, 1H), 1.35 (d, *J* = 6.5 Hz, 3H). **^{13}C-NMR** product **16f** (151 MHz, CD_2Cl_2): δ 164.1, 163.8, 159.3, 145.3, 129.2, 128.0, 114.5, 114.4, 103.0, 98.3, 77.4, 55.6, 47.5, 34.4, 28.3, 21.3, 20.7, 20.6. **HRMS**-ESI (m/z) product **16f**: $[M + H]^+$ calculated for $C_{20}H_{24}NO_4^+$, 342.1670; found, 342.1707. **^{1}H-NMR** product **14g** (400 MHz, MeOH-d_4): δ 7.01 (d, *J* = 8.6 Hz, 2H), 6.86 (d, *J* = 8.6 Hz, 2H), 5.86 (s, 1H), 5.31-5.21 (m, 2H), 4.36-4.18 (m, 1H), 3.93 (dd, *J* = 11.3, 4.3 Hz, 1H), 3.76 (bs, 4H), 3.56 (t, *J* = 11.3 Hz, 1H), 2.16 (s, 3H), 1.79-1.52 (m, 4H), 1.02 (d, *J* = 6.2 Hz, 3H). **^{13}C-NMR** product **14g** (126 MHz, MeOH-d_4): δ 164.8, 160.4, 160.3, 146.7, 130.3, 128.4, 115.2, 111.4, 101.0, 76.5 69.4, 55.7, 47.3, 40.1, 28.2, 28.1, 20.4. **HRMS**-ESI (m/z) product **14g**: $[M + H]^+$ calculated for $C_{20}H_{26}NO_4^+$, 344.1856; found, 344.1865.

(±) 6-(4-fluorobenzyl)-2,7-dimethyl-4a,9a-dihydro-2H-pyrano[3',2':4,5]furo[3,2-c]pyridin-5(6H)-one (15g)

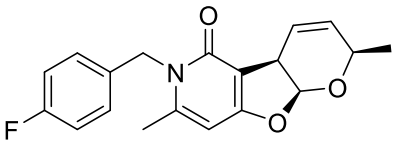

According to GP2, **3b**-*trans* (75.9 mg, 0.25 mmol) was reacted with **2h** (45.0 mg, 0.19 mmol) at 100 °C for 1 hour. After filtration over celite the crude was purified by FC (cyclohexane/EtOAc 1:0 to 1:1) to afford the product (15.9 mg, 25%). **^{1}H-NMR** (700 MHz, CD_2Cl_2): δ 7.13 (dd, *J* = 8.6, 5.4 Hz, 2H), 7.02 (t, *J* = 8.6 Hz, 2H), 6.23 (ddd, *J* = 10.4, 3.9, 2.3 Hz, 1H), 6.16 (d, *J* = 6.2 Hz, 1H), 5.99 (s, 1H), 5.89 (ddd, *J* = 10.4, 2.7, 1.8 Hz, 1H), 5.37 (d, *J* = 16.1 Hz, 1H), 5.15 (d, *J* = 16.1 Hz, 1H), 4.37 (qq, *J* = 6.9, 2.7 Hz, 1H), 3.77 (dq, *J* = 6.2, 2.3 Hz, 1H), 2.30 (s, 3H), 1.29 (d, *J* = 6.9 Hz, 3H). **^{13}C-NMR** (176 MHz, CD_2Cl_2): δ 166.0, 163.1,

161.7, 161.9, 149.6, 133.0, 130.1, 128.6, 121.7, 115.9, 109.4, 106.1, 97.1, 68.2, 46.7, 38.1, 22.2, 21.5. **HRMS**-ESI (m/z): $[M + H]^+$ calculated for $C_{19}H_{19}FNO_3^+$, 328.1344; found, 328.1343.

(±) 8-methyl-1,2,3,4,5b,9a-hexahydro-5H,8H-cyclopenta[b]pyrano[3',2':4,5]furo[2,3-d]pyridin-5-one (15h)

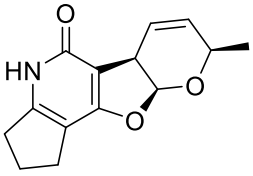

According to GP2, **3b**-*trans* (50.0 mg, 0.17 mmol) was reacted with **2x** (25.0 mg, 0.17 mmol) at 110 °C for 1 hour. The catalyst was filtered off and the filtrate was diluted with EtOAc (10 mL) and washed with water (15 mL). The aqueous phase was extracted with EtOAc (3 x 10 mL) and the combined organic layers were washed with brine (50 mL), dried over $MgSO_4$ and concentrated in vacuo. The crude was purified by prep. HPLC to afford the product (0.80 mg, 2%). **^{1}H-NMR** (700 MHz, CD_2Cl_2): δ 6.22-6.17 (m, 2H), 5.88 (dt, *J* = 10.4, 2.4 Hz, 1H), 4.37 (dq, *J* = 6.9, 2.4 Hz, 1H), 3.75-3.72 (m, 1H), 2.86 (t, *J* = 7.5 Hz, 2H), 2.80-2.70 (m, 2H), 2.16 (p, *J* = 7.3 Hz, 2H), 1.27 (d, *J* = 6.9 Hz, 1H). **HRMS**-ESI (m/z): $[M + H]^+$ calculated for $C_{14}H_{16}NO_3^+$, 246.1125; found, 246.1127.

(±) 6-(2-chlorobenzyl)-2,7-dimethyl-4a,9a-dihydro-2H-pyrano[3',2':4,5]furo[3,2-c]pyridin-5(6H)-one (15i); (±) 8-(2-chlorobenzyl)-1,7-dimethyl-8,9b-dihydro-1H-pyrano[3',4':4,5]furo[3,2-c]pyridin-9(4aH)-one (12i)

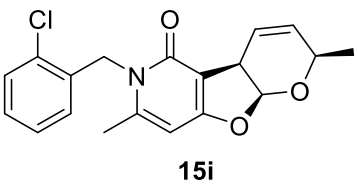

15i

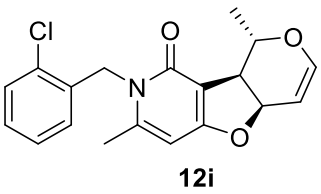

12i

According to GP2, **3b**-*trans* (67.8 mg, 0.22 mmol) was reacted with **2i** (28.0 mg, 0.11 mmol) at 110 °C for 1 hour. The catalyst was filtered off and the filtrate was diluted with DCM (10 mL) and washed with saturated $NaHCO_3$ solution (15 mL). The aqueous phase was extracted with DCM (3 x 10 mL) and the combined organic layers were washed with brine (50 mL), dried over $MgSO_4$ and concentrated in vacuo. The crude was purified by prep. HPLC to afford product **15i** (7.7 mg, 20%) and **12i** (1.0 mg, 3%) in separated fractions. **^{1}H-NMR** product **15i** (600 MHz, CD_2Cl_2): δ 7.41 (dd, *J* = 7.7, 1.5 Hz, 1H), 7.23 (td, *J* = 7.7, 1.8 Hz, 1H), 7.19 (td, *J* = 7.9, 1.5 Hz, 1H), 6.72 (d, *J* = 7.9 Hz, 1H), 6.26 (ddd, *J* = 10.3, 3.9, 2.0 Hz, 1H), 6.14 (d, *J* = 6.5 Hz, 1H), 5.95 (s, 1H), 5.88 (ddd, *J* = 10.3, 2.6, 1.8 Hz, 1H), 5.41 (d, *J* = 16.9 Hz, 1H), 5.23 (d, *J* = 16.9 Hz, 1H), 4.36 (qq, *J* = 6.9, 2.6 Hz, 1H), 3.80-3.73 (m, 1H), 2.19 (s, 3H), 1.29 (d, *J* = 6.9 Hz, 1H). **^{13}C-NMR** product **15i** (151 MHz, CD_2Cl_2): δ 165.5, 161.5, 149.3, 134.8, 132.7, 130.5, 129.9, 128.8, 128.7, 126.7, 122.1, 108.8, 105.7, 96.3, 68.1, 44.6, 38.5, 22.1, 21.2. **HRMS**-ESI (m/z) product **15i**: $[M + H]^+$ calculated for

$C_{19}H_{19}ClNO_3^+$, 344.1048; found, 344.1050. **^{1}H-NMR** product **12i** (600 MHz, CD_2Cl_2): δ 7.41 (dd, *J* = 7.7, 1.5 Hz, 1H), 7.23 (td, *J* = 7.7, 1.9 Hz, 1H), 7.19 (td, *J* = 7.5, 1.5 Hz, 1H), 6.79 (d, *J* = 6.2 Hz, 1H), 6.71 (dd, *J* = 7.5, 1.9 Hz, 1H), 5.92 (s, 1H), 5.40 (d, *J* = 16.9 Hz, 1H), 5.28 (d, *J* = 16.9 Hz, 1H), 5.26 (dd, *J* = 6.2, 4.7 Hz, 1H), 4.98 (ddd, *J* = 7.0, 4.7, 1.1 Hz, 1H), 3.53 (dq, *J* = 10.7, 6.3 Hz, 1H), 3.03 (dd, *J* = 10.7, 7.0 Hz, 1H), 2.19 (s, 3H), 1.46 (d, *J* = 6.3 Hz, 3H). **^{13}C-NMR** product **12i** (151 MHz, CD_2Cl_2): δ 168.4, 161.9, 150.0, 149.5, 134.9, 132.7, 129.9, 128.8, 127.7. 126.5, 107.6, 98.5, 96.3, 79.4, 74.0, 44.8, 44.0, 21.2, 19.8. **HRMS**-ESI (m/z) product **12i**: $[M + H]^+$ calculated for $C_{19}H_{19}ClNO_3^+$, 344.1048; found, 344.1045.

(±) 2,7-dimethyl-6-(thiophen-2-ylmethyl)-4a,9a-dihydro-2H-pyrano[3',2':4,5]furo[3,2-c]pyridin-5(6H)-one (15j); (±) 1,7-dimethyl-8-(thiophen-2-ylmethyl)-8,9b-dihydro-1H-pyrano[3',4':4,5]furo[3,2-c]pyridin-9(4aH)-one (12j)

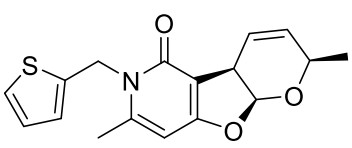

15j

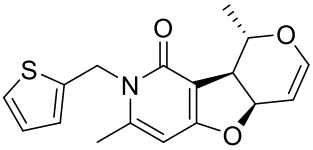

12j

According to GP2, **3b**-*trans* (66.5 mg, 0.22 mmol) was reacted **2l** (44.3 mg, 0.20 mmol) at 110 °C for 1 hour. After filtration over celite the crude was purified by MPLC (cyclohexane/EtOAc 1:0 to 0:1) to afford a mixture of products a and b. The product mixture was subjected for separation by prep. HPLC to afford pure product **15j** (9.8 mg, 16%) and **12j** (3.4 mg, 5%). **^{1}H-NMR** product **15j** (700 MHz, CD_2Cl_2): δ 7.24 (dd, *J* = 5.1, 1.2 Hz, 1H), 7.00 (dd, *J* = 3.5, 1.2 Hz, 1H), 6.94 (dd, *J* = 5.1, 3.5 Hz, 1H), 6.23 (ddd, *J* = 10.4, 3.8, 2.0 Hz, 1H), 6.15 (d, *J* = 6.6 Hz, 1H), 5.89 (ddd, *J* = 10.4, 2.7, 1.8 Hz, 1H), 5.97 (s, 1H), 5.47 (d, *J* = 15.5 Hz, 1H), 5.28 (d, *J* = 15.5 Hz, 1H), 4.37 (qq, *J* = 6.9, 2.7 Hz, 1H), 3.79-3.75 (m, 1H), 2.44 (s, 1H), 1.27 (d, *J* = 6.9 Hz, 3H). **^{13}C-NMR** product **15j** (176 MHz, CD_2Cl_2): δ 166.1, 161.5, 149.2, 139.4, 130.7, 127.0, 126.9, 126.1, 121.6, 109.4, 106.2, 97.3, 68.2, 43.0, 37.9, 22.3, 21.4. **HRMS**-ESI (m/z) product **15j**: $[M + H]^+$ calculated for $C_{17}H_{18}NO_3S^+$, 316.1002; found, 316.1016. **^{1}H-NMR** product **12j** (700 MHz, CD_2Cl_2): δ 7.24 (dd, *J* = 5.1, 1.2 Hz, 1H), 7.02 (dd, *J* = 3.5, 1.2 Hz, 1H), 6.95 (dd, *J* = 5.1, 3.5 Hz, 1H), 6.78 (d, *J* = 6.2 Hz, 1H), 5.94 (s, 1H), 5.42-5.37 (bs, 2H), 5.24 (dd, *J* = 6.2, 4.7 Hz, 1H), 4.96 (ddd, *J* = 6.8, 4.7, 1.1 Hz, 1H), 3.47 (dq, *J* = 10.8, 6.3 Hz, 1H), 3.05 (dd, *J* = 10.8, 6.8 Hz, 1H), 2.45 (s, 3H), 1.48 (d, *J* = 6.3 Hz, 3H). **^{13}C-NMR** product **12j** (176 MHz, CD_2Cl_2): δ 168.9, 161.9, 150.2, 149.5, 139.6, 127.0, 126.8, 126.2, 108.2, 98.3, 97.2, 79.7, 73.9, 43.7, 43.1, 21.5, 19.6. **HRMS**-ESI (m/z) product **12j**: $[M + H]^+$ calculated for $C_{17}H_{18}NO_3S^+$, 316.1002; found, 316.1004.

(±) 6,7-dimethyl-4a,9a-dihydro-2H-pyrano[3',2':4,5]furo[3,2-c]pyridine-3,5(4H,6H)-dione (26a)

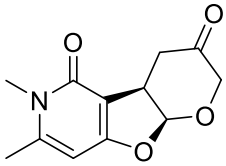

According to GP7, **4a** (50.0 mg, 0.32 mmol) was reacted with **2b** (44.6 mg, 0.32 mmol). Purification by MPLC (cyclohexane/EtOAc 1:0 to 0:1) afforded the product (4.9 mg, 7%). **^{1}H-NMR** (700 MHz, $CDCl_3$): δ 5.91 (s, 1H), 5.86 (bs, 1H), 3.87 (d, *J* = 11.7 Hz, 1H), 3.73 (dd, *J* = 11.7, 3.0 Hz, 1H), 3.55-3.45 (m, 4H), 2.56 (dd, *J* = 12.7, 3.0 Hz, 1H), 2.33 (s, 3H), 1.80 (dt, *J* = 12.7, 3.3 Hz, 1H). **^{13}C-NMR** (176 MHz, $CDCl_3$): δ 208.5, 163.6, 163.0, 146.3, 103.9, 101.0, 90.6, 69.5, 32.9, 31.5, 28.3, 21.2. **HRMS**-ESI (m/z): $[M + H]^+$ calculated for $C_{12}H_{14}NO_4^+$, 236.0917; found, 236.0917.

(±) 6-benzyl-7-methyl-4a,9a-dihydro-2H-pyrano[3',2':4,5]furo[3,2-c]pyridine-3,5(4H,6H)-dione (**26b)**

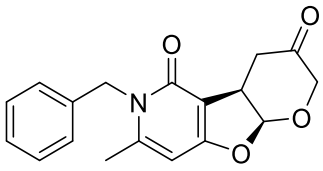

According to GP7, **4a** (100.0 mg, 0.64 mmol) was reacted with **2g** (137.9 mg, 0.64 mmol). Purification by MPLC (cyclohexane/EtOAc 1:0 to 0:1) afforded the product (56.0 mg, 30%). **^{1}H-NMR** (500 MHz, $CDCl_3$): δ 7.33-7.28 (m, 3H), 7.12-7.09 (m, 2H), 5.93 (s, 1H), 5.88 (bs, 1H), 5.33-5.29 (m, 2H), 3.89 (d, *J* = 11.6 Hz, 1H), 3.76 (dd, *J* = 11.6, 3.0 Hz, 1H), 3.55-3.52 (m, 1H), 2.59 (dd, *J* = 12.7, 3.0 Hz, 1H), 2.26 (s, 3H), 1.85 (dt, *J* = 12.7, 3.2 Hz, 1H). **^{13}C-NMR** (126 MHz, $CDCl_3$): δ 169.5, 164.1, 163.1, 146.8, 136.2, 129.0, 127.7, 126.5, 104.1, 101.8, 90.6, 69.4, 47.7, 32.9, 28.2, 20.8. **HRMS**-ESI (m/z): $[M + H]^+$ calculated for $C_{18}H_{18}NO_4^+$, 312.1230; found, 312.1234.

(±) 6-(4-fluorobenzyl)-7-methyl-4a,9a-dihydro-2H-pyrano[3',2':4,5]furo[3,2-c]pyridine-3,5(4H,6H)-dione (26c)

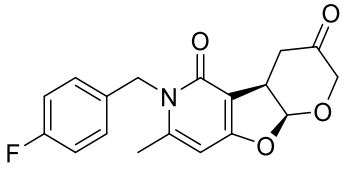

According to GP7, **4a** (50.0 mg, 0.32 mmol) was reacted with **2h** (74.7 mg, 0.32 mmol). Purification by MPLC (cyclohexane/EtOAc 1:0 to 0:1) afforded the product (24.5 mg, 23%). **^{1}H-NMR** (700 MHz, $CDCl_3$): δ 7.11 (dd, *J* = 8.6, 5.2 Hz, 2H), 7.00 (t, *J* = 8.6 Hz, 2H), 5.90-5.87 (m, 2H), 5.25 (bs, 2H), 3.88 (d, *J* = 11.6 Hz, 1H), 3.75 (dd, *J* = 11.6, 3.0 Hz, 1H), 3.52 (d, *J* = 2.5 Hz 1H), 2.57 (dd, *J* = 12.8, 3.0 Hz, 1H), 2.25 (s, 3H), 1.83 (dt, *J* = 12.8, 3.2 Hz, 1H). **^{13}C-NMR** (176 MHz, $CDCl_3$): δ 207.5, 169.4, 164.0, 163.0, 161.6, 146.4, 132.2, 128.4, 115.9, 104.1, 101.6, 90.7, 69.5, 46.9, 32.9, 28.2, 20.8. **HRMS**-ESI (m/z): $[M + H]^+$ calculated for $C_{18}H_{17}FNO_4^+$, 330.1136; found, 330.1141.

(±) 6-(4-methoxybenzyl)-7-methyl-4a,9a-dihydro-2H-pyrano[3',2':4,5]furo[3,2-c]pyridine-3,5(4H,6H)-dione (26d)

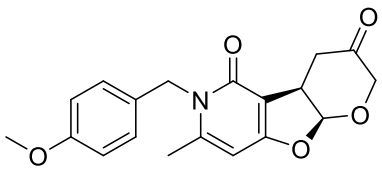

According to GP7, **4a** (50.0 mg, 0.32 mmol) was reacted with **2k** (78.5 mg, 0.32 mmol). Purification by MPLC (cyclohexane/EtOAc 1:0 to 0:1) afforded the product (33.3 mg, 30%). **^{1}H-NMR** (700 MHz, $CDCl_3$): δ 7.08 (d, *J* = 8.5 Hz, 2H), 6.83 (d, *J* = 8.5 Hz, 2H), 5.89-5.88 (m, 1H), 5.83 (s, 1H), 5.24-5.17 (m, 2H), 3.87 (d, *J* = 11.6 Hz, 1H), 3.77 (s, 3H), 3.74 (dd, *J* = 11.6, 3.0 Hz, 1H), 3.52 (q, *J* = 2.8 Hz, 1H), 2.56 (dd, *J* = 12.7, 3.0 Hz, 1H), 2.25 (s, 3H), 1.82 (dt, *J* = 12.7, 3.2 Hz, 1H). **^{13}C-NMR** (176 MHz, $CDCl_3$): δ 207.2, 163.5, 162.8, 158.9, 146.3, 128.5, 128.0, 114.2, 103.8, 100.9, 90.6. 69.4, 55.3, 46.8, 32.8, 28.2, 20.7. **HRMS**-ESI (m/z): $[M + H]^+$ calculated for $C_{19}H_{20}NO_5^+$, 342.1336; found, 342.1340.

(±) 7-methyl-4a,9a-dihydro-2H,5H-furo[2,3-b:4,5-c']dipyran-3,5(4H)-dione (26e)

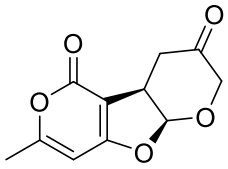

According to GP7, **4a** (50.0 mg, 0.32 mmol) was reacted with 4-hydroxy-6-methyl-2H-pyran-2-one (**1a**) (40.4 mg, 0.32 mmol). Purification by MPLC (cyclohexane/EtOAc 1:0 to 0:1) afforded the product (65.1 mg, 91%). **^{1}H-NMR** (500 MHz, $CDCl_3$): δ 6.38 (d, *J* = 8.3 Hz, 1H), 5.99 (s, 1H), 4.11 (d, *J* = 18.3 Hz, 1H), 4.04-3.97 (m, 1H), 3.90 (d, *J* = 18.3 Hz, 1H), 3.15 (dd, *J* = 16.1, 2.0 Hz, 1H), 2.80 (dd, *J* = 16.1, 6.3 Hz, 1H), 2.26 (s, 3H). **^{13}C-NMR** (126 MHz, $CDCl_3$): δ 207.1, 170.5, 167.4, 160.6, 105.4, 99.3, 94.8, 67.4, 36.5, 35.2, 20.7. **HRMS**-ESI (m/z): $[M + H]^+$ calculated for $C_{11}H_{11}O_5^+$, 223.0601; found, 223.0600.

(±) 2,6,7-trimethyl-4a,9a-dihydro-2H-pyrano[3',2':4,5]furo[3,2-c]pyridine-3,5(4H,6H)-dione (27a)

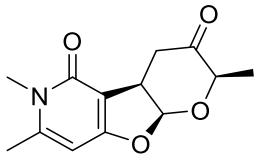

According to GP7, **4b** (53.0 mg, 0.31 mmol) was reacted with **2b** (43.3 mg, 0.31 mmol). Purification by MPLC (cyclohexane/EtOAc 1:0 to 0:1) afforded the product (66.9 mg, 86%). **^{1}H-NMR** (500 MHz, CD_2Cl_2): δ 6.15 (d, *J* = 7.8 Hz, 1H), 5.87 (s, 1H), 4.21 (q, *J* = 7.3 Hz, 1H), 3.90 (q, *J* = 6.7 Hz, 1H), 3.44 (s, 3H), 2.97 (dd, *J* = 14.7, 5.4 Hz, 1H), 2.89 (dd, *J* = 14.7, 6.7 Hz, 1H), 2.31 (s, 3H), 1.28 (d, *J* = 7.3 Hz, 3H).**^{13}C-NMR** (126 MHz, CD_2Cl_2): δ 211.1, 164.9, 161.8, 150.3, 106.5, 105.2, 94.6, 77.7, 39.8, 36.6, 30.6, 22.0, 17.7. **HRMS**-ESI (m/z): $[M + H]^+$ calculated for $C_{13}H_{16}NO_4^+$, 250.1074; found, 250.1073.

(±) 2,2,7-trimethyl-4a,9a-dihydro-2H-pyrano[3',2':4,5]furo[3,2-c]pyridine-3,5(4H,6H)-dione (28a)

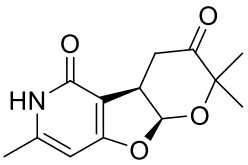

According to GP7, **4c** (50.0 mg, 0.27 mmol) was reacted with **2a** (34.0 mg, 0.27 mmol). Purification by MPLC (cyclohexane/EtOAc 1:0 to 0:1) afforded the product (3.5 mg, 5%). **^{1}H-NMR** (700 MHz, $CDCl_3$): δ 6.36 (d, *J* = 8.3 Hz, 1H), 5.93 (s, 1H), 4.10-4.06 (m, 1H), 3.08 (dt, *J* = 14.4, 2.5 Hz, 1H), 2.93 (dd, *J* = 14.4, 6.8 Hz, 1H), 2.34 (s, 3H), 1.36 (s, 3H), 1.27 (s, 3H). **^{13}C-NMR** (176 MHz, $CDCl_3$): δ 207.1, 186.6, 161.7, 149.3, 106.4, 105.4, 95.6, 82.4, 39.2, 34.6, 27.2, 25.6, 19.7. **HRMS**-ESI (m/z): $[M + H]^+$ calculated for $C_{13}H_{16}NO_4^+$, 250.1001; found, 250.1070.

(±) 2,2,6,7-tetramethyl-4a,9a-dihydro-2H-pyrano[3',2':4,5]furo[3,2-c]pyridine-3,5(4H,6H)-dione (28b)

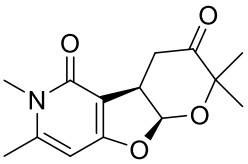

According to GP7, **4c** (50.0 mg, 0.27 mmol) was reacted with **2b** (37.7 mg, 0.27 mmol). Purification by MPLC (cyclohexane/EtOAc 1:0 to 0:1) afforded the product (18.2 mg, 25%). **^{1}H-NMR** (700 MHz, $CDCl_3$): δ 6.32 (d, *J* = 8.3 Hz, 1H), 5.94 (s, 1H), 4.12-4.08 (m, 1H), 3.50 (s, 3H), 3.06 (dd, *J* = 14.3, 2.9 Hz, 1H), 2.92 (dd, *J* = 14.3, 7.0 Hz, 1H), 2.35 (s, 3H), 1.34 (s, 3H), 1.26 (s, 3H). **^{13}C-NMR** (176 MHz, $CDCl_3$): δ 212.2, 165.7, 161.3, 150.1, 106.9, 105.2, 96.0, 82.3, 40.1, 34.5, 31.2, 27.2, 25.1, 21.9. **HRMS**-ESI (m/z): $[M + H]^+$ calculated for $C_{14}H_{18}NO_4^+$, 264.1230; found, 264.1235.

(±) 6-benzyl-2,2,7-trimethyl-4a,9a-dihydro-2H-pyrano[3',2':4,5]furo[3,2-c]pyridine-3,5(4H,6H)-dione (28c)

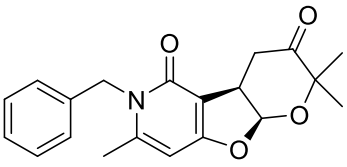

According to GP7, **4c** (50.0 mg, 0.27 mmol) was reacted with **2g** (58.4 mg, 0.27 mmol). Purification by MPLC (cyclohexane/EtOAc 1:0 to 0:1) afforded the product (31.2 mg, 34%). **^{1}H-NMR** (700 MHz, $CDCl_3$): δ 7.31 (t, *J* = 7.4 Hz, 2H), 7.24 (t, *J* = 7.4 Hz, 1H), 7.07 (d, *J* = 7.4 Hz, 2H), 6.36 (d, *J* = 8.3 Hz, 1H), 5.94 (s, 1H), 5.44 (d, *J* = 15.9 Hz, 1H), 5.19 (d, *J* = 15.9 Hz, 1H), 4.19-4.13 (m, 1H), 3.12 (dd, *J* = 14.2, 3.0 Hz, 1H), 2.95 (dd, *J* = 14.2, 6.9 Hz, 1H), 2.27 (s, 3H), 1.37 (s, 3H), 1.30 (s, 3H). **^{13}C-NMR** (176 MHz, $CDCl_3$): δ 212.2, 165.9, 161.3, 150.5, 136.2, 129.0, 127.6, 126.4, 107.0, 105.4, 96.5, 82.3, 47.2, 40.2, 34.4, 27.1, 25.0, 21.5. **HRMS**-ESI (m/z): $[M + H]^+$ calculated for $C_{20}H_{22}NO_4^+$, 340.1543; found, 340.1546.

(±) 6-(2-chlorobenzyl)-2,2,7-trimethyl-4a,9a-dihydro-2H-pyrano[3',2':4,5]furo[3,2-c]pyridine-3,5(4H,6H)-dione (28d)

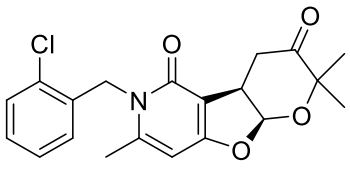

According to GP7, **4c** (50.0 mg, 0.27 mmol) was reacted with **2i** (67.8 mg, 0.27 mmol). Purification by MPLC (cyclohexane/EtOAc 1:0 to 0:1) afforded the product (19.9 mg, 20%). **^{1}H-NMR** (700 MHz, $CDCl_3$): δ 7.40-7.36 (m, 1H), 7.22-7.18 (m, 2H), 6.63 (dd, *J* = 7.0, 2.3 Hz, 1H), 6.38 (d, *J* = 8.3 Hz, 1H), 5.99 (s, 1H), 5.45 (d, *J* = 16.8 Hz, 1H), 5.33 (d, *J* = 16.8 Hz, 1H), 4.19-4.15 (m, 1H), 3.10 (dd, *J* = 14.2, 2.9 Hz, 1H), 2.96 (dd, *J* = 14.2, 6.9 Hz, 1H), 2.22 (s, 3H), 1.37 (s, 3H), 1.31 (s, 3H). **^{13}C-NMR** (176 MHz, $CDCl_3$): δ 212.2, 166.1, 161.3, 150.3, 133.5, 132.4, 129.7, 128.8, 127.7, 126.4, 107.0, 105.5, 96.7, 82.4, 44.8, 40.2, 34.4, 27.2, 25.0, 21.2. **HRMS**-ESI (m/z): $[M + H]^+$ calculated for $C_{20}H_{21}NO_4Cl^+$, 374.1154; found, 374.1156.

(±) 6-(4-fluorobenzyl)-2,2,7-trimethyl-4a,9a-dihydro-2H-pyrano[3',2':4,5]furo[3,2-c]pyridine-3,5(4H,6H)-dione (28e)

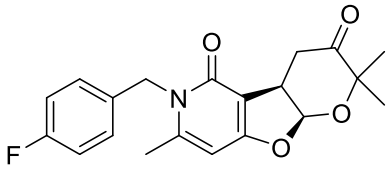

According to GP7, **4c** (50.0 mg, 0.27 mmol) was reacted with **2h** (63.3 mg, 0.27 mmol). Purification by MPLC (cyclohexane/EtOAc 1:0 to 0:1) afforded the product (15.6 mg, 16%). **^{1}H-NMR** (700 MHz, $CDCl_3$): δ 7.08 (dd, *J* = 8.7, 5.3 Hz, 2H), 7.00 (t, *J* = 8.7 Hz, 2H), 6.35 (d, *J* = 8.3 Hz, 1H), 5.92 (s, 1H), 5.37 (d, *J* = 15.7 Hz, 1H), 5.15 (d, *J* = 15.7 Hz, 1H), 4.17-4.12 (m, 1H), 3.12 (dd, *J* = 14.1, 2.9 Hz, 1H), 2.95 (dd, *J* = 14.1, 6.8 Hz, 1H), 2.27 (s, 3H), 1.37 (s, 3H), 1.29 (s, 3H). **^{13}C-NMR** (176 MHz, $CDCl_3$): δ 212.2, 165.8, 163.0, 161.6, 161.2, 150.1, 132.1, 128.3, 116.0, 106.9, 105.3, 96.3, 82.4, 46.5, 40.3, 34.4, 27.2, 24.8, 21.5. (700 MHz, $CDCl_3$): δ **HRMS**-ESI (m/z): $[M + H]^+$ calculated for $C_{20}H_{21}NO_4F^+$, 358.1449; found, 358.1453.

(±) 6-(4-methoxybenzyl)-2,2,7-trimethyl-4a,9a-dihydro-2H-pyrano[3',2':4,5]furo[3,2-c]pyridine-3,5(4H,6H)-dione (28f)

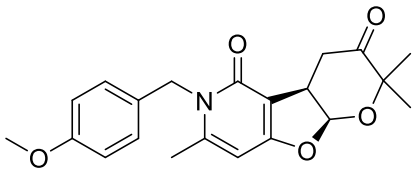

According to GP7, **4c** (50.0 mg, 0.27 mmol) was reacted with **2k** (66.6 mg, 0.27 mmol). Purification by MPLC (cyclohexane/EtOAc 1:0 to 0:1) afforded the product (9.3 mg, 9%). **^{1}H-NMR** (700 MHz, $CDCl_3$): δ 7.04 (d, *J* = 8.8 Hz, 2H), 6.85 (d, *J* = 8.8 Hz, 2H), 6.36 (d, *J* = 8.3 Hz, 1H), 5.94 (s, 1H), 5.36 (d, *J* = 15.7 Hz, 1H), 5.14 (d, *J* = 15.7 Hz, 1H), 4.19-4.14 (m, 1H), 3.77 (s, 3H), 3.11 (dd, *J* = 14.2, 2.9 Hz, 1H),

2.96 (dd, *J* = 14.2, 6.9 Hz, 1H), 2.30 (s, 3H), 1.37 (s, 3H), 1.29 (s, 3H). **^{13}C-NMR** (176 MHz, $CDCl_3$): δ 212.2, 166.0, 161.4, 159.2, 150.5, 128.1, 128.0, 114.5, 107.1, 105.4, 96.7, 82.4, 55.4, 46.8, 34.5, 27.2, 25.1, 21.6. (700 MHz, $CDCl_3$): δ **HRMS**-ESI (m/z): $[M + H]^+$ calculated for $C_{21}H_{23}NO_5Na^+$, 392.1468; found, 392.1457.

(±) *Tert*-butyl-7'-methyl-3',5'-dioxo-3',4',4a',5',6',9a'-hexahydrospiro[piperidine-4,2'-pyrano[3',2':4,5]furo[3,2-c]pyridine]-1-carboxylate (29a)

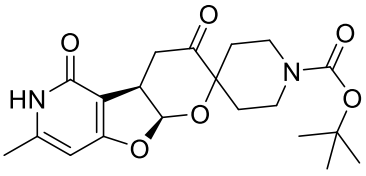

According to GP7, **4d** (97.6 mg, 0.30 mmol) was reacted with **2a** (37.5 mg, 0.30 mmol). Purification by prep. HPLC afforded the product (17.4 mg, 15%). **^{1}H-NMR** (700 MHz, $CDCl_3$): δ 6.47 (d, *J* = 8.4 Hz, 1H), 6.06 (s, 1H), 4.14 (td, *J* = 8.4, 7.3, 2.6 Hz, 1H), 4.00-3.81 (m, 2H), 3.25-3.13 (m, 2H), 3.07 (dd, *J* = 14.5, 2.6 Hz, 1H), 2.93 (dd, *J* = 14.5, 7.3 Hz, 1H), 2.40 (s, 3H), 1.81-1.63 (m, 3H), 1.46-1.42 (m, 10H). **^{13}C-NMR** (176 MHz, $CDCl_3$): δ 210.0, 169.4, 161.5, 154.8, 150.4, 106.5, 105.7, 97.0, 82.0, 80.0, 39.2, 38.8, 38.2, 34.6, 31.8, 28.6, 19.6. **HRMS**-ESI (m/z): $[M + H]^+$ calculated for $C_{20}H_{27}N_2O_6^+$, 391.1864; found, 391.1866.

(±) 7'-methyl-3',5'-dioxo-3',4',4a',5',6',9a'-hexahydrospiro[piperidine-4,2'-pyrano[3',2':4,5]furo[3,2-c]pyridin]-1-ium triflate (30a)

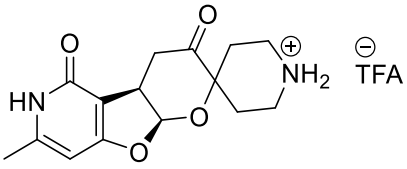

29a (17.4 mg, 0.04 mmol) was dissolved in DCM (3 mL) and cooled to 0 °C. HCl in dioxane (0.03 mL, 4 M, 10 equiv) was added slowly and the mixture was stirred at 0 °C for 1 hour and at room temperature for 30 min. The reaction was quenched by slow addition of saturated Na_2CO_3 solution at 0 °C and dilution with EtOAc (10 mL). The layers were separated and the aqueous phase was extracted with EtOAc (3 x 10 mL). The combined organic layers were washed with brine (20 mL), dried over $MgSO_4$ and concentrated in vacuo. Purification by prep. HPLC afforded the product (2.4 mg, 18%). **^{1}H-NMR** (700 MHz, DMSO): δ 11.34 (s, 1H), 8.72 (s, 1H), 8.34 (s, 1H), 6.45 (d, *J* = 8.3 Hz, 1H), 5.84 (s, 1H), 4.09-4.06 (m, 1H), 3.27-3.19 (m, 2H), 3.11-3.03 (m, 3H), 2.90 (dd, *J* = 14.4, 2.7 Hz, 1H), 2.14 (s, 3H), 2.01-1.97 (m, 1H), 1.93-1.87 (m, 1H), 1.78-1.73 (m, 1H), 1.55-1.51 (m, 1H). **^{13}C-NMR** (176 MHz, DMSO): δ 210.8, 165.9, 160.3, 149.1, 105.1, 103.9, 92.1, 78.0, 38.9, 38.7, 38.2, 34.4, 30.8, 28.2, 18.8. **HRMS**-ESI (m/z): $[M + H]^+$ calculated for $C_{15}H_{19}N_2O_4^+$, 291.1339; found, 291.1342.

(±) *Tert*-butyl-6',7'-dimethyl-3',5'-dioxo-3',4',4a',5',6',9a'-hexahydrospiro[piperidine-4,2'-pyrano[3',2':4,5]furo[3,2-c]pyridine]-1-carboxylate (29b)

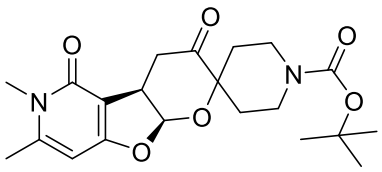

According to GP7, **4d** (116.9 mg, 0.36 mmol) was reacted with **2b** (50.0 mg, 0.36 mmol). Purification by MPLC (EtOAc/MeOH 1:0 to 9:1) afforded the product (39.8 mg, 27%). **^{1}H-NMR** (700 MHz, CD_2Cl_2): δ 6.35 (d, *J* = 8.6 Hz, 1H), 5.80 (s, 1H), 4.06 (ddd, *J* = 8.6, 6.8, 2.7 Hz, 1H), 3.90-3.88 (m, 2H), 3.41 (s, 3H), 3.22-3.10 (m, 2H), 3.08 (dd, *J* = 14.4, 2.7 Hz, 1H), 2.88 (dd, *J* = 14.4, 6.8 Hz, 1H), 2.30 (s, 3H), 1.71-1.64 (m, 2H), 1.59 (ddd, *J* = 13.4, 11.9, 4.7 Hz, 1H), 1.49-1.44 (m, 1H), 1.41 (s, 9H). **^{13}C-NMR** (176 MHz, CD_2Cl_2): δ 211.6, 165.1, 161.0, 154.8, 150.7, 105.8, 105.0, 94.4, 81.8, 79.6, 40.2, 39.6, 38.6, 35.1, 34.9, 31.9, 30.6, 28.5, 21.9. **HRMS**-ESI (m/z): $[M + H]^+$ calculated for $C_{21}H_{29}N_2O_6^+$, 405.2020; found, 405.2016.

(±) 6',7'-dimethyl-4a',9a'-dihydrospiro[piperidine-4,2'-pyrano[3',2':4,5]furo[3,2-c]pyridine]-3',5'(4'H,6'H)-dione (30b)

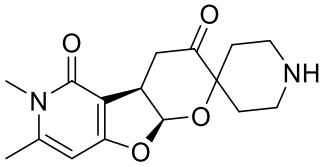

29b (19.5 mg, 0.05 mmol) was dissolved in dioxane (0.5 mL) and cooled to 0 °C. HCl in dioxane (0.12 mL, 4 M, 10 equiv) was added slowly and the mixture was stirred at 0 °C for 1 hour and at room temperature for 30 min. The reaction was quenched by slow addition of saturated Na_2CO_3 solution at 0 °C and diluted with EtOAc (10 mL). The layers were seperated and the aqueous phase was extracted with EtOAc (3 x 10 mL). The combined organic layers were washed with brine (20 mL), dried over $MgSO_4$ and concentrated in vacuo to afford the product (6.6 mg, 45%). **^{1}H-NMR** (700 MHz, MeOH-d_4): δ 6.46 (d, *J* = 8.3 Hz, 1H), 6.05 (s, 1H), 4.11-4.09 (m, 1H), 3.54- 3.47 (m, 4H), 3.21-3.11 (m, 1H), 3.04-2.98 (m, 2H), 2.87 (tt, *J* = 12.8, 4.0 Hz, 2H), 2.40 (s, 3H), 1.79-1.73 (m, 2H), 1.63 (ddd, *J* = 13.5, 11.9, 4.4 Hz, 1H), 1.52-1.45 (m, 1H). **^{13}C-NMR** (176 MHz, MeOH-d_4): δ 212.7, 167.1, 162.7, 152.7, 107.3, 106.5, 96.3, 82.4, 41.6, 41.4, 40.8, 35.8, 32.8, 31.2, 30.7, 21.5. **HRMS**-ESI (m/z): $[M + H]^+$ calculated for $C_{16}H_{20}N_2O_4^+$, 305.1496; found, 305.1501.

(±) *Tert*-butyl-6'-isopentyl-7'-methyl-3',5'-dioxo-3',4',4a',5',6',9a'-hexahydrospiro[piperidine-4,2'-pyrano[3',2':4,5]furo[3,2-c]pyridine]-1-carboxylate (29c)

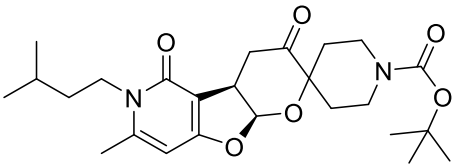

According to GP7, **4d** (97.6 mg, 0.30 mmol) was reacted with **2d** (58.6 mg, 0.30 mmol). Purification by MPLC (cyclohexane/EtOAc 1:0 to 0:1) afforded the product (100.0 mg, 72%). **^{1}H-NMR** (700 MHz, CD_2Cl_2): δ 6.34 (d, *J* = 8.4 Hz, 1H), 5.77 (s, 1H), 4.09-4.02 (m, 2H), 3.91-3.77 (m, 3H), 3.23-3.10 (m, 2H), 3.08 (dd, *J* = 14.3, 2.7 Hz, 1H), 2.87 (dd, *J* = 14.4, 6.7 Hz, 1H), 2.33 (s, 3H), 1.71-1.64 (m, 2H), 1.62-1.56 (m, 2H), 1.54-1.43 (m 3H), 1.42 (s, 9H), 0.97 (dd, *J* = 6.6, 1.6 Hz, 6H). **^{13}C-NMR** (176 MHz, CD_2Cl_2): δ 211.6, 165.0, 160.6, 154.8, 149.9, 106.1, 105.0, 94.6, 81.8, 79.6, 42.9, 40.3, 39.6, 38.6, 37.8, 35.0, 34.8, 32.0, 28.5, 27.0, 22.6, 21.3. **HRMS**-ESI (m/z): $[M + H]^+$ calculated for $C_{25}H_{37}N_2O_6^+$, 461.2646; found, 461.2638.

(±) 6'-isopentyl-7'-methyl-4a',9a'-dihydrospiro[piperidine-4,2'-pyrano[3',2':4,5]furo[3,2-c]pyridine]-3',5'(4'H,6'H)-dione (30c)

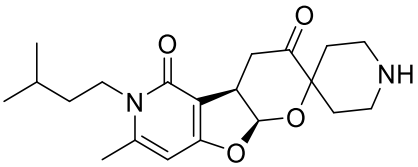

29c (90.0 mg, 0.20 mmol) was dissolved in DCM (3 mL) and cooled to 0 °C. TFA (0.15 mL, 10 equiv) was added slowly and the mixture was stirred at 0 °C for 1 hour and at room temperature for 30 min. The reaction was quenched by slow addition of saturated Na_2CO_3 solution at 0 °C and dilution with EtOAc (10 mL). The layers were separated and the aqueous phase was extracted with EtOAc (3 x 10 mL). The combined organic layers were washed with brine (20 mL), dried over $MgSO_4$ and concentrated in vacuo to afford the product (61.0 mg, 87%). **^{1}H-NMR** (700 MHz, CD_2Cl_2): δ 6.33 (d, *J* = 8.3 Hz, 1H), 5.76 (s, 1H), 4.09-3.99 (m, 2H), 3.83-3.78 (m, 1H), 3.03 (dd, *J* = 14.2, 2.9 Hz, 1H), 3.01-2.95 (m, 2H), 2.89-2.83 (m, 2H), 2.33 (s, 3H), 1.72-1.65 (m, 3H), 1.59 (ddd, *J* = 13.4, 11.5, 4.5 Hz, 1H), 1.53-1.40 (m, 3H), 0.97 (dd, *J* = 6.6, 1.6 Hz, 6H). **^{13}C-NMR** (176 MHz, CD_2Cl_2): δ 211.7, 165.1, 160.7, 149.8, 106.3, 105.4, 94.7, 82.4, 42.9. 41.6, 41.4, 40.4, 37.8, 35.9, 34.8, 32.9, 27.0, 22.6, 21.3. **HRMS**-ESI (m/z): $[M + H]^+$ calculated for $C_{20}H_{29}N_2O_4^+$, 361.2122; found, 361.2119.

(±) *Tert*-butyl 6'-benzyl-7'-methyl-3',5'-dioxo-3',4',4a',5',6',9a'-hexahydrospiro[piperidine-4,2'-pyrano[3',2':4,5]furo[3,2-c]pyridine]-1-carboxylate (29d)

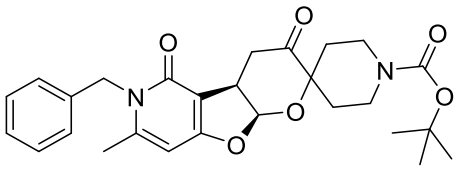

According to GP7, **4d** (97.6 mg, 0.30 mmol) was reacted with **2g** (64.6 mg, 0.30 mmol). Purification by MPLC (cyclohexane/EtOAc 1:0 to 0:1) afforded the product (94.7 mg, 66%). **^{1}H-NMR** (500 MHz, CD_2Cl_2): δ 7.35-7.20 (m, 3H), 7.10-7.02 (m, 2H), 6.40 (d, *J* = 8.3 Hz, 1H), 5.84 (s, 1H), 5.40 (d, *J* = 16.1 Hz, 1H), 5.10 (d, *J* = 16.1 Hz, 1H), 4.16-4.10 (m, 1H), 3.94-3.77 (m, 2H), 3.26-3.08 (m, 3H). 2.92 (dd, *J* = 14.5, 6.5 Hz, 1H), 2.22 (s, 3H), 1.93-1.55 (m, 4H), 1.42 (s, 9H). **^{13}C-NMR** (126 MHz, CD_2Cl_2): δ 211.5, 165.5, 160.1, 154.8, 150.8, 137.2, 129.1, 127.6, 126.5, 106.2, 105.2, 95.2, 81.9, 79.6, 46.7, 40.3, 39.5, 38.7, 35.0, 34.8, 31.8, 28.5, 21.6. **HRMS**-ESI (m/z): $[M + H]^+$ calculated for $C_{27}H_{33}N_2O_6^+$; 481.2333; found, 481.2328.

(±) 6'-benzyl-7'-methyl-4a',9a'-dihydrospiro[piperidine-4,2'-pyrano[3',2':4,5]furo[3,2-c]pyridine]-3',5'(4'H,6'H)-dione (30d)

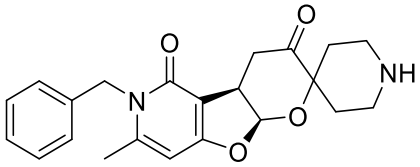

29d (90.2 mg, 0.19 mmol) was dissolved in DCM (3 mL) and cooled to 0 °C. TFA (0.14 mL, 10 equiv) was added slowly and the mixture was stirred at 0 °C for 1 hour and at room temperature for 30 min. The reaction was quenched by slow addition of saturated Na_2CO_3 solution at 0 °C and dilution with EtOAc (10 mL). The layers were separated and the aqueous phase was extracted with EtOAc (3 x 10 mL). The combined organic layers were washed with brine (20 mL), dried over $MgSO_4$ and concentrated in vacuo to afford the product (60.1 mg, 84%). **^{1}H-NMR** (700 MHz, DMSO): δ 7.32 (t, *J* = 7.5 Hz, 2H), 7.25 (t, *J* = 7.5 Hz, 1H), 7.04 (d, *J* = 7.5 Hz, 2H), 6.48 (d, *J* = 8.3 Hz, 0H), 6.06 (s, 1H), 5.32 (d, *J* = 15.9 Hz, 1H), 5.16 (d, *J* = 15.9 Hz, 1H), 4.12-4.08 (m, 1H), 2.99 (dd, *J* = 14.1, 6.7 Hz, 1H), 2.86 (dd, *J* = 14.1, 2.7 Hz, 1H), 2.83-2.71 (m, 4H), 2.21 (s, 3H9, 1.67 (dd, *J* = 13.1, 2.9 Hz, 1H), 1.61 (ddd, *J* = 14.0, 11.4, 4.4 Hz, 1H), 1.45 (td, *J* = 12.4, 4.5 Hz, 1H), 1.38-1.33 (m, 1H). **^{13}C-NMR** (176 MHz, DMSO): δ 212.0, 165.0, 160.4, 160.0, 151.0, 137.7, 129.1, 127.5, 126.5, 105.9, 105.0, 94.8, 82.0, 45.9, 41.2, 40.9, 39.5, 35.2, 34.6, 32.3, 21.0. **HRMS**-ESI (m/z): $[M + H]^+$ calculated for $C_{22}H_{25}N_2O_4^+$, 381.1809; found, 381.1809.

(±) *Tert*-butyl-6'-(4-fluorobenzyl)-7'-methyl-3',5'-dioxo-3',4',4a',5',6',9a'-hexahydrospiro[piperidine-4,2'-pyrano[3',2':4,5]furo[3,2-c]pyridine]-1-carboxylate (29e)

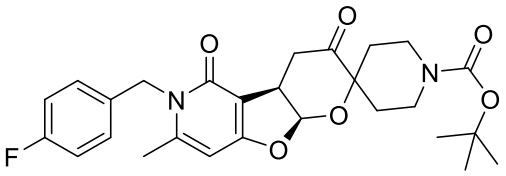

According to GP7, **4d** (97.6 mg, 0.30 mmol) was reacted with **2h** (70.0 mg, 0.30 mmol). Purification by MPLC (cyclohexane/EtOAc 1:0 to 0:1) afforded the product (119.8 mg, 80%). **^{1}H-NMR** (500 MHz, CD_2Cl_2): δ 7.10-6.99 (m, 4H), 6.40 (d, *J* = 8.0 Hz, 1H), 5.83 (s, 1H), 5.36 (d, *J* = 15.5 Hz, 1H), 5.07 (d, *J* = 15.5 Hz, 1H), 4.12 (ddd, *J* = 8.0, 6.5, 2.7 Hz, 1H), 3.95-3.79 (m, 2H), 3.25-3.13 (m, 2H), 3.12 (dd, *J* = 14.2, 2.7 Hz, 1H), 2.92 (dd, *J* = 14.2, 6.5 Hz, 1H), 2.23 (s, 3H), 1.77-1.57 (m, 3H), 1.51-1.46 (m, 1H), 1.42 (s, 9H). **^{13}C-NMR** (126 MHz, CD_2Cl_2): δ 211.2, 165.3, 163.1, 160.7, 154.4, 150.4, 132.9, 128.2, 115.6, 106.0, 105.0, 95.0, 81.7, 79.3, 45.9, 40.1, 38.7, 34.9, 34.5, 31.8, 28.2, 21.3. **HRMS**-ESI (m/z): $[M + H]^+$ calculated for $C_{27}H_{32}FN_2O_6^+$, 499.2239; found, 499.2236.

(±) 6'-(4-fluorobenzyl)-7'-methyl-4a',9a'-dihydrospiro[piperidine-4,2'-pyrano[3',2':4,5]furo[3,2-c]pyridine]-3',5'(4'H,6'H)-dione (30e)

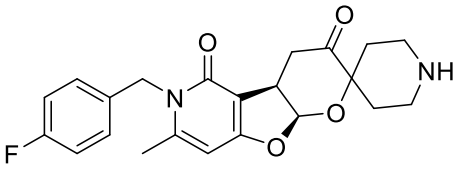

29e (119.8 mg, 0.24 mmol) was dissolved in DCM (3 mL) and cooled to 0 °C. TFA (0.19 mL, 10 equiv) was added slowly and the mixture was stirred at 0 °C for 1 hour and at room temperature for 30 min. The reaction was quenched by slow addition of saturated Na_2CO_3 solution at 0 °C and dilution with EtOAc (10 mL). The layers were separated and the aqueous phase was extracted with EtOAc (3 x 10 mL). The combined organic layers were washed with brine (20 mL), dried over $MgSO_4$ and concentrated in vacuo to afford the product (57.8 mg, 60%). **^{1}H-NMR** (500 MHz, DMSO): δ 7.18-7.08 (m, 4H), 6.47 (d, *J* = 8.7 Hz, 1H), 6.07 (s, 1H), 5.31 (d, *J* = 15.9 Hz, 1H), 5.11 (d, *J* = 15.9 Hz, 1H), 4.10 (ddd, *J* = 8.7, 6.8, 2.7 Hz, 1H), 3.00 (dd, *J* = 14.1, 6.8 Hz, 1H), 2.89-2.71 (m, 5H), 2.22 (s, 3H), 1.67 (dq, *J* = 13.3, 2.9 Hz, 1H), 1.61 (ddd, *J* = 13.6, 11.2, 4.7 Hz, 1H), 1.44 (ddd, *J* = 13.2, 11.4, 4.7 Hz, 1H), 1.35 (dq, *J* = 13.5, 2.9 Hz, 1H). **^{13}C-NMR** (126 MHz, DMSO): δ 211.6, 164.6, 162.2, 160.2, 160.0, 150.5, 133.4, 128.2, 115.5, 105.5, 104.5, 94.5, 81.5, 44.8, 40.7, 40.5, 39.0, 34.7, 34.2, 31.8. 20.5. **HRMS**-ESI (m/z): $[M + H]^+$ calculated for $C_{22}H_{24}FN_2O_4^+$, 399.1715; found, 399.1706.

(±) *Tert*-butyl-6'-(4-methoxybenzyl)-7'-methyl-3',5'-dioxo-3',4',4a',5',6',9a'-hexahydrospiro[piperidine-4,2'-pyrano[3',2':4,5]furo[3,2-c]pyridine]-1-carboxylate (29f)

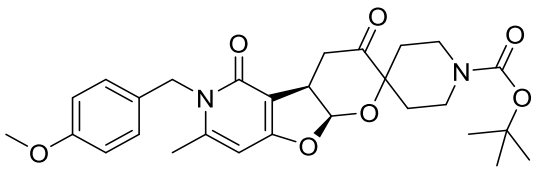

According to GP7, **4d** (97.6 mg, 0.30 mmol) was reacted with **2k** (73.6 mg, 0.30 mmol). Purification by MPLC (cyclohexane/EtOAc 1:0 to 0:1) afforded the product (65.0 mg, 42%). **^{1}H-NMR** (500 MHz, CD_2Cl_2): δ 7.01 (d, *J* = 8. Hz, 2H), 6.84 (d, *J* = 8.7 Hz, 2H), 6.39 (d, *J* = 8.4 Hz, 1H), 5.81 (s, 1H), 5.31 (d, *J* = 15.2 Hz, 1H), 5.03 (d, *J* = 15.2 Hz, 1H), 4.12 (ddd, *J* = 8.4, 6.6, 2.67Hz, 1H), 3.94-3.80 (m, 2H), 3.76 (s, 3H), 3.25-3.14 (m, 2H), 3.13 (dd, *J* = 14.2, 2.7 Hz, 1H), 2.91 (dd, *J* = 14.2, 6.6 Hz, 1H), 2.24 (s, 3H), 1.77-1.57 (m, 3H), 1.52-1.45 (m, 1H), 1.42 (s, 9H). **^{13}C-NMR** (126 MHz, CD_2Cl_2): δ 211.5, 165.4, 161.0, 159.3, 154.8, 150.8, 129.2, 128.0, 114.4, 106.1, 105.1, 95.1, 81.9, 79.6, 55.6, 46.2, 40.3, 39.1, 34.8, 31.8, 28.5, 21.6. **HRMS**-ESI (m/z): $[M + H]^+$ calculated for $C_{28}H_{35}N_2O_7^+$, 511.2439; found, 511.2436.

(±) 6'-(4-methoxybenzyl)-7'-methyl-4a',9a'-dihydrospiro[piperidine-4,2'-pyrano[3',2':4,5]furo[3,2-c]pyridine]-3',5'(4'H,6'H)-dione (30f)

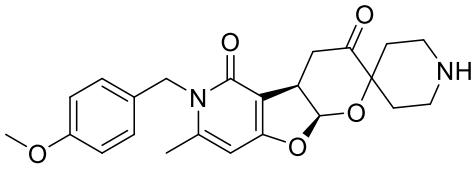

29f (55.0 mg, 0.11 mmol) was dissolved in DCM (3 mL) and cooled to 0 °C. TFA (0.08 mL, 10 equiv) was added slowly and the mixture was stirred at 0 °C for 1 hour and at room temperature for 30 min. The reaction was quenched by slow addition of saturated Na_2CO_3 solution at 0 °C and dilution with EtOAc (10 mL). The layers were separated and the aqueous phase was extracted with EtOAc (3 x 10 mL). The combined organic layers were washed with brine (20 mL), dried over $MgSO_4$ and concentrated in vacuo to afford the product (21.0 mg, 48%). **^{1}H-NMR** (500 MHz, DMSO): δ 7.01 (d, *J* = 8.8 Hz, 2H), 6.87 (d, *J* = 8.8 Hz, 2H), 6.49 (d, *J* = 8.7 Hz, 1H), 6.04 (s, 1H), 5.25 (d, *J* = 15.5 Hz, 1H), 5.08 (d, *J* = 15.5 Hz, 1H), 4.13 (ddd, *J* = 8.7, 6.9, 2.7 Hz, 1H), 3.72 (s, 3H), 3.05 (dd, *J* = 14.2, 6.9 Hz, 1H), 3.01-2.88 (m, 5H), 2.23 (s, 3H), 1.87-1.72 (m, 2H), 1.64-1.57 (m, 1H), 1.47-1.41 (m, 1H). **^{13}C-NMR** (126 MHz, DMSO): δ 211.6, 164.8, 160.4, 158.8, 151.2, 129.6, 128.1, 114.6, 105.9, 104.9, 94.7, 80.3, 55.5, 45.4, 40.5, 39.5, 34.6, 33.5, 30.4,

(±) *Tert*-butyl-7'-methyl-3',5'-dioxo-6'-(thiophen-2-ylmethyl)-3',4',4a',5',6',9a'-hexahydrospiro[piperidine-4,2'-pyrano[3',2':4,5]furo[3,2-c]pyridine]-1-carboxylate (29g)

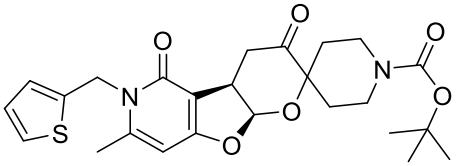

According to GP7, **4d** (97.6 mg, 0.30 mmol) was reacted with **2l** (66.4 mg, 0.30 mmol). Purification by MPLC (cyclohexane/EtOAc 1:0 to 0:1) afforded the product (92.5 mg, 64%). **^{1}H-NMR** (500 MHz, CD_2Cl_2): δ 7.25-7.20 (m, 1H), 6.95-6.92 (m, 2H), 6.37 (d, *J* = 8.4 Hz, 1H), 5.80 (s, 1H), 5.47 (d, *J* = 15.5 Hz, 1H), 5.18 (d, *J* = 15.5 Hz, 1H), 4.11 (ddd, *J* = 8.4, 6.7, 2.6 Hz, 1H), 3.95-3.78 (m, 2H), 3.24-3.14 (m, 2H), 3.13 (dd, *J* = 14.3, 2.6 Hz, 1H), 2.91 (dd, *J* = 14.3, 6.7 Hz, 1H), 2.38 (s, 3H), 1.75-1.65 (m, 2H), 1.63-1.59 (m 2H), 1.42 (s, 9H). **^{13}C-NMR** (126 MHz, CD_2Cl_2): δ 211.4, 165.5, 160.6, 154.8, 150.2, 139.8, 126.9, 126.6, 125.9, 106.2, 105.2, 95.2, 81.9, 79.6, 42.5, 40.2, 39.5, 35.0, 34.8, 31.9, 28.5, 21.4. **HRMS**-ESI (m/z): $[M + H]^+$ calculated for $C_{25}H_{31}N_2O_6S^+$, 487.1897; found, 487.1894.

(±) 7'-methyl-6'-(thiophen-2-ylmethyl)-4a',9a'-dihydrospiro[piperidine-4,2'-pyrano[3',2':4,5]furo[3,2-c]pyridine]-3',5'(4'H,6'H)-dione (30g)

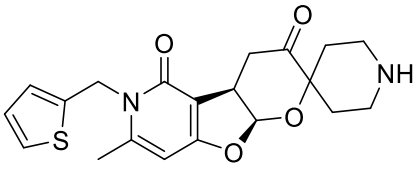

29g (80.0 mg, 0.16 mmol) was dissolved in DCM (3 mL) and cooled to 0 °C. TFA (0.13 mL, 10 equiv) was added slowly and the mixture was stirred at 0 °C for 1 hour and at room temperature for 30 min. The reaction was quenched by slow addition of saturated Na_2CO_3 solution at 0 °C and dilution with EtOAc (10 mL). The layers were separated and the aqueous phase was extracted with EtOAc (3 x 10 mL). The combined organic layers were washed with brine (20 mL), dried over $MgSO_4$ and concentrated in vacuo to afford the product (51.0 mg, 80%). **^{1}H-NMR** (600 MHz, DMSO): δ 8.74 (s, 1H), 8.48 (s, 1H), 7.43 (dd, *J* = 5.1, 1.2 Hz, 1H), 7.02 (dd, *J* = 3.5, 1.2 Hz, 1H), 6.97 (dd, *J* = 5.1, 3.5 Hz, 1H), 6.50 (d, *J* = 8.3 Hz, 1H), 6.05 (s, 1H), 5.40 (d, *J* = 15.6 Hz, 1H), 5.27 (d, *J* = 15.6 Hz, 1H), 4.20-4.14 (m, 1H), 3.28-3.19 (m, 2H), 3.16-3.01 (m, 3H), 2.95 (dd, *J* = 14.4, 2.7 Hz, 1H), 2.39 (s, 3H), 2.01 (dq, *J* = 14.4, 3.1 Hz, 1H), 1.90 (ddd, *J* = 14.6, 12.5, 4.2 Hz, 1H), 1.76 (ddd, *J* = 14.2, 12.4, 4.5 Hz, 1H), 1.53 (dq, *J* = 14.7, 3.0 Hz, 1H). **^{13}C-NMR** (151 MHz, DMSO): δ 210.9, 164.8, 160.0, 150.9, 139.9, 127.1, 127.0, 126.6, 105.8, 104.7, 94.7, 78.6, 41.9, 39.3, 39.1, 34.8, 31.3, 28.8, 20.9. **HRMS**-ESI (m/z): $[M + H]^+$ calculated for $C_{20}H_{23}N_2O_4S^+$, 387.1373; found, 387.1375.

(±) *Tert*-butyl-7'-methyl-3',5'-dioxo-6'-(pyridin-2-ylmethyl)-3',4',4a',5',6',9a'-hexahydrospiro[piperidine-4,2'-pyrano[3',2':4,5]furo[3,2-c]pyridine]-1-carboxylate (29h)

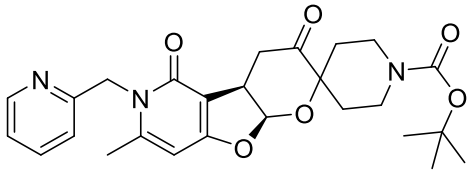

According to GP7, **4d** (97.6 mg, 0.30 mmol) was reacted with **2m** (64.9 mg, 0.30 mmol). Purification by MPLC (cyclohexane/EtOAc 4:1 to 0:1) afforded the product (79.2 mg, 55%). **^{1}H-NMR** (700 MHz, CD_2Cl_2): δ 8.48 (dd, *J* = 4.9, 1.8 Hz, 1H), 7.65 (td, *J* = 7.7, 1.8 Hz, 1H), 7.18 (dd, *J* = 7.7, 4.9 Hz, 1H), 7.10 (d, *J* = 7.7 Hz, 1H), 6.38 (d, *J* = 8.6 Hz, 1H), 5.85 (s, 1H), 5.47 (d, *J* = 16.0 Hz, 1H), 5.15 (d, *J* = 16.0 Hz, 1H), 4.09 (ddd, *J* = 8.6, 6.7, 2.7 Hz, 1H), 3.94-3.77 (m, 2H), 3.25-3.10 (m, 2H), 3.09 (dd, *J* = 14.3, 2.7 Hz, 1H), 2.89 (dd, *J* = 14.3, 6.7 Hz, 1H), 2.32 (s, 3H), 1.77-1.57 (m, 3H), 1.53-1.48 (m, 1H), 1.42 (s, 9H). **^{13}C-NMR** (176 MHz, CD_2Cl_2): δ 211.5, 165.6, 160.8, 157.0, 154.8, 151.2, 149.7, 137.2, 122.8, 121.8, 106.0, 105.2, 95.0, 81.9, 79.6, 48.8, 40.3, 39.7, 38.7, 35.0, 34.8, 31.9, 28.5, 21.9. **HRMS**-ESI (m/z): $[M + H]^+$ calculated for $C_{26}H_{32}N_3O_6^+$, 482.2286; found, 482.2278.

(±) 7'-methyl-3',5'-dioxo-6'-(pyridin-2-ylmethyl)-3',4',4a',5',6',9a'-hexahydrospiro[piperidine-4,2'-pyrano[3',2':4,5]furo[3,2-c]pyridin]-1-ium triflate (30h)

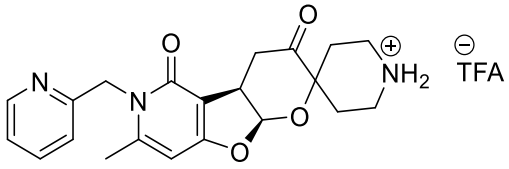

29h (79.4 mg, 0.14 mmol) was dissolved in DCM (3 mL) and cooled to 0 °C. HCl in dioxane (0.13 mL, 4 M, 10 equiv) was added slowly and the mixture was stirred at 0 °C for 1 hour and at room temperature for 30 min. The reaction was quenched by slow addition of saturated Na_2CO_3 solution at 0 °C and dilution with EtOAc (10 mL). The layers were separated and the aqueous phase was extracted with EtOAc (3 x 10 mL). The combined organic layers were washed with brine (20 mL), dried over $MgSO_4$ and concentrated in vacuo. Purification by prep. HPLC afforded the product (41.8 mg, 66%). **^{1}H-NMR** (700 MHz, DMSO): δ 8.72 (s, 1H), 8.53 (s, 1H), 8.48 (d, *J* = 4.9 Hz, 1H), 7.77 (td, *J* = 7.7, 1.9 Hz, 1H), 7.30 (dd, *J* = 7.7, 4.9 Hz, 1H), 7.13 (d, *J* = 7.7 Hz, 1H), 6.49 (d, *J* = 8.3 Hz, 1H), 6.09 (s, 1H), 5.42 (d, *J* = 16.3 Hz, 1H), 5.16 (d, *J* = 16.3 Hz, 1H), 4.14-4.11 (m, 1H), 3.28-3.19 (m, 2H), 3.13-3.04 (m, 3H), 2.88 (dd, *J* = 14.4, 2.8 Hz, 1H), 2.30 (s, 3H), 2.00 (dq, *J* = 14.6, 3.3 Hz, 1H), 1.93 (ddd, *J* = 16.7, 13.4, 3.7 Hz, 1H), 1.77 (ddd, *J* = 16.5, 12.9, 4.2 Hz, 1H), 1.59-1.55 (m, 1H). **^{13}C-NMR** (176 MHz, DMSO): δ 210.6, 164.4, 159.7, 156.1, 151.3, 148.9, 137.2, 122.5, 121.2, 105.1, 104.2, 94.0, 78.1, 47.5, 40.0, 38.8, 38.6, 34.3, 30.7,

28.4, 20.9. **HRMS**-ESI (m/z): $[M + H]^+$ calculated for $C_{21}H_{24}N_3O_4^+$, 382.1761; found, 382.1762.

(±) *Tert*-butyl-7'-methyl-3',5'-dioxo-6'-(pyridin-4-ylmethyl)-3',4',4a',5',6',9a'-hexahydrospiro[piperidine-4,2'-pyrano[3',2':4,5]furo[3,2-c]pyridine]-1-carboxylate (29i)

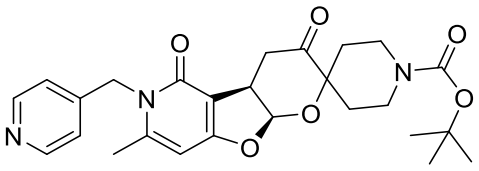

According to GP7, **4d** (97.6 mg, 0.30 mmol) was reacted with **2n** (64.8 mg, 0.30 mmol). Purification by MPLC (cyclohexane/EtOAc 1:0 to 0:1) afforded the product (95.0 mg, 66%). **^{1}H-NMR** (700 MHz, CD_2Cl_2): δ 8.74 (d, *J* = 6.4 Hz, 2H), 7.45 (d, *J* = 6.4 Hz, 2H), 6.45 (d, *J* = 8.2 Hz, 1H), 5.52 (d, *J* = 17.2 Hz, 1H), 5.30 (d, *J* = 17.2 Hz, 1H), 4.15 (ddd, *J* = 8.2, 6.6, 2.6 Hz, 1H), 3.93-3.81 (m, 2H), 3.25-3.13 (m, 2H), 3.06 (dd, *J* = 14.2, 2.6 Hz, 1H), 2.94 (dd, *J* = 14.2, 6.6 Hz, 1H), 2.22 (s, 3H), 1.77 (ddd, *J* = 14.1, 11.9, 4.5 Hz, 1H), 1.72 (d, *J* = 13.2 Hz, 1H), 1.60 (ddd, *J* = 13.4, 11.8, 4.7 Hz, 1H), 1.51-1.47 (m, 1H), 1.43 (s, 9H). **^{13}C-NMR** (176 MHz, CD_2Cl_2): δ 210.8, 165.8, 160.2, 154.7, 154.4, 149.3, 143.5, 123.7, 106.2, 105.2, 96.1, 81.7, 79.3, 46.0, 39.9, 38.4, 34.7, 34.3, 31.5, 28.1, 21.2. **HRMS**-ESI (m/z): $[M + H]^+$ calculated for $C_{26}H_{32}N_3O_6^+$, 482.2286; found, 482.2274.

(±) 7'-methyl-6'-(pyridin-4-ylmethyl)-4a',9a'-dihydrospiro[piperidine-4,2'-pyrano[3',2':4,5]furo[3,2-c]pyridine]-3',5'(4'H,6'H)-dione (30i)

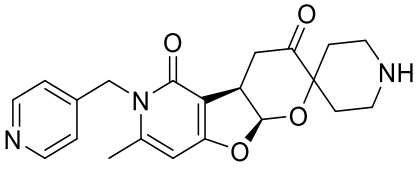

29i (87.1 mg, 0.18 mmol) was dissolved in DCM (2 mL) and cooled to 0 °C. TFA (0.14 mL, 10 equiv) was added slowly and the mixture was stirred at 0 °C for 1 hour and at room temperature for 30 min. The reaction was quenched by slow addition of saturated Na_2CO_3 solution at 0 °C and dilution with EtOAc (10 mL). The layers were separated and the aqueous phase was extracted with EtOAc (3 x 10 mL). The combined organic layers were washed with brine (20 mL), dried over $MgSO_4$ and concentrated in vacuo to afford the product (50.0 mg, 72%). **^{1}H-NMR** (500 MHz, DMSO): δ 8.51-8.49 (m, 2H), 7.02-6.99 (m, 2H), 6.49 (d, *J* = 8.6 Hz, 1H), 6.12 (s, 1H), 5.34 (d, *J* = 16.9 Hz, 1H), 5.17 (d, *J* = 17.0 Hz, 1H), 4.11 (ddd, *J* = 8.6, 7.0, 2.7 Hz, 1H), 2.99 (dd, *J* = 14.0, 6.7 Hz, 1H), 2.86-2.70 (m, 5H), 2.20 (s, 3H), 1.70-1.58 (m, 2H), 1.44 (td, *J* = 12.8, 12.3, 4.6 Hz, 1H), 1.38-1.32 (m, 1H). **^{13}C-NMR** (126 MHz, DMSO): δ 211.6, 164.8, 159.8, 150.4, 149.9, 146.4, 121.1, 105.5, 104.6, 94.6, 81.6, 44.8, 40.8, 40.5, 39.0, 34.8, 34.2, 31.9, 20.5. **HRMS**-ESI (m/z): $[M + H]^+$ calculated for $C_{21}H_{24}N_3O_4^+$, 382.1761; found, 382.1761.

(±) *Tert*-butyl-6'-((2-chloropyridin-4-yl)methyl)-7'-methyl-3',5'-dioxo-3',4',4a',5',6',9a'-hexahydrospiro[piperidine-4,2'-pyrano[3',2':4,5]furo[3,2-c]pyridine]-1-carboxylate (29j)

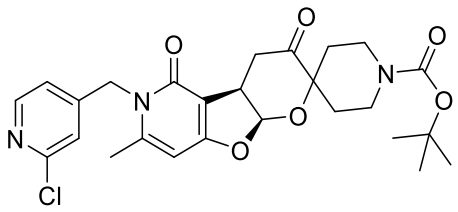

According to GP7, **4d** (97.6 mg, 0.30 mmol) was reacted with **2p** (75.2 mg, 0.30 mmol). Purification by MPLC (cyclohexane/EtOAc 1:0 to 0:1) afforded the product (94.7 mg, 66%). **^{1}H-NMR** (500 MHz, CD_2Cl_2): δ 8.28 (d, *J* = 5.2 Hz, 1H), 6.99 (s, 1H), 6.94 (dd, *J* = 5.2, 1.6 Hz, 1H), 6.42 (d, *J* = 8.7 Hz, 1H), 5.89 (s, 1H), 5.38 (d, *J* = 16.4 Hz, 1H), 5.07 (d, *J* = 16.4 Hz, 1H), 4.13 (ddd, *J* = 8.7, 6.6, 2.6 Hz, 1H), 3.94-3.80 (m, 2H), 3.26-3.09 (m, 2H), 3.08 (dd, *J* = 14.2, 2.6 Hz, 1H), 2.92 (dd, *J* = 14.2, 6.6 Hz, 1H), 2.19 (s, 3H), 1.78-1.66 (m, 2H), 1.63-1.56 (m, 1H), 1.51-1.45 (m, 1H), 1.41 (s, 9H). **^{13}C-NMR** (126 MHz, CD_2Cl_2): δ 211.3, 165.8, 160.6, 154.7, 152.4, 150.4, 150.1, 149.9, 121.9, 120.5, 106.3, 105.3, 95.8, 81.9, 79.6, 45.5, 40.2, 39.3, 38.6, 34.9, 34.7, 31.8, 28.4, 21.5. **HRMS**-ESI (m/z): $[M + H]^+$ calculated for $C_{26}H_{31}ClN_3O_6^+$, 516.1896; found, 516.1882.

(±) 6'-((2-chloropyridin-4-yl)methyl)-7'-methyl-4a',9a'-dihydrospiro[piperidine-4,2'-pyrano[3',2':4,5]furo[3,2-c]pyridine]-3',5'(4'H,6'H)-dione (30j)

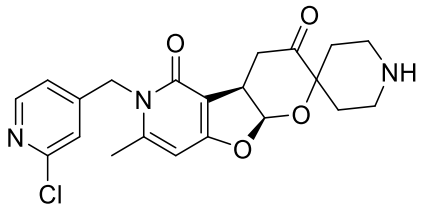

29j (92.1 mg, 0.18 mmol) was dissolved in DCM (3 mL) and cooled to 0 °C. TFA (0.14 mL, 10 equiv) was added slowly and the mixture was stirred at 0 °C for 1 hour and at room temperature for 30 min. The reaction was quenched by slow addition of saturated Na_2CO_3 solution at 0 °C and dilution with EtOAc (10 mL). The layers were separated and the aqueous phase was extracted with EtOAc (3 x 10 mL). The combined organic layers were washed with brine (20 mL), dried over $MgSO_4$ and concentrated in vacuo to afford the product (58.7 mg, 79%). **^{1}H-NMR** (700 MHz, DMSO): δ 8.35 (d, *J* = 5.2 Hz, 1H), 7.08 (s, 1H), 7.04 (d, *J* = 5.2 Hz, 1H), 6.49 (d, *J* = 8.3 Hz, 1H), 6.14 (s, 1H), 5.31 (d, *J* = 17.1 Hz, 1H), 5.22 (d, *J* = 17.1 Hz, 1H), 4.14-4.11 (m, 1H), 3.01 (dd, *J* = 14.1, 6.7 Hz, 1H), 2.88-2.80 (m, 5H), 2.21 (s, 1H), 1.75-1.65 (m, 2H), 1.53-1.48 (m, 1H), 1.41-1.37 (m, 1H). **^{13}C-NMR** (176 MHz, DMSO): δ 211.3, 164.9, 160.0, 150.7, 150.6, 150.1, 121.4, 120.6, 105.4, 104.6, 94.8, 81.0, 44.6, 40.4, 40.2, 39.0, 34.1, 34.0, 31.2, 20.5. **HRMS**-ESI (m/z): $[M + H]^+$ calculated for $C_{21}H_{23}ClN_3O_4^+$, 416.1372; found, 416.1367.

(±) *Tert*-butyl-6'-(2-(5-methoxy-1H-indol-3-yl)ethyl)-7'-methyl-3',5'-dioxo-3',4',4a',5',6',9a'-hexahydrospiro[piperidine-4,2'-pyrano[3',2':4,5]furo[3,2-c]pyridine]-1-carboxylate (29k)

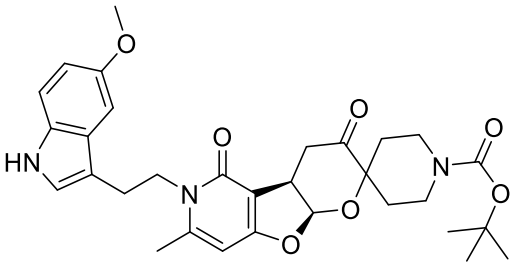

According to GP7, **4d** (97.6 mg, 0.30 mmol) was reacted with **2s** (98.5 mg, 0.30 mmol). Purification by MPLC (cyclohexane/EtOAc 1:0 to 0:1) afforded the product (89.0 mg, 52%). **^{1}H-NMR** (700 MHz, CD_2Cl_2): δ 8.18 (s, 1H), 7.26 (d, *J* = 8.7 Hz, 1H), 7.12 (d, *J* = 2.5 Hz, 1H), 6.91 (s, 1H), 6.82 (dd, *J* = 8.7, 2.5 Hz, 1H), 6.37 (d, *J* = 8.3 Hz, 1H), 5.71 (s, 1H), 4.32-4.25 (m, 1H), 4.14-4.08 (m, 2H), 3.93-3.80 (m, 5H), 3.24-3.08 (m, 4H), 3.05-3.00 (m, 1H), 2.92 (dd, *J* = 14.3, 6.7 Hz, 1H), 2.11 (s, 3H), 1.77-1.67 (m, 2H), 1.64-1.59 (m, 1H), 1.52-1.47 (m, 1H), 1.43 (s, 9H). **^{13}C-NMR** (176 MHz, CD_2Cl_2): δ 211.7, 165.2, 160.8, 154.9, 154.6, 150.4, 131.8, 128.2, 123.6, 112.4, 112.3, 106.3, 105.1, 100.9, 94.6, 81.8, 79.6, 56.1, 45.1, 40.4, 39.7, 38.8, 35.0, 34.9, 31.9, 28.5, 24.6, 21.5. **HRMS**-ESI (m/z): $[M + H]^+$ calculated for $C_{31}H_{38}N_3O_7^+$, 564.2704; found, 564.2700.

(±) 6'-(2-(5-methoxy-1H-indol-3-yl)ethyl)-7'-methyl-4a',9a'-dihydrospiro[piperidine-4,2'-pyrano[3',2':4,5]furo[3,2-c]pyridine]-3',5'(4'H,6'H)-dione (30k)

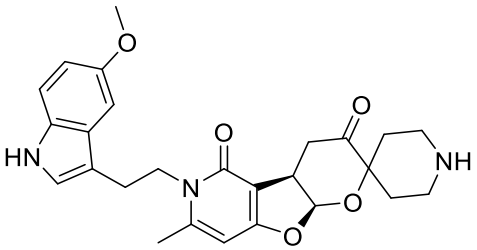

29k (80.0 mg, 0.14 mmol) was dissolved in DCM (3 mL) and cooled to 0 °C. TFA (0.11 mL, 10 equiv) was added slowly and the mixture was stirred at 0 °C for 1 hour and at room temperature for 30 min. The reaction was quenched by slow addition of saturated Na_2CO_3 solution at 0 °C and dilution with EtOAc (10 mL). The layers were separated and the aqueous phase was extracted with EtOAc (3 x 10 mL). The combined organic layers were washed with brine (20 mL), dried over $MgSO_4$ and concentrated in vacuo to afford the product (40.0 mg, 61%). **^{1}H-NMR** (700 MHz, DMSO): δ 10.73 (s, 1H), 7.24 (dd, *J* = 9.0, 3.5 Hz, 1H), 7.12 (s, 1H), 7.02 (s, 1H), 6.73 (dt, *J* = 9.0, 2.0 Hz, 1H), 6.45 (d, *J* = 8.2 Hz, 1H), 5.94 (s, 1H), 4.24-4.16 (m, 1H), 4.13-4.07 (m, 1H), 4.06-3.98 (m, 1H), 3.76 (s, 1H), 3.01 (dd, *J* = 14.2, 6.7 Hz, 1H), 2.97-2.79 (m, 7H), 2.18 (s, 3H), 1.74-1.65 (m, 2H), 1.57-1.48 (m, 1H), 1.42-1.36 (m, 1H). **^{13}C-NMR** (176 MHz, DMSO): δ 212.1, 164.7, 160.2, 153.6, 150.8, 131.8, 127.9, 124.2, 112.5, 111.6, 111.0, 105.9, 104.7, 100.7, 94.2, 81.4, 55.8, 44.7, 40.8, 40.6, 39.5, 34.7, 34.4, 31.7, 24.3, 20.8. **HRMS**-ESI (m/z): $[M + H]^+$ calculated for $C_{26}H_{30}N_3O_5^+$, 464.2180; found, 464.2172.

(±) *Tert*-butyl-6',8'-dioxo-5',6',6b',7',8',10a'-hexahydrospiro[piperidine-4,9'-pyrano[3',2':4,5]furo[3,2-c]quinoline]-1-carboxylate (29l)

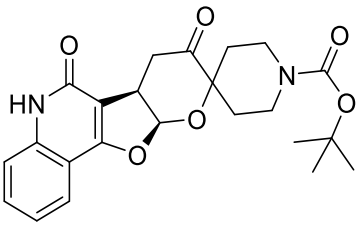

According to GP7, **4d** (97.6 mg, 0.30 mmol) was reacted with **2u** (48.3 mg, 0.30 mmol). Purification by MPLC (cyclohexane/EtOAc 1:0 to 0:1) afforded the product (24.5 mg, 20%). **^{1}H-NMR** (500 MHz, CD_2Cl_2): δ 11.75 (s, 1H), 7.68 (dd, *J* = 7.8, 1.5 Hz, 1H), 7.57 (ddd, *J* = 8.3, 7.2, 1.5 Hz, 1H), 7.41 (d, *J* = 8.3 Hz, 1H), 7.24 (td, *J* = 7.8, 7.2, 1.0 Hz, 1H), 6.61 (d, *J* = 8.7 Hz, 1H), 4.29 (ddd, *J* = 8.7, 6.9, 2.7 Hz, 1H), 3.99-3.75 (m, 2H), 3.31-3.17 (m, 3H), 3.04 (dd, *J* = 14.6, 6.9 Hz, 1H), 1.78-1.59 (m, 4H), 1.40 (s, 9H). **^{13}C-NMR** (126 MHz, CD_2Cl_2): δ 210.6, 162.7, 161.9, 154.4, 139.9, 131.8, 122.5, 122.4, 116.2, 110.8, 108.2, 105.3, 81.8, 79.3, 40.0, 39.1, 38.2, 34.8, 34.5, 31.7, 28.1. **HRMS**-ESI (m/z): $[M + H]^+$ calculated for $C_{23}H_{27}N_2O_6^+$, 427.1864; found, 427.1863.

(±) 6b',10a'-dihydrospiro[piperidine-4,9'-pyrano[3',2':4,5]furo[3,2-c]quinoline]-6',8'(5'H,7'H)-dione (30l)

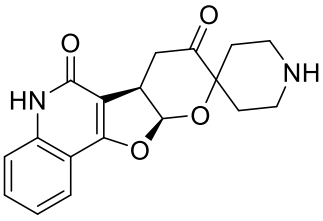

29l (22.0 mg, 0.05 mmol) was dissolved in DCM (3 mL) and cooled to 0 °C. HCl in dioxane (0.13 mL, 4 M, 10 equiv) was added slowly and the mixture was stirred at 0 °C for 1 hour and at room temperature for 30 min. The reaction was quenched by slow addition of saturated Na_2CO_3 solution at 0 °C and dilution with EtOAc (10 mL). The layers were separated and the aqueous phase was extracted with EtOAc (3 x 10 mL). The combined organic layers were washed with brine (20 mL), dried over $MgSO_4$ and concentrated in vacuo to afford the product (12.3 mg, 73%). **^{1}H-NMR** (500 MHz, DMSO): δ 11.55 (s, 1H), 7.60-7.53 (m, 2H), 7.35 (d, *J* = 8.3 Hz, 1H), 7.23-7.19 (m, 1H), 6.66 (d, *J* = 8.5 Hz, 1H), 4.23 (ddd, *J* = 8.5, 6.9, 2.8 Hz, 1H), 3.10 (dd, *J* = 14.3, 6.9 Hz, 1H), 2.96-2.78 (m, 5H), 1.81-1.76 (m, 1H), 1.65-1.50 (m, 2H), 1.30-1.25 (m, 1H). **^{13}C-NMR** (126 MHz, DMSO): δ 211.3, 160.9, 159.9, 139.9, 131.6, 122.0, 121.9, 115.7, 110.0, 108.6, 104.8, 80.9, 40.1, 39.6, 34.5, 33.6. 31.0. **HRMS**-ESI (m/z): $[M + H]^+$ calculated for $C_{18}H_{19}N_2O_4^+$, 327.1339; found, 327.1343.

(±) 5'-methyl-6',8'-dioxo-5',6',6b',7',8',10a'-hexahydrospiro[piperidine-4,9'-pyrano[3',2':4,5]furo[3,2-c]quinolin]-1-ium triflate (30m)

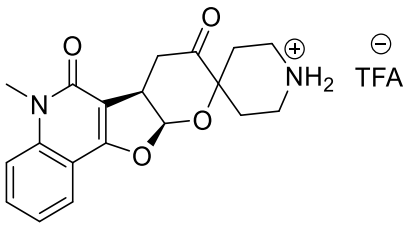

According to GP7, **4d** (97.6 mg, 0.30 mmol) was reacted with **2w** (66.4 mg, 0.30 mmol). Purification by MPLC (cyclohexane/EtOAc 1:0 to 0:1) afforded the product which was directly dissolved in DCM (3 mL) and cooled to 0 °C. TFA (0.23 mL, 10 equiv) was added slowly and the mixture was stirred at 0 °C for 1 hour and at room temperature for 30 min. The reaction was quenched by slow addition of saturated Na_2CO_3 solution at 0 °C and dilution with EtOAc (10 mL). The layers were separated and the aqueous phase was extracted with EtOAc (3 x 10 mL). The combined organic layers were washed with brine (20 mL), dried over $MgSO_4$ and concentrated in vacuo. The crude was purified by MPLC (cyclohexane/EtOAc 1:0 to 0:1) and repurified by prep. HPLC to afford the product (22.1 mg, 17% over two steps). **^{1}H-NMR** (600 MHz, DMSO): δ 8.78 (s, 1H), 8.48 (s, 1H), 7.74-7.68 (m, 2H), 7.59 (d, *J* = 8.6 Hz, 1H), 7.33 (t, *J* = 7.5 Hz, 1H), 6.71 (d, *J* = 8.5 Hz, 1H), 4.32 (ddd, *J* = 8.5, 7.1, 2.8 Hz, 1H), 3.59 (s, 3H), 3.27-3.11 (m, 5H), 2.99 (dd, *J* = 14.6, 2.8 Hz, 1H), 2.04 (dq, *J* = 14.3, 3.1 Hz, 1H), 1.85 (ddd, *J* = 14.6, 12.1, 4.5 Hz, 1H), 1.78 (ddd, *J* = 14.2, 12.3, 4.4 Hz, 1H), 1.44 (dq, *J* = 14.7, 3.2 Hz, 1H). **^{13}C-NMR** (151 MHz, DMSO): δ 210.5, 159.6, 159.0, 140.5, 132.2, 122.5, 122.3, 115.6, 110.6, 108.0, 104.7, 78.4, 40.1, 38.9, 38.6, 34.6, 30.8, 28.7, 28.5. **HRMS**-ESI (m/z): $[M + H]^+$ calculated for $C_{19}H_{21}N_2O_4^+$, 341.1496; found, 341.1494.

(±) *Tert*-butyl-6',8'-dioxo-6b',7',8',10a'-tetrahydro-6'H-spiro[piperidine-4,9'-pyrano[3',2':4,5]furo[3,2-c]chromene]-1-carboxylate (29n)

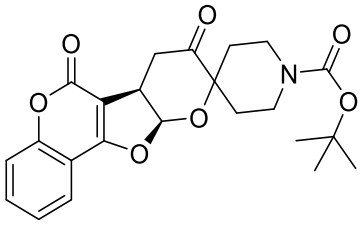

According to GP7, **4d** (116.9 mg, 0.36 mmol) was reacted with 4-hydroxy-2H-chromen-2-one (1H)-one (**1b**) (58.3 mg, 0.36 mmol). Purification by MPLC (cyclohexane/EtOAc 1:0 to 0:1) afforded the product (134.3 mg, 87%). **^{1}H-NMR** (500 MHz, CD_2Cl_2): δ 7.66-7.63 (m, 1H), 7.63-7.61 (m, 1H), 7.38 (d, *J* = 8.4 Hz, 1H), 7.33 (td, *J* = 7.6, 1.0 Hz, 1H), 6.65 (d, *J* = 8.7 Hz, 1H), 4.20 (ddd, *J* = 8.7, 6.6, 2.7 Hz, 1H), 3.95-3.76 (m, 2H), 3.30-3.14 (m, 2H), 3.08-2.94 (m, 2H), 1.77-1.61 (m, 3H), 1.41 (s, 9H), 1.39-1.36 (m, 1H). **^{13}C-NMR** (126 MHz, CD_2Cl_2): δ 210.0, 165.3, 159.1, 155.6, 154.7, 133.7, 124.8, 123.2, 117.5, 112.0, 106.5, 103.1, 82.6, 79.7, 39.9, 38.6, 34.9, 32.1, 28.5. **HRMS**-ESI (m/z): $[M + H]^+$ calculated for $C_{23}H_{26}NO_7^+$, 428.1704; found, 428.1703.

(±) 6b',10a'-dihydro-6'H-spiro[piperidine-4,9'-pyrano[3',2':4,5]furo[3,2-c]chromene]-6',8'(7'H)-dione (30n)

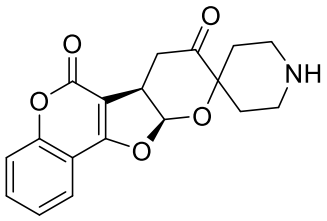

29n (130.0 mg, 0.30 mmol) was dissolved in DCM (3 mL) and cooled to 0 °C. TFA (0.23 mL, 10 equiv) was added slowly and the mixture was stirred at 0 °C for 1 hour and at room temperature for 30 min. The reaction was quenched by slow addition of saturated Na_2CO_3 solution at 0 °C and dilution with EtOAc (10 mL). The layers were separated and the aqueous phase was extracted with EtOAc (3 x 10 mL). The combined organic layers were washed with brine (20 mL), dried over $MgSO_4$ and concentrated in vacuo to afford the product (74.5 mg, 75%). **^{1}H-NMR** (700 MHz, DMSO): δ 7.72 (ddd, *J* = 8.6, 7.5, 1.7 Hz, 1H), 7.67 (dd, *J* = 7.5, 1.7 Hz, 1H), 7.48 (dd, *J* = 8.6, 1.0 Hz, 1H), 7.41 (td, *J* = 7.5, 1.0 Hz, 1H), 6.78 (d, *J* = 8.4 Hz, 1H), 4.26 (ddd, *J* = 8.4, 6.9, 2.9 Hz, 1H), 3.14 (dd, *J* = 14.5, 6.9 Hz, 1H), 2.85 (tt, *J* = 11.9, 3.4 Hz, 2H), 2.80-2.75 (m, 2H), 2.72 (dt, *J* = 12.6, 4.0 Hz, 1H), 1.74 (dq, *J* = 13.3, 2.9 Hz, 1H), 1.60 (ddd, *J* = 13.7, 11.5, 4.3 Hz, 1H), 1.51 (ddd, *J* = 13.2, 11.4, 4.5 Hz, 1H), 1.23 (dd, *J* = 13.8, 2.8 Hz, 1H). **^{13}C-NMR** (176 MHz, DMSO): δ 210.6, 164.2, 158.2, 154.4, 133.6, 124.8, 122.7, 116.9, 111.2, 106.2, 102.8, 82.1, 40.5, 40.2, 38.6, 34.4, 34.2, 31.8. **HRMS**-ESI (m/z): $[M + H]^+$ calculated for $C_{18}H_{18}NO_5^+$, 328.1180; found, 328.1180.

(±) *Tert*-butyl 7-methyl-3,5-dioxo-3,4,4a,9a-tetrahydro-5H-spiro[furo[2,3-b:4,5-c']dipyran-2,4'-piperidine]-1'-carboxylate (29o)

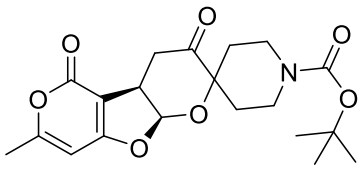

According to GP7, **4d** (116.9 mg, 0.36 mmol) was reacted with 4-hydroxy-6-methyl-2H-pyran-2-one (1H)-one (**1a**) (45.3 mg, 0.36 mmol). Purification by MPLC (cyclohexane/EtOAc 1:0 to 0:1) afforded the product (118.9 mg, 85%). **^{1}H-NMR** (500 MHz, CD_2Cl_2): δ δ 6.44 (d, *J* = 8.5 Hz, 1H), 5.92 (s, 1H), 4.04-4.00 (m, 1H), 3.93-3.80 (m, 2H), 3.23-3.08 (m, 2H), 2.96-2.88 (m, 2H), 2.24 (s, 3H), 1.76 (ddd, *J* = 14.2, 11.9, 4.5 Hz, 1H), 1.72-1.66 (m, 1H), 1.62 (ddd, *J* = 13.5, 11.6, 4.7 Hz, 1H), 1.46-1.43 (m, 1H), 1.42 (s, 9H). **^{13}C-NMR** (126 MHz, CD_2Cl_2): δ 210.3, 169.9, 167.8, 160.6, 154.7, 106.0, 99.9, 95.3, 82.3, 79.7, 39.5, 38.8, 35.0, 34.8, 31.9, 28.5, 20.8. **HRMS**-ESI (m/z): $[M + H]^+$ calculated for $C_{20}H_{26}NO_7^+$, 392.1704; found, 392.1704.

(±) 7-methyl-4a,9a-dihydro-5H-spiro[furo[2,3-b:4,5-c']dipyran-2,4'-piperidine]-3,5(4H)-dione (30o)

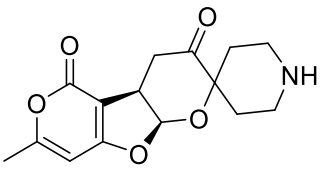

29o (110.0 mg, 0.28 mmol) was dissolved in DCM (3 mL) and cooled to 0 °C. TFA (0.21 mL, 10 equiv) was added slowly and the mixture was stirred at 0 °C for 1 hour and at room temperature for 30 min. The reaction was quenched by slow addition of saturated Na_2CO_3 solution at 0 °C and dilution with EtOAc (10 mL). The layers were separated and the aqueous phase was extracted with EtOAc (3 x 10 mL). The combined organic layers were washed with brine (20 mL), dried over $MgSO_4$ and concentrated in vacuo to afford the product (62.3 mg, 76%). **^{1}H-NMR** (700 MHz, DMSO): δ 6.56 (d, *J* = 8.4 Hz, 1H), 6.34 (s, 1H), 4.08-4.05 (m, 1H), 3.05 (dd, *J* = 14.4, 6.8 Hz, 1H), 2.85-2.75 (m, 4H), 2.66 (dd, *J* = 14.4, 2.7 Hz, 1H), 2.22 (s, 3H), 1.71 (dq, *J* = 13.5, 3.0 Hz, 1H), 1.66 (ddd, *J* = 13.8, 8.8, 7.1 Hz, 1H), 1.49 (ddd, *J* = 13.3, 11.2, 4.8 Hz, 1H), 1.30 (dq, *J* = 13.7, 3.0 Hz, 1H). **^{13}C-NMR** (176 MHz, DMSO): δ 210.7, 169.2, 167.2, 159.7, 105.5, 99.3, 95.0, 81.6, 40.5, 40.2, 37.5, 34.3, 34.2, 31.4, 19.9. **HRMS**-ESI (m/z): $[M + H]^+$ calculated for $C_{15}H_{18}NO_5^+$, 292.1180; found, 292.1178.

5.2. Cheminformatics

Similarity search for bipodal connections in Scifinder:

The Scifinder database was systematically browsed for chemical similarity to following structure queries:

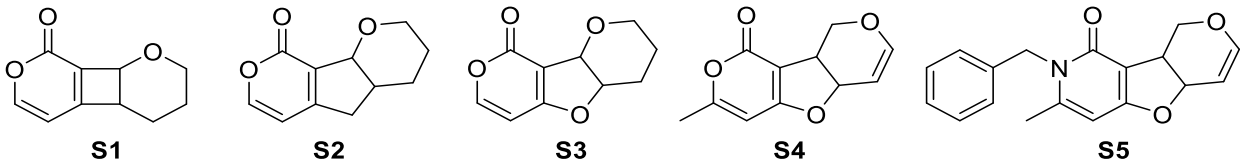

Scheme 32. Bipodal queries for combination of 2-pyrone or 2-pyridone and DHP or THP assessed in a Scifinder search.

Query **S3** resulted in a list of 20 molecules out of which entry 15 (structure **S4**) incorporated all desired features for a bipodal connection between pyr(id)ones and DHPs and for which a feasible synthesis was reported.[50] Furthermore, it was reported that the pyrone moiety can be exchanged to a pyridone (structure **S5**).[50] The other queries resulted in no hits.

Natural-Product-Likeness scores[66] were calculated and provided by Dr. Axel Pahl.

MW vs AlogP scatter plots and PMI-Plots were calculated and displayed with the open source software LLAMA[69]:
https://llama.leeds.ac.uk/

5.3. Biology

5.3.1. Cell Painting Assay

Morphological Profiling by means of the cell painting assay was performed by the Compound Management and Screening Center Dortmund (COMAS)

The described assay follows closely the method described by Bray *et al*.[39] and was performed by the Compound Management and Screening Center (COMAS). Initially, 5 µl U2OS medium were added to each well of a 384-well plate (PerkinElmer CellCarrier-384 Ultra). Subsequently, U2OS cells were seeded with a density of 1600 cells per well in 20 µl medium. The plate was incubated for 5 min at the ambient temperature, followed by an additional 4 h incubation (37 °C, 5% CO_2). Compound treatment was performed with the Echo 520 acoustic dispenser (Labcyte) at final concentrations of 50, 30, 10, 3 or 1 µM for 20 h (37 °C, 5% CO_2). Subsequently, mitochondria were stained with Mito Tracker Deep Red (Thermo Fisher Scientific, Cat. No. M22426). The MitoTracker Deep Red stock solution (1 mM) was diluted to a final concentration of 100 nM in prewarmed medium. The medium was removed from the plate leaving 10 µl residual volume and 25 µl of the Mito Tracker solution were added to each well. The plate was incubated for 30 min in the dark (37 °C, 5% CO_2). To fix the cells 7 µl of 18.5 % formaldehyde in PBS were added, resulting in a final formaldehyde concentration of 3.7 %. Subsequently, the plate was incubated for another 20 min in the dark (37 °C, 5% CO_2) and washed three times with 70 µl of PBS using the Biotek Washer Elx405. Cells were permeabilized by addition of 25 µl 0.1% Triton X-100 to each well, followed by 15 min incubation (37 °C, 5% CO2) in the dark. The cells were washed three times with PBS leaving a final volume of 70 µl. To each well 25 µl of a staining solution were added, which contains 1% BSA, 50 µl phalloidin (Thermo Fisher Scientific, A12381), 25 µg/ml concanavalin A (Thermo Fisher Scientific, Cat. No. C11252), 50 µl/ml Hoechst 33342 (Sigma, Cat. No. B2261-25mg), 15 µl/ml WGA-Alexa594 conjugate (Thermo Fisher Scientific, Cat. No. W11262) and 0.3 µl/ml SYTO 14 solution (Thermo Fisher Scientific, Cat. No. S7576). The plate was incubated for 30 min (37 °C, 5% CO_2) in the dark and washed three times with 70 µl PBS. After

the final washing step, the PBS was not aspirated. The plates were sealed and centrifuged for 1 min at 500 rpm.

The plates were prepared in triplicates with shifted layouts to reduce plate effects and imaged using a Micro XL High-Content Screening System (Molecular Devices, 5 channels, 9 sites per well, 20x magnification, binning 2).

The generated images were processed with the CellProfiler package (https://cellprofiler.org/) on a computing cluster of the Max Planck Society to extract 1716 cell features (parameters).

Further analysis was performed with custom Python (https://www.python.org/) scripts using the Pandas (https://pandas.pydata.org/) and Dask (https://dask.org/) data processing libraries (separate publication to follow).

In a first step, the data was aggregated as overall medians per well. A subset of highly reproducible parameters was determined using the procedure described by Woehrmann et al.[113] in the following way: Two biological replicates of one plate containing reference compounds were analyzed. For every parameter, its full profile over each whole plate was calculated. If the profiles from the two repeats showed a similarity >= 0.8 (see below), the parameter was added to the set. This was carried out once and resulted in a set of 579 parameters that was used for all further analyses.

Z-scores were then calculated for each parameter as how many times the MAD of the controls the measured value deviates from the median of the controls:

The phenotypic compound profile is then the list of z-scores of all parameters for one compound.

In addition to the phenotypic profile, an induction value was determined for each compound as the fraction of significantly changed parameters, in percent:

$$Induction\ [\%] = \frac{number\ of\ parameters\ with\ abs.\quad values\ >\ 3}{total\ number\ of\ parameters}$$

Similarities of phenotypic profiles (BioSim) were calculated from the correlation distances between two profiles (https://docs.scipy.org/doc/scipy/reference/generated/scipy.spatial.distance.correlation.html; Similarity = 1 - Correlation Distance) and the compounds with the most similar profiles were

determined from a set of approximately 3500 reference compounds that was also measured in the assay.

5.3.2. Cell Painting Data Analysis

Data Analysis was carried out employing various tools on the Datavis server:
http://datavis.mpi-dortmund.mpg.de/

Clustering of compounds was performed on the Datavis server employing the "cluster compounds" application. The compounds were sorted by descending induction and therefore the highest inducing compound was put into the first cluster. Compounds exhibiting a fingerprint similarity above 80% to that first compound would be added to this cluster. When no more compounds could be added, a new analysis of the remaining compounds was started. The procedure was repeated until all compounds were distributed into clusters.

Biological similarity and chemical similarity calculations as well as heatmap visualizations were performed on the Datavis server employing the "heat maps" application. For the calculation of biological similarity all parameters were used. The top line in the heatmap is set as a reference fingerprint (100% BioSim) to which subjacent fingerprints are compared, respectively; blue indicates a decreased value of a specific parameter compared to the DMSO control; red indicates an increased value of a specific parameter compared to the DMSO control.

Common references for a given data set of profiles were searched on the Datavis server employing the "common references" application. Only references that were found by at least two compounds and only compounds that share at least one reference with another compound are displayed. References targeting GPCRs were excluded for the analysis as they were found to occur ubiquitous in the whole data set for yet unresolved reasons.

Cross similarity was displayed employing the "compound cross similarity" application on the Datavis server. The tool generates a N x N cross table with biological similarities displayed between each of the N entered compounds.

5.3.3. Cell Culture

HeLa (ACC 57) cells were purchased from DSMZ GmbH (Germany) and cultured in DMEM with 10% FBS, sodium pyruvate, non-essential amino acids, penicillin and streptomycin. Cells were incubated at 37°C, 5% CO_2 in a humidified atmosphere. During regular testing for mycoplasma infections, cells were found negative.

5.3.4. Mito Stress Test

The Mito Stress Test was performed by Aylin Binici and Julian Wilke

The influence of test compounds on mitochondrial respiration was assessed using the Seahorse XFp analyzer (Agilent, USA) in combination with the Cell Mito Stress Test kit (Agilent, USA) according to the manufacturer's protocol. 20,000 HeLa cells per well were seeded into XFp cell culture plates (Agilent, USA) and incubated at 37°C, 5% CO_2 overnight. XFp cartridges were hydrated using XF Calibrant and incubated overnight at 37°C. Seeding medium was exchanged for pH 7.4 DMEM-based assay medium (Agilent, USA) containing 2 mM GlutaMAX (ThermoFisher), 1 mM sodium pyruvate (PAN Biotech, Germany) and 25 mM glucose (Sigma-Aldrich, Germany). Oxygen consumption rate (OCR) and extracellular acidification rate (ECAR) were measured in intervals of 6 min. After five measurement intervals of baseline recording, the test compounds were injected, followed by ten measurement intervals. Subsequently, Oligomycin, FCCP and Rotenone/Antimycin A were injected, followed by three measurement intervals after each injection. Data was background-subtracted and normalized to the last baseline measurement (=100%), using the Wave software (Agilent, USA).

5.3.5. Inhibition of mitochondrial complexes I-IV

The Semi-Intact Assay for Mitochondrial Respiration was performed by Aylin Binici and Julian Wilke

Inhibition of mitochondrial complexes I-IV was tested using the Seahorse XFp analyzer. Seeding of 10,000 HeLa cells per well and hydration of XFp cartridges were performed as described for the Cell Mito Stress Test. The assay was performed using MAS buffer (220 mM mannitol, 70 mM sucrose, 10 mM KH_2PO_4, 5 mM $MgCl_2$, 2 mM HEPES, 1 mM EGTA, pH 7.4). The buffer was supplemented with 0.5% (w/v) fatty acid free BSA for complex I-III. Oxygen consumption rate (OCR) was measured in intervals of 8 min. After three baseline measurement intervals, the test compound, 1 nM of Seahorse XF Plasma membrane

permeabilizer (Agilent) and 1 mM ADP were injected together with 10 mM pyruvate / 1 mM malate for complex I, 10 mM succinate / 1 µM rotenone for complex II, 0.2 mM duroquinol for complex III or 0.5 mM tetramethylphenylenediamine (TMPD) / 2 mM ascorbate for complex IV, followed by three measurement intervals. Subsequently, first 1 µM Oligomycin, then 1 µM antimycin A (complex I and II) or 20 mM sodium azide (complex III and IV) were injected, followed by three measurement intervals each. Data analysis was performed as described for the Cell Mito Stress Test.

5.3.6. MitoSOX Red Assay

The MitoSOX Red assay was performed by Aylin Binici and Julian Wilke

Mitochondrial superoxide levels were determined using the indicator dye MitoSOX Red[99] (ThermoFisher, USA). 15,000 Hela cells were seeded per well into black 96 well plates with clear flat bottom and incubated at 37°C, 5% CO_2 overnight. Seeding medium was exchanged for staining medium comprising DMEM without additives containing 5 µM MitoSOX Red and 5 µg/µL Hoechst-33342 (ThermoFisher, USA). Cells were incubated for 30 min at 37°C, 5% CO_2. Subsequently, the medium was exchanged for DMEM with additives containing test compounds, followed by 60 min of incubation at 37°C, 5% CO_2. Cells were fixed in PBS containing 0.5% paraformaldehyde for 10 min at room temperature and washed three times with PBS. Cells were imaged using an Axiovert 200M automated microscope (Carl Zeiss, Germany) at 10x magnification. MetaMorph 7.7.8.0 (Visitron, Germany) was used to quantify the integrated fluorescence intensity of MitoSOX Red per cell. The data was normalized to control cells treated with either DMSO (=0%) or 10 µM CDNB (=100%). Non-linear regression via four-parameter fit was performed using Prism 7 (GraphPad Software, USA) and EC_{50} values were obtained by interpolating X values for 50% staining intensity.

6. List of Abbreviations

Abbreviation	Meaning
ADME	Absorption/administration, distribution, metabolism, excretion
ADP	Adenosine diphosphate
AlogP	Estimated hydrophobicity
ATP	Adenosine triphosphate
BIOS	Biology-oriented synthesis
BioSim	Biological similarity = morphological profile similarity
bpy	2,2'-Bipyridine
BSA	Bovine serum albumin
CDNB	1-Chloro-2,4-dinitrobenzene
ChEMBL	Chemical database of bioactive molecules of the European Molecular Biology Labaratory
ChemSim	Chemical similarity = Tanimoto similarity
Cmpd	Compound
COMAS	Compound management and screening center
Conc.	Concentration
CtD	Complexity-to-diversity
DCM	Dichloromethane
DHP	Dihydropyran
DMA	Dimethylacetamide
DMAP	4-(Dimethylamino)pyridine
DMEM	Dulbecco´s modified eagle medium
DMF	Dimethylformamide
DMSO	Dimethyl sulfoxide
DNP	Dictionary of natural products
dppf	1,1′-Ferrocenediyl-bis(diphenylphosphine)
ECAR	Extracellular acidification rate
EGTA	Ethylene glycol-bis(β-aminoethyl ether)-*N*,*N*,*N*‘,*N*‘-tetraacetic acid
ESI	Electrospray ionization
EtOAc	Ethyl acetate

FBS	Fetal bovine serum
FBDD	Fragment-based drug design
FCG	Forward chemical genetics
FDA	Food and Drug Administration
PFP	Pyrano-furo-pyridones
GLUT	Glucosetransporter
GPCR	G-protein coupled receptor
HEPES	4-(2-Hydroxyethyl)-1-peperazineethanesulfonic acid
(U)HPLC	(Ultra)-high pressure liquid chromatography
HRMS	High-resolution mass spectrometry
HTS	High throughput screening
Ind.	Induction
LCMS	Liquid chromatography mass spectrometry
LLAMA	Lead-likeness and molecular analysis
MAD	Mean absolute deviation
MAP kinase	Mitogen-activated protein kinase
*m*CPBA	*Meta*-chloroperoxybenzoic acid
MeCN	Acetonitrile
MPLC	Medium pressure liquid chromatography
MLCK1	Myosin light chain kinase 1
MW	Microwave
NBS	*N*-bromosuccinimide
NOESY	Nuclear Overhauser effect spectroscopy
NMR	Nuclear magnetic resonance spectroscopy
OAc	Acetoxy group
OCR	Oxygen consumption rate
OTf	Triflate group
Pd-AAC	Palladium catalyzed allylic alkylation cascade
PBS	Phosphate-buffered saline
PMI	Principal moments of inertia
NP	Natural product

RCG	Reverse chemical genetics
SAR	Structure-activity relationship
SCONP	Structural classification of natural products
SPR	Structure-phenotype relationship
TBSCl	*Tert*-butyldimethylsilyl chloride
TFA	Trifluoroacetic acid
THF	Tetrahydrofuran
THP	Tetrahydropyran
TMPD	Tetramethylphenylenediamine
TMSOTf	Trimethylsilyl trifluoromethanesulfonate
XPhos	2-Dicyclohexylphosphino-2′,4′,6′-triisopropylbiphenyl

7. References

[1] K. Kumar, H. Waldmann, *Isr. J. Chem.* **2019**, *59*, 41-51.

[2] D. R. Spring, *Chem. Soc. Rev.* **2005**, *34*, 472-482.

[3] E. Zamir, P. I. H. Bastiaens, *Nat. Chem. Biol.* **2008**, *4*, 643-647.

[4] R. S. Lokey, *Curr. Opin. Chem. Biol.* **2003**, *7*, 91-96.

[5] W. P. Walters, *J. Med. Chem.* **2018**.

[6] J. Eder, R. Sedrani, C. Wiesmann, *Nat. Rev. Drug Discov.* **2014**, *13*, 577-587.

[7] A. L. Harvey, R. Edrada-Ebel, R. J. Quinn, *Nat. Rev. Drug Discov.* **2015**, *14*, 111-129.

[8] L. Laraia, H. Waldmann, *Drug Discov. Today* **2017**, *23*, 75-82.

[9] D. J. Newman, G. M. Cragg, *J. Nat. Prod.* **2012**, *75*, 311-335.

[10] T. E. Nielsen, S. L. Schreiber, *Angew. Chem. Int. Ed.* **2008**, *47*, 48-56.

[11] H. Hattum, H. Waldmann, *J. Am. Chem. Soc.* **2014**, *136*, 11853-11859.

[12] R. W. Huigens, K. C. Morrison, R. W. Hicklin, T. A. Flood, M. F. Richter, P. J. Hergenrother, *Nat. Chem.* **2013**, *5*, 195-202.

[13] B. Over, S. Wetzel, C. Grütter, N. Yasushi, S. Renner, D. Rauh, H. Waldmann, *Nat. Chem.* **2013**, *5*, 21-28.

[14] M. A. Koch, A. Schuffenhauer, M. Scheck, S. Wetzel, M. Casaulta, A. Odermatt, P. Ertl, H. Waldmann, *Proc. Natl. Acad. Sci.* **2005**, *102*, 17272-17277.

[15] M. Kaiser, S. Wetzel, K. Kumar, H. Waldmann, *Cell. Mol. Life. Sci.* **2008**, *65*, 1186-1201.

[16] S. Wetzel, R. S. Bon, K. Kumar, H. Waldmann, *Angew. Chem. Int. Ed.* **2011**, *50*, 10800-10826.

[17] C. R. Pye, M. J. Bertin, R. S. Lokey, W. H. Gerwick, R. G. Linington, *Proc. Natl. Acad. Sci.* **2017**, *114*, 5601-5606.

[18] R. J. Rafferty, R. W. Hicklin, K. A. Maloof, P. J. Hegenrother, *Angew. Chem. Int. Ed.* **2014**, *53*, 220-224.

[19] N. G. Paciaroni, R. R., J. H. Matthews, V. M. Norwood, A. C. Arnold, L. H. Dang, H. Luesch, R. W. Huigens, *Chemistry* **2017**, *23*, 4327-4335.

[20] A. Garcia, B. S. Drown, P. J. Hergenrother, *Org. Lett.* **2016**, *18*, 4852-4855.

[21] S. Z. Tasker, A. E. Cowfer, P. J. Hergenrother, *Org. Lett.* **2018**, *20*, 5894-5898.

[22] E. Llabani, R. W. Hicklin, H. Y. Lee, S. E. Motika, L. A. Crawford, E. Weerapana, P. J. Hergenrother, *Nat. Chem.* **2019**, *11*, 521-532.

[23] P. J. Hajduk, J. Greer, *Nat. Rev. Drug Discov.* **2007**, *6*, 211-219.

[24] C. W. Murray, D. C. Rees, *Nat. Chem.* **2009**, *1*, 187-192.

[25] J. Klein, J. R. Heal, W. D. O. Hamilton, T. Boussembhoune, O. T. Tange, F. Delegrange, G. Jaeschke, A. Hatsch, J. Heim, *ACS Synth. Biol.* **2014**, *3*, 314-323.

[26] G. Karageorgis, E. S. Reckzeh, J. Ceballos, M. Schwalfenberg, S. Sievers, C. Ostermann, A. Pahl, S. Ziegler, H. Waldmann, *Nat. Chem.* **2018**, *10*, 1103-1111.

[27] W. H. B. Sauer, M. K. Schwarz, *J. Chem. Inf. Comput. Sci* **2003**, *43*, 987-1003.

[28] G. Karageorgis, D. J. Foley, L. Laraia, H. Waldmann, *unpublished results* **2019**.

[29] T. Schneidewind, S. Kapoor, G. Garivet, G. Karageorgis, R. Narayan, G. Vendrell-Navarro, A. P. Antonchick, S. Ziegler, H. Waldmann, *Cell Chem. Biol.* **2019**, *26*, 512-523.e515.

[30] C. J. O´Connor, L. Laraia, D. R. Spring, *Chem. Soc. Rev.* **2011**, *40*, 4332-4345.

[31] J. G. Moffat, F. Vincent, J. A. Lee, J. Eder, M. Prunotto, *Nat. Rev. Drug Discov* **2017**, *16*, 531-543.

[32] F. Vincent, P. Loria, M. Pregel, R. Stanton, L. Kitching, K. Nocka, R. Doyonas, C. Steppan, A. Gilbert, T. Schroeter, M.-C. Peakman, *Sci. Transl. Med.* **2015**, *7*, 293ps 215.

[33] B. K. Wagner, *Expert Opin. Drug Discov.* **2016**, *11*, 121-125.

[34] B. K. Wagner, S. L. Schreiber, *Cell Chem. Biol.* **2016**, *23*, 3-9.

[35] J. C. Caicedo, S. Singh, A. E. Carpenter, *Curr. Opin. Biothechnol.* **2016**, *39*, 134-142.

[36] S. M. Gustafsdottir, V. Ljosa, K. L. Sokolnicki, J. A. Wilson, D. Walpita, M. M. Kemp, K. P. Seiler, H. A. Carrel, T. R. Golub, S. L. Schreiber, P. A. Clemons, A. E. Carpenter, A. F. Shamji, *Plos One* **2013**, *8*, 1-7.

[37] D. C. Swinney, A. J., *Nat. Rev. Drug Discov.* **2011**, *10*, 507-519.

[38] Y. Feng, T. J. Mitchison, A. Bender, D. W. Young, J. A. Talarico, *Nat. Rev. Drug Discov.* **2009**, *8*, 567-578.

[39] M.-A. Bray, S. Singh, H. Han, C. T. Davis, B. Borgeson, C. Hartland, M. Kost-Alimova, S. M. Gustafsdottir, C. C. Gibson, A. E. Carpenter, *Nat. Protoc.* **2016**, *11*, 1757-1774.

[40] J. C. Caicedo, S. Cooper, F. Heigwer, S. Warchal, P. Qiu, C. Molnar, A. S. Vailevich, J. D. Barry, H. S. Bansal, O. Krau, M. J. Wawer, L. Paavolainen, M. D. Herrmann, M. Rohban, J. Hung, H. Hennig, J. Concannon, I. Smith, P. A. Clemons, S. Singh, P. Rees, P. Horvath, R. G. Linington, A. E. Carpenter, *Nat. Methods* **2017**, *14*, 849-863.

[41] A. E. Carpenter, T. R. Jones, M. R. Lamprecht, C. Clarke, I. H. Kang, O. Friman, D. A. Guertin, J. H. Chang, R. A. Lindguist, J. G. Moffat, P. Golland, D. M. Sabatini, *Genome Biol* **2006**, *7*, doi:10.1186/gb-2006-1187-1110-r1100.

[42] M. J. Wawer, S. M. Gustafsdottir, V. Ljosa, N. E. Bodycobe, M. A. Marton, K. L. Sokolnicki, M.-A. Bray, M. M. Kemp, E. Winchester, B. Taylor, G. B. Grant, C. S.-Y. Hon, J. R. Duvall, A. Wilson, J. A. Bittker, V. Dancik, R. Narayan, A. Subramanian, W. Winckler, T. R. Golub, A. E. Carpenter, A. F. Shamji, S. L. Schreiber, P. A. Clemons, *Proc. Natl. Acad. Sci.* **2014**, *111*, 10911-10916.

[43] B. Melillo, J. Zoller, B. K. Hua, O. Verho, J. C. Borghs, S. D. Nelson, M. Maetani, M. J. Wawer, P. A. Clemons, S. L. Schreiber, *J. Am. Chem. Soc.* **2018**, *140*, 11784-11790.

[44] C. J. Gerry, B. K. Hua, M. J. Wawer, J. P. Knowles, N. J. S. D., O. Verho, S. Dandapani, B. K. Wagner, P. A. Clemons, K. I. Booker-Milburn, Z. V. Boskovic, S. L. Schreiber, *J. Am. Chem. Soc.* **2016**, *138*, 8920-8927.

[45] M. R. Redinbo, L. Stewart, P. Kuhn, J. J. Champoux, W. G. J. Hol, *Science* **1998**, *279*, 1504-1513.

[46] A. A. Alfatafta, J. B. Gloer, J. A. Scott, D. Malloch, *J. Nat. Prod.* **1994**, *57*, 1696-1702.

[47] X. Lan, W. Whang, W. Li, J. Wang, *Mol. Neurobiol.* **2016**, *53*, 1794-1801.

[48] R. Tundis, M. R. Loizzo, F. Menichini, G. A. Statti, F. Menichini, *Mini-Rev. in Med. Chem.* **2008**, *8*, 399-420.

[49] http://dnp.chemnetbase.com/faces/chemical/ChemicalSearch.xhtml;jsessionid=EDA27818EB1DD19C06C55F78A73C4520, *last visited* **23.07.2019**.

[50] M. J. Bartlett, C. A. Turner, J. E. Harvey, *Org. Lett.* **2013**, *15*, 2430-2433.

[51] J. Yu, H. Ma, H. Yao, H. Cheng, R. Tong, *Org. Chem. Front.* **2016**, *3*, 714-719.

[52] R. H. Wiley, N. R. Smith, L. H. Knabeschuh, *J. Am. Chem. Soc.* **1953**, *75*, 4482-4484.

[53] O. Achmatowicz, P. Bukowski, B. Szechner, Z. Zwierzchowska, A. Zamojski, *Tetrahedron* **1971**, *21*, 1973-1996.

[54] M. B. Plutschack, P. H. Seeberger, K. Gilmore, *Org. Lett.* **2017**, *19*, 30-33.

[55] A. Jakab, Z. Dalicsek, T. Holczbauer, A. Hamza, I. Pápai, Z. Finta, G. Timári, T. Soós, *Eur. J. Org. Chem.* **2015**, *2015*, 60-66.

[56] R. J. Ferrier, N. Prasad, *J. Chem. Soc. (C)* **1969**, 570-575.

[57] K. L. Granberg, J.-E. Bäckvall, *J. Am. Chem. Soc.* **1992**, *114*, 6858-6863.

[58] D. L. Van Vranken, B. M. Trost, *Chem. Rev.* **1996**, *96*, 395-422.

[59] M.-R. Brescia, Y. C. Shimshok, P. DeShong, *J. Org. Chem.* **1997**, *62*, 1257-1263.

[60] S. Dharuman, Y. D. Vankar, *Org. Lett.* **2014**, *16*, 1172-1175.

[61] Y. Bai, J. Zeng, S. Cai, X.-W. Liu, *Org. Lett.* **2011**, *13*, 4394-4397.

[62] D.-C. Xiong, L.-H. Zhang, X.-S. Ye, *Org. Lett.* **2009**, *11*, 1709-1712.

[63] J. Ramnauth, O. Poulin, S. Rakhit, S. P. Maddaford, *Org. Lett.* **2001**, *3*, 2013-2015.

[64] A. J. Zhang, D. H. Russell, J. Zhu, K. Burgess, *Tetrahedron Lett.* **1998**, *39*, 7439-7442.

[65] P. Vincetti, F. Caporuscio, S. Kaptein, A. Gioiello, V. Mancino, Y. Suzuki, N. Yamamoto, E. Crespan, A. Lossani, G. Maga, G. Rastelli, D. Castagnolo, J. Neyts, P. Leyssen, G. Costantino, M. Radi, *J. Med. Chem.* **2015**, *58*, 4964-4975.

[66] P. Ertl, S. Roggo, A. Schuffenhauer, *J. Chem. Inf. Model* **2008**, *48*, 68-74.

[67] V. Law, C. Knox, Y. Djoumbou, T. Jewison, A. C. Guo, Y. Liu, A. Maciejewski, D. Arndt, M. Wilson, V. Neveu, A. Tang, G. Gabirel, C. Ly, S. Adamjee, Z. Dame, B. Han, Y. Zhou, D. S. Wishart, *Nucleic Acids Res.* **2014**, *42*, D1091-D1097.

[68] C. A. Lipinski, F. Lombardo, B. W. Dominy, P. J. Feeney, *Adv. Drug Deliv. Rev.* **1997**, *23*, 3-25.

[69] I. Colomer, C. J. Empson, P. Craven, Z. Owen, R. Doveston, I. Churcher, S. P. Marsden, A. Nelson, *Chem. Commun.* **2016**, *52*, 7209-7212.

[70] R. Doveston, S. Marsden, A. Nelson, *Drug Discov. Today* **2014**, *19*, 813-819.

[71] N. Bougen-Zhukov, S. Y. Loh, H. K. Lee, L.-H. Loo, *Cytom. A* **2017**, *91A*, 115-125.

[72] S. Brand, S. Roy, P. Schröder, B. Rathmer, J. Roos, S. Kapoor, S. Patil, C. Pommerenke, T. Maier, P. Janning, S. Eberth, D. Steinhilber, D. Schade, G. Schneider, K. Kumar, S. Ziegler, H. Waldmann, *Cell Chem. Biol.* **2018**, *25*, 1095-1106.

[73] K. Kiquchi, L. Ruffino, T. Kawamoto, T. Ajiki, J. Digiovanni, *Clin. Cancer Res.* **2005**, *11*, 5572-5580.

[74] L. Kremer, E. Hennes, A. Brause, A. Ursu, L. Robke, H. T. Matsubayashi, Y. Nihongaki, I. Mejdrová, J. Eickhoff, M. Baumann, R. Nencka, P. Janning, S. Kordes, H. R. Schöler, J. Sterneckert, T. Inoue, S. Ziegler, H. Waldmann, *unpublished results*.

[75] L. Robke, Y. Futamura, G. Konstantinidis, J. Wilke, H. Aono, M. Zhwan, N. Watanabe, Y.-W. Wu, H. Osada, L. Laraia, H. Waldmann, *Chem. Sci.* **2018**, *9*, 3014-3022.

[76] Y. Chen, S. B. Gibson, *Autophagy* **2008**, *4*, 246-248.

[77] A. Gugliucci, L. Ranzato, L. Scorrano, R. Colonna, V. Petronilli, C. Cusan, M. Prato, M. Mancini, F. Pagano, P. Bernardi, *J. Biol. Chem.* **2002**, *35*, 31789-31795.

[78] M. R. Hart, H. Y. Su, D. Broka, A. Goverdhan, J. A. Schroeder, *Mol. Ther.* **2013**, *21*, 1996-2007.

[79] S. Andrisse, R. M. Koehler, J. E. Chen, G. D. Patel, V. R. Vallurupalli, B. A. Ratliff, D. E. Warren, J. S. Fischer, *Redox. Biol.* **2014**, *25*, 764-771.

[80] R.-Y. Zhang, Z.-Y. Quiao, H.-J. Liu, J.-W. Ma, *Exp. Ther. Med.* **2018**, *16*, 4193-4200.

[81] S. B. Le, M. K. Hailer, S. Buhrow, Q. Wang, K. Flatten, P. Pediaditakis, K. C. Bible, L. L. D., E. A. Sausville, Y. P. Pang, M. M. Ames, J. J. Lemasters, E. L. Holmuhamedov, S. H. Kaufmann, *J. Biol. Chem.* **2007**, *282*, 8860-8872.

[82] N. Li, K. Raqheb, G. Lawler, J. Sturgis, B. Rajwa, J. A. Melendez, J. P. Robinson, *J. Biol. Chem.* **2003**, *278*, 8516-8525.

[83] N. Kaiser, D. Corkery, Y. Wu, L. Laraia, H. Waldmann, *Bioorg. Med. Chem.* **2019**, *21*, 2444-2448.

[84] A. Binici, *Master Thesis* **2019**.

[85] J. K. Salabei, A. A. Gibb, B. G. Hill, *Nat. Protoc.* **2014**, *9*, 421-438.

[86] G. Palmer, D. J. Horgan, H. Tisdale, T. P. Singer, H. Beinert, *J. Biol. Chem.* **1968**, *243*, 844-847.

[87] F. M. Drawnel, J. D. Zhang, E. Kueng, N. Aoyama, F. Benmansour, A. A. Del Rosario, S. J. Zoffmann, F. Delobel, M. Prummer, F. Weibel, C. Carlson, B. Anson, R. Iacone, U. Certa, T. Singer, M. Ebeling, *Cell Chem. Biol.* **2017**, *24*, 624-634.

[88] F. Reisen, A. Saut de Chalon, M. Pfeifer, X. Zhang, D. Gabriel, P. Selzer, *Assay. Drug. Dev. Technol.* **2015**, *13*, 415-427.

[89] D. W. Young, A. Bender, J. Hoyt, E. McWhinnie, G.-W. Chirn, C. Y. Tao, J. A. Tallarico, M. Labow, J. L. Jenkins, T. J. Mitchison, Y. Feng, *Nat. Chem. Biol.* **2008**, *4*, 59-68.

[90] M. D. Esposti, A. Ghelli, M. Crimi, E. Estornell, R. Fato, G. Lenaz, *Biochem. Biophys. Res. Commun.* **1993**, *190*, 1090-1096.

[91] M. D. Esposti, *Biochim. Biophys. Acta Bioenerg.* **1998**, *1364*, 222-235.

[92] U. Fendel, M. A. Tocilescu, S. Kerscher, U. Brandt, *Biochim. Biophys. Acta* **2008**, *1777*, 660-665.

[93] J. G. Okun, P. Lümmen, U. Brandt, *J. Biol. Chem.* **1999**, *274*, 2625-2630.

[94] K. Bhattacharya, A. K. Bag, R. Tripathi, S. K. Samanta, B. C. Pal, C. Shaha, C. Mandal, *Am. J. Cancer. Res.* **2014**, *4*, 629-647.

[95] D. Xia, C. A. Yu, H. Kim, J. Z. Xia, A. M. Kachurin, L. Zhang, L. Yu, J. Deisenhofer, *Science* **1997**, *277*, 60-66.

[96] M. D. Brand, C. Affourtit, T. C. Esteves, K. Green, A. J. Lambert, S. Miwa, J. L. Pakay, N. Parker, *Free Radic. Biol. Med.* **2004**, *37*, 755-767.

[97] I. Liguori, G. Russo, F. Curcio, G. Bulli, L. Aran, D. Della-Morte, G. Gargiulo, G. Testa, F. Cacciatore, D. Bonaduce, P. Abete, *Clin. Interv. Aging.* **2018**, *13*, 757-772.

[98] D. Trachootham, J. Alexandre, P. Huang, *Nat. Rev. Drug Discov* **2009**, *8*, 579-591.

[99] https://www.thermofisher.com/order/catalog/product/M36008, *last visited* **07.07.2019**.

[100] G. R. Fulmer, A. J. M. Miller, H. N. Sherden, H. E. Gottlieb, A. Nudelman, B. M. Stoltz, J. E. Bercaw, K. I. Goldberg, *Organometallics* **2010**, *29*, 2176-2179.

[101] B. H. Patel, A. M. Mason, A. G. M. Barrett, *Org. Lett.* **2011**, *13*, 5156-5159.

[102] M.-T. Nolan, J. T. W. Bray, K. Eccles, M. S. Cheung, Z. Lin, S. E. Lawrence, A. C. Whitwood, J. S. Fairlamb, G. P. McGlacken, *Tetrahedron* **2014**, *70*, 7120-7127.

[103] J. Vucicevic, T. Srdic-Rajic, M. Pieroni, J. M. M. Laurila, V. Perovic, S. Tassini, E. Azzali, G. Costantino, S. Glisic, D. Agbaba, M. Scheinin, K. Nikolic, M. Radi, N. Veljkovic, *Bioorg. Med. Chem.* **2016**, *24*, 3174-3183.

[104] G. P. Tokmakov, N. M. Przheval'skii, E. N. Rozhkova, N. L. Nam, *Izvestiya Timiryazevskoi Sel'skokhozyaistvennoi Akademii* **2009**, *2*, 169-175.

[105] N. M. Przheval'skii, E. N. Rozhkova, *Doklady TSKhA* **2009**, *281*, 114-118.

[106] S. R. Selness, R. V. Devraj, J. B. Monahan, T. L. Boehm, J. K. Walker, B. Devadas, R. C. Durley, R. Kurumbail, H. Shieh, L. Xing, M. Hepperle, P. V. Rucker, K. D. Jerome, A. G. Benson, L. D. Marrufo, H. M. Madsen, J. Hitchcock, T. J. Owen, L. Christie, M. A. Promo, B. S. Hickory, E. Alvira, W. Naing, R. Blevis-Bal, *Bioorg. Med. Chem. Lett.* **2009**, *19*, 5851-5856.

[107] S. L. Clarke, G. P. McGlacken, *Tetrahedron* **2015**, *71*, 2906-2913.

[108] G. Dannhardt, W. Meindl, S. Gussmann, S. Ajili, T. Kappe, *J. Med. Chem.* **1987**, *22*, 505-510.

[109] W.-Z. Song, N. Zheng, M. Li, K. Ullah, J.-H. Li, K. Dong, Y.-B. Zheng, *Heterocycles* **2018**, *96*, 1779-1785.

[110] H. Takayama, Z.-J. Jia, L. Kremer, J. Bauer, C. Strohmann, S. Ziegler, A. P. Antonchick, H. Waldmann, *Angew. Chem. Int. Ed.* **2013**, *52*, 12404-12408.

[111] C. Zhao, D. A. Glazier, D. Yang, D. Yin, I. A. Guzei, M. M. Aristov, P. Liu, W. Tang, *Angew. Chem. Int. Ed.* **2019**, *58*, 887-891.

[112] J. Yu, H. Ma, H. Yao, G. Cheng, R. Tong, *Org. Chem. Front.* **2016**, *3*, 714-719.

[113] M. H. Woehrmann, W. M. Bray, J. K. Durbin, S. C. Nisam, A. K. Michael, E. Glassey, J. M. Stuart, R. S. Lokey, *Mol. BioSyst.* **2013**, *9*, 2604-2617.

8. Appendix

8.1. Supplemental Spectra

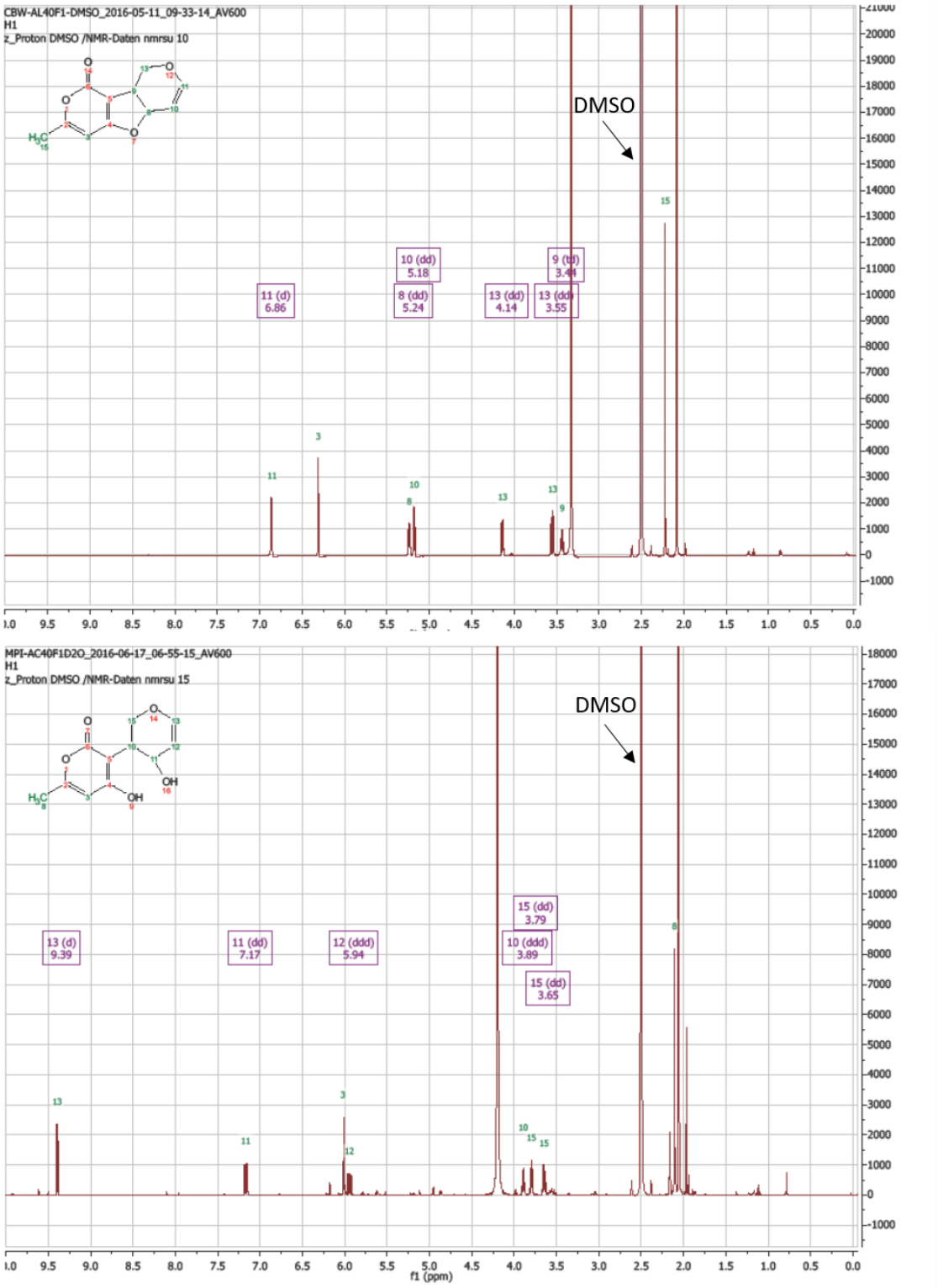

Supplemental Spectra S1. Top: ^{1}H-NMR of **9a** in DMSO-d_6, recorded immediately after dissolving the compound. Bottom: ^{1}H-NMR of **9a** in DMSO-d_6/D_2O (4:1), recorded 24 hours after dissolving the compound and storing it at room temperature in the NMR tube.

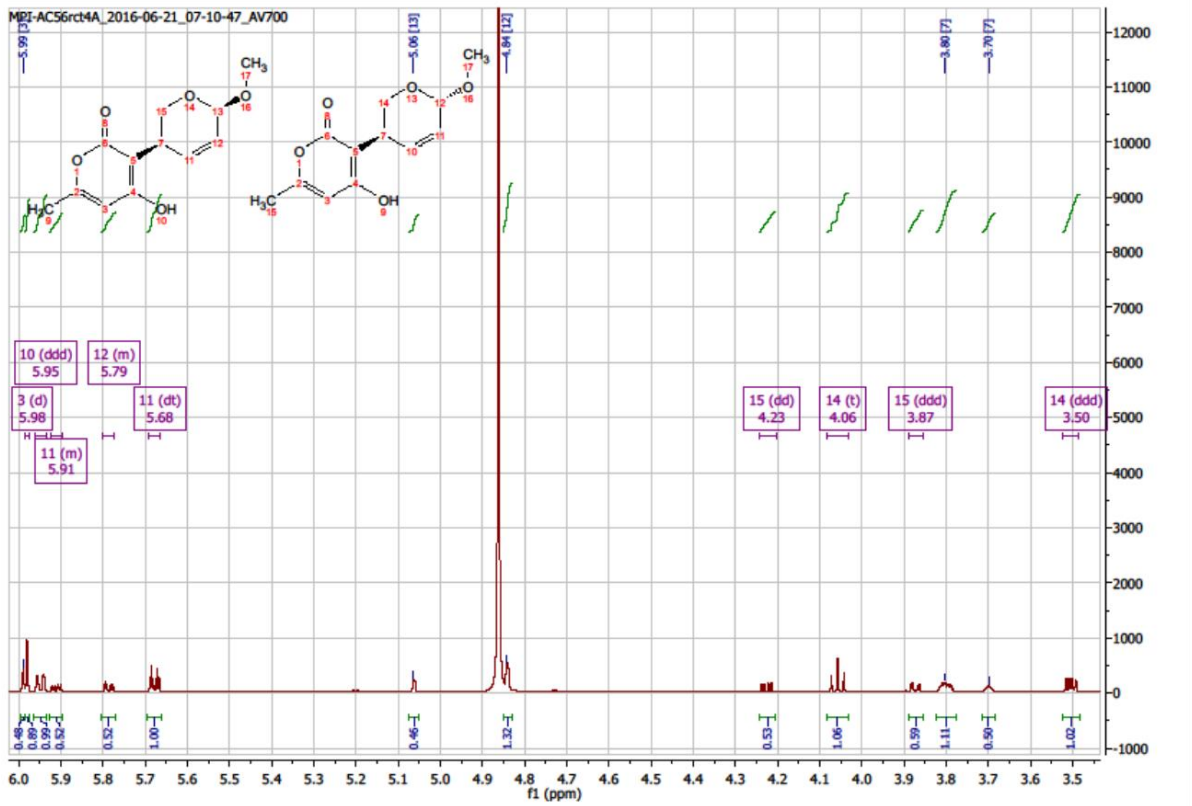

Supplemental Spectra S2. ^{1}H-NMR of **9a** in MeOH-d_4, recorded 24 hours after dissolving the compound and storing it at room temperature in the NMR tube.

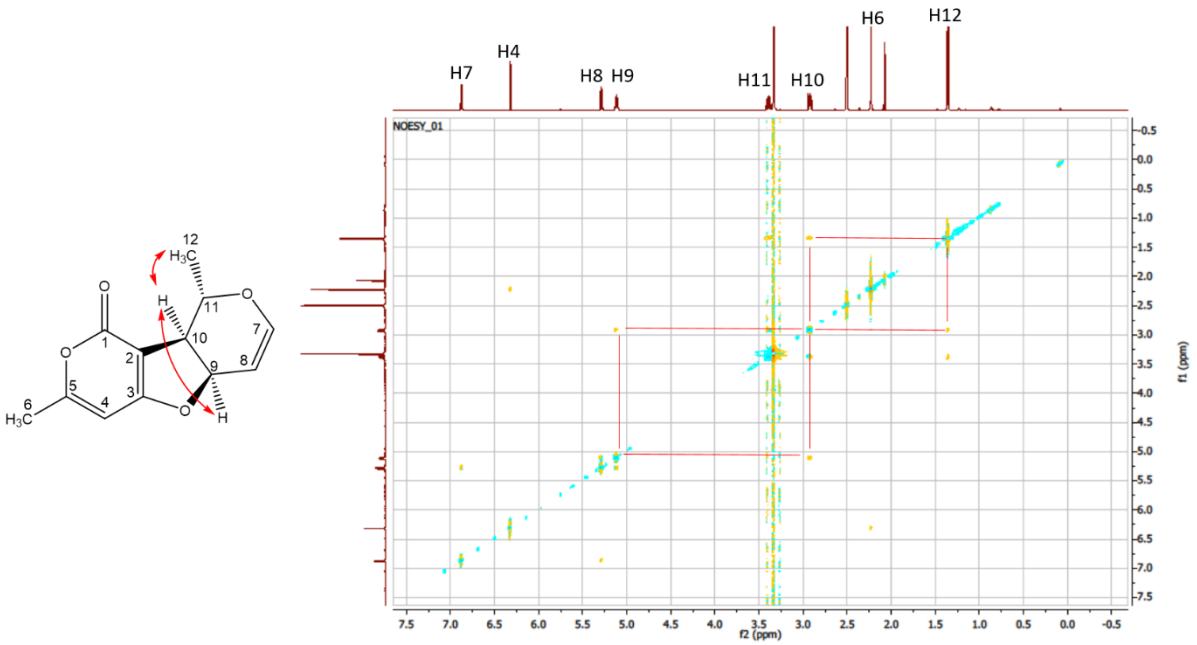

Supplemental Spectra S3. 2D-NOESY spectrum of **12a** in DMSO-d_6.

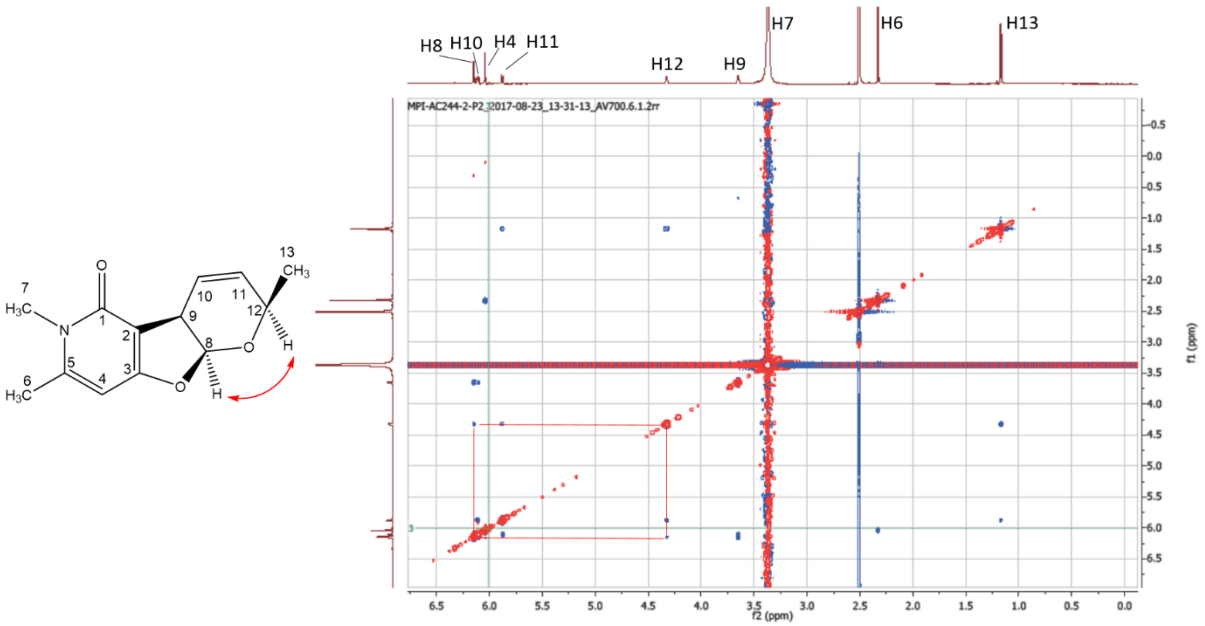

Supplemental Spectra S4. 2D-NOESY spectrum of **15a** in DMSO-d_6.

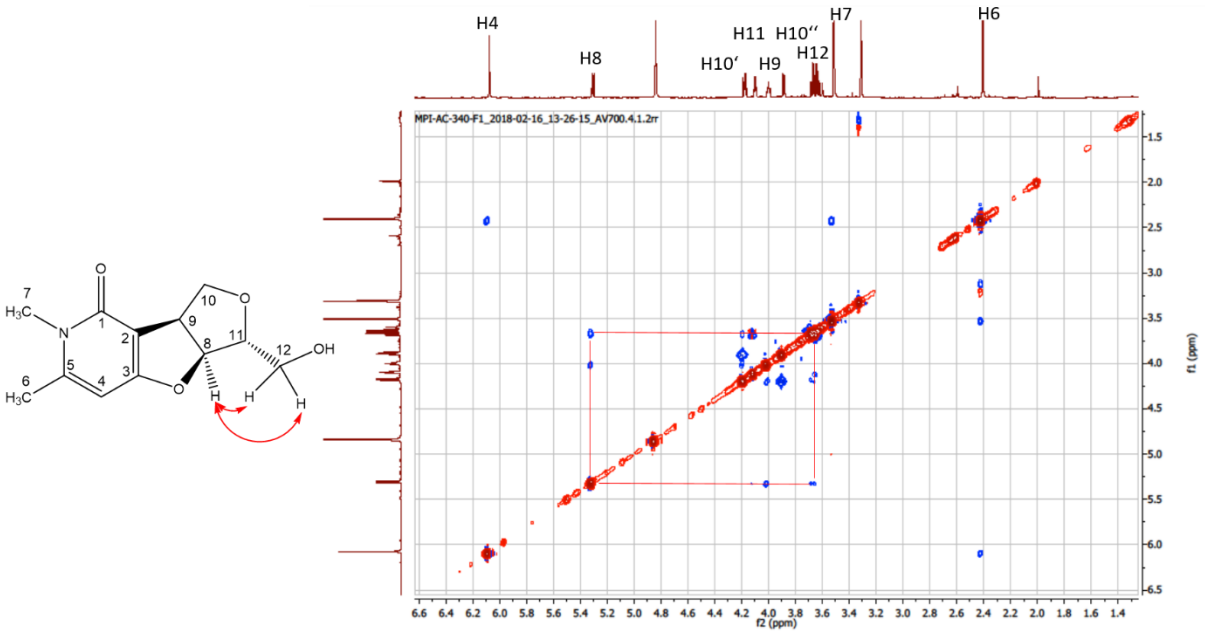

Supplemental Spectra S5. 2D-NOESY spectrum of **19b** in MeOH-d_4.

8.2. Representative Cell Painting Images

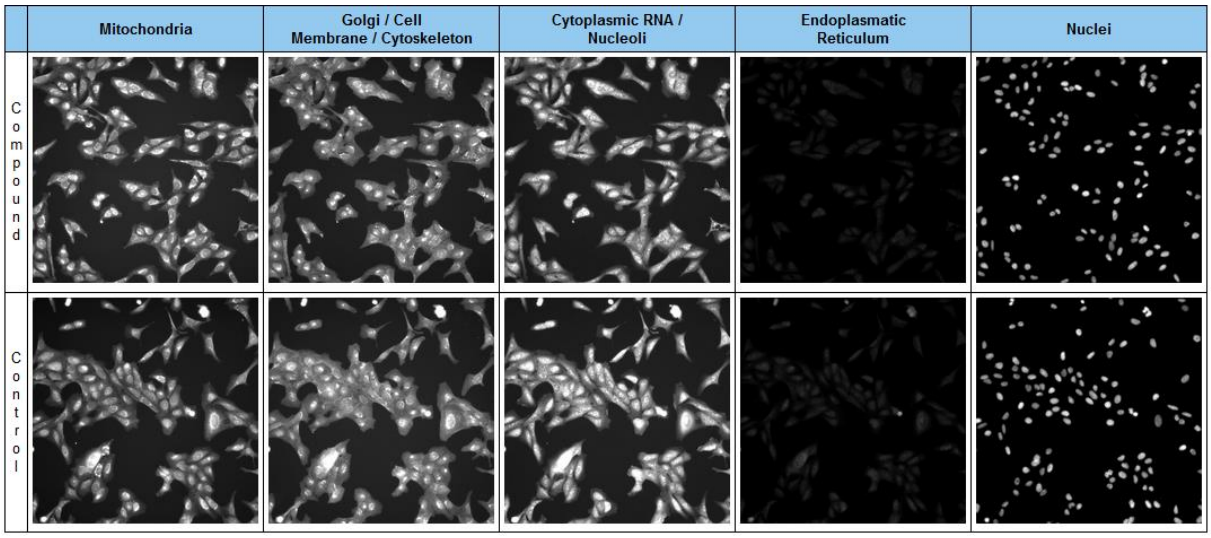

Figure 21. Microscopy images recorded for **29k** at 10 µM; cell-count = 90%

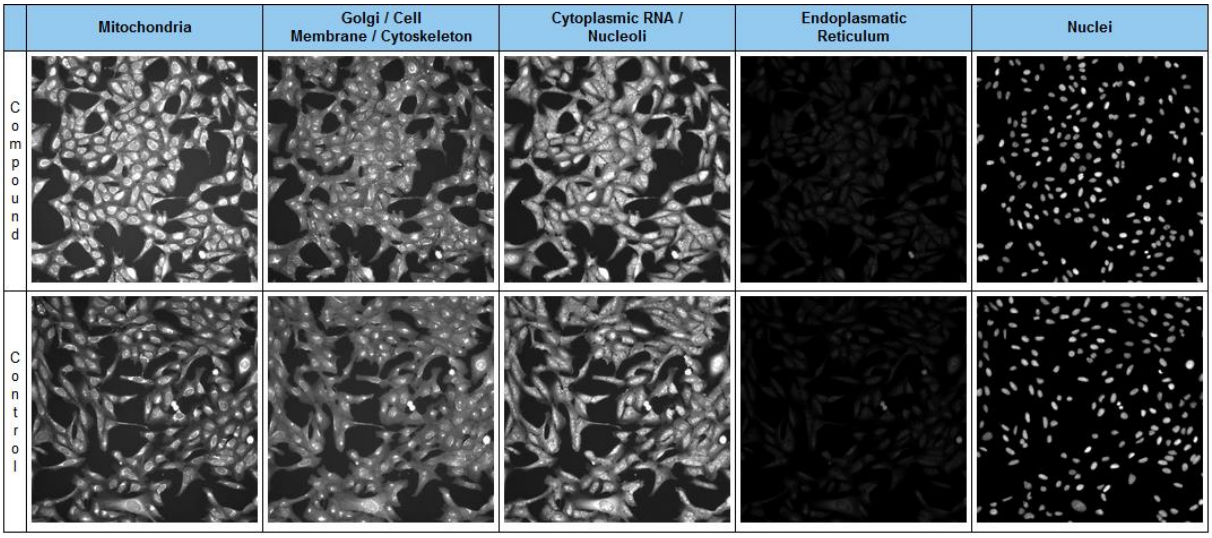

Figure 22. Microscopy images recorded for **29k** at 30 µM; cell-count = 96%

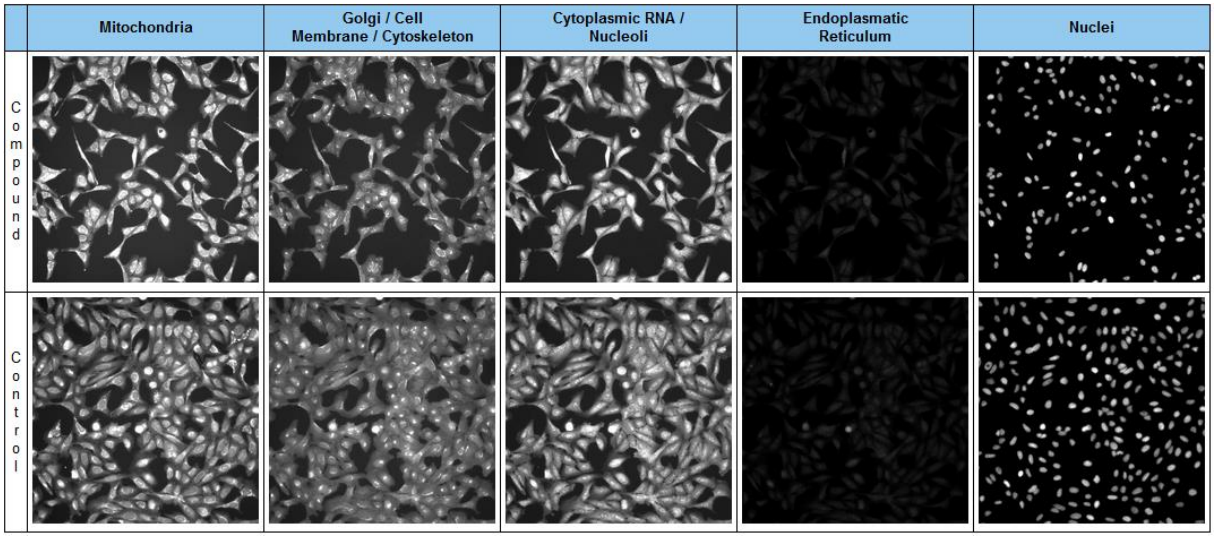

Figure 23. Microscopy images recorded for **29k** at 50 µM; cell-count = 93%

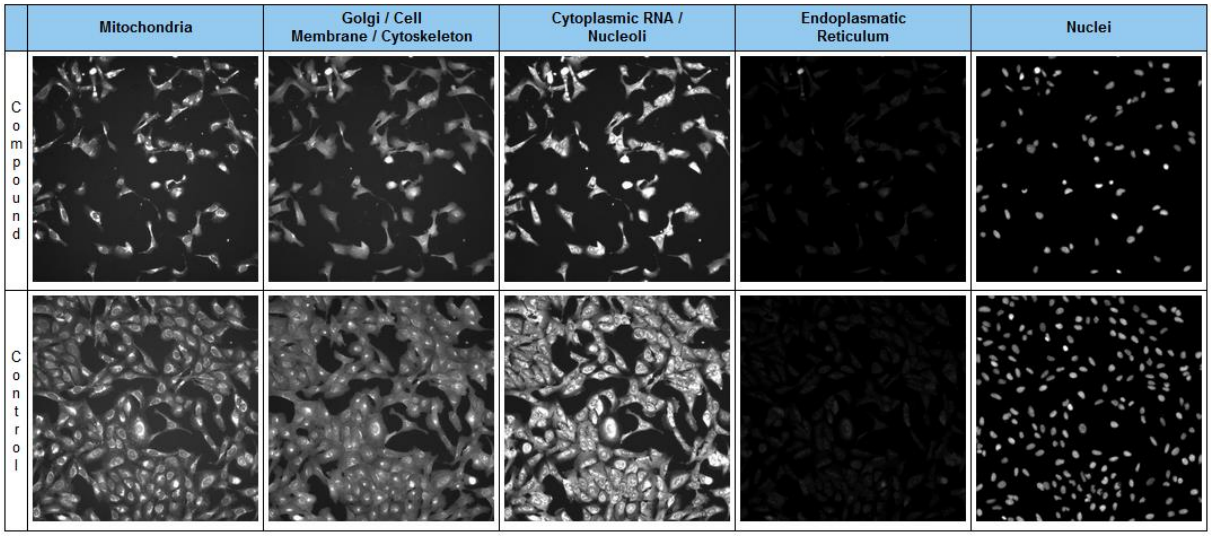

Figure 24. Microscopy images recorded for **4d** at 10 µM; cell-count = 50%

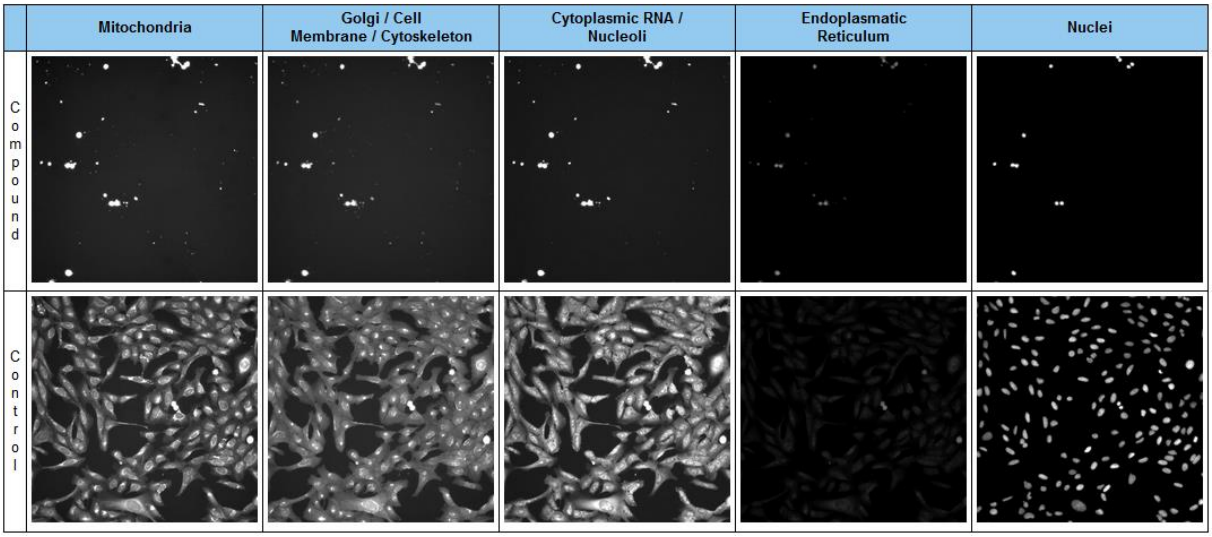

Figure 25. Microscopy images recorded for **4d** at 30 µM; cell-count = 34%

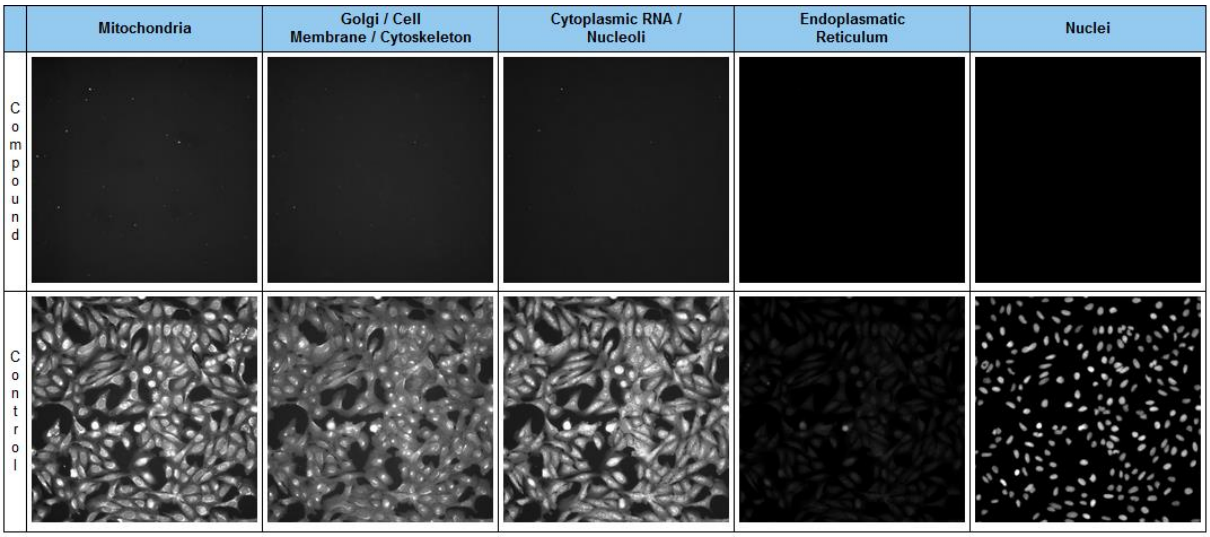

Figure 26. Microscopy images recorded for **4d** at 50 µM; cell-count = 7%

8.3. Acknowledgments

First, I would like to thank Prof. Dr. Herbert Waldmann for giving me the opportunity to work on this interesting and challenging project in such an excellent scientific environment. I highly appreciate the freedom to work independently and I am thankful for his encouragement, constant input and guidance throughout the time of my PhD. I truly value his interdisciplinary mindset and all the facets of chemical biology I was able to experience during his supervision.

I would like to express my gratitude to Prof. Dr. Markus Kaiser for being my second examiner.

I am truly thankful to Dr. Slava Ziegler, Dr. Saad Shaaban and Dr. Michael Grigalunas for proofreading this thesis.

I am deeply grateful to Aylin Binici whom I supervised during her master thesis and who contributed to this thesis by synthesizing compounds for the PFP library and performing the Mito Stress Test assay, the semi-intact assay for mitochondrial respiration and the MitoSOX Red assays. Likewise, I want to thank Julian Wilke and Dr. Slava Ziegler for supervising the biological experiments of Aylin Binici and for the fruitful discussions on the cell painting data.

I would like to express my gratitude to Dr. Axel Pahl who established the cell painting assay at COMAS and the corresponding data analysis tools. The countless discussions on data analysis strategies and cheminformatic analysis significantly influenced the successful completion of this project. I also gratefully acknowledge Dr. Sonja Sievers, Dr. Claude Ostermann and all co-workers of the COMAS team for their work on the cell painting assay as well as the management and screening of my compounds.

A special thanks goes to my trainees Julian Dyrda and Maike Wolters as well as to my bachelor student Joseph Hoock for being a great help in the synthesis of the pseudo NP library.

I would like to thank Dr. Kamal Kumar, Dr. Andrey Antonchick, Dr. Charles Loh. Dr. Luca Laraia, Dr. Tom Mejuch, Dr. Michael Grigalunas, Dr. George Karageorgis and Dr. Daniel Foley for their highly valuable input on organic chemistry issues and pseudo NPs in general as well as my former laboratory partner of room D 3.12 Dr. Peter t'Hart for interesting scientific discussions and his great company.

I further acknowledge all analytic departments involved in the characterization of the synthesized compounds emphasizing my gratitude to Jens Warmers for the maintenance of the

analytical and preparative HPLCs, Dr. Petra Janning and her Team for HRMS measurements as well as Bernhard Griewel and the NMR-Team of the TU Dortmund for all NMR experiments.

I would like to thank the whole department IV for the great working atmosphere and the scientific input that made me enjoy the exciting and demanding journey of a PhD every day. I want to especially name Hélène Adihou, Mahyar Akbarzadeh, Luis Bering, Aylin Binici, Annina Burhop, Gregor Cremosnik, Tim Foerster, Guillaume Garivet, Michael Grigalunas, Peter t'Hart, Elisabeth Hennes, Nadine Kaiser, Luca Laraia, Tom Mejuch, Georg Niggemeyer, Elena Reckzeh, Marjorie Rummelt, Saad Shaaban, Julian Wilke, Michael Winzker and Stefan Zimmermann.

любимые родители, Дорогой брат, Дорогая семья,
Я благодарю вас за вашу постоянную поддержку.

Finally, my deepest and heartfelt appreciation goes to Mayken Visser for her everlasting support and encouragement.

8.4. Curriculum Vitae

Date and	13.08.1989
place of birth	Nishnajaja Alarca (Kyrgyzstan)
Nationality	German
Address	Dammannstraße 41, 45138 Essen, Germany
Email	andreas.christoforow@gmx.net

Academic education

Since 02/2016 — **PhD in chemical Biology** (Prof. Dr. Waldmann, Max-Planck-Institut of molecular Physiology, Dortmund, Germany)

- *„Design and Synthesis of Pyrano-furopyridone Pseudo Natural Products“*
- Designed and carried out multi-step library synthesis
- Performed cheminformatic calculations and data visualization
- Analyzed and interpreted structure-phenotype relationship of morphological fingerprints
- Supervised trainees, bachelor- and master students
- Trained other scientists for utilization of in-house NMR-spectrometer

10/2013 – 07/2015 — **M.Sc. Molecular Science** (Grade: 1.1; Friedrich-Alexander-University, Erlangen, Germany)

- Courses: Drug Discovery, Medicinal Chemistry, Advanced Organic Chemistry

Master thesis (Grade: 1.0; Prof. Dr. Gmeiner, Friedrich-Alexander-University, Erlangen, Germany)

- *„Synthesis of Selective Ligands for the Protease Activated Receptor 2“*

10/2010 – 07/2013 — **B.Sc. Molecular Science** (Grade: 2.1; Friedrich-Alexander-University, Erlangen, Germany)

- Courses: Organic and inorganic chemistry, medicinal chemistry, biochemistry, theoretical and physical chemistry

DAAD-ISAP scholarship for semester abroad and Bachelor thesis (Grade: 1.3; Prof. Dr. Keller, University of Wollongong, Australia)

- *„Design and Synthesis of Potential Drugs for the Treatment of Human African Trypanosomiasis“*

School education

07/2009	Abitur, Aventinus Gymnasium, Burghausen (Germany, grade: 2.1)
09/2000 – 07/2009	Aventinus Gymnasium, Burghausen (Germany)

8.5. Eidesstattliche Versicherung (Affidativ)

Christoforow, Andreas — Name, Vorname (Surname, first name)

190895 — Matrikel-Nr. (Enrolment number)

Belehrung:

Wer vorsätzlich gegen eine die Täuschung über Prüfungsleistungen betreffende Regelung einer Hochschulprüfungsordnung verstößt, handelt ordnungswidrig. Die Ordnungswidrigkeit kann mit einer Geldbuße von bis zu 50.000,00 € geahndet werden. Zuständige Verwaltungsbehörde für die Verfolgung und Ahndung von Ordnungswidrigkeiten ist der Kanzler/die Kanzlerin der Technischen Universität Dortmund. Im Falle eines mehrfachen oder sonstigen schwerwiegenden Täuschungsversuches kann der Prüfling zudem exmatrikuliert werden, § 63 Abs. 5 Hochschulgesetz NRW.

Die Abgabe einer falschen Versicherung an Eides statt ist strafbar.

Wer vorsätzlich eine falsche Versicherung an Eides statt abgibt, kann mit einer Freiheitsstrafe bis zu drei Jahren oder mit Geldstrafe bestraft werden, § 156 StGB. Die fahrlässige Abgabe einer falschen Versicherung an Eides statt kann mit einer Freiheitsstrafe bis zu einem Jahr oder Geldstrafe bestraft werden, § 161 StGB.

Die oben stehende Belehrung habe ich zur Kenntnis genommen:

Official notification:

Any person who intentionally breaches any regulation of university examination regulations relating to deception in examination performance is acting improperly. This offence can be punished with a fine of up to EUR 50,000.00. The competent administrative authority for the pursuit and prosecution of offences of this type is the chancellor of the TU Dortmund University. In the case of multiple or other serious attempts at deception, the candidate can also be unenrolled, Section 63, paragraph 5 of the Universities Act of North Rhine-Westphalia.

The submission of a false affidavit is punishable.

Any person who intentionally submits a false affidavit can be punished with a prison sentence of up to three years or a fine, Section 156 of the Criminal Code. The negligent submission of a false affidavit can be punished with a prison sentence of up to one year or a fine, Section 161 of the Criminal Code.

I have taken note of the above official notification.

Dortmund, — Ort, Datum (Place, date)

Unterschrift (Signature)

Titel der Dissertation:
(Title of the thesis):

Pyrano-Furo-Pyridones:
Design, Synthesis and Morphological Profiling of
a Novel Pseudo Natural Product Class

Ich versichere hiermit an Eides statt, dass ich die vorliegende Dissertation mit dem Titel selbstständig und ohne unzulässige fremde Hilfe angefertigt habe. Ich habe keine anderen als die angegebenen Quellen und Hilfsmittel benutzt sowie wörtliche und sinngemäße Zitate kenntlich gemacht.
Die Arbeit hat in gegenwärtiger oder in einer anderen Fassung weder der TU Dortmund noch einer anderen Hochschule im Zusammenhang mit einer staatlichen oder akademischen Prüfung vorgelegen.

I hereby swear that I have completed the present dissertation independently and without inadmissible external support. I have not used any sources or tools other than those indicated and have identified literal and analogous quotations.

The thesis in its current version or another version has not been presented to the TU Dortmund University or another university in connection with a state or academic examination.*

*Please be aware that solely the German version of the affidavit ("Eidesstattliche Versicherung") for the PhD thesis is the official and legally binding version.

Dortmund, — Ort, Datum (Place, date)

Unterschrift (Signature)